Gymnosperm woods of the Upper Jurassic Morrison Formation in the Western Interior of North America: Systematics, anatomy, growth ring analysis, tree height reconstruction, and plant–insect–fungal interactions

Dissertation
zur
Erlangung des Doktorgrades (Dr. rer. nat.)
der
Mathematisch-Naturwissenschaftlichen Fakultät
der
Rheinischen Friedrich-Wilhelms-Universität Bonn

vorgelegt von

Aowei XIE

aus
Henan, China

Bonn, 2022

Angefertigt mit Genehmigung der Mathematisch-Naturwissenschaftlichen Fakultät
der Rheinischen Friedrich-Wilhelms-Universität Bonn

Gutachterin: PD Dr. Carole T. Gee
Gutachter: Prof. Dr. P. Martin Sander

Tag der Promotion: September 17, 2022
Erscheinungsjahr: 2022

Hiermit erkläre ich an Eides statt, die vorliegende Arbeit selbstständig verfasst und keine anderen Hilfsmittel als die angegebenen verwendet zu haben. Inhaltlich und wörtlich aus anderen Werken entnommene Stellen und Zitate sind als solche gekennzeichnet.

Aowei Xie

Tao begets One, One begets Two, Two begets Three, Three begets all things.[1]

Tao Te Ching, Laozi (Lao Tzu)[2]

[1] Original text in Chinese, “道生一，一生二，二生三，三生万物”.

[2] Laozi, ca. 6th–4th century BCE, is an ancient Chinese philosopher and writer, and worshipped as a deity in the traditional Chinese religion of Taoism.

Acknowledgments

Time is fleeting; more than three years have gone by. At the time of completion of this doctoral dissertation, many things are appreciated here, on learning or living.

This dissertation was written under the guidance of my supervisor PD Dr. Carole Gee, which is highly appreciated. During the time of my Ph.D. studies, Dr. Gee has given me lots of generous support, helpful discussions, and valuable advice, which benefit my academic career a lot. I also express many thanks to my Master's degree supervisor Prof. Dr. Yongdong Wang at Nanjing Institute of Geology and Palaeontology, Chinese Academy of Sciences (CAS), for generously guiding me throughout my career. I would also like to thank Prof. Dr. P. Martin Sander for helping me in various ways, especially paying time to review this dissertation, Dr. Moritz Liesegang (Freie Universität Berlin) for wonderful office time and teaching me the knowledge of silicification of silicified woods, Prof. Dr. Eva Maria Griebeler (University of Mainz) for collaborating with the height–diameter growth models of conifer trees, and Assoc. Prof. Dr. Ning Tian (Shenyang Normal University) for help in my career.

Paleontological study is inseparable from field work, thus, great appreciation to my supervisor PD Dr. Carole Gee, Prof. Dr. Yongdong Wang and Dr. Xiaoqing Zhang (Nanjing Institute of Geology and Palaeontology, CAS) for help in the field, Mary Beth Bennis and Dale E. Gray (Utah Field House of Natural History State Park Museum) for guiding us to the field site, as well as Steven Sroka (Utah Field House of Natural History State Park Museum) for logistical support.

I am greatly indebted to the Division of Paleontology, Institute of Geosciences and the University of Bonn for offering academic conditions for the last nearly four years. Special thanks go to Prof. Dr. A. Rahman Ashraf for generous help and support, Olaf Dülfer for the guidance of making thin-sections, and Peter Göddertz for solving technical problems on the Internet, computer, and printer.

I also express gratitude to my colleagues and friends Prof. Dr. Jun Liu, Dr. Shook Ling Low, Dr. Tong Bao, Dr. Tzu-Ruei Yang, Felicitas Hoff, Gustavo Pereira, Kelly Shunn, Luis Pauly, Mariah Howell, Philipp Knaus, and Qiang Li for a great time in Bonn and helpful academic communications; to Mariah for proofreading some of the dissertation; and to my friend Christopher Sander for a

wonderful time and logistical support in Bonn.

Many thanks to my family for encouraging me and chatting with me when I feel lonely far away from home.

Financial support from the China Scholarship Council for the doctoral studies (CSC no. 201804910527) is greatly appreciated. Financial support for fieldwork in Utah from Open Funding grant no. 193101 from the State Key Laboratory of Palaeobiology and Stratigraphy (Nanjing Institute of Geology and Palaeontology, CAS) State Grant is also gratefully acknowledged.

Thank you so much to all the reviewers who have worked hard for reviewing this dissertation.

Preface

In today's world, the greenhouse effect has caused abnormal climate change for many years, which urges people to be more and more aware of the importance of protecting the environment. However, can you imagine there was once a period of CO_2 concentration in earth's history (Bice and Norris, 2002) that was 4–10 times greater than today? This period had a typical greenhouse climate and the highest temperature throughout the 540 million years of the Phanerozoic Eon: the Mesozoic.

The Mesozoic Era, a geological time interval ranging from 252 to 66 million years ago (Ma), consists of three periods—the Triassic (252–201 Ma), Jurassic (201–145 Ma), and Cretaceous (145–66 Ma) (Cohen et al., 2013). When speaking about the Mesozoic, dinosaurs governing the world are frequently mentioned with enthusiasm. Nevertheless, the forest was the dominant terrestrial ecosystem.

Roaming around in the Triassic–Jurassic world, you would have seen flourishing gymnosperm forests dominated by bennettitaleans, cycads, ginkgos, and conifers come into view instead of angiosperms (flowering plants). However, the bennettitaleans are now extinct. The cycads and ginkgos had a much broader global distribution then than now, even extending northward to Siberia and Greenland in the Middle Triassic. The conifers obtained the pivotal period of radiation at this time, and became an increasingly significant component of the vegetation, although the once widely spread conifer family Cheirolepidiaceae went extinct. In the Cretaceous forests, you would have seen the vegetation become recognizable as today's forms, that is, as the angiosperms that obtained ecological dominance owing to rapid radiation and diversification of flowering plants during this time (e.g., Willis and McElwain, 2014; Gee et al., 2020).

Such spectacular reconstruction of the Mesozoic vegetation have resulted from the numerous studies on plant fossils found in Mesozoic deposits, including fossil leaves, wood, seed cones, pollen grains, and spores. Hence, a deeper and more comprehensive knowledge of the fossil flora is essential to further understand the vegetation of ancient forest ecosystems during the Mesozoic.

Contents

Abstract

Silicified wood is one of the most important types of plant fossils that can be used for reconstructing terrestrial ecosystems and paleoclimate in deep time. Abundant fossil woods occur in the world-famous Upper Jurassic Morrison Formation of Western Interior of North America. However, the normally poorly preserved internal structures of the woods are unattractive to formal paleobotanical study, making the diversity of the Morrison woods understudied. Here, the primary objectives of this dissertation are the taxonomic identification and anatomical study of newly discovered silicified woods with well-preserved cellular structures from the Morrison Formation in Utah and Wyoming to better understand the diversity of the Morrison woods during the Late Jurassic times. In addition to the taxonomy and anatomy, analyzing growth rings, establishing height–diameter growth models for ancient trees, describing multitrophic interactions among plants, insect, and fungi, as well as identifying the preservation potential of organic compounds in fossil wood were carried out.

In chapter 2, for instance, a systematic paleobotanic study on a fossil log from Miners Draw in the Morrison Formation of Utah recognizes the most southerly occurrence of *Xenoxylon* tree in North America so far and confirms that *Xenoxylon* trees were not only limited to the cool circumpolar zone. Furthermore, the reconstruction of ancient tree height on the basis of maximum preserved diameter was applied to this fossil log, which measured 90 cm in diameter and resulted in a reconstructed tree height of ca. 40 m using our newly established height–diameter growth models for conifer-like trees. When a closer look was taken at the wood thin sections of the Miner Draw log, in chapter 4, we were able to describe abundant white rot features and fossil mycelia with typical Basidiomycota characters, which represents now the first reliable record of Jurassic basidiomycetes in Utah. Similar white rot characters were also noticed in a fossil wood from an araucariaceous fossil log in Rainbow Draw, 30 km northwest of the Miners Draw, along with two insect boreholes (chapter 3). To understand the preservation quality of the Morrison woods, in chapter 6, a silicified wood with visible color zones in the Morrison Formation in Utah was studied, that is, the preservation potential of wood organic compounds was investigated, and the related primary and secondary trace element distribution were analyzed. Outside of Utah, an araucariaceous wood flora in the Upper Jurassic Morrison Formation in

the Howe-Stephens Quarry of north-central Wyoming was described in chapter 7, which reconstructed these ancient trees based on their maximum preserved diameters using our newly established araucariaceous height–diameter growth models given in chapter 5.

In summary, the new knowledge related to paleobotany of Morrison Formation in this dissertation contributes to further understand the floristics of ancient forest ecosystems and paleohabitats during the Morrison times, as well as the preservation of Morrison woods.

Structure of dissertation

This dissertation is comprised of eight chapters, which are already published, in review, or in preparation to be submitted to peer-reviewed scientific journals. Therefore, chapters 2 and 3 are shown in the respective journal format with light modifications; that is, the page header, footer, and margin are fitted to the dissertation format. For the original published papers, please see DOIs: 10.1016/j.revpalbo.2021.104451 and 10.1016/j.revpalbo.2022.104627. Additionally, author contributions and a summary of the publication are presented at the beginning of chapters 2 and 3. Chapters 4, 5, and 6 are prepared in their respective submitted format with modifications—the headings follow the dissertation format, along with the author contributions and abstract of the manuscript. The last two chapters are produced in the dissertation format.

Chapter 1
Introduction

1.1. Research background

Since the first fossil cycad trunks *Cycadeoidea wyomingensis* were reported from the Upper Jurassic Morrison Formation in Wyoming of western USA in 1900 (Ward, 1900), abundant plant fossils have been found in this formation in the Western Interior of North America. Based on these fossil plants, Morrison ecosystems have been accepted as a conifer-dominated forest by many paleobotanists, with other tall trees such as ginkgophytes and an understory of ferns, fern allies, cycads, and bennettitaleans (Tidwell, 1990; Ash and Tidwell, 1998; Tidwell et al., 1998; Hotton and Baghai-Riding, 2010; Gee et al., 2014; Foster, 2020; Xie et al., 2021). Some studies, however, have suggested a semiarid to arid climate with sparse plants (Demko and Parrish, 1998; Demko et al., 2004; Parrish et al. 2004; Rees et al. 2004; Turner and Peterson, 2004), which is inconsistent with the paleohabitats that large-bodied herbivores and carnivores needed during the Morrison time (cf. Foster, 2020).

Fossil logs and woods are abundant at some Morrison sites. Up to now, more than 20 localities have been documented in Utah, Colorado, Wyoming, South Dakota, and Montana (Fig. 1) (e.g., Medlyn and Tidwell, 1975; 1979; Tidwell, 1990a; 1990b; Tidwell and Medlyn, 1992; 1993; Ash and Tidwell, 1998; Tidwell et al., 1998; Gee and Tidwell, 2010; Gee et al., 2019; Richmond et al., 2019; Xie et al., 2021). However, only a small number of taxa of fossil woods have been recognized. In 2018, the Morrison wood flora comprised six genera and eight species of fossil gymnosperm woods: *Araucarioxylon hoodii* Tidwell et Medlyn (1993), *Cupressinoxylon jurassicum* Lutz (1930), *Mesembrioxylon carterii* Tidwell et al. (1998), *M. obscurum* (Knowlton) Medlyn et Tidwell (2002), *Protocupressinoxylon medlynii* Tidwell et al. (1998), *Protopiceoxylon resiniferous* Medlyn et Tidwell (1979), *Xenoxylon moorei* Tidwell et al. (1998), and *X. morrisonense* Medlyn et Tidwell (1975).

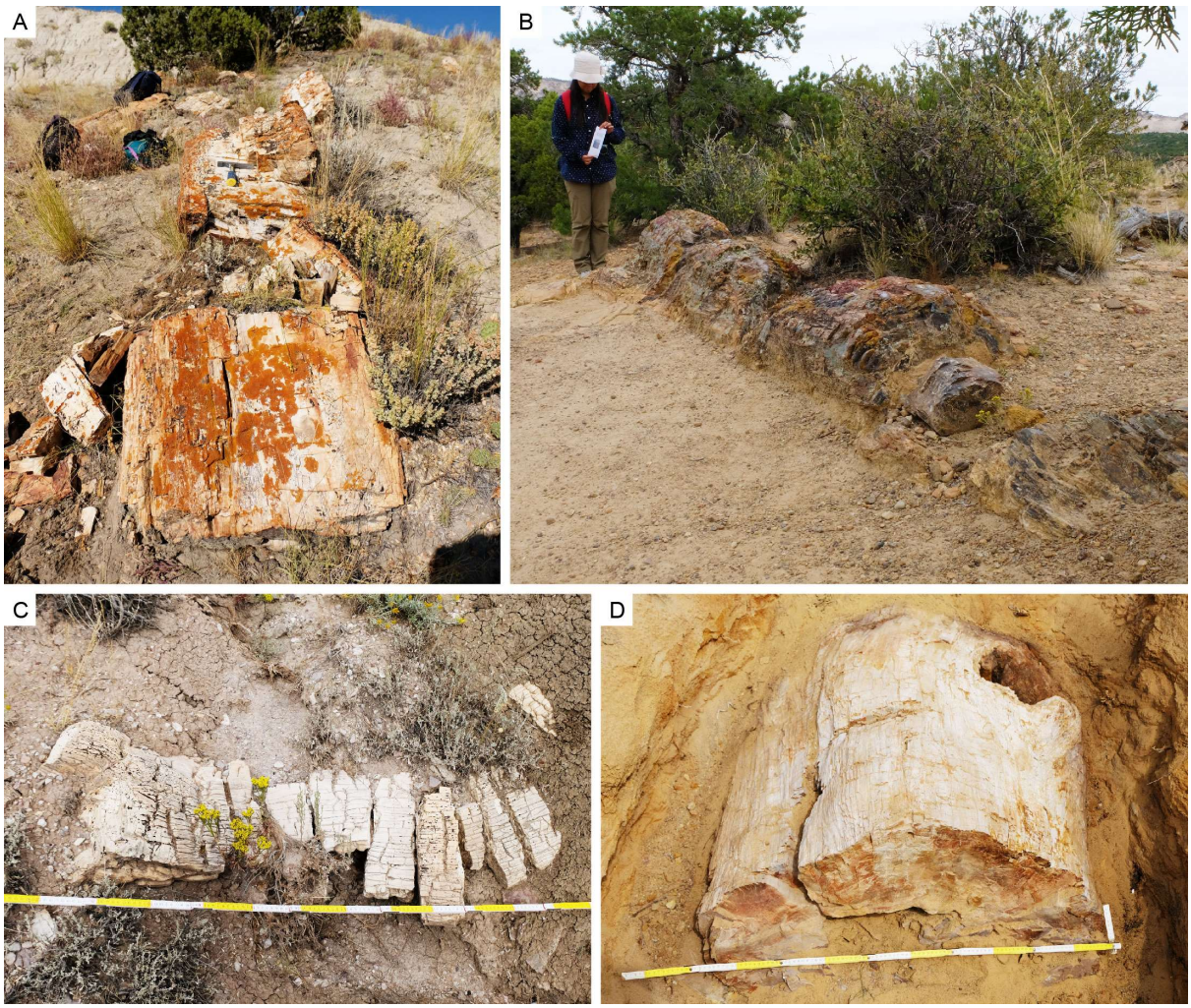

Figure 1. Fossil logs from the Upper Jurassic Morrison Formation at different localities: (A) Rainbow Draw near Vernal, northeastern Utah, (B) Escalante Petrified Forest State Park in Escalante, southern Utah, (C) Six Mile Draw near Vernal, northeastern Utah, and (D) Manwell Log Site near Vernal, northeastern Utah.

The next year, in 2019, *Araucarioxylon hoodii*, *Xenoxylon moorei*, and *X. morrisonense* underwent taxonomic revision. *Araucarioxylon hoodii* was established as a new combination, *Agathoxylon hoodii* (Tidwell et Medlyn) Gee et al. (2019), while *Xenoxylon moorei* and *X. morrisonense* were excluded from the genus based on their anatomy (Richmond et al., 2019). Moreoever, Richmond et al. (2019) described a new occurrence of *Xenoxylon*, *X. meisteri*, in Montana. In 2021, Xie and colleagues established a new species of *Xenoxylon*, *X. utahense*, in Utah (Xie et al., 2021). Consequently, the Morrison wood flora consisted now of six genera and eight species of fossil gymnosperm woods. This seemed to point to continued low diversity in the Morrison wood flora. However, according to Gee et al. (2019), the small number of taxa of fossil wood does not

reflect the real landscape of Morrison flora because of the generally poorly-preserved anatomical structures of the woods, which makes them unattractive to formal paleobotanical study. For example, the fossil woods in the Escalante Petrified Forest State Park of south-central Utah, called "agatized wood" with green, blue, pink, black, and red colors, are not good enough for paleobotanical study due to the lack of the fine anatomical characters essential for systematic identification (cf. Morgan et al., 2010; Gee and Xie, own data).

1.2. Aim of dissertation

This dissertation aims to present my recent paleobotanical studies, which provide new insights into the floristics of ancient forest ecosystems and paleohabitats of the Morrison Formation. These studies were done in collaboration with colleagues who are experts in paleobotany, statistical analysis, wood rot fungi, micro-CT, and fossilization. My studies focus on the fossil woods and logs from the Upper Jurassic Morrison Formation in Utah and Wyoming, USA, to describe wood anatomy (chapters 2 and 7), reconstruct the minimum height of the ancient trees based on the preserved maximum diameter of the fossil logs (chapter 2), establish good height–diameter models for ancient trees (chapter 5), interpret the paleoclimatic signals shown by the growth rings in the woods (chapter 2), elucidate plant–fungi–insect interactions in the Morrison ecosystems (chapters 3 and 4), and analyze the fossilization of Morrison woods (chapter 6).

1.3. The Morrison Formation geology

In the main study area of my dissertation research in northeastern Utah, the Morrison Formation is generally divided into four members—the Windy Hill Member, Tidwell Member, Salt Wash Member, and Brushy Basin Member in ascending chronostratigraphic order (Sprinkel et al., 2019). In terms of lithology and paleontology, these four members are comprised of different depositional environments. For example, the Windy Hill and Tidwell members indicate a marine to marginal marine to coastal plain depositional environment (Turner and Peterson, 2004), but the Salt Wash and Brushy Basin members represent a fluvial–lacustrine depositional environment (Turner and Peterson, 2004; Sprinkel et al., 2019).

In general, the Morrison Formation crops out in the western United States, mostly in the Rocky Mountain region. Outcrops are exposed in Arizona, New Mexico, Oklahoma, Utah, Colorado, Wyoming, South Dakota, and Montana, encompassing ca. 1 million square kilometers (Fig. 2) (Foster, 2020). This formation is regarded as Upper Jurassic (e.g., Turner and Peterson, 2004; Trujillo and Kowallis, 2015; Foster, 2020), largely Kimmeridgian (Trujillo and Kowallis, 2015), ca. 152 million years old. Morrison sediments generally indicate terrestrial environments, but also some marginal marine sediments occur at the base of the Morrison Formation northwards northern Utah and Colorado (Turner and Peterson, 2004).

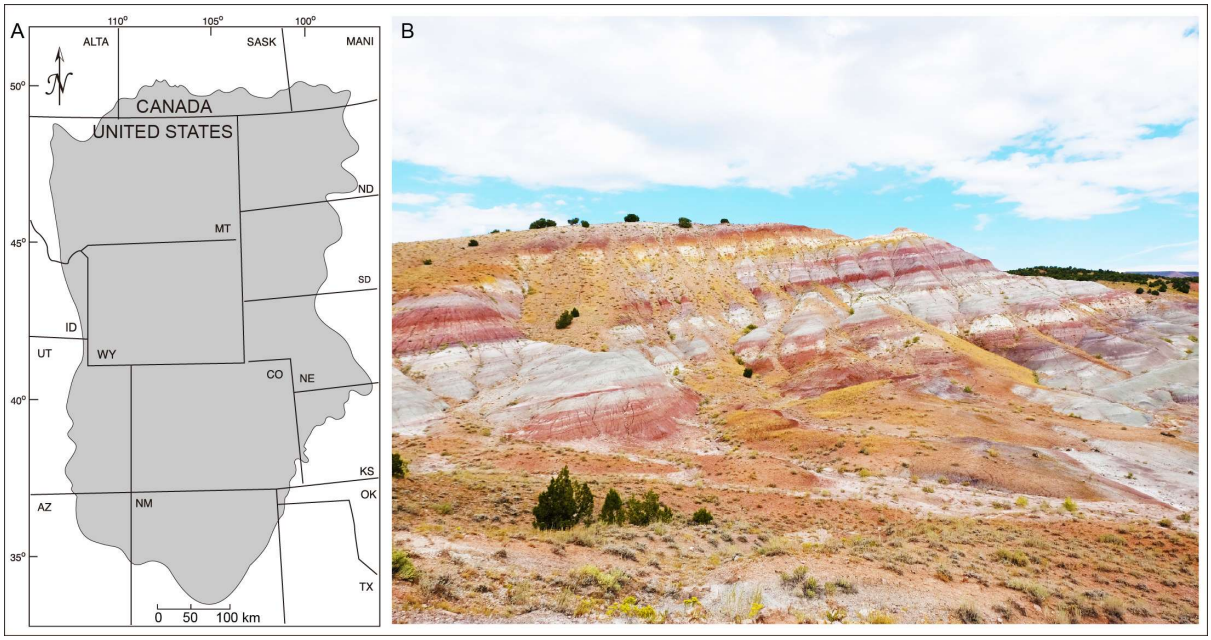

Figure 2. (A) Sketch map of the distribution of the Upper Jurassic Morrison Formation in the Western Interior of North America (gray area) (modified after Hasiotis, 2004). (B) The typically colorful outcrops of the Upper Jurassic Morrison Formation with a mix of sandstones and mudstones in Six Mile Draw, near Vernal, northeastern Utah.

1.4. New insights into the Morrison flora and paleoclimate

Increasing evidence of fossil plants, pollen grains, and spores has been found in the Morrison Formation in the last two decades, which makes it clearer that the Morrison flora was mainly composed of conifers, cycads, bennettitaleans, ginkgophytes, seed ferns, and ferns. Among the woody plants, the conifers were dominant. Evidence for the dominance of conifers throughout the Morrison Formation is evident in the occurrence of fossil woods and logs throughout Utah, Colorado,

Wyoming, South Dakota, and Montana (e.g., Tidwell, 1990; Ash and Tidwell, 1998; Tidwell et al., 1998; Gee and Tidwell, 2010; Gee et al., 2019; Richmond et al., 2019; Sprinkel et al. 2019; Xie et al., 2021). The most common conifer family is the Araucariaceae. For example, a silicified log flora from the Morrison Formation at Rainbow Draw area in Utah contained variously sized tree trunks ranging from 70 to 130 cm in maximum preserved diameter, which was interpreted as forming a monospecific forest of large araucariaceous trees that attained individual ages of over 100 years (Gee et al., 2019). The other conifer families that have been found as fossil wood include the Cupressaceae, Podocarpaceae, and the extinct conifer family coniferous family Miroviaceae (cf. Lutz, 1930; Tidwell et al., 1998; Medlyn and Tidwell, 1979; 2002; Xie et al., 2021).

Another line of evidence for the dominance and diversity of conifers growing throughout the Morrison Formation is also supported by the occurrence of conifer seed cones. For instance, in Utah and Wyoming, the fossil seed cones pertain to at least three conifer families, the Araucariaceae, Pinaceae, and extinct family Cheirolepidiaceae (Gee and Tidwell, 2010; Gee, 2013; Gee et al., 2014).

A third line of evidence supporting a variety of conifers in the Morrison Formation are fossil leaves and shoots. In Utah, more than ten fossil localities yielding fossil leaves and shoots have been discovered, including *Cupressinocladus*, *Elatides*, *Brachyphyllum*, *Behuninia*, and *Steinerocaulis* (Ash and Tidwell, 1998; Gee and Tidwell, 2010), which pertain to the Cupressaceae and Araucariaceae.

The last line of evidence for a diversified conifer flora in the Morrison Formation is pollen. Palynological studies demonstrate that a variety of conifers dominated in the Morrison Formation, including the Araucariaceae, Pinaceae, Podocarpaceae, and Cheirolepidiaceae (Litwin et al., 1998; Hotton and Baghai-Riding, 2010).

The evidence of the Morrison flora presented here suggests that conifers comprised much of the vegetation of the Morrison Formation and formed a framework of forests during the Late Jurassic times. The composition of Morrison flora indicates that a warm and humid climate with mild seasonality prevailed. For example, the fossil woods found in the Rainbow Draw and Miners Draw area of northeastern Utah contain growth rings with narrow latewood (Xie et al., 2021), or no true growth rings (Gee et al., 2019), which suggests that the growing conditions of Morrison trees were lightly variable with mild seasonality during the entire year, such as mild summer–winter changes or light moisture cyclicity that influenced the growth of the Morrison trees (Fig. 3). Similar growth ring

characters were also found in the fossil woods from other localities in Utah and Colorado: *Xenoxylon morrisonense* in southeastern Utah (Medlyn and Tidwell, 1975), and *Mesembrioxylon carterii*, *Protocupressinoxylon medlynii*, and *Xenoxylon moorei* in western Colorado (Tidwell et al., 1998).

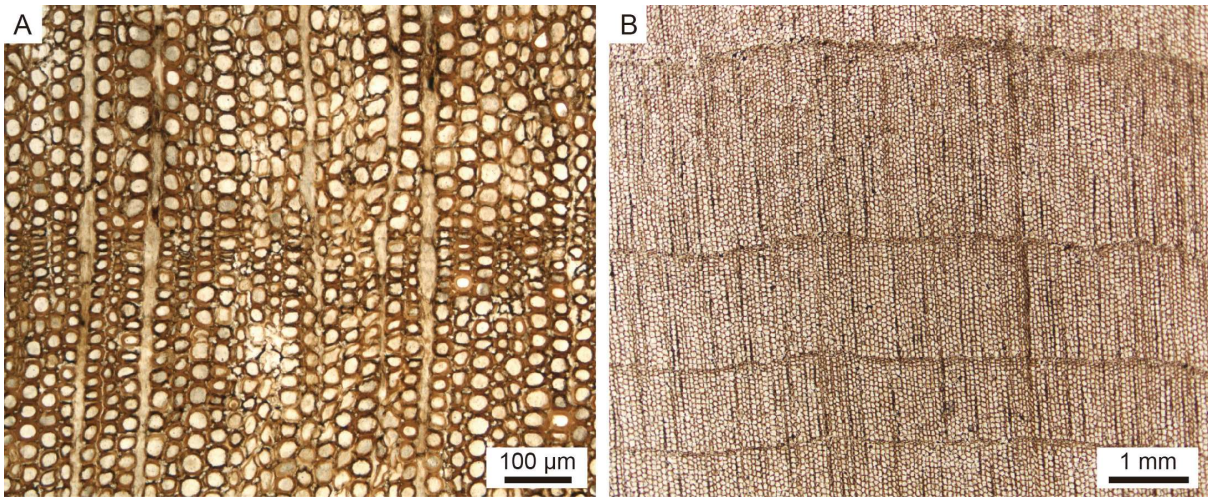

Figure 3. Fossil woods containing growth rings with narrow latewood or distinct growth rings from the Upper Jurassic Morrison Formation in Utah. (A) *Agathoxylon hoodii* in Rainbow Draw, northeastern Utah. Thin section RDW-005a. (B) *Xenoxylon utahense* in Miners Draw, northeastern Utah. Thin section BMT-001a (modified after Xie et al., 2021).

1.5. Description of chapters

This dissertation is comprised of eight chapters. Chapters 2–7 present my recent research papers written in collaboration with colleagues that are already published, in review, or are in preparation for submission to peer-reviewed scientific journals. These studies include the taxonomy and anatomy of silicified woods, growth ring analysis, establishment of height–diameter growth models for ancient trees, plant–insect–fungal interactions, and preservation process of silicified wood.

Chapter 2, published in May 2021, describes a new *Xenoxylon* species, *X. utahense* Xie et Gee, based on well-preserved silicified wood from a fossil log in the Upper Jurassic Morrison Formation in northeastern Utah. This new species is anatomically characterized by distinct xenoxylean radial tracheary pitting and the window-like crossfield pitting of *Xenoxylon* wood. The occurrence of *Xenoxylon* from Utah offers new insights into the Upper Jurassic conifer diversity in Utah, the height and composition of the forest vegetation in the Morrison Formation, and paleoclimatic implications for the Morrison flora. It is worth pointing out that this chapter sheds new light on whether *Xenoxylon* should be re-considered a consistently reliable indicator of cool climate, as had been commonly

suggested previously.

Chapter 3, published in February 2022, describes multitrophic interactions between a Morrison tree, fungi, and wood-boring insect in the Morrison Formation with an extant bee in northeastern Utah. A giant araucariaceous tree of *Agathoxylon hoodii* was infected and decayed by white rot fungi when alive, and then bored by an insect, likely a beetle, that produced large-diameter galleries. One gallery was later inhabited by a living orchard mason bee, *Osmia lignaria*.

Chapter 4, in revision with the *Journal of Paleontology* since May 2022, describes well-preserved fossil mycelia in a silicified wood, *Xenoxylon utahense* Xie and Gee, from the Upper Jurassic Morrison Formation at Blue Mountain near Vernal City in northeastern Utah. This fossil fungus is interpreted as saprotroph due to the wood-decay structures and assigned to the Basidiomycota based on the typical clamp connections. Moreover, this wood-decay fungus possesses a close affinity with the extant *Polyporus squamosus* in the Basidiomycota. This fossil fungus represents now the first reliable record of Jurassic basidiomycetes in Utah and sheds new light on the plant–fungal interactions in the Morrison ecosystems during Jurassic times.

Chapter 5, which is a manuscript nearing completion and subsequent submission, establishes good height–diameter growth models for ancient araucariaceous trees based on the height–diameter relationships of extant *Araucaria* trees in New Guinea and Queensland in Australia. In this study, four living populations of *Araucaria* were modeled. Nineteen nonlinear growth models (1, 2, or 3-parameter models) were considered for each population. A detailed statistical analysis shows that the modified Mosbrugger and von Bertalanffy models were among the best models for each population, but with variable parameter estimates; the median modified Mosbrugger, Power, and Curtis models are always the best growth models for *Araucaria*. Additionally, all three median models were used to estimate the tree heights of Upper Jurassic araucariaceous logs in Utah to test our growth models established.

Chapter 6, in review by *Geochimica et Cosmochimica Acta* since April 2022, investigates a silicified, gymnospermous wood with visible color zones observable to the naked eye from the Upper Jurassic Morrison Formation in Utah to identify the preservation potential of wood organic compounds and the related primary and secondary trace element distribution using MALDI-ToF-MS, FT-IR, and Raman spectroscopy. Electron probe microanalysis of trace elements reveals that the quality and quantity of the organic compounds reflect the primary calcium and secondary sulfur

distribution in cell walls overprinted chemically and structurally during fossilization and diagenesis.

Chapter 7 describes the fossil woods and logs from the Upper Jurassic Morrison Formation in the Howe-Stephens Quarry on Howe Ranch, north-central Wyoming. The fossil woods pertain to *Agathoxylon hoodii*, which represents the first unequivocal occurrence of this genus in Wyoming. The fossil logs measure 1.15 m and 1.49 m in diameter. Based on our height–diameter growth models for ancient araucariaceous trees, the fossil logs attained at least 63 m and 75 m in height, respectively, and may have represented two individuals in a larger forest community with many more trees of similar size that reached individual ages of over 500 years. Interestingly, abundant dinosaur remains have also been found in the same quarry that represent a megaherbivorous and carnivorous dinosaur fauna, which suggests that these dinosaurs might inhabit an araucariaceous forest.

Chapter 2

A more southerly occurrence of *Xenoxylon* in North America: *X. utahense* Xie et Gee sp. nov. from the Upper Jurassic Morrison Formation in Utah, USA, and its paleobiogeographic and paleoclimatic significance

Publication

Xie, A.[1], Gee, C.T., Bennis, M.B., Gray, D., and Sprinkel, D.A., 2021, A more southerly occurrence of *Xenoxylon* in North America: *X. utahense* Xie et Gee sp. nov. from the Upper Jurassic Morrison Formation in Utah, USA, and its paleobiogeographic and paleoclimatic significance: Review of Palaeobotany and Palynology, v. 291, 104451, DOI: 10.1016/j.revpalbo.2021.104451.

Author contributions

Xie and Gee designed the study and collected the fossil wood in the field. Xie measured and mapped the fossil log in the field, made the thin-sections in the lab, studied the thin-sections, took micrographs, analyzed the anatomical structures, wrote the preliminary manuscript, and created all the figures and plates. Gee revised the manuscript, and guided the research with her excellent supervision. Bennis and Gray originally discovered the fossil log and assisted in the field. Sprinkel studied the stratigraphy of the site in earlier work and contributed his knowledge on geology.

Summary

The boreal Mesozoic conifer-like fossil wood genus *Xenoxylon* has a circumpolar distribution,

[1] Corresponding author.

which has led to it being considered as an indicator of cool and wet climate. In North America, the first report of *Xenoxylon* was from the Upper Jurassic Morrison Formation in Utah, USA, as two species, *X. moorei* and *X. morrisonense*. However, in 2019, Richmond and colleagues declared these two species as invalid based on the anatomical characters in a review of all North American reports of *Xenoxylon*, and described a new occurrence of *Xenoxylon* in Montana, *X. meisteri*. In 2021, a more southerly occurrence of another *Xenoxylon* species in North America was reported by Xie and colleagues.

In the study by Xie et al. (2021), we described a new fossil wood with xenoxylean anatomical structures from the Morrison Formation in Miners Draw, near Vernal of northeastern Utah, and established a new species, *X. utahense* Xie et Gee, based on a unique combination of characters of the radial tracheid pitting, crossfield pitting, and ray height. For example, the *X. utahense* wood in Miners Draw distinctly differs from the *Xenoxylon* species in Montana by pertaining to the *phyllocladoides* group which is characterized by mostly uniseriate and locally xenoxylean radial tracheid pits, whereas the *Xenoxylon* species of Montana belongs to the *meisteri* group which generally shows xenoxylean, uniseriate, but locally distant, radial tracheid pits. In a worldwide comparison of species, *X. utahense* from Miners Draw resembles *X. huttonianum* in Yorkshire, UK, in having *phyllocladoides*-type radial tracheid pitting, although the two wood species show minor differences in their ray height and number of pits per crossfield.

Because growth rings are well-preserved in the Miners Draw wood, mean sensitivity analysis of the growth rings was carried out, which interprets the growth conditions of this *Xenoxylon* tree during Late Jurassic times. The results produced by the *X. utahense* wood, a mean sensitivity equal to 0.53, falls within the range of the mean sensitivity of the living conifers and suggest warm and wet growth conditions. We therefore argued that *Xenoxylon* is not only limited to a cool climate, as was previously suggested.

The paleolatitude of ca. 36° N shows that *Xenoxylon utahense* is the most southerly occurrence of *Xenoxylon* in the North America, which indicates that the Mesozoic *Xenoxylon* trees were not only limited to the circumpolar zone that suggested before. Additionally, the new occurrence of a new species of *Xenoxylon* offers new evidence on the fossil wood diversity in western USA during the Late Jurassic times and provides more knowledge in understanding the Morrison flora.

Contents lists available at ScienceDirect

Review of Palaeobotany and Palynology

journal homepage: www.elsevier.com/locate/revpalbo

Research papers

A more southerly occurrence of *Xenoxylon* in North America: *X. utahense* Xie et Gee sp. nov. from the Upper Jurassic Morrison Formation in Utah, USA, and its paleobiogeographic and paleoclimatic significance

Aowei Xie [a,*], Carole T. Gee [a,b,c], Mary Beth Bennis [d], Dale Gray [d], Douglas A. Sprinkel [e]

[a] Institute of Geosciences, Division of Paleontology, University of Bonn, Nussallee 8, 53115 Bonn, Germany
[b] Huntington Botanical Gardens, 1151 Oxford Road, San Marino, CA 91108, USA
[c] State Key Laboratory of Palaeobiology and Stratigraphy, Nanjing Institute of Geology and Palaeontology, CAS, Nanjing 210008, China
[d] Utah Field House of Natural History State Park Museum, 496 E. Main, Vernal, UT 84078, USA
[e] Azteca Geosolutions, 3260 N 1350 W, Pleasant View, UT 84414, USA

ARTICLE INFO

Article history:
Received 6 March 2021
Received in revised form 10 May 2021
Accepted 13 May 2021
Available online 15 May 2021

Keywords:
Growth ring analysis
Mean sensitivity
Miroviaceae
Salt Wash Member
Xenoxylean

ABSTRACT

Although *Xenoxylon* is a global genus of Mesozoic wood in the Northern Hemisphere, it is striking that the valid records in North America occur only in the northernmost parts of the continent. Decades ago, two species of *Xenoxylon* were described from the Upper Jurassic Morrison Formation in Utah, USA. However, a recent review of all North American reports of *Xenoxylon* excluded both species from the genus based on their anatomy, rendering all records of this genus south of Montana invalid in 2019. Here we describe a fossil log from the Morrison Formation near Vernal, northeastern Utah, USA, with true *Xenoxylon* anatomy with locally xenoxylean radial tracheid pitting and fenestriform crossfield pitting. Due to a novel combination of radial tracheid pitting, crossfield pitting and ray height, a new species, *Xenoxylon utahense* Xie et Gee sp. nov., is recognized here. Located at the southernmost occurrence of *Xenoxylon* in North America during the Mesozoic, this new species confirms that *Xenoxylon* trees were not only restricted to a circumpolar zone, but also grew in more southerly areas. In comparison with other fossil plants in the Morrison Formation of Utah, along with growth ring characteristics and climatic preferences of living conifers, the new fossil log with true growth rings with abundant, well-formed earlywood and extremely little latewood argues for a warm and humid climate with very mild seasonality for the Late Jurassic in this region, which is inconsistent with previous interpretations of *Xenoxylon* as a reliable indicator of cool climates.

1. Introduction

Fossil plants have been known in the Upper Jurassic Morrison Formation for over a century. The first report was made by Ward (1990) on the cycad trunks of *Cycadeoidea wyomingensis* from the Freezeout Hills in Wyoming. In paleobotanical studies of the last three decades, the Morrison flora has been described as lush forests of conifers and ginkgophytes with a dense understory of ferns, fern allies, cycads, and bennettitaleans (Tidwell, 1990; Ash and Tidwell, 1998; Tidwell et al., 1998; Chure et al., 2006; Gorman II et al., 2008; Hotton and Baghai-Riding, 2010; Gee et al., 2014; Foster, 2020), although some geological studies have argued for sparse vegetation (Demko and Parrish, 1998; Demko et al., 2004; Parrish et al., 2004; Turner and Peterson, 2004).

Fossil logs and woods are locally abundant in the Morrison Formation (Tidwell, 1990; Tidwell et al., 1998; Chure et al., 2006; Gee et al., 2019; Sprinkel et al., 2019; Foster, 2020). Up to now, more than 20 localities with fossil wood remains have been documented in the states of Utah, Colorado, Wyoming, South Dakota, and Montana (e.g., Tidwell, 1990; Ash and Tidwell, 1998; Tidwell et al., 1998; Gee and Tidwell, 2010; Gee et al., 2019; Richmond et al., 2019). In 2018, there were six genera and eight species of fossil conifer-like woods: *Araucarioxylon hoodii* Tidwell et Medlyn (1993), *Cupressinoxylon jurassicum* Lutz (1930), *Mesembrioxylon carterii* Tidwell et al. (1998), *M. obscurum* (Knowlton) Medlyn et Tidwell (2002), *Protocupressinoxylon medlynii* Tidwell et al. (1998), *Protopiceoxylon resiniferous* Medlyn et Tidwell (1979), *Xenoxylon moorei* Tidwell et al. (1998), and *X. morrisonense* Medlyn et Tidwell (1975). In 2019, however, *Araucarioxylon hoodii* was established as a new combination, *Agathoxylon hoodii* (Tidwell et Medlyn) Gee et al. (2019), *Xenoxylon moorei* and *X. morrisonense* were declared invalid species, and a new occurrence of *Xenoxylon*, *X. meisteri* (Richmond et al., 2019) was recognized, which decreased the diversity of fossil wood taxa to seven species. This relatively low number of taxa compared to the number of localities where fossil wood has been

* Corresponding author.
E-mail address: s6aoxiee@uni-bonn.de (A. Xie).

found does not necessarily reflect low species diversity of conifer in the Morrison flora, but is more likely due to the poor preservation of anatomical structures in most fossil wood specimens found in the Morrison Formation (Gee et al., 2019).

A fossil log with well-preserved wood was discovered in the Salt Wash Member of the Morrison Formation in Miners Draw of northeast Utah, USA, that was initially grouped with other logs in a nearby locality and assigned to *Agathoxoylon hoodii* (Gee et al., 2019). Here we take a closer look at the log from Miners Draw to describe its wood anatomy in detail and revise the taxonomic determination of the wood, reconstruct the minimum height of the tree based on preserved log diameter, interpret the paleoclimatic signals shown by the growth rings in the wood, and shed new light into the paleobiogeography of Mesozoic *Xenoxylon* in North America. The fossil log is recognized as a new species of *Xenoxylon*, *X. utahense* Xie et Gee, and is now the only valid occurrence of *Xenoxylon* from the Upper Jurassic Morrison Formation in Utah.

2. Geological setting

The fossil log under investigation here (Fig. 1, A, B) was discovered by Mary Beth Bennis and Dale Gray in 2013 as part of a greater reconnaissance for logs in the Morrison Formation in northeast Utah. The fossil log occurs in Miners Draw, Blue Mountain, about 30 km southeast of the city of Vernal, Utah, USA (Fig. 1, C). Exact locality information is on file at the Utah Field House of Natural History State Park Museum in Vernal. Altogether, three specimens of fossil wood were taken from the log during two different collecting campaigns; the last two were collected as field specimen numbers 091119-8 and 091119-9.

The fossil log occurs in the Upper Jurassic Morrison Formation, a widespread formation cropping out across the Colorado Plateau (e.g., Sprinkel et al., 2019; Foster, 2020). Outcrops of the Morrison Formation are common in the northeastern Uinta Basin and the southeastern flank of the Uinta Mountains, for example, in the Rainbow Draw and Miners Draw areas (Sprinkel et al., 2019; Gee et al., 2019). In northeastern Utah, the Morrison Formation consists of four members, namely, the Windy Hill, Tidwell, Salt Wash, and Brushy Basin Members in ascending chronostratigraphic order (Hasiotis, 2004; Sprinkel et al., 2019). Based on lithological and paleontological analysis, the Windy Hill and Tidwell members represent a marine to marginal marine to coastal plain depositional environment (Turner and Peterson, 1999; Sprinkel et al., 2019), while the Salt Wash and Brushy Basin members indicate a fluvial–lacustrine depositional environment (Peterson, 1980; Turner and Peterson, 1999, 2004; Sprinkel et al., 2019).

The stratigraphic section at the fossil log site at Miners Draw was previously measured as part of a larger study on the occurrence of fossil logs in northeastern Utah (Fig. 2) (Sprinkel et al., 2019). The fossil log studied occurs in the light greenish-gray to brownish-gray, silty to very fine-grained sandstone of the Salt Wash Member of the Morrison Formation in Miners Draw. Here, it crops out 3.0 m above the base of the Salt Wash Member and 7.8 m below its top at its contact with the Brushy Basin Member. According to single-crystal $^{40}Ar/^{39}Ar$ laser fusion dating, the Salt Wash Member in the Rainbow Draw area is between 156 and 152 million years old (Trujillo and Kowallis, 2015).

In general, the Morrison Formation is regarded as Upper Jurassic (Litwin et al., 1998; Schudack et al., 1998; Turner and Peterson, 2004; Gee et al., 2019), largely Kimmeridgian (Trujillo and Kowallis, 2015). The fossil flora of the entire Morrison Formation consists of conifers and ginkgophytes, with an understory of ferns, seed ferns, cycads, bennettitaleans, which reflect warm and humid climatic conditions (Tidwell, 1990; Tidwell and Medlyn, 1992; Ash, 1994; Ash and Tidwell, 1998; Gee and Tidwell, 2010; Hotton and Baghai-Riding, 2010; Gee et al., 2019). The major vegetation type of the Morrison Formation is conifer forest (e.g., Gee and Tidwell, 2010; Hotton and Baghai-Riding, 2010; Gee et al., 2019).

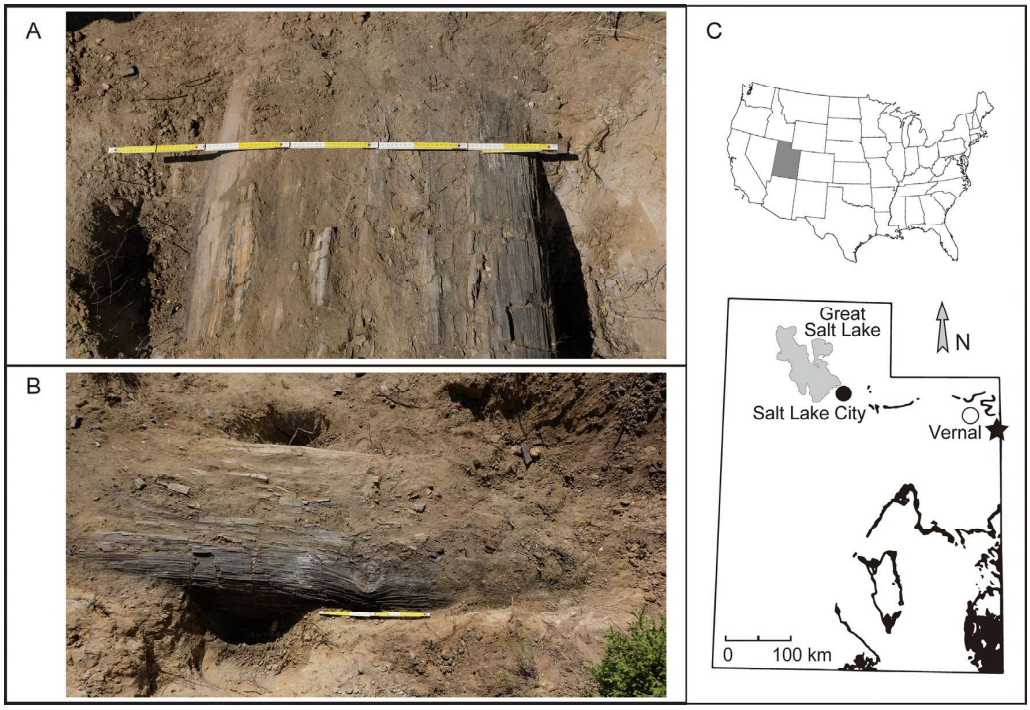

Fig. 1. (A) Fossil log cropping out in Miners Draw. (B) Fossil log showing branch scar (near scale bar). (C) Sketch map of fossil locality (star) for fossil log in Miners Draw near Vernal (open circle), Utah (dark gray state in USA map), USA, superimposed on the outcrops of the Upper Jurassic Morrison Formation. Map of Morrison outcrops courtesy of Kenneth Carpenter.

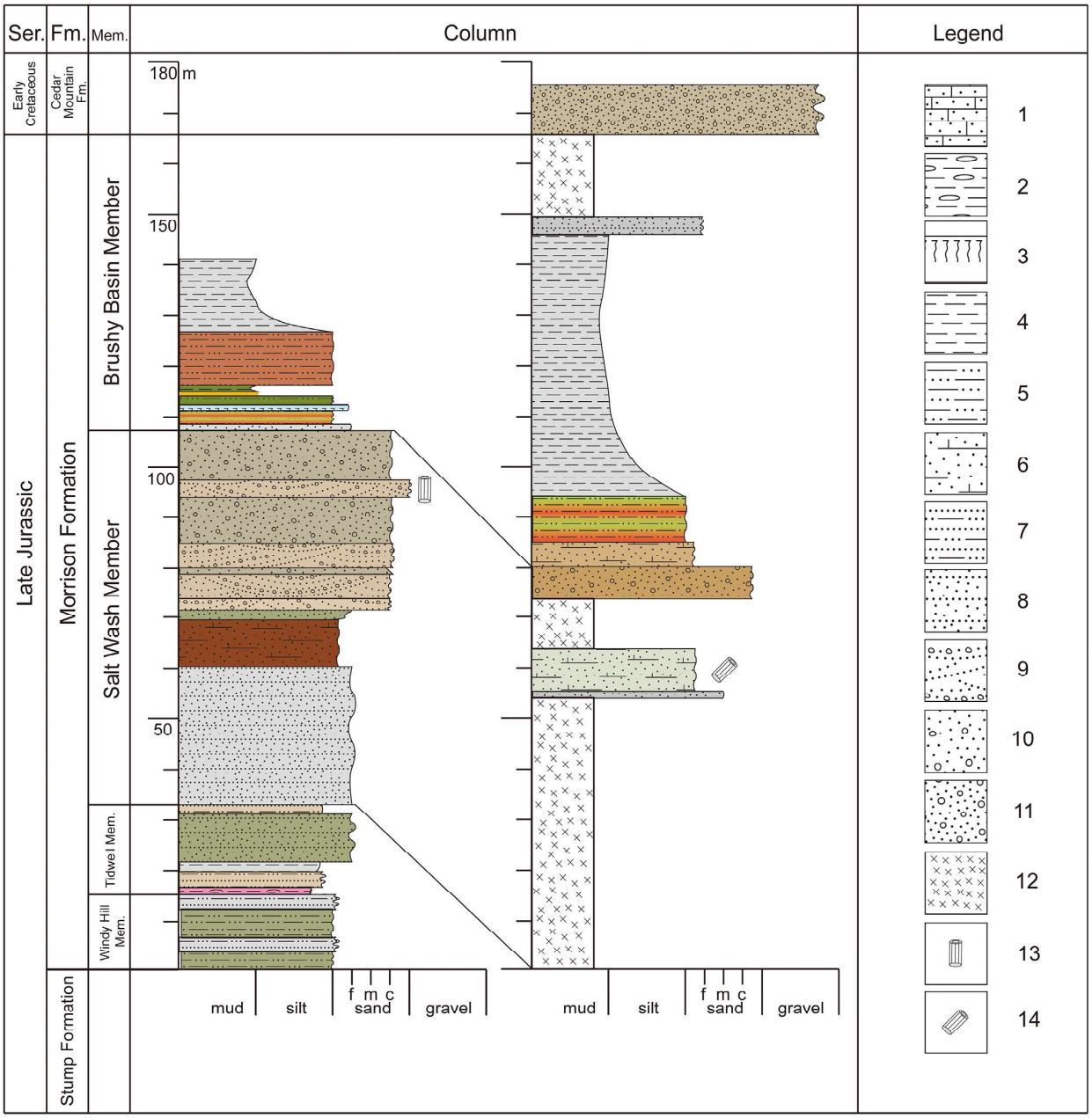

Fig. 2. The stratigraphic column and fossil log horizon of the Upper Jurassic Morrison Formation in the Miners Draw area near Vernal, Utah, USA (modified after Sprinkel et al., 2019). Legend: (1) sandy limestone; (2) pink amygdaloidal chert; (3) calcrete; (4) mudstone; (5) siltstone; (6) silty sandstone; (7) siltstone and sandstone; (8) sandstone; (9) cross-bedded sandstone; (10) conglomeratic sandstone; (11) conglomerate; (12) covered and not measured outcrop; (13) fragmentary fossil wood; (14) fossil log.

3. Materials and methods

Three samples of fossil wood were collected from different parts of the log. For anatomical study, each sample was cut transversely, radially, and tangentially to make standard petrographic thin-sections in the three planes of section for wood identification. Thin-sections were studied and photos were taken with a Leica DM2500 compound photomicroscope. Cellular structures were measured with the integrated measurement software ImageAccess easyLab 7. Wood samples and thin-sections of the holotype are deposited at the Utah Field House of Natural History State Park Museum (FHNHM) under FHPR Catalog Number FHPR 11386. Thin-sections of the three samples are logged into the system at the University of Bonn as BMT-001a, BMT-001b, and BMT-001c.

4. Results

Systematic paleobotany
GYMNOSPERMAE
Family: UNKNOWN

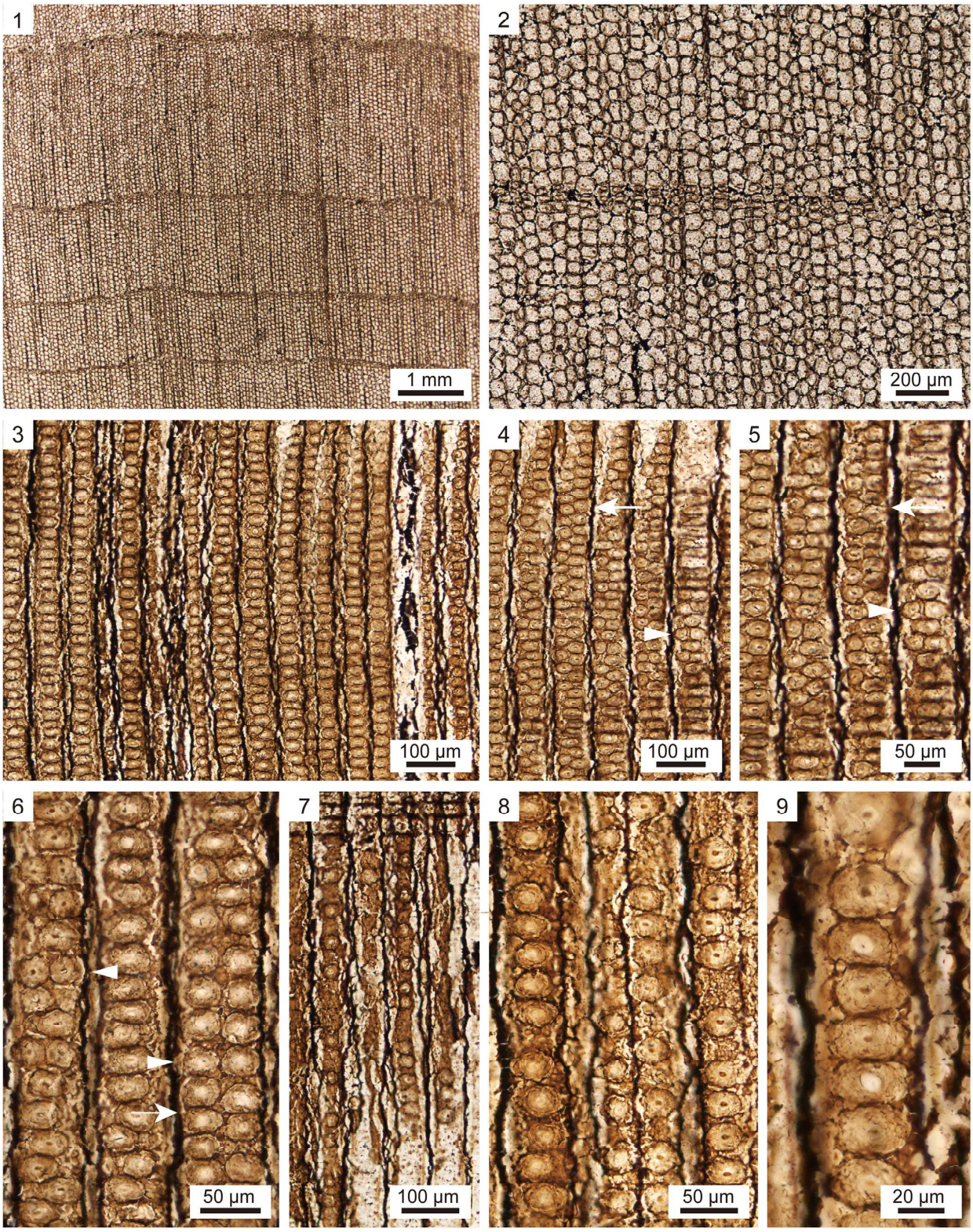
1
1 mm
2
200 µm
3
100 µm
4
100 µm
5
50 µm
6
50 µm
7
100 µm
8
50 µm
9
20 µm

Genus: **Xenoxylon** Gothan, 1905

Species: *Xenoxylon utahense* Xie et Gee sp. nov. (Plates I and II)

Synonymy: *Agathoxylon hoodii* (Tidwell et Medlyn) Gee, Sprinkel, Bennis et Gray, 2019 – FHPR 11747 from site 10 in the Blue Mountain area, thin-section RDW-013 (not figured)

Etymology: The specific epithet *utahense* refers to the fossil locality in the American state of Utah.

Locality: Miners Draw, Blue Mountain, Uintah County, Utah. Exact geographic coordinates for the collecting site are on file at the FHNHM.

Holotype: FHPR Catalog Number FHPR 11386, field specimen number 091119-8, thin-section BMT-001b. Thin-sections BMT-001a and c are isotypes (see below under Remarks).

Material studied: Three specimens arising from different parts of the same fossil log in the field, which were thin-sectioned in the three planes of section at the University of Bonn as BMT-001a to BMT-001c.

Horizon and age: Salt Wash Member, Morrison Formation; Late Jurassic (Kimmeridgian)

Repository: Utah Field House of Natural History State Park Museum in Vernal, Utah, USA, as FHPR catalog number FHPR 11386.

Diagnosis: Secondary xylem with distinct growth rings; transition from earlywood to latewood abrupt. Earlywood wide; latewood narrow, only one to a few cells wide. Radial tracheid pitting typically strongly flattened (xenoxylean radial pitting) and uniseriate; otherwise variable, from uniseriate contiguous to distant, from biseriate alternate to subopposite to opposite. Crossfield pitting fenestriform with normally one pit per crossfield, but up to two pits. Rays uniseriate, or occasionally biseriate; ray height variable, from very low to high (1–34 cells). No tangential tracheid pitting. Resin canals, axial parenchyma, idioblasts, and rims of Sanio absent.

Description: This description is based on secondary xylem from a large, 6 m-long log measuring 90 cm in diameter. Bark and primary tissues such as pith are absent. On the exposed length of the fossil log, there is only one branch scar measuring 15.5 cm × 13.0 cm (Fig. 1, B).

In cross section, distinct growth rings are evident (Plate I, 1, 2). The earlywood contains on average 20 (6–35) rows of tracheids and has a mean width of 1.39 mm (0.40–2.54 mm; n = 11). Earlywood tracheids are large, thin-walled, with an oval to polygonal shape in cross section (Plate I, 2). Lumina of earlywood cells measure on average 54 μm (34–79 μm; n = 123) in tangential diameter. The latewood is composed of narrow bands of tracheids, 1–(2)–6 rows wide, with an average width of 63.40 μm; the latewood tracheids are somewhat thicker-walled than those of the earlywood tracheids (Plate I, 2). The cross-sectional shape of tracheids in the latewood is narrow, from narrowly elliptical to narrowly rectangular (Plate I, 2). The abrupt transition between earlywood and latewood is marked by size differences in radial diameter and wall thickness in the tracheids, type D of Brison et al. (2001) (Plate I, 1, 2). Width ratio between the bands of earlywood and latewood is on average 0.05 (0.02–0.08; n = 11). Tracheid ratio between the bands of earlywood and latewood is on average 0.11 (0.06–0.18; n = 13). Axial parenchyma, resin canals, and idioblasts are absent.

In radial section, tracheids measure on average 63 μm wide (49–85 μm; n = 21). Bordered pits on the radial tracheid walls are mostly uniseriate, but also biseriate; when uniseriate, they are strongly flattened (Plate I, 3–6), locally distant (Plate I, 7). When biseriate, the arrangement of tracheid pits is mixed, sometimes opposite (Plate I, 4–6, arrowhead) and sometimes alternate (Plate I, 4–6, arrow). The bordered pits are generally an oblate to transversely elliptic in outline, with a width of 31 μm and a height of 22 μm (n = 200); at times, they can be greatly flattened with a width of 35 μm and a height of 19 μm (n = 67), giving the appearance of typical xenoxylean radial tracheid pitting sensu Philippe and Bamford (2008). Bordered pits are mostly contiguous, and each of them bears a circular or subround aperture with a diameter up to 10 μm (Plate I, 8–9). Crassulae were not observed. Crossfield pitting is fenestriform (Plate II, 1–3). Each crossfield generally bears a single large pit that occupies nearly the entire crossfield (Plate II, 1, 2); occasionally there are two smaller oopores within one crossfield (Plate II, 3, arrow). Crossfield pits are elongate, elliptical to oblong elliptical in shape (Plate II, 2, 3). The rays consist of parenchymatous cells with thin, smooth horizontal and end walls (Plate II, 2, 3). Axial parenchyma cells, resin canals, idioblasts and rims of Sanio are absent.

In the tangential section, rays are homogenous, parenchymatous, uniseriate or occasionally biseriate (Plate II, 5, 6, arrowhead). The rays are variable in height, ranging from very low to high, 1–34 cells tall; the majority of rays are on average from very low to medium in height, from 3 to 13 cells (Plate II, 4–6; Fig. 3).

Comparison: Since *Xenoxylon* was established by Gothan for fossil wood in 1905, the genus has been widely applied to Mesozoic woods. More than 31 *Xenoxylon* species had been proposed from Laurasia, although more recent work has pared this number down to 11 valid species (Philippe et al., 2013). *Xenoxylon* is a well-defined wood that is typified by strongly flattened, or obround, contiguous radial tracheid pits, a trait called xenoxylean radial tracheid pitting (Müller-Stoll, 1951; Philippe et al., 2009; Philippe et al., 2013). The proportion of the longitudinal to horizontal diameter in any individual radial tracheid pit, called the xenoxylean height/width ratio, should be equal to or less than 0.60 when the pit is contiguous (adjacent and touching) the pits above and below it (Philippe et al., 2013). Each pit is areolated, that is, it has a border around a central opening.

The second distinctive feature of *Xenoxylon* is its fenestriform crossfield pitting (IAWA Committee, 2004; Philippe et al., 2009, 2013), which is exemplified by a single, large, unbordered pore, or in rare cases, two pores. This so-called borderless "oopore" (Philippe and Bamford, 2008) occupies all or nearly all of the space of the crossfield which is typical of *Xenoxylon* wood (e.g., Philippe and Hayes, 2010).

The fossil wood from Upper Jurassic Morrison Formation in Miners Draw described here can be assigned to the genus *Xenoxylon* based on its locally strongly flattened radial tracheid pitting and fenestriform crossfield pitting. To quantify the amount of flattening in individual radial tracheid pits and frequency of these obround pits in the wood, we measured the height to width proportions (longitudinal diameter divided by radial diameter) of 200 radial tracheid pits in the earlywood. In the Miners Draw wood, 30% of all contiguous radial tracheid pits qualify as xenoxylean pitting (Fig. 4), as their height to width proportion is equal to or less than the criterion of 0.6 proposed by Philippe et al. (2013).

In 2013, Philippe and colleagues defined three informal subgeneric morphogroups within *Xenoxylon*, namely, the *latiporosum*, *phyllocladoides*, and *meisteri* groups (Philippe et al., 2013). The *latiporosum* group is defined by exclusively xenoxylean, contiguous, uniseriate radial tracheid pits, along with rare, uniseriate, spaced tangential tracheid pits (Philippe et al., 2013). The *phyllocladoides* group is characterized by mostly uniseriate, locally xenoxylean radial tracheid pits, while the tangential tracheid pits are rare, uniseriate, and spaced

Plate I. *Xenoxylon utahense* Xie et Gee sp. nov. from the Upper Jurassic Morrison Formation in Miners Draw, Blue Mountain, east of Vernal, Utah State, USA; holotype specimen BMT-001b. (1) Cross section, showing growth rings with narrow bands of latewood. (2) Close-up of 1, cross section, showing details of a growth ring. (3) Radial section, showing tracheids with contiguous uniseriate or alternate biseriate bordered pits. (4) Radial section, showing tracheids with contiguous uniseriate or alternate biseriate or opposite biseriate bordered pits. (5) Radial section, showing details of alternate biseriate or opposite biseriate bordered pits. (6) Radial section, showing details of bordered pits, arranged opposite or subopposite or alternate one another. (7) Radial section, showing tracheids with uniseriate distant bordered pits. (8) Radial section, showing details of bordered pits, arranged closely spaced to one another. (9) Radial section, showing details of contiguous and strongly flattened uniseriate bordered pits. Arrows mark alternate biseriate bordered pits, while arrowheads point to opposite biseriate bordered pits.

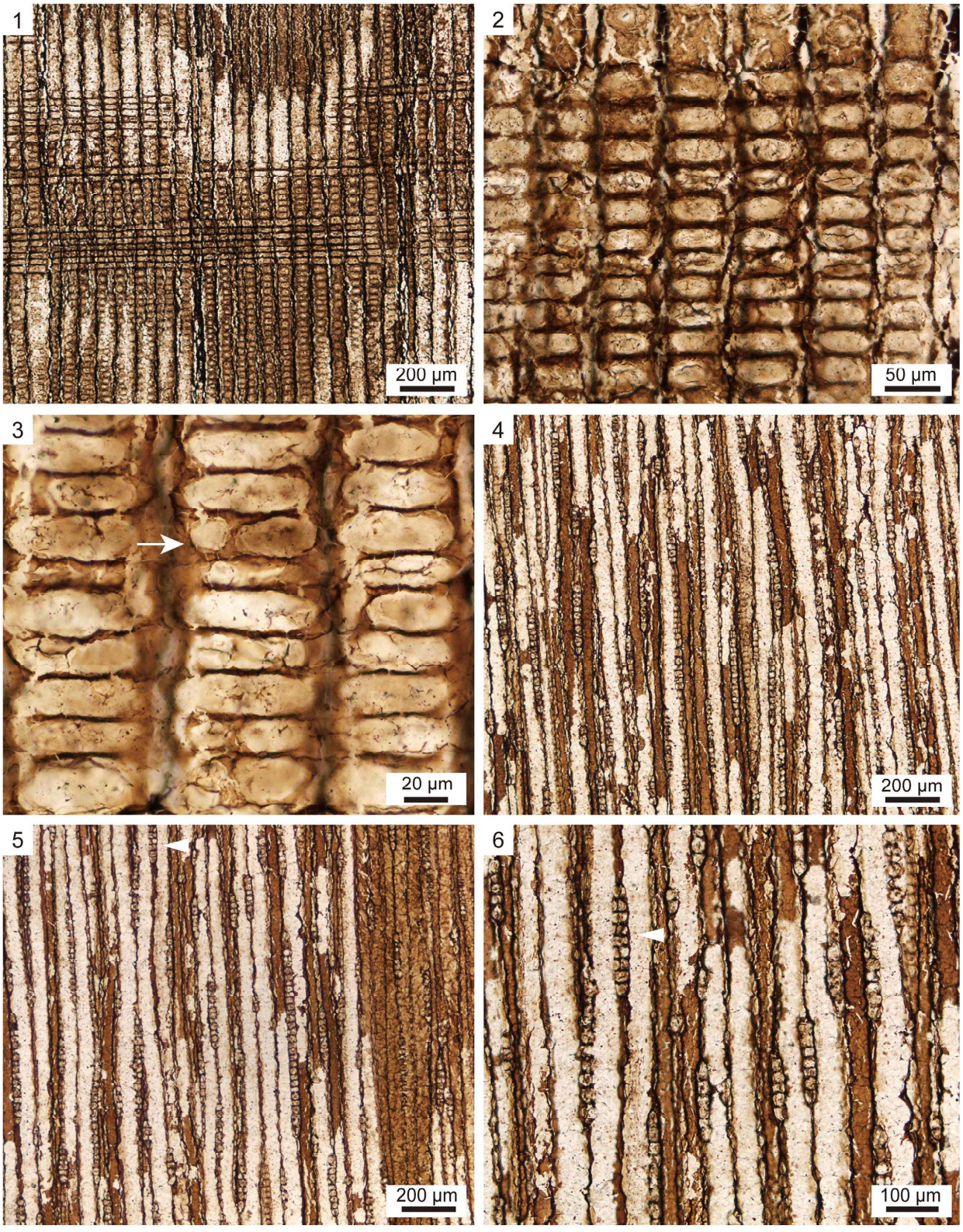
1
200 µm
2
50 µm
3
20 µm
4
200 µm
5
200 µm
6
100 µm

(Philippe et al., 2013). The *meisteri* group is described by generally xenoxylean, uniseriate radial tracheid pits, but locally interrupted; when biseriate, the pits are alternate or opposite, spaced or contiguous. The tangential tracheid pits in the *meisteri* type range from occasional to common, commonly biseriate or triseriate in a crowded, alternate arrangement (Philippe et al., 2013).

In the Miners Draw wood, radial tracheid pits are contiguous and flattened. About 30% of the radial tracheid pitting consists of this type of xenoxylean pitting. Otherwise, the arrangement of radial tracheid pitting is mixed, mostly uniseriate contiguous or biseriate alternate, but also at times, uniseriate spaced, and occasionally biseriate opposite or subopposite. Striking is the lack of tangential tracheid pitting. Given this suite of characters in the Miners Draw wood, it falls into the *phyllocladoides* group put forth by Philippe et al. (2013).

Within the *phyllocladoides* group, only four species of *Xenoxylon* have been described from all parts of the world that exhibit a combination of locally xenoxylean radial tracheid pitting and mixed type pitting, namely, *X. hopeiense* Chang, *X. jakutiense* Shilkina, *X. phyllocladoides* Gothan, and *X. huttonianum* (Witham) Philippe et Hayes (Gothan, 1905; Chang, 1929; Shilkina and Khudaiberdyev, 1971; Philippe and Hayes, 2010). *X. hopeiense* is marked by generally uniseriate radial tracheid pitting, scattered xylem parenchyma, rims of Sanio, and tall rays (1–65 cells high) (Chang, 1929; Zheng et al., 2008), whereas the Miners Draw specimens lack xylem parenchyma and rims of Sanio. *X. jakutiense* is characterized by consistently uniseriate radial tracheid pitting and rims of Sanio (Shilkina and Khudaiberdyev, 1971; Philippe et al., 2013), however, the Miners Draw wood lack rims of Sanio. *X. phyllocladoides* bears the characters typical of *phyllocladoides* type, that is, local radial tracheid xenoxylean pitting, and otherwise a mixed type of pitting; mostly uniseriate radial tracheid pitting; and rare, uniseriate, spaced tangential tracheid pitting (Gothan, 1905; Philippe et al., 2013), which are also observed in the Miners Draw specimens. However, it differs from our wood in having some crossfields with phyllocladoid or podocarpoid oopores (Philippe and Bamford, 2008).

Our specimens are more akin to *X. huttonianum* in its mixed type radial tracheid pitting, local radial tracheid xenoxylean pitting, and fenestriform crossfield pitting. The species *X. huttonianum* was established by Philippe and Hayes (2010) when they reappraised the type material of *Peuce huttoniana* Witham. However, the Miners Draw wood differs from *X. huttonianum* by having a relatively higher ray height and occasionally bearing two oopores per crossfield, while *X. huttonianum* has only one large window-like oopore that occupies entire crossfield.

Within each the *phyllocladoides* group, ray height, radial tracheid pit size, occurrence of axial parenchyma, and the occurrence of tangential tracheid pitting are features used to distinguish *Xenoxylon* species from one another (Philippe et al., 2013). Because our comparison shows that our wood differs from the four species in *phyllocladoides* group in least two anatomical characteristics, we recognize here the *Xenoxylon* wood from Miners Draw as a new species, *X. utahense* sp. nov. Xie et Gee.

Remarks: Due to mislabeling by a lab technician, the wood thin-section of the fossil log from Miners Draw, Blue Mountain, that was first studied (Gee et al., 2019) was misidentified as *Agathoxylon hoodii* (see synonymy). The collection of two new specimens in September 2019 and study of their thin-sections have since clarified the situation. The misidentified thin-section, originally labeled RDW-013, is now given a new specimen number, BMT-001a, and recognized as an isotype. Thin-sections of the new specimens collected in September 2019 are designated BMT-001b (holotype) and BMT-001c (a second isotype).

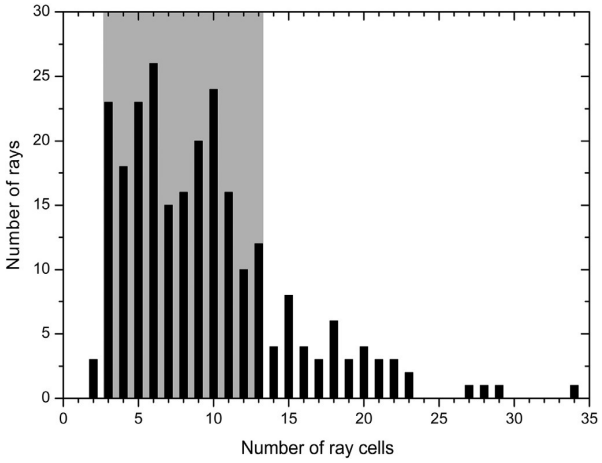

Fig. 3. Histogram showing ray cell height in 250 rays as observed in a tangential section of *Xenoxylon utahense* Xie et Gee sp. nov. (BMT-001b) from the Upper Jurassic Morrison Formation in Miners Draw, Blue Mountain, near Vernal, Utah, USA. Shaded area shows that the majority of rays are very low to medium in height, from 3 to 13 cells high.

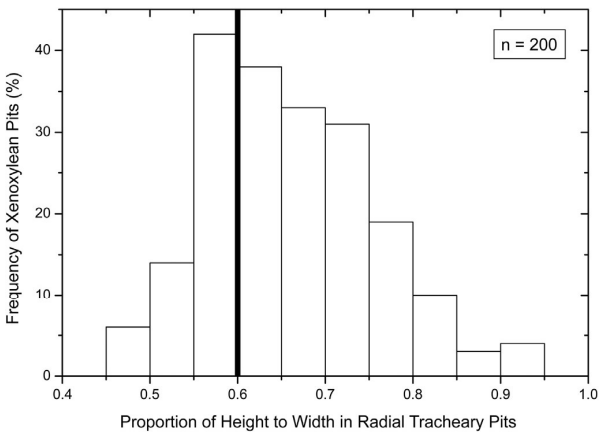

Fig. 4. Histogram showing height to width proportions of contiguous radial tracheid pits in *Xenoxylon utahense* Xie et Gee sp. nov. from the Upper Jurassic Morrison Formation in Miners Draw, Blue Mountain, near Vernal, Utah, USA. Measurements were made on 200 radial tracheid pits; the counts are divided up into size classes on the x-axis and shown as frequency on the y-axis. Area to the left of thick solid line marks a height to width proportion equal to or less than 0.6, which is typifies the xenoxylean shape in radial tracheid pits (cf. Philippe et al., 2013).

4.1. Growth ring characteristics of Xenoxylon utahense *sp. nov*

As mentioned earlier, there are distinct growth rings in *X. utahense* sp. nov. (Plate I, 1; Fig. 5). On average, the growth ring consists of 20 (7–41) rows of tracheids and has a mean width of 1.46 mm (0.43–2.68 mm). The earlywood contains on average 20 (6–35) rows of tracheids and has a mean width of 1.39 mm (0.40–2.54 mm), whereas the latewood is composed of narrow bands of tracheids, 1–(2)–6 rows wide, with an average width of 63.40 μm. The transition between earlywood and latewood is abrupt. Width ratio between the bands of earlywood and latewood is on average 0.05 (0.02–0.08). The

Plate II. *Xenoxylon utahense* Xie et Gee sp. nov. from the Upper Jurassic Morrison Formation in Miners Draw, Blue Mountain, east of Vernal, Utah State, USA; holotype specimen BMT-001b. (1) Radial section, showing fenestriform crossfield pits. (2) Close-up of 1, radial section, showing detail of fenestriform crossfield pits in which each crossfield bears a single large pit. (3) Radial section, with arrow showing two oopores in one crossfield. (4) Tangential section, showing uniseriate rays. (5) Tangential section, showing biseriate rays (arrowhead). (6) Tangential section, showing detail of biseriate rays (arrowhead).

Growth ring number	Growth ring width (mm)	Annual sensitivity	Mean sensitivity
16	0.825	0.71	0.53
15	1.732	0.27	
14	1.318	0.31	
13	0.966	0.77	
12	2.181	0.21	
11	2.685	0.47	
10	1.657	0.39	
9	1.115	0.24	
8	1.425	0.39	
7	0.962	0.67	
6	0.479	0.12	
5	0.424	0.90	
4	1.114	0.91	
3	0.419	1.33	
2	2.094	0.23	
1	1.655		

Fig. 5. Measurements of growth ring width, annual and mean sensitivity of *Xenoxylon utahense* sp. nov., spec. BMT-001b, from the Upper Jurassic Morrison Formation in Miners Draw, Utah, USA. The line between rings 15 and 16 is merely dark organic material, not a false ring. Scale bar = 2 mm.

tracheid ratio between the bands of earlywood and latewood is on average 0.11 (0.06–0.18).

4.2. *Mean sensitivity of* Xenoxylon utahense *sp. nov*

To document interannual climatic variation, we carried out statistical analysis for mean sensitivity on 16 growth rings of Xenoxylon utahense in spec. no. BMT-001b using the method proposed by Fritts (1976). The results reveal that the annual sensitivity varies from 0.12–1.33, and the mean sensitivity is 0.53 (Fig. 5). In general, a value of mean sensitivity that is less than 0.3 indicates stable growing conditions for the tree year after year ("complacent tree-ring growth"), while a value greater than 0.3 illustrates variable growing conditions for the trees ("sensitive tree-ring growth") (Fritts, 1976).

4.3. *Reconstruction of minimum tree height of* Xenoxylon utahense *sp. nov*

As a result of an ongoing analysis of living conifers (Xie and Gee, unpubl. data), a formula has been developed for the extrapolation of minimum tree height from preserved diameter in fossil logs. Drawn from the best-fit curves of trunk diameter at breast height vs. total tree height data for four taxa of living conifers, the formula for conifers of unknown familial affinity can be given as:

$$H = 0.48\,(E/w)^{1/3}\,r^{2/3}$$

where E = Young's modulus (a measure of the stiffness of solid wood), w = specific weight of conifer wood, related to the density of conifer wood and obtained by equation $w = \rho\, g$ (g, standard gravity, approximately equal to 9.8 m/s^2), and r = radius of the fossil log. $E/w = 2.2 \times 10^6$ m is the value of a generalized conifer when the botanical affinity of a conifer is unknown.

The preserved diameter of the fossil log at the Miners Draw area is 90 cm. Hence, this results in a reconstructed minimum height of the *Xenoxylon* tree at Miners Draw of about 40 m since *Xenoxylon* has conifer-like wood.

5. Discussion

Although the fossil log described from Miners Draw is only a single occurrence, it represents the only valid systematic report of the fossil wood *Xenoxylon* from the Upper Jurassic Morrison Formation in Utah. Previously, Medlyn and Tidwell (1975) and Tidwell et al. (1998) had described two new species of *Xenoxylon* from Morrison Formation of Utah, *X. morrisonense* and *X. moorei*, respectively, but these taxa have been determined as invalid by Richmond et al. (2019). Thus, the recognition of a valid occurrence of *Xenoxylon*, which is described here as *X. utahense* sp.

nov. from Miners Draw, contributes to the deeper understanding of Upper Jurassic gymnosperm diversity in Utah as well as to the composition of the forest vegetation in the Morrison Formation.

In the Northern Hemisphere, the genus *Xenoxylon* Gothan, 1905 is an integral member of the Mesozoic wood flora (Philippe et al., 2013). While the systematic affinity of the genus is still unclear, it is considered to be a likely member of Coniferales (Marynowski et al., 2008) and has been linked to various coniferous genera and families, such as *Podozamites*, *Baiera*, *Sciadopitys*, Podocarpaceae, and Protopinaceae (Nathorst, 1897; Jarmolenko, 1933; Arnold, 1952; Bailey, 1953; Shilkina and Khudaiberdyev, 1971; Youssef, 2002). However, the most credible hypothesis for the taxonomic affinity of *Xenoxylon* is the extinct coniferous family Miroviaceae based on the similarity in crossfield pitting of *Xenoxylon* and *Mirovia eximia* (Miroviaceae). The stratigraphic range of Miroviaceae also agrees well with that of *Xenoxylon* (Nosova and Kiritchkova, 2008; Philippe et al., 2013). Up to now, there is no evidence for linking fossil leaves, cones, or pollen to *Xenoxylon* wood.

5.1. Tree and forest height

The preserved length of 6 m and diameter of 90 cm of the fossil log at Miners Draw site, as well as its calculated height of at least 40 m, confirms the presence of tall forest trees in the Morrison Formation. Large fossil trunks of a similarly large size ranging from 71 to 127 cm in preserved diameter have been found at nearby Rainbow Draw, NE Utah (Gee et al., 2019), which is located about 30 km northwest of the Miners Draw. Based on the formula proposed by Mosbrugger et al. (1994) to estimate ancient tree height, Gee et al. (2019) reconstructed the minimum heights of Rainbow Draw trees as 19–28 m (Gee et al., 2019; Sprinkel et al., 2019). However, the results of an ongoing analysis of living conifers (Xie and Gee, unpubl. data) indicates that the reconstructed heights of Rainbow Draw trees may have been underestimated by approximately one-third and that the greater reconstructed heights of Rainbow Draw trees may have instead reached greater heights up to 31–46 m. It should be noted, however, that the Rainbow Draw wood flora is different from the one at Miners Draw, because up to now, the Upper Jurassic forest at Rainbow Draw consists exclusively of a monospecific wood flora of the araucariaceaeous tree *Agathoxylon hoodii* (Gee et al., 2019).

In general, fossil logs or trunks complete with their bark layer are rarely preserved in the deep time, because the bark is easily detached from the central cylinder of secondary xylem after the tree has died or fallen (Staccioli et al., 1998). Bark thickness is strongly positively correlated with diameter at breast height (DBH) (Pinard and Huffman, 1997; Paine et al., 2010; Zeibig-Kichas et al., 2016). Although the ratio of bark thickness to DBH varies widely among families, an average ratio of 5% may be generally applied when estimating ancient tree heights (Pinard and Huffman, 1997; Zeibig-Kichas et al., 2016). Thus, the DBH of 1 m in living conifers would be roughly equivalent in size to fossil trunks or logs lacking bark that have a preserved diameter of 90 cm. Mature trees of *Thuja plicata* (western redcedar, Cupressaceae), a common species in the NW USA, reach an average height of 40 m (25–52 m) when DBH equals 1 m (VanderSchaaf, 2013). In northern California, the native coastal redwood *Sequoia sempervirens* (Cupressaceae) generally obtains tree heights of about 33–70 m, averaging about 50 m, when DBH equals 1 m (Sillett et al., 2019; Earle, 2020; Vaden, 2020). In the subtropical forests of southern Brazil, the native tree of *Araucaria angustifolia* generally attains heights of about 18–32 m, averaging about 28 m, when DBH reaches 1 m. Giant individuals of *A. angustifolia* (Araucariaceae) reach a maximum height of about 45 m when DBH equals 2 m (Scipioni et al., 2019). In the case of *Araucaria* in New Guinea, the native species of *A. cunninghamii* and *A. hunsteinii* in primeval forests reach heights of about 60 m when DBH is 1 m (Gray, 1975). Thus, the reconstructed minimum tree height of 40 m of the Miners Draw log demonstrates that the ancient tree has a size similar to many living conifer trees when fully grown and that the ancient tree at Miners Draw was a mature tree, presumably one individual within a larger forest community of many more trees of similar size.

5.2. Paleobiodiversity in the West–Central Morrison Formation

If the Mygatt-Moore Quarry in Colorado at the eastern boundary of Utah is included, there are now four taxa of conifer-like woods in the Morrison Formation of Utah: *Agathoxylon hoodii* (Tidwell et Medlyn) Gee, Sprinkel, Bennis et Gray 2019, *Protocupressinoxylon medlynii* Tidwell, Britt et Ash 1998, *Mesembrioxylon carterii* Tidwell, Britt et Ash 1998, and *Xenoxylon utahense* sp. nov. Xie et Gee. When identified to family level, the first two conifer taxa represent two families, the Araucariaceae and Cupressaceae, while the last two taxa pertain to unknown gymnosperm families. These four fossil taxa show a variety of trees formed a vegetation of mixed forest during the Late Jurassic in what is now the state of Utah.

A diversity of conifers growing throughout the Morrison Formation in the Upper Jurassic is also supported by the occurrence of conifer seed cones in Utah and Wyoming (Gee and Tidwell, 2010; Gee et al., 2014). These fossil seed cones pertain to at least three conifer families, the Araucariaceae, Pinaceae, and extinct family Cheirolepidiaceae. An additional two fossil seed cones figured by Gee et al. (2014) could not be referred to a family based on the two single-species specimens known so far, but they clearly represent two different morphotypes. Another line of evidence supporting a diversity of conifers in the Upper Jurassic Morrison Formation are the fossil leaves and shoots that have been found at more than 10 fossil localities in Utah, including *Cupressinocladus*, *Elatides*, *Brachyphyllum*, *Behuninia*, and *Steinerocaulis* (Ash and Tidwell, 1998; Gee and Tidwell, 2010), which represent at least two families of conifers, the Cupressaceae and Araucariaceae.

Palynological studies also play an important role in demonstrating that a variety of conifers grew throughout the Morrison Formation (Hotton and Baghai-Riding, 2010). The studies demonstrate that the conifer pollen is referable to the Araucariaceae, Pinaceae, Podocarpaceae, and Cheirolepidiaceae (Hotton and Baghai-Riding, 2010). Cheirolepidiaceous pollen is less abundant in the northern parts of the Morrison Formation and more abundant in the southern parts, forming a general north–south gradient (Hotton and Baghai-Riding, 2010), which indicates that the conifer flora may have been varied geographically throughout the Morrison Formation in accordance with climatic differences.

Although abundant evidence supporting a diversity of conifers growing throughout the Morrison Formation in the Upper Jurassic, it is not possible to determine if these species lived in the same forests at the same time, owing to the lack of finer stratigraphic resolution in the Salt Wash and Brushy Basin Members (Gee et al., 2014). However, wood, cone, and pollen data suggest that conifers dominated the vegetation of the Morrison Formation and formed a framework of widespread forests during Late Jurassic times (Hotton and Baghai-Riding, 2010; Gee et al., 2014).

5.3. Paleobiogeography of Mesozoic Xenoxylon in North America

With the discovery of our new species from Miners Draw, Utah, the occurrence of *X. utahense* sp. nov. extends the paleobiogeographic range of *Xenoxylon* southward in North America. From the Jurassic to the Lower Cretaceous, *Xenoxylon* was widespread in the Northern Hemisphere with a circumpolar distribution (Philippe and Thévenard, 1996; Philippe et al., 2009). The first report of *Xenoxylon* in North America was made by Arnold in 1952, namely, *X. latiporosum* from the Nanushuk Formation (Albian–Cenomanian) in northern Alaska (Arnold, 1952; Mull et al., 2003). Since then, Philippe et al. (2013) remarked that the specimens described by Arnold (1952) may pertain to *X. japonicum*, while Richmond et al. (2019) suggested that it should be assigned to *X. meisteri*.

For many years, the North American occurrences of *Xenoxylon* were known only from the very high latitudes in what is today the Polar Circle (Fig. 6), before *X. meisteri* was described from the Upper Jurassic Morrison Formation of central Montana (Philippe and Thévenard, 1996; Richmond et al., 2019). In their recent review of *Xenoxylon* species, Richmond et al. (2019) posit that there are only five valid species of *Xenoxylon* in North America. They show that nearly all of the valid fossil records of *Xenoxylon* in North America occur in a broad zone in what is currently at very high latitudes, from Alaska in the west, to Sverdrup Basin in the Arctic in the center, and Jameson Land in Greenland in the east. In contrast, *Xenoxylon* species are less common south of what is today the Canadian–USA border and are restricted to only two localities: one in Montana (Richmond et al., 2019) and now the second one in Utah described here in our study.

The paleobiogeographic distribution of *Xenoxylon* in North America varied during the Mesozoic (Fig. 6). For the Lower Jurassic, one species is recorded, that is, *X. phyllocladoides* in Jameson Land of eastern Greenland (Oh et al., 2015). For the Middle Jurassic, the same species occurs at the same fossil locality, namely, *X. phyllocladoides* from Jameson Land of eastern Greenland (Oh et al., 2015). For the Upper Jurassic, *Xenoxylon* reaches its maximum diversity in the Mesozoic with three species, namely, *X. phyllocladoides* from Jameson Land of eastern Greenland (Oh et al., 2015), and the other two species, *X. meisteri* and *X. utahense* sp. nov. from Montana and Utah, USA, respectively. For the Lower Cretaceous, one species, *X. hopeiense* is recorded from the Sverdrup Basin of the Arctic, which was originally described as *Dacrydioxylon* (Selmeier and Grosser, 2011; Philippe et al., 2013). For the Upper Cretaceous, one species, *X. latiporosum* is documented from northern Alaska (Arnold, 1952; Parrish and Spicer, 1988; Spicer and Parrish, 1990). To date, the most common subgeneric morphogroup occurring in North America is the *phyllocladoides* group, which includes *X. phyllocladoides*, *X. hopeiense*, and *X. utahense* sp. nov.

In regard to paleolatitudes, the occurrence of *Xenoxylon utahense* sp. nov. in Utah, extends the biogeographic range of *Xenoxylon* further to the southwest by ca. 800 km. During Late Jurassic times, the locality with *X. meisteri* in what is now Montana was located at a paleolatitude between 49° and 50° N (Richmond et al., 2019), whereas the paleolatitude of what is today Miners Draw was at a more southerly location at about 36° N (cf., van Hinsbergen et al., 2015). Hence, *X. utahense* sp. nov. now represents the southernmost occurrence of the genus in North America in the Mesozoic, as well as also offers new evidence that *Xenoxylon* trees were not only restricted to a circumpolar zone, but also grew in more southerly areas.

5.4. Paleoclimatic implications of Xenoxoylon utahense *sp. nov. for the Morrison Formation*

In all trees, growth rings reflect the climate under which the tree grew (Fritts, 1962, 1966; Creber and Chaloner, 1984; Tidwell et al., 1998; Brison et al., 2001). Hence, the growth rings of the well-preserved wood from Miners Draw represent an excellent data archive for the paleoclimate that the *Xenoxylon* utahense nov. sp. tree grew under. To aid in interpreting growth rings in fossil wood, Creber and Chaloner (1984) suggested six growth ring types to characterize different relationships between earlywood and latewood, illustrated by Brison and others in 2001. The growth rings of Miners Draw wood are very similar to the growth rings type D in that the growth rings are distinct with abundant, well-formed earlywood and a thin band of latewood, usually 1–2 cells wide. The true growth rings referable to type D of Brison et al. (2001) in *X. utahense* sp. nov. suggest that growth conditions were slightly variable in regard to mild seasonality during the entire year, namely, that mild summer–winter changes or slight moisture cyclicity affected the growth of the Morrison trees.

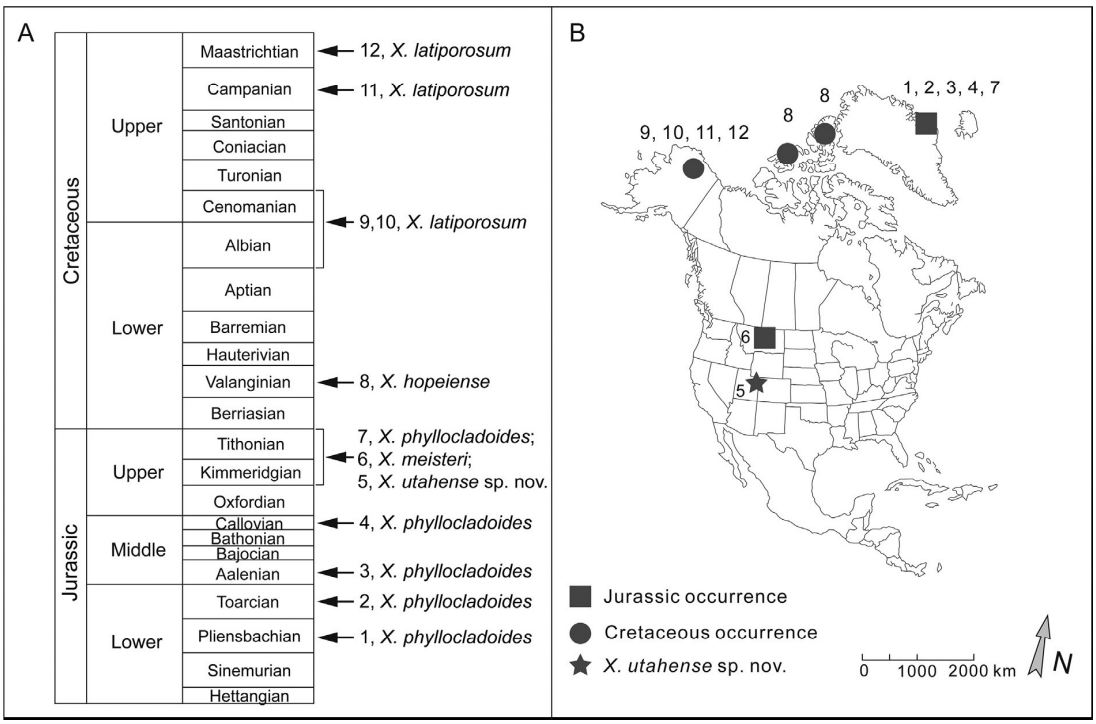

Fig. 6. (A) Temporal distribution of *Xenoxylon* occurrences in the Mesozoic of North America. (B) Geographic distribution of *Xenoxylon* occurrences in North America (modified after Richmond et al., 2019).

In general, the percentage of latewood in a growth ring reflects climatic seasonality, that is, the suitability of growth conditions toward the end of the growing season (cf. Creber and Chaloner, 1984; Parrish and Spicer, 1988; Keller and Hendrix, 1997). In the Miners Draw *Xenoxylon* wood, the narrow latewood zones, which are only at very most six cells wide, indicate that the tree enjoyed a long, optimal, main growing season, then underwent slower growth for a short time, similar to the living conifer *Callitris intratropica* native to the seasonal tropical forest in northern Australia (Baker et al., 2008).

Another line of evidence supporting mild seasonality during the deposition of the Late Jurassic Morrison Formation are the other fossil woods from the Morrison Formation in Utah and western Colorado. For example, the invalid fossil wood species *X. morrisonense* from Clay Point of southeastern Utah has either indistinct growth rings or growth rings with a very narrow band of latewood that is only 2–3 rows wide (Medlyn and Tidwell, 1975). The fossil wood of *Protopiceoxylon resiniferous*, occurring at the same locality as *X. morrisonense*, has distinct growth rings with a gradual transition from earlywood to latewood, which documents that this tree experienced seasonal cyclicity (Medlyn and Tidwell, 1979). The fossil flora from Mygatt-Moore Quarry of western Colorado yielded fossil woods exhibiting a conflicting spectrum of growth ring patterns (Tidwell et al., 1998). For example, although *Protocupressinoxylon medlynii* has distinct growth rings with an abrupt or gradual transition from earlywood to latewood, *Mesembrioxylon carterii* has either indistinct growth rings or no growth rings and the invalid fossil wood species *Xenoxylon moorei* has indistinct growth rings or distinct growth rings with an abrupt transition from earlywood to latewood (Tidwell et al., 1998). To reconcile the conflicting data, Tidwell et al. (1998) suggested that the fossil woods found in the same quarry probably did not grow in the same environment, but that the woods with growth rings had been transported from an upland environment with a more seasonal climate, while the woods lacking growth rings may have been components of a lowland flora.

It should be noted that some fossil woods from the Morrison Formation in Utah show little to no seasonality. *Agathoxylon hoodii* from the eastern flank of Mt. Ellen in southcentral Utah as well as from Rainbow Draw in northeastern Utah have either indistinct growth rings, or discontinuous growth rings with an abrupt or indistinct transition from earlywood to latewood. Gee et al. (2019) interpreted these unusual growth ring patterns as likely caused by biological and not environmental factors, and that the well-formed wood lacking true growth rings indicates an equable climate, similar to rainforest conifers in a warm, humid climate with little or no seasonal instability, such as the living araucarian trees growing in Australia (Gee et al., 2019).

Mean sensitivity (MS) is a method widely used to measure the variability between growth ring widths year by year, indicating environmental fluctuation (cf. Jefferson, 1982; Francis, 1984, 1986; Morgans et al., 1999; Falcon-Lang et al., 2001, 2004). In extant conifers, the mean sensitivity is generally higher in cool-to-cold, dry climates (MS, 0.15–0.75) and lower in warm, wet climatic conditions (MS, 0.15–0.3) (Falcon-Lang, 2005). Based on the mean sensitivity of living conifers collected from 554 sites worldwide, Falcon-Lang (2005) found that the conifers growing in warm, humid climatic conditions in the southeastern United States and on the North Island of New Zealand have a mean sensitivity value varying from 0.35 to 0.6, especially when they grow in flooding-disturbed, streamside habitats (Falcon-Lang, 2005). Growth ring analysis on the fossil wood from Miners Draw shows that *X. utahense* sp. nov. had a mean sensitivity of 0.53, which suggests that it grew in a warm, humid climate, when compared to mean sensitivity values of the global living conifer flora. A warm and humid climate is also consistent with the Late Jurassic paleoclimate interpreted from the abundant fossil plant records in the Morrison Formation (Tidwell, 1990; Tidwell and Medlyn, 1992; Ash, 1994; Ash and Tidwell, 1998; Gee and Tidwell, 2010; Hotton and Baghai-Riding, 2010; Gee et al., 2019).

Up to now, the presence of the genus *Xenoxylon* in the fossil record has been accepted as an indicator of cool and/or wet climate (Philippe and Thévenard, 1996; Philippe et al., 2009; Amiot et al., 2011; Oh et al., 2015). Thus, the occurrence of *X. utahense* sp. nov. in the warm and humid paleoclimate in the Upper Jurassic Morrison Formation of Utah, suggests that *X. utahense* offers a different climate signal compared to the previously described species of *Xenoxylon* (Philippe and Thévenard, 1996).

6. Conclusions

A new species of the fossil wood genus *Xenoxylon* is described as *Xenoxylon utahense* Xie et Gee sp. nov. from Miners Draw near Vernal in northeastern Utah as the first unequivocal occurrence of this genus in this state. This new species of fossil wood is characterized by xenoxylean radial tracheid pitting and fenestriform crossfield pitting. The fossil log itself measures 6 m long and 90 cm in diameter. Based on preserved diameter–height calculations, the fossil log of *Xenoxylon utahense* sp. nov. represents a tall, mature tree that attained at least 90 cm in diameter and 40 m in height. It presumably represents one individual within a larger forest community with many more trees of similar size. Growth ring analysis of the *X. utahense* wood indicates that the local paleoclimate experienced extremely light seasonality consisting of a long, optimal, main growth season and a shorter, mild season with slower growth. A Late Jurassic paleoclimate of warm and humid conditions with little to no seasonality in Utah is consistent with other evidence of fossil conifer foliage and seed cones in the Morrison Formation and the growth rings of living conifers. *Xenoxylon utahense* Xie et Gee sp. nov. from Miners Draw near Vernal in northeast Utah now represents the southernmost occurrence of the genus in North America in the Upper Jurassic.

Declaration of Competing Interest

The authors declare that they have no known competing financial interests or personal relationships that they could have appeared to influence the work reported in this paper.

Acknowledgments

We thank Yongdong Wang, Nanjing Institute of Geology and Palaeontology, Chinese Academy of Sciences for help in the field, Steven Sroka, Utah Field House of Natural History State Park Museum for logistical support, as well as Victoria Egerton, The University of Manchester, and an anonymous reviewer for helpful suggestions. Financial support from the China Scholarship Council for the doctoral studies of AX (CSC no. 201804910527) is greatly appreciated. Financial support for fieldwork in Utah from Open Funding grant no. 193101 from the State Key Laboratory of Palaeobiology and Stratigraphy (Nanjing Institute of Geology and Palaeontology, CAS) State Grant to CTG is also gratefully acknowledged.

References

Amiot, R., Wang, X., Zhou, Z.H., Wang, X.L., Buffetaut, E., Lécuyer, C., Ding, Z.L., Fluteau, F., Hibino, T., Kusuhashi, N., Mo, J.Y., Suteethorn, V., Wang, Y.Q., Xu, X., Zhang, F.S., 2011. Oxygen isotopes of East Asian dinosaurs reveal exceptionally cold Early Cretaceous climates. Proc. Natl. Acad. Sci. U. S. A. 108, 5179–5183.

Arnold, C.A., 1952. Silicified plant remains from the Mesozoic and Tertiary of western North America. II. Some fossil woods from northern Alaska. Pap. Mich. Acad. Sci. 28, 9–20.

Ash, S., 1994. First occurrence of *Czekanowskia* (Gymnospermae, Czekanowskiales) in the United States. Rev. Palaeobot. Palynol. 81 (2–4), 129–140.

Ash, S.R., Tidwell, W.D., 1998. Plant megafossils from the Brushy Basin Member of the Morrison Formation near Montezuma Creek Trading Post, southeastern Utah. Mod. Geol. 22, 321–339.

Bailey, I.W., 1953. Evolution of the tracheary tissue of land plants. Am. J. Bot. 40, 4–8.

Baker, P.J., Palmer, J.G., D'Arrigo, R., 2008. The dendrochronology of *Callitris intratropica* in northern Australia: annual ring structure, chronology development and climate correlations. Aust. J. Bot. 56 (4), 311–320.

Brison, A.L., Philippe, M., Thévenard, F., 2001. Are Mesozoic wood growth rings climate induced? Paleobiology 27, 531–538.

Chang, C.Y., 1929. A new *Xenoxylon* from North China. Bull. Geol. Soc. China 8, 243–251.

Chure, D.J., Litwin, R., Hasiotis, S.T., Evanoff, E., Carpenter, K., 2006. The fauna and flora of the Morrison Formation: 2006. In: Foster, J.R., Lucas, S.G. (Eds.), Paleontology and Geology of the Upper Jurassic Morrison Formation. N. Mex. Mus. Nat. Hist. Sci. Bull vol. 36, pp. 233–249.

Creber, G.T., Chaloner, W.G., 1984. Influence of environmental factors on the wood structure of living and fossil trees. Bot. Rev. 50, 357–448.

Demko, T.M., Parrish, J.T., 1998. Paleoclimatic setting of the Upper Jurassic Morrison Formation. Mod. Geol. 22, 283–296.

Demko, T.M., Currie, B.S., Nicoll, K.A., 2004. Regional paleoclimatic and stratigraphic implications of paleosols and fluvial/overbank architecture in the Morrison Formation (Upper Jurassic), Western Interior, USA. Sediment. Geol. 167 (3–4), 115–135.

Earle, C.J., 2020. The Gymnosperm Database. Available online at https://www.conifers.org/cu/Sequoia.php. Accessed on 13 Feb 2020.

Falcon-Lang, H.J., 2005. Global climate analysis of growth rings in woods, and its implications for deep-time paleoclimate studies. Paleobiology 31 (3), 434–444.

Falcon-Lang, H.J., Cantrill, D.J., Nichols, G.J., 2001. Biodiversity and terrestrial ecology of a mid-Cretaceous, high-latitude floodplain, Alexander Island, Antarctica. J. Geol. Soc. London 158, 709–725.

Falcon-Lang, H.J., MacRae, R.A., Csank, A.Z., 2004. Palaeoecology of Late Cretaceous polar vegetation preserved in the Hansen Point Volcanics, NW Ellesmere Island, Canada. Palaeogeogr. Palaeoclimatol. Palaeoecol. 212, 45–64.

Foster, J., 2020. Jurassic West: The Dinosaurs of the Morrison Formation and Their World. Indiana Univ. Press, Bloomington.

Francis, J.E., 1984. The seasonal environment of the Purbeck (Upper Jurassic) fossil forests. Palaeogeogr. Palaeoclimatol. Palaeoecol. 48, 285–307.

Francis, J.E., 1986. Growth rings in Cretaceous and Tertiary wood from Antarctica and their palaeoclimatic implications. Palaeontology 29, 665–684.

Fritts, H.C., 1962. An approach to dendroclimatology: screening by means of multiple regression techniques. J. Geophys. Res. 67 (4), 1413–1420.

Fritts, H.C., 1966. Growth-rings of trees: their correlation with climate. Science 154 (3752), 973–979.

Fritts, H.C., 1976. Tree Rings and Climate. Acad. Press, London, pp. 1–567.

Gee, C.T., Tidwell, W.D., 2010. A mosaic of characters in a new whole-plant *Araucaria*, *A. delevoryasii* Gee sp. nov., from the Late Jurassic Morrison Formation. In: Gee, C.T. (Ed.), Plants in Mesozoic Time: Morphological Innovations, Phylogeny, Ecosystems. Indiana Univ. Press, Bloomington, pp. 67–94

Gee, C.T., Dayvault, R.D., Stockey, R.A., Tidwell, W.D., 2014. Greater palaeobiodiversity in conifer seed cones in the Upper Jurassic Morrison Formation of Utah, USA. Palaeobio. Palaeoenv. 94, 363–375.

Gee, C.T., Sprinkel, D., Bennis, M.B., Gray, D.E., 2019. Silicified logs of *Agathoxylon hoodii* (Tidwell et Medlyn) comb. nov. from Rainbow Draw, near Dinosaur National Monument, Uintah County, Utah, USA, and their implications for araucariaceous conifer forests in the Upper Jurassic Morrison Formation. Geol. Intermountain West 6, 77–92.

Gorman II, M.A., Miller, I.M., Pardo, J.D., Small, B.J., 2008. Plants, fish, turtles, and insects from the Morrison Formation: a Late Jurassic ecosystem near Canon City, Colorado. Geol. Soc. Am. Field Guide 10, 295–310.

Gothan, W., 1905. Zur Anatomie lebender und fossiler Gymnospermen-Hölzer. Abh. preußische geol. Landesanst. 44, 1–108 (in German).

Gray, B., 1975. Size-composition and regeneration of *Araucaria* stands in New Guinea. J. Ecol. 273–289.

Hasiotis, S.T., 2004. Reconnaissance of Upper Jurassic Morrison Formation ichnofossils, Rocky Mountain Region, USA: paleoenvironmental, stratigraphic, and paleoclimatic significance of terrestrial and freshwater ichnocoenoses. Sediment. Geol. 167, 177–268.

Hotton, C.L., Baghai-Riding, N.L., 2010. Palynological evidence for conifer dominance within a heterogeneous landscape in the Late Jurassic Morrison Formation, USA. In: Gee, C.T. (Ed.), Plants in Mesozoic Time: Morphological Innovations, Phylogeny, Ecosystems. Indiana Univ. Press, Bloomington, pp. 295–328.

IAWA Committee, 2004. IAWA list of microscopic features for softwood identification. IAWA J. 25, 1–70.

Jarmolenko, A.V., 1933. The experimental application of stem secondary wood anatomy to investigation of conifer phylogeny. Sov. Bot. 6, 46–63.

Jefferson, T.H., 1982. Fossil forests from the Lower Cretaceous of Alexander Island, Antarctica. Palaeontology 25, 681–708.

Keller, A.M., Hendrix, M.S., 1997. Paleoclimatological analysis of a Late Jurassic petrified forest, Southeastern Mongolia. Palaios 12, 282–291.

Litwin, R.J., Turner, C.E., Peterson, F., 1998. Palynological evidence on the age of the Morrison Formation, Western Interior U.S. Mod. Geol. 22, 297–319.

Lutz, H.T., 1930. A new species of *Cupressionoxylon* (Goeppert) Gothan from the Jurassic of South Dakota. Bot. Gaz. 90 (1), 92–107.

Marynowski, L., Philippe, M., Zatoń, M., Hautevelle, Y., 2008. Systematic relationships of Mesozoic wood genus *Xenoxylon*: integrative biomolecular and palaeobotanical approach. Neues Jahrb. Geol. Paläontol. 247, 177–189.

Medlyn, D.A., Tidwell, W.D., 1975. Conifer wood from the Upper Jurassic of Utah. Part I: *Xenoxylon morrisonense* sp. nov. Am. J. Bot. 62 (2), 203–208.

Medlyn, D.A., Tidwell, W.D., 1979. A review of the genus *Protopiceoxylon* with emphasis on North American species. Can. J. Bot. 57, 1451–1463.

Medlyn, D.A., Tidwell, W.D., 2002. *Mesembrioxylon obscurum*, a new combination for *Araucarioxylon? obscurum* Knowlton, from the Upper Jurassic Morrison Formation, Wyoming. West. N. Am. Nat. 62 (2), 210–217.

Morgans, H.S., Hesselbo, S.P., Spicer, R.A., 1999. Seasonal climate of the Early–Middle Jurassic, Cleveland Basin, England. Palaios 14, 261–272.

Mosbrugger, V., Gee, C.T., Belz, G., Ashraf, A.R., 1994. Three-dimensional reconstruction of an in-situ Miocene peat forest from the Lower Rhine Embayment, northwestern Germany—new methods in palaeovegetation analysis. Palaeogeogr. Palaeoclimatol. Palaeoecol. 110 (3–4), 295–317.

Mull, C.G., Houseknecht, D.W., Bird, K.J., 2003. Revised Cretaceous and Tertiary stratigraphic nomenclature in the Colville Basin, northern Alaska. US Geol. Surv. Prof. Pap. 1673, 51.

Müller-Stoll, W.R., 1951. Mikroskopie des zersetzen und fossilierten Holzes. In: Freund, H. (Ed.), Handbuch der Mikroskopie in der Technik. 5, pp. 727–816.

Nathorst, A.G., 1897. Zur mesozoischen Flora Spitzbergens. K. Svenska Vetenskapsakademiens Handligar 30, 1–77.

Nosova, N.V., Kiritchkova, A.I., 2008. First records of the genus *Mirovia reymanówna* (Miroviaceae, Coniferales) from the Lower Jurassic of western Kazakhstan (Mangyshlak). Paleontol. J. 42, 1383–1392.

Oh, C., Philippe, M., Kim, K., 2015. *Xenoxylon* synecology and palaeoclimatic implications for the Mesozoic of Eurasia. Acta Palaeontol. Polonica 60 (1), 245–256.

Paine, C.E.T., Stahl, C., Courtois, E.A., Patino, S., Sarmiento, C., Baraloto, C., 2010. Functional explanations for variation in bark thickness in tropical rain forest trees. Funct. Ecol. 24 (6), 1202–1210.

Parrish, J.T., Spicer, R.A., 1988. Middle Cretaceous wood from the Nanushuk Group, Central North Slope, Alaska. Palaeontology 31, 19–34.

Parrish, J.T., Peterson, F., Turner, C.E., 2004. Jurassic "savannah": plant taphonomy and climate of the Morrison Formation (Upper Jurassic, western USA). Sediment. Geol. 167, 137–162.

Peterson, F., 1980. Sedimentology of the uranium-bearing Salt Wash Member and Tidwell unit of the Morrison Formation in the Henry and Kaiparowits Basins, Utah. In: Picard, M.D. (Ed.), Henry Mountains Symposium. Utah Geol. Assoc. Publ, pp. 305–322.

Philippe, M., Bamford, M.K., 2008. A key to morphogenera used for Mesozoic conifer-like woods. Rev. Palaeobot. Palynol. 148 (2), 184–207.

Philippe, M., Hayes, P., 2010. Reappraisal of two of Witham's species of fossil wood with taxonomical and nomenclatural notes on *Planoxylon* Stopes, *Protocedroxylon* Gothan and *Xenoxylon* Gothan. Rev. Palaeobot. Palynol. 162, 54–62.

Philippe, M., Thévenard, F., 1996. Distribution and palaeoecology of the Mesozoic wood genus *Xenoxylon*: palaeoclimatological implications for the Jurassic of Western Europe. Rev. Palaeobot. Palynol. 91, 353–370.

Philippe, M., Jiang, H.E., Kim, K., Oh, C., Gromyko, D., Harland, M., Paik, I.S., Thévenard, F., 2009. Structure and diversity of the Mesozoic wood genus *Xenoxylon* in Far East Asia: implications for terrestrial palaeoclimates. Lethaia 42, 393–406.

Philippe, M., Thévenard, F., Nosova, N., Kim, K., Naugolnykh, S., 2013. Systematics of a palaeoecologically significant boreal Mesozoic fossil wood genus, *Xenoxylon* Gothan. Rev. Palaeobot. Palynol. 193, 128–140.

Pinard, M.A., Huffman, J., 1997. Fire resistance and bark properties of trees in a seasonally dry forest in eastern Bolivia. J. Trop. Ecol. 727–740.

Richmond, D., Lupia, R., Philippe, M., Klimek, J., 2019. First occurrence of the boreal fossil wood *Xenoxylon meisteri* from the Jurassic of North America: Morrison Formation of central Montana, USA. Rev. Palaeobot. Palynol. 267, 39–53.

Schudack, M.E., Turner, C.E., Peterson, F., 1998. Biostratigraphy, paleoecology, and biogeography of charophytes and ostracodes from the Upper Jurassic Morrison Formation, Western Interior, USA. Mod. Geol. 22, 379–414.

Scipioni, M.C., Dobner, J.M., Longhi, S.J., Vibrans, A.C., Schneider, P.R., 2019. The last giant *Araucaria* trees in southern Brazil. Sci. Agric. 76 (3), 220–226.

Selmeier, A., Grosser, D., 2011. Lower Cretaceous conifer drift wood from Sverdrup Basin, Canadian Arctic Archipelago. Zitteliana 51, 19–35.

Shilkina, I.A., Khudaiberdyev, R.Kh., 1971. Novyie nakhodki i obzor rodov *Protocedroxylon* i *Xenoxylon*. Paleobot. Uzbekistana 2, 117–142 (in Russian).

Sillett, S.C., Van Pelt, R., Carroll, A.L., Campbell-Spickler, J., Coonen, E.J., Iberle, B., 2019. Allometric equations for *Sequoia sempervirens* in forests of different ages. For. Ecol. Manag. 433, 349–363.

Spicer, R.A., Parrish, J.T., 1990. Latest Cretaceous woods of the central North Slope, Alaska. Palaeontology 33, 225–242.

Sprinkel, D.A., Bennis, M.B., Gray, D.E., Gee, C.T., 2019. Stratigraphic setting of fossil log sites in the Morrison Formation (Upper Jurassic) near Dinosaur National Monument, Uintah County, Utah, USA. Geol. Intermountain West 6, 61–76.

Staccioli, G., Uçar, G., Bartolini, G., Coppi, C., Mochi, M., 1998. Investigation on a fossil Sequoia bark from Turkey. Holz als Roh- Werkst. 56 (6), 426.

Tidwell, W.D., 1990. Preliminary report on the megafossil flora of the Upper Jurassic Morrison Formation. Hunteria 2 (8), 1–11.

Tidwell, W.D., Medlyn, D.A., 1992. Short shoots from the Upper Jurassic Morrison Formation, Utah, Wyoming, and Colorado, USA. Rev. Palaeobot. Palynol. 71 (1–4), 219–238.

Tidwell, W.D., Medlyn, D.A., 1993. Conifer wood from the Upper Jurassic of Utah, Part II—*Araucarioxylon hoodii* sp. nov. Palaeobotanist 42, 1–7.

Tidwell, W.D., Britt, B.B., Ash, S.R., 1998. Preliminary floral analysis of the Mygatt-Moore Quarry in the Jurassic Morrison Formation, west-central Colorado. Mod. Geol. 22, 341–378.

Trujillo, K.C., Kowallis, B.J., 2015. Recalibrated legacy $^{40}Ar/^{39}Ar$ ages for the Upper Jurassic Morrison Formation, Western Interior, U.S.A. Geol. Intermountain West 2, 1–8.

Turner, C.E., Peterson, F., 1999. Biostratigraphy of dinosaurs in the Upper Jurassic Morrison Formation of the Western Interior, U.S.A. In: Gillette, D.D. (Ed.), Vertebrate Paleontology in Utah. Utah Geol. Surv. Miscellaneous Publ vols. 99–1, pp. 77–114.

Turner, C.E., Peterson, F., 2004. Reconstruction of the Upper Jurassic Morrison Formation extinct ecosystem—a synthesis. Sediment. Geol. 167, 309–355.

Vaden, M.D., 2020. Tallest & Largest redwoods. Avaliable online at https://mdvaden.com/redwood_dimensions.shtml. Accessed on 13 Feb 2020.

van Hinsbergen, D.J.J., de Groot, L.V., van Schaik, S.J., Spakman, W., Bijl, P.K., Sluijs, A., Langereis, C.G., Brinkhuis, H., 2015. A paleolatitude calculator for paleoclimate studies. PLoS One 10 (6), e0126946.

VanderSchaaf, C.L., 2013. Mixed-effects height–diameter models for ten conifers in the inland Northwest, USA. South. For. J. For. Sci. 76 (1), 1–9.

Ward, L.F., 1990. Description of a new genus and twenty new species of fossil cycadean trunks from the Jurassic of Wyoming. Wash. Acad. Sci. Proc. 1, 253–300.

Youssef, S.G.M., 2002. *Xenoxylon* wood from late Jurassic–Early Cretaceous of Gebal Kâmil, Egypt. IAWA J. 23, 69–76.

Zeibig-Kichas, N.E., Ardis, C.W., Berrill, J.P., King, J.P., 2016. Bark thickness equations for mixed-conifer forest type in Klamath and Sierra Nevada Mountains of California. Int. J. For. Res. 1–10.

Zheng, S.L., Li, Y., Zhang, W., Li, N., Wang, Y.D., Yang, X.J., Yi, T.M., Yang, J., Fu, X.P., 2008. Fossil Wood of China. China For. Publ. House, Beijing, pp. 1–356.

Chapter 3

Multitrophic plant–insect–fungal interactions across 150 million years: A giant *Agathoxylon* tree, ancient wood-boring beetles and fungi from the Morrison Formation of NE Utah, and the brood of an extant orchard mason bee

Publication

Gee, C.T.[1], Xie, A.[2], and Zajonz, J., 2022, Multitrophic plant–insect–fungal interactions across 150 million years: A giant *Agathoxylon* tree, ancient wood-boring beetles and fungi from the Morrison Formation of NE Utah, and the brood of an extant orchard mason bee: Review of Palaeobotany and Palynology, v. 300, 104627, DOI: 10.1016/j.revpalbo.2022.104627.

Author contributions

Gee and Xie designed the study. Gee analyzed and interpreted the data, wrote the manuscript, and created the photo plates. Xie and Gee collected the fossil material in the field. Xie made the thin-section of fossil wood, took micrographs, analyzed the wood decay, created one figure, and proofread the manuscript. Zajonz scanned the fossil wood specimen using microCT and created the 3D reconstructions using Avizo. Gee obtained funding for fieldwork.

Summary

A new discovery of ecological associations between a Morrison plant, insect, and fungus in a fossil log from the Upper Jurassic Morrison Formation in Utah is presented in this chapter, which also

[1,2] Corresponding author.

provides evidence of an interrelationship between these Upper Jurassic organisms and a modern bee. Up to now, few records of ancient plant–insect interactions have been documented from the Morrison Formation compared to those of the abundant fossil plants preserved in this formation.

The tree host is a large fossil araucariaceous log measuring ca. 1.3 m in diameter, with an estimated tree height of ca. 70 m. When this tree was alive, the fungi infected and decayed its wood tissue, which appears in the cut face (in cross section) of fossil specimen as numerous pores. The fungi are recognized as white rot fungi based on the irregular pocket-like decay structures in the thin section of the wood. Afterwards, a Morrison insect, likely a beetle, bored into the tree trunk in the woody tissue weakened by the white rot fungi, which is interpreted on the basis of the two large boreholes measuring 9 mm and 4 mm in diameter, respectively.

The most surprising finding in this study is that an extant orchard mason bee utilized the larger borehole as a nest with at least three chambers separated by thin walls of sand. However, only the lower two chambers are intact, and each of them bears one cocoon of an orchard mason bee, which is easily visible in the microCT imaging.

Hence, this study shows not only the ecological associations between plant, insect, and fungi during the Late Jurassic time, but also the interrelationship between ancient and modern organisms.

Contents lists available at ScienceDirect

Review of Palaeobotany and Palynology

journal homepage: www.elsevier.com/locate/revpalbo

Multitrophic plant–insect–fungal interactions across 150 million years: A giant *Agathoxylon* tree, ancient wood-boring beetles and fungi from the Morrison Formation of NE Utah, and the brood of an extant orchard mason bee

Carole T. Gee [a,b,c,*], Aowei Xie [a,*], Jonas Zajonz [a,d]

[a] Institute of Geosciences, Division of Paleontology, University of Bonn, Nussallee 8, 53115 Bonn, Germany
[b] Huntington Botanical Gardens, 1151 Oxford Road, San Marino, California 91108, USA
[c] State Key Laboratory of Palaeobiology and Stratigraphy, Nanjing Institute of Geology and Palaeontology, CAS, Nanjing 210008, China
[d] Department of Geology, University of Cincinnati, 345 Clifton Court, Cincinnati, Ohio 45220, USA

ARTICLE INFO

Article history:
Received 3 November 2021
Received in revised form 4 February 2022
Accepted 11 February 2022
Available online 17 February 2022

Keywords:
Araucariaceae
Blue orchard bee
MicroCT
Osmia lignaria
Upper Jurassic
Xylophagy

ABSTRACT

Although plant–insect interactions can be traced back to the Silurian, little is known from Upper Jurassic to mid-Cretaceous ecosystems. In the Upper Jurassic Morrison Formation, evidence is limited to insect body fossils and trace fossils in mostly wood. However, until now, multitrophic interactions have not been reported from the Morrison Formation. Here we describe a complex web of interrelationships between an ancient tree, fungi, and wood-boring insect from the Morrison Formation with an extant bee in NE Utah, USA, using microscopy, thin sectioning, and microCT for non-destructive internal imaging. The tree is *Agathoxylon hoodii* (Araucariaceae), one of the largest individuals in a monospecific forest, whose trunk was infected and decayed by white rot while the tree was alive during the Jurassic. Fungal formation of voids in the wood facilitated the boring of large-diameter galleries by an insect, likely a beetle. One gallery was repurposed by a modern orchard mason bee, *Osmia lignaria*, as a linear nest for her brood. The fossil wood specimen was serendipitously collected with two bee larvae plus food provisions in cocoons in the lowermost two chambers. Thus, this example is not only a simple interaction between fossil plants and insects, but transcends 150 million years between the ancient tree–insect–fungal relationship and a living insect.

1. Introduction

Although interactions between land plants and arthropods are as ancient as the Upper Silurian, about 417 million years ago (e.g., Grimaldi and Engel, 2005; Labandeira, 2007, 2013; Taylor et al., 2009), relatively little is known about plant–insect interactions in Upper Jurassic to mid-Cretaceous ecosystems (Labandeira, 1998). This comes as a surprise given the onset of the dramatic turnover in the global flora from tall forests dominated by arborescent gymnosperms to vegetation featuring the morphologically varied and biodiverse angiosperms that expanded into nearly all land habitats during this time interval. Furthermore, the Upper Jurassic has yielded one of the most spectacular terrestrial faunas in earth history—the gigantic sauropods of the Morrison Formation in the Western Interior of North America.

Nevertheless, there is little evidence of the insect body fossils in the Morrison Formation. Examples are limited to a locustopsid orthopterna (Smith et al., 2011), an enigmatic nepomorphan (Lara et al., 2020), and some aquatic insect larvae (Gorman II et al., 2008). Trace fossils of insects are more common and include ground-dwelling anthophorid or halictid bee nests; terraphilic wasp nests with cocoons; mud-loving beetle or mole cricket burrows; tiger beetle burrows; insect larvae burrows; dung beetle nests; rove beetle burrows; and nests pertaining to various genera of ants (Hasiotis, 2004). Nests of other social insects have been described as well (Smith et al., 2020).

Plant–animal interactions in the Morrison Formation are also documented by trace fossils. Insect-bored tunnels of *Paleobuprestis* and *Paleoscolytus* beetles have been found in fossil conifer wood, while smooth cavities in fossil wood have been attributed to wood-feeding beetles, termites, or ants (Hasiotis, 2004). Other small-diameter tunnels found in the silicified wood of the enigmatic gymnosperm *Hermatophyton* have been ascribed to Cupedidae, the reticulated beetles (Tidwell and Ash, 1990). Insect-feeding on Morrison seeds has also been reported (Dayvault and Hatch, 2003).

* Corresponding authors.
E-mail addresses: cgee@uni-bonn.de (C.T. Gee), awxie@uni-bonn.de (A. Xie).

With the continued interest in the fossil plants of the Morrison Formation, the chances of finding evidence of plant–insect interactions increase. While earlier paleobotanical studies on the megaflora may have concentrated on fossil leaf compressions and single pieces of wood (older work reviewed by Ash and Tidwell, 1998; Tidwell and Skog, 1999; Gorman II et al., 2008; Gee and Tidwell, 2010), investigations carried out in the last decade have expanded into other fossil plant organs, such as conifer seed cones (Gee, 2013; Gee et al., 2014), other gymnospermous reproductive organs (Manchester et al., 2021), and large conifer logs (Gee et al., 2019; Richmond et al., 2019; Sprinkel et al., 2019; Xie et al., 2021). The potential of finding interactions between conifers and insects is thus enhanced.

Here we report on a new, multitrophic, plant–insect–fungal interaction from the Upper Jurassic Morrison Formation, namely, an insect-bored gallery in intimate association with the fungally infected wood of an *Agathoxylon* tree trunk from Rainbow Draw in northeastern Utah, USA. Surprisingly, the fossil insect-bored gallery was repurposed 150 million years later by an extant orchard mason bee as a nest to brood her offspring. Thus, in this case, we not only describe a simple interaction between fossil plants and insects, but also show evidence of an interrelationship between an ancient tree–insect–wood-decay fungi and an extant insect.

2. Geological setting and previous studies

The fossil material under study was collected during paleobotanical fieldwork in Rainbow Draw in Uintah County, northeastern Utah, USA, in September 2019 (Fig. 1A). Rainbow Draw is located on the southeastern flank of the Uinta Mountains, 36 km east–northeast of the city of Vernal and nearly 1 km north of the entrance to Dinosaur National Monument.

Most of the Jurassic sediments in Rainbow Draw pertain to the Morrison Formation which can be subdivided into the Windy Hill, Tidwell, Salt Wash, and Brushy Basin Members (Trujillo and Kowallis, 2015;

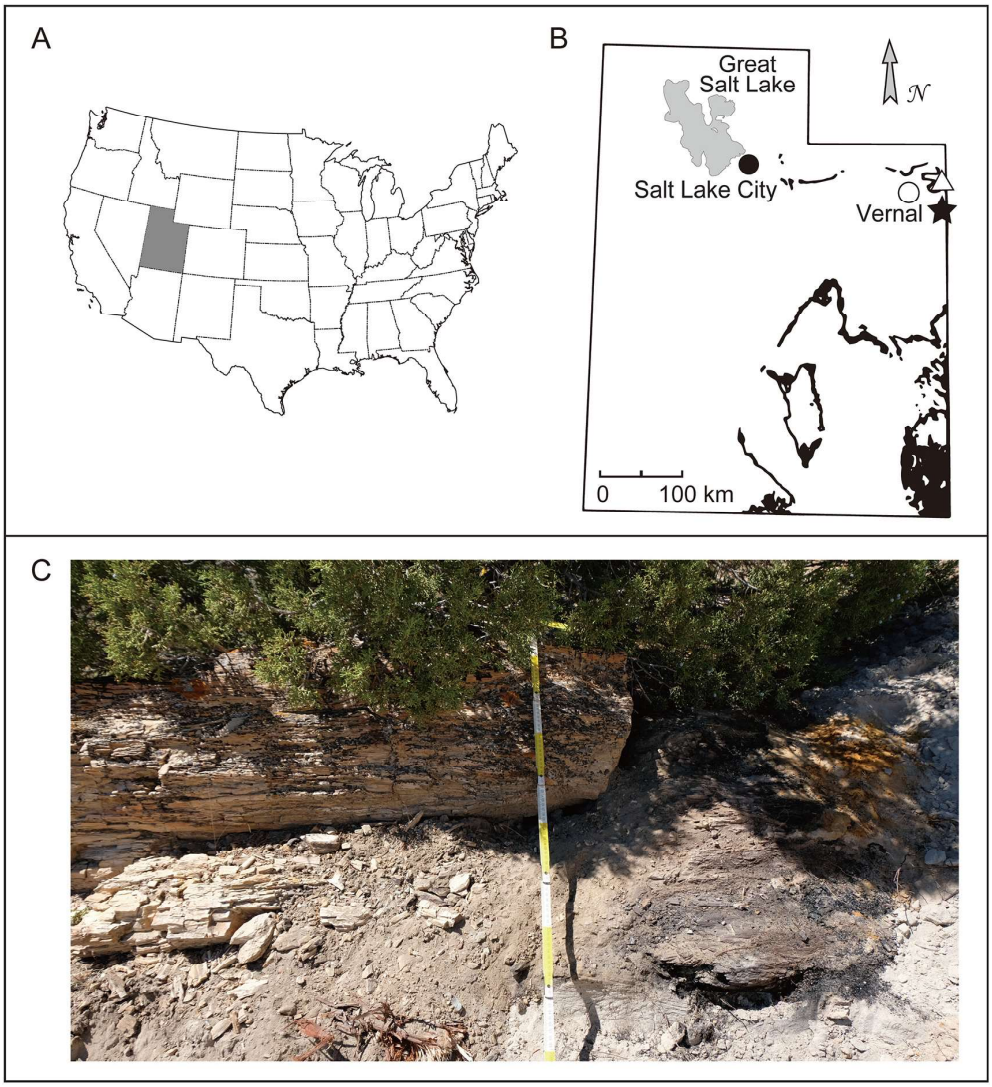

Fig. 1. (A) Sketch map of the USA highlighting the state of Utah (gray). (B) Sketch map of Utah showing the locality of the fossil log (star) in Rainbow Draw near Vernal (open circle) and Dinosaur National Monument (triangle), superimposed on the outcrops of the Upper Jurassic Morrison Formation (black). Map of Morrison outcrops courtesy of Kenneth Carpenter. (C) Fossil conifer log under study in Rainbow Draw, which yielded field specimen #091319–22, FHPR accession #2020.7.8.

Sprinkel et al., 2019). It is the Salt Wash Member that is fossiliferous, containing numerous occurrences of fossil logs and pieces of wood. This member consists of light to medium greenish-gray, very fine to fine, friable sandstone and siltstone with indistinct bedding and no discernable sedimentary structures (Gee et al., 2019; Sprinkel et al., 2019). The log-bearing intervals of the Salt Wash Member are interpreted as overbank deposits in a floodplain depositional environment (Sprinkel et al., 2019). According to single-crystal $^{40}Ar/^{39}Ar$ laser fusion dating, the Salt Wash Member in the Rainbow Draw area is between 156 to 152 million years old (Trujillo and Kowallis, 2015), which corresponds to a Kimmeridgian age (Cohen et al., 2013).

In regard to previous studies on this specific fossil log, a formal systematic treatment described the wood as *Agathoxylon hoodii* (Tidwell et Medlyn) Gee, Sprinkel, Bennis et Gray (Gee et al., 2019). Mineralogical analysis of the fossil wood shows that it is silicified, with the cell lumina, primary and secondary cell walls consisting of granular quartz (Pereira, 2020).

3. Materials and methods

The main fossil specimen is a block of silicified wood collected from log 1 at site 4 in Rainbow Draw (Fig. 1B), which is entered into the collections at the Utah Field House of Natural History State Park Museum in Vernal, Utah, USA, as field specimen number 091319–22 and accession number FHNH 2020.7.8. The boreholes in the fossil wood were discovered during routine handling of the block prior to thin sectioning. A thin section of ca. 30 μm thickness was consequently made in transverse section through the block of wood using standard petrological methods and bears the number RDW-004-2019. The fossil wood specimen and thin section are deposited in the Utah Field House of Natural History State Park Museum in Vernal, Utah, USA.

Binocular microscopy of the fossil wood specimen was carried out with a Leica S APO zoom microscope, while the thin section was studied with a Leica DM 2500 compound microscope. Digital images were taken and processed with the integrated measurement software ImageAccess easyLab 7.

High-resolution X-ray microcomputer tomography (microCT) scans were performed with a v|tome|x s 240D (phoenix|x-ray, General Electric Measurement & Control Solutions, Wunstorf, Germany), scanning software phoenix datos|×2, version 2.7.0. The resulting projections were converted into orthoslices in imagestacks with VG Studio Max (version 3.2; Volume Graphics, Heidelberg, Germany) and enhanced with Preview (version 11.0) on MacBook Air (version 10.15.5). The orthoslice imagestacks served as the basis of the three-dimensional reconstruction created with the visualization and analysis software Avizo (version 8.1; FEI Visualization Sciences Group, Düsseldorf, Germany).

4. Results

4.1. Fossil conifer tree

The fossil log from which the wood specimen was collected (Fig. 1C) has a preserved minimum diameter of 1.3 m. Using new models to extrapolate the height of an araucarian tree from its diameter based on height–diameter correlations of living *Araucaria* spp. (Xie, Griebeler, and Gee, unpubl. data), this fossil log represents a tall tree with a minimum height of 68 to 72 m.

As previously mentioned, the fossil log pertains to *Agathoxylon hoodii* (Tidwell et Medlyn) Gee, Sprinkel, Bennis et Gray, of the conifer family Araucariaceae. It has the same anatomical structure as the wood identified and described from this particular fossil log and from 12 other fossil logs or wood occurrences in Rainbow Draw (Gee et al., 2019). *Agathoxylon hoodii* is a tracheid-dominated wood that lacks axial parenchyma or resin canals, but contains abundant resin in the ray cells and occasionally in the axial tracheids. The tracheary pitting on the radial walls of the tracheids consists mostly of uniseriate, contiguous circular bordered pits; when biseriate, the circular bordered pits are arranged variously, from opposite to alternate. Rays are uniseriate, homocellular, parenchymatous, with smooth ray-cell end walls. Crossfield pitting is araucaroid in type, with numerous, crowded, slit-like, and obliquely oriented cupressoid pits in the crossfields.

4.2. Features on cut face of the wood specimen

On the cut face of the specimen, which represents an oblique transverse plane of section through the fossil log, most of the surface is intact (Plate I, 1). However, the uniformly dense surface is disturbed by three patches (Plate I, 1A, B, C) where the anatomical integrity of the wood is destroyed (see Section 4.3, fossil fungal damage). Two patches are each associated with a single borehole (see Section 4.4, fossil insect gallery).

The largest patch with disturbed wood grain (Plate I, 1A) includes a borehole occupying approximately one-third of the surface area (Plate I, arrow), which runs into the wood, parallel to the wood grain. Within this borehole, there is a partition of sand running across the gallery, perpendicular to the wood grain. Through this partition is a circular hole (see Section 4.6, recent nest of mason bees).

4.3. Fossil fungal damage

Around the two boreholes described above (Plate I, 1A, 1B) and at a third spot (Plate I, 1C), the wood structure appears macroscopically as roughened and pitted (Plate II, 1). In thin section, it becomes clear that the roughened area is caused by irregularly shaped pockets of decay where the tracheid wood cells have been broken down and are missing (Plate II, 2). The greatest loss in cellular structure is located in the wood tissue closest to the boreholes. The loss of tracheids is patchy, forming pocket-like cavities in the wood tissue (Plate II, 3). In the areas with severe wood tissue damage and cellular deterioration, there are minute, irregularly spaced, angular bodies of dark-colored resin (Plate II, 3, arrow). In adjacent areas with a more moderate amount of tissue damage, the resin appears as larger, more fluid accumulations. There are also areas of intact wood tissue that do not show any cellular damage and do not contain any resin.

While there is no evidence of fungal bodies such as hyphae or mycelia, nor spores, the fungal damage to the *Agathoxylon* wood can be also observed on the microscopic level. In thin section, the decay is evident as damage to the cell wall of individual tracheid cells in different parts of the wood. The stages of progressive deterioration to the tracheid cell walls can also be described. As a response to infection by fungi or other pathogens, the first visible line of defense of a living plant against fungal invasion is to actively reenforce its cell wall with the deposition of cell wall apposition at the site of attempted penetration of the fungus, which shows up as a thickening of the cell wall or so-called papillae (Collinge, 2009; Underwood, 2012). In the case of the *Agathoxylon* wood from Rainbow Draw, cell wall apposition can be clearly observed in some tracheids and appears as papillae of cell wall material in the tracheid lumen (Plate III, 1, 2, arrowheads).

The various stages in progressive fungal decay can be noted in adjacent cells. While the cell walls of one tracheid can appear seemingly intact, as well as uniform and dark in color (Plate III, 3A), a neighboring tracheid can appear to have lost color in only one small part of its cell wall (Plate III, 3B). Such a color loss is characteristic of selective delignification caused by the more rapid breakdown of lignin than hemicellulose or cellulose in the secondary cell wall, especially in early stages of wood decay (Schwarze et al., 2000). As time and fungal damage progresses, more of the secondary cell wall loses its dark brown color through delignification, leaving a ghostly outline of the former cell wall (Plate III, 3C). These lighter zones of cell wall consist of pure cellulose (cf., Schwarze et al., 2000). Left unchecked, the cell walls of a tracheid will become completely destroyed, leaving holes and gaps between wood cells like those in *Agathoxylon* (Plate III, 4).

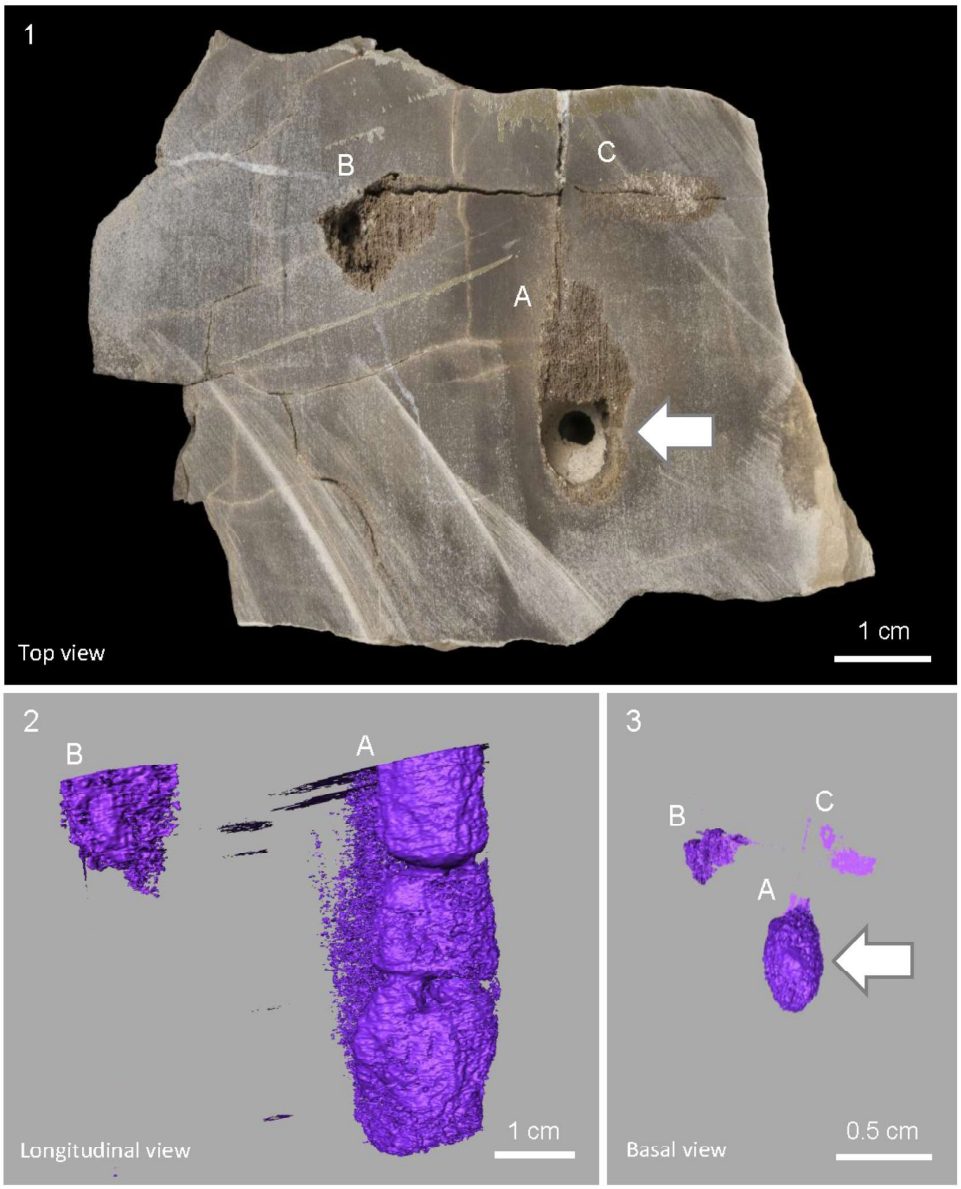

Plate I. Fossil wood specimen from the Upper Jurassic Morrison Formation in Utah and microCT reconstructions. (1) Cut face in transverse section of the wood block of *Agathoxylon hoodii*, showing three patches of fungal damage (A, B, C), and two boreholes (A, B). Arrow indicates the largest borehole in the wood (A), as well as the circular hole through the sand partition of the orchard mason bee nest. (2) Lateral view of the two largest patches of fungal damage (A, B), as reconstructed by Avizo in 3D with microCT orthoslices. The image of (A) shows the longitudinal extent of the fossil insect-bored gallery, as well as the segmentation of the gallery into three cells made by the extant orchard mason bee. (3) Basal view of all three patches of fungal damage, as reconstructed by Avizo in 3D with microCT orthoslices. Arrow indicates the transverse view of the largest borehole in the wood (A).

As more wood tissue is destroyed, these holes can then be observed on the macroscopic level.

4.4. Fossil insect gallery

In transverse section, the largest borehole on the cut surface of the fossil wood is elliptical on one end and truncated on the other end (Plate I, 1A, arrow). The borehole measures about 8.1 mm in width and 10.2 mm in length. The oblique angle of the transverse saw cut across the surface of the block of wood is evident in the lateral 3D reconstruction based on the microCT orthosections (Plate I, 2).

The largest borehole leads to a linear gallery oriented parallel to wood grain, namely, a vertical gallery running parallel to the longitudinal axis of the fossil tree trunk. The gallery is simple and unbranched, and there is no evidence of side galleries. The preserved length of the gallery measures approximately 5 cm, and its original full length is unknown. In diameter, this gallery is relatively large, averaging about 1.3 cm in width (Plate I, 2A). In top view, it measures 1.0 × 0.8 cm. In lateral view, it varies little in diameter, ranging from 1.0 cm near preserved top of the gallery to 1.4 at its base, widening to 1.5 cm at its widest point (Plate I, 2A). The irregular elliptical shape in transverse section in which one end is rounded and the other is truncate is maintained until the very

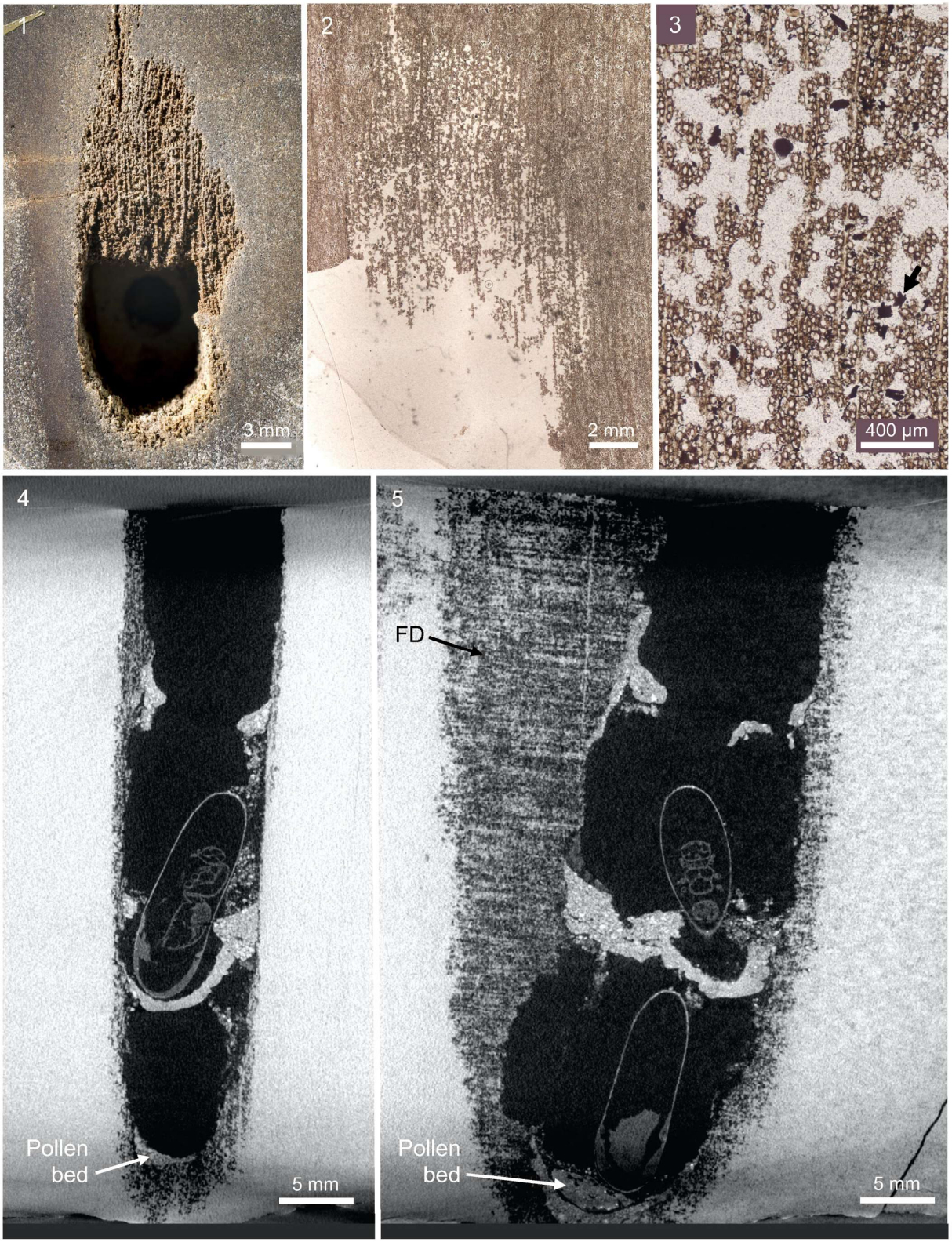

Plate II. Fossil fungal damage in wood and extant orchard mason bee nest in gallery. (1) Close-up of the largest patch of fungal damage and the borehole made by the wood-boring fossil insect, as also shown in Plate I, 1A. (2) Thin section image through the largest patch of fungal damage in the *Agathoxylon hoodii* wood. (3) Close-up of the fossil wood structure damaged by fungal activity. Note the non-damaged tracheids in radial rows alongside rays. Black arrow indicates amorphous fossil resin. (4) Longitudinal section through the largest gallery, microCT orthoslice YZ_572/904. Evident in this view are the three cells of the orchard mason bee next, the cell partitions made of sand, a cocoon with an immature bee in the middle cell, and the pollen bed in the lowermost cell. (5) Longitudinal section through the largest gallery at an 90° angle from (4), microCT orthoslice XZ_981/1836. In this view, the fossil insect-bored gallery is much wider. Evident are the three cells of the orchard mason bee next, the cell partitions made of sand, one cocoon each in the middle and lowermost cell, each one containing the remains of an immature bee, and the pollen bed in the lowermost cell. FD indicates the fossil fungal damage in the fossil wood.

base of the gallery (Plate I, 2A), as is seen in basal view when reconstructed in 3D (Plate I, 3A). In lateral 3D view, the end of the gallery is naturally rounded truncate (Plate I, 2A).

There are partitions that divide the larger gallery into three cells. The middle cell measures 1.5 cm in length, while the lowermost one measures 2.2 cm in length; the full length of the uppermost cell is unknown. See Section 4.6, recent nest of mason bees, for a more detailed description.

The second borehole on the block of wood is much smaller and apparent on the cut surface of the specimen (Plate I, 1B). In top view, the smaller borehole is more evenly shaped into a symmetrical elliptical form than the larger borehole and measures 4 mm × 3.7 mm. It is unclear how deep this borehole is preserved here, as it cannot be viewed in the reconstruction in lateral view (Plate I, 2B).

4.5. Juxtaposition of wood cells, fungal damage, and gallery

A thin section in oblique transverse section shows the juxtaposition of the wood anatomy, fungal damage, and gallery (Plate II, 2). The main layer is composed of the tracheid and ray cells of the fossil wood. The fungal damage, evident in the loss of wood cells, creates gaps into the wood. The insect-bored gallery then cuts through the parts of the wood that has been damaged by fungi, producing an uneven edge (Plate II, 1, 2).

4.6. Recent nest of mason bees

Within the largest borehole, there is a thin wall or partition of sand that is oriented perpendicular to the longitudinal axis of the gallery. In this partition of sand, there is a small, circular hole with a diameter of roughly 3.5 mm (Plate I, 1A, arrow).

In lateral view, it can be observed that the largest gallery contains a linear nest with cells that are each separated by partitions of sand (Plate I, 1A, 2A; Plate II, 4, 5). MicroCT imaging and 3D reconstruction show that three cells have been preserved, although the full length of the uppermost one was cut off by collecting (Plate I, 2A; Plate II, 4, 5). The middle and lowermost cells, both of which are complete, are roughly equivalent in length, the middle one measuring 1.7 cm and the lowermost one 1.8 cm (measurements based on Plate II, 5). The partitions between cells consist of light colored, very fine to fine, well-sorted sand with some small, angular clasts (Plate I, 1A, arrow), which is characteristic of the Morrison Formation sediments near the log site.

Cocoons are present in the lower two cells, one cocoon per chamber. In the cocoon in the middle cell, a well-formed bee can be seen (Plate II, 4, 5). In the lower cell, there is a well-formed cocoon, but the insect in this one is less well-developed (Plate II, 5). Maximum length and width of the cocoons are about 14.5 mm × 4.5 mm. A disk-shaped bed presumably of pollen and nectar that was collected and stored by the mother bee as food provisions for the growing larva appears at the bottom of the lowermost cell (Plate II, 4, 5, arrows).

5. Discussion

5.1. Ancient tree–ancient fungi–ancient insect–living insect interactions

A fossil tree trunk with coeval internal trace fossils reflecting fungal activity and insect boring reflects interactions on multiple trophic levels that occurred during Late Jurassic times. As the primary producer, the *Agathoxylon* tree represents the base of the ecological web of interactions. The tree provided nutrition to the xylophagous white-rot fungi which subsisted on the lignin in the wood cell walls. The tree also provided nutrition and shelter for wood-boring insects, which were likely beetles. The white-rot fungi facilitated insect boring in the tree by breaking down the cell walls in the normally very hard wood tissue and creating areas of weakness or even cell-less voids within the tree trunk. One gallery bored by the ancient beetle in the tree provided an appropriate shelter for extant orchard mason bee larvae some 150 million years later. The repurposing and adaption of the fossil-bored gallery in the wood by a living insect adds an unusual twist and the fourth dimension of time to this network of interrelationships.

5.2. Fossil wood, log, and forest

The previous identification of the fossil wood as *Agathoxylon hoodii*, a species that has been described from 12 fossil log or wood occurrences in Rainbow Draw near Vernal and from fossil wood collected from Mt. Ellen in southeastern Utah, places it in the family Araucariaceae (Gee et al., 2019). Given this familial assignment and a preserved diameter of 1.3 m, the ancient tree was at least 68 to 72 m in height, using a new height–diameter models for Araucariaceae trees based on the size data of 157 living trees (Xie, Griebeler, and Gee, unpubl. data). Using the same new models, the minimum height of the trees in this forest reconstructed from the six fossil logs known thus far is estimated to be 42 m (Xie and Gee, own data). Thus, the ancient tree under discussion here was thus one of the tallest, mature trees that grew in a monospecific, araucariaceous forest during Late Jurassic times in what is today Rainbow Draw in northeastern Utah.

The wood of *Agathoxylon hoodii* is characterized by resin which is abundant in the fossil wood cells as so-called resin plugs in both radial ray cells and in axial tracheids (Tidwell and Medlyn, 1993). At times, the dark, red-brown resin also collects in the corners of the ray cells. In the living tree, the resin was certainly a viscous substance that could flow copiously. In general, resin is a well-known defense mechanism against fungi and insects which occurs in several families of conifers (Langenheim, 2003). The flow, production, or mobilization of resin in trees can be stimulated by wounding or infection (Schwarze et al., 2000). In certain species of *Araucaria*, for example, *Araucaria humboldtensis* in New Caledonia, extensive resin exudation can be triggered by the damage of the branches and branchlets by two different species of wood-boring beetles (Beimforde et al., 2017).

In the severely, fungally damaged parts of the *Agathoxylon hoodii* wood under study here, the small, angularly shaped resin bodies found scattered among the wood cells likely represent a direct reaction by the tree to repel or hinder the fungal pathogens. Similarly, the larger flows of resin in adjacent parts of the wood can also be attributed to infection or wounding by fungi in these parts of the wood tissue. The difference in the size and shape characteristics between the small resin bodies and the larger flows are probably due to the desiccation of the resin bodies in the less intact areas of the wood where the cellular tissue received greater damage and was open to the air. The release of resin into areas between the tracheid cells from the storage areas in the ray parenchyma in some axial tracheids (cf. Gee et al., 2019) also suggests that tree was alive when the fungal damage happened.

5.3. Fossil fungi

Of the three major types of wood-decay fungi—brown rot, soft rot, and white rot—the fungal damage in the wood of *Agathoxylon hoodii* was most likely caused by white rot. White rot decay fungi are not defined by taxonomical affinity, but by the type of decay that they cause in comparison to damage by brown and soft rot fungi. Indicators for white rot damage are the macroscopic zones and pockets of decay in the wood, and the selective decoloration and delignification of the tracheid cell walls, whereby the lignin is broken down before the cellulose and hemicellulose in the cell wall. Hence, the areas of the delignified cell walls appear light-colored and not deep brown.

The division of fungi most commonly responsible for white rot in the present day is the Basidiomycota, although there is one family in the Ascomycota, the Xylariaceae, that produces white rot as well (Schwarze et al., 2000). While white rot subsists on the lignin-rich cell walls in wood, they are not limited to any particular taxon, but occur in a wide range of woody plant groups and plant parts. Today, white rot is a

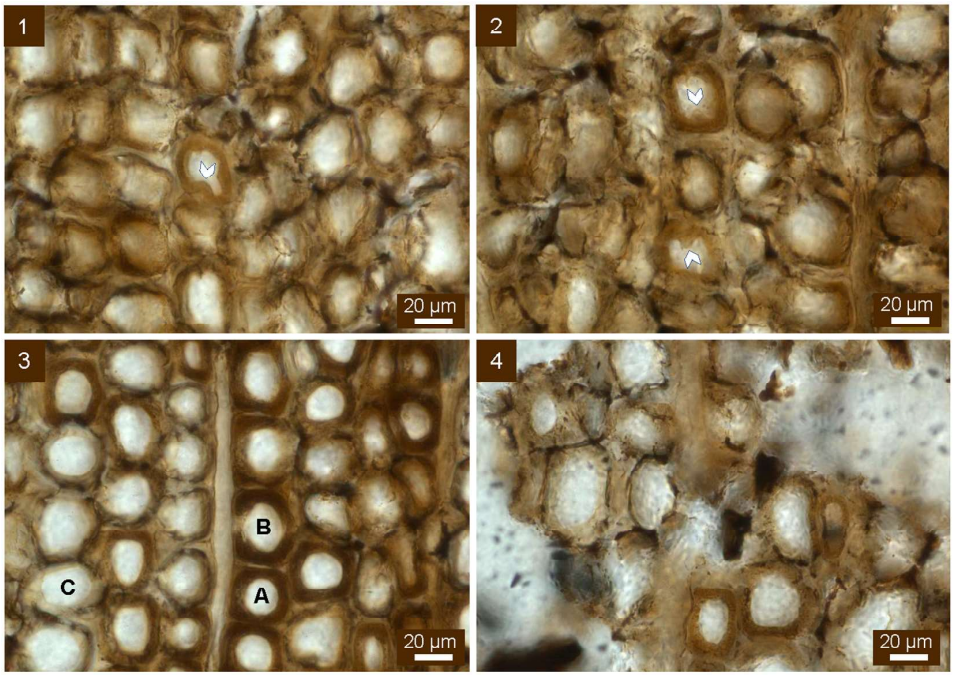

Plate III. Fossil fungal damage on the cellular level in transverse thin section. (1) Cell wall apposition in two spots in one tracheid (arrowhead points to apposition on left; the second one is to the right in the same cell). (2) Cell wall apposition in two different tracheids (arrowheads). (3) White-rot decay sequence in the delignification of cell walls in neighboring tracheids. The cell wall of one tracheid (A) is uniformly dark in color, whereas its neighbor (B) has lost brown color and presumably lignin in a small section of cell wall on the left side of the cell. In other tracheids, such as (C), the entire cell wall is at a more advanced stage of decoloration and delignification. (4) A very advanced stage of white rot decay in which the destruction of some tracheids is so complete that their absence forms holes in the wood tissue.

common xylophagous fungus that carries out selective delignification in both angiosperm and conifer wood (Schwarze et al., 2000).

Wood-rotting fungi appear in the fossil record as soon as the first woody plants evolve. The geologically oldest white rot is found in Upper Devonian progymnosperm wood (Stubblefield et al., 1985; Taylor et al., 2015). Other occurrences of white rot have been reported from the Permian (Stubblefield and Taylor, 1985, 1986; Harper et al., 2016; Wei et al., 2019), Triassic (Stubblefield and Taylor, 1986; Harper et al., 2016), Jurassic (Xia et al., 2020), and Cretaceous (Tian et al., 2020). Hence, it is not surprising to find white-rot fungal damage in the conifer wood from the Upper Jurassic Morrison Formation described here.

5.4. Fossil insect

The gallery in the fossil wood was most likely bored by a fossil insect into the trunk of the *Agathoxylon hoodii* tree. Although no frass was found in the gallery, the diameter of the gallery offers a clue to the identity of the Upper Jurassic insect borer. In the case of the *Agathoxylon hoodii* tree from Rainbow Draw, the insect must have been rather large to bore a hole roughly 1 cm in diameter through the wood.

Today, the wood-boring insects in the modern fauna causing the most damage through xylophagy, or feeding on wood, are the nymphal and adult stages of Isoptera (termites) and the larval stages of Coleoptera (beetles) (USDA Forest Service, 2013; Zabel and Morrell, 2020). To a lesser extent, both the nymphal and adult stages of Hymenoptera (horntail wasps, carpenter bees, and carpenter ants), the larvae of Lepidoptera (clearwinged moths), and the larvae and adults of Curculionidae (ambrosia beetles) damage or utilize trunk wood as well (USDA Forest Service, 2013; Zabel and Morrell, 2020).

In the order Coleoptera, there are nine families of beetles that produce wood damage (Zabel and Morrell, 2020). Of these wood-boring taxa, the largest insect larvae are those of the Buprestidae (flatheaded borers) and Cerambycidae (roundheaded borer) beetles, which can produce galleries up to 1.3 cm in diameter (Brown, 2011). The Buprestidae and Cerambycidae, in addition to 15 other beetle families, are known to depend on trees of *Araucaria* spp. as hosts. It has been found, for example, that 32 species of the family Cerambycidae interact with the *Araucaria* trees growing in Brazil, New Zealand, and New Caledonia (Mecke et al., 2005), although there are a few species of the Buprestidae that are known to be closely associated with *Araucaria cunninghamii* in Australia (Hawkeswood, 2006; Bellamy et al., 2013).

Thus, based on gallery diameter size in the fossil *Agathoxylon* wood, as well as the sizes of living beetles, the most likely fossil candidate responsible for the insect-bored gallery in the Upper Jurassic *Agathoxylon* wood is the larva of a beetle with large-diameter larvae such as those pertaining to the living families Cerambycidae or Buprestidae.

5.5. Extant mason bee

While the body of the extant bee can be observed in microCT images, the determination of the bee to genus and species is possible based exclusively on its reproductive behavior. Judging from the repurposing of the previously existing, long, and narrow gallery in the fossil wood, this nest was very likely made by a living female orchard mason bee, *Osmia lignaria* ssp. *propinqua* of the family Megachlidae, order Hymemoptera. Indicative of this native solitary bee is also the use of locally available fine-grained substrate such as mud to create the partitions between the cells; in this case, it was the very fine to fine sand of the Morrison Formation. *O. lignaria* ssp. *propinqua* is the subspecies found in North America west of the Rocky Mountains (Bosch and Kemp, 2001).

The reproductive behavior of *Osmia lignaria*, commonly called the orchard mason bee or blue orchard bee, is well known (Bosch and Kemp, 2001). In the spring, the female bees make a nest composed of

a linear series of cells in naturally occurring, previously existing spaces which include tubular cavities, hollow stems, and holes in wood. After finding an appropriate nesting cavity, she collects pollen and nectar to form a pollen nest at the bottom of the lowermost cell, into which a single egg is deposited. The cell is then sealed with mud (or very fine sand to fine sand, as in this case) from the immediate surroundings, and beyond the mud partition, a new cell is prepared for the next egg, with its own pollen bed and is sealed with the fine sediment. The pollen and nectar of the pollen bed serve as provisions for the developing larva in each cell. Once the provisions are largely consumed, the larva spins a cocoon around itself and matures into an adult. The bees develop ontogenetically in their respective cells for many months and do not emerge until the spring of the following year. Extrapolating from observations of living bees, the two bees in the lowermost part of gallery in the fossil wood are likely female, because eggs with male bees are deposited in the upper end of the nest.

In general, it is not unusual for orchard mason bees seeking appropriate nest sites to reuse beetle-bored tunnels in wood. In the wild, orchard mason bees are usually known to build nests in abandoned beetle burrows in dead logs and stumps (Bosch and Kemp, 2001). In wild populations in Utah, it has been reported that orchard mason bees commonly build their nest in the galleries of large wood-boring beetles in living tree trunks (Kervin, 2011). When designing artificial nesting units for the bees, the optimal cavity diameter is 7.5 mm (Bosch and Kemp, 2001), which is just slightly smaller, by about one-half millimeter, than the 8.1 mm diameter of the fossil insect-bored gallery. Thus, the linear and narrow gallery in the fossil wood of *Agathoxylon* and abundance of very fine to fine sand of the Morrison Formation in the immediate environs made for an ideal site for an orchard mason bee nest, even if the shaft was drilled 150 million years ago.

5.6. Timeline of events

The timeline of events between interactions can be reconstructed based on the fossil evidence. In Late Jurassic times, a tall tree of *Agathoxylon hoodii* grew to at least 1.30 m in diameter, 68 to 72 m in height, and an age of at least 100 years old (Gee et al., 2019), thus becoming one of the largest trees in the Morrison forest. Its trunk became infected in part by white rot fungi. When the fungus tried to invade individual cells, each cell tried to keep the pathogen out by actively reinforcing its cell wall with the deposition of apposition at the site of attempted penetration.

Once the wood cells began to be destroyed by white rot, the tree tried to repel or at least control the fungal infection by releasing resin. At first, the resin was discharged between cells with small amounts of resin, which appear as small, angular, isolated pieces of resin 150 million years later. Later, as the white rot continued to destroy the woody tissue, great amounts of more viscous resin was released in the voids between more intact cells.

The weakened and decomposed areas of wood tissue made it easier for beetles or other insects to bore large-diameter, vertical galleries into this part of the wood. The number of galleries and their individual lengths in this *Agathoxylon* tree trunk is unknown, since the area of study is limited to a small, fist-sized specimen of fossil wood.

Approximately 150 million years later, one end of one insect-bored gallery became exposed to the atmosphere. This gallery, measuring 1.0 to 1.5 cm in diameter, was repurposed by a female orchard mason bee, *Osmia lignaria* ssp. *propinqua*. Orchard mason bees normally nest in tubular cavities such as hollow stems or holes in trunk wood of living trees, although it seems that this gallery in a fossil tree trunk was deemed to be an appropriate nesting site. The female bee collected pollen and nectar to form a pollen nest at the bottom of gallery, deposited a single egg in the nest, then sealed the chamber by making a partition with the very fine to fine, moist sand of the Morrison Formation near the fossil log. The action of providing food provisions, depositing an egg, and forming a sand partition by the mother bee was then repeated until her linear nest was completed.

A fist-sized specimen of fossil wood was then serendipitously sampled by paleobotanists (AX and CTG) in September 2019 from this particular part of the ancient tree trunk that happened to have been infested while alive 150 million years ago with white-rot fungi and bored into by beetles. Coincidentally, this small block of Upper Jurassic wood also contained a section of the ancient burrow gallery that had been adapted by an extant orchard mason bee to serve a linear nest, which still contained the lowermost two chambers and the remains of two female bees that would have emerged a few months later in the spring of 2020.

6. Conclusions

Study of a small specimen of fossil wood for identification reveals complex interactions between an ancient tree, fungi, insect-boring beetles, and a living orchard mason bee that began in the Upper Jurassic of western North America. Some 150 million years ago, a monospecific forest of tall trees grew in what is today the Morrison Formation of northeastern Utah. The trees were araucariaceous, pertaining to *Agathoxylon hoodii*. One tree in particular attained a diameter of at least 130 cm, a minimum height of 68 to 72 m, and an individual age of 100 years, and was thus one of the largest and oldest trees in the Morrison forest. While the tree was still alive, parts of its trunk were infested by white rot. The tree tried to combat the fungal invasion by various means, including strengthening its cell walls at the entry point of the fungus into individual tracheids and the release of increasing amounts of resin. In the weakened parts of the tissue, wood-boring insects, likely beetles, were able to make large-diameter, vertical galleries. One of these galleries was repurposed in the spring of 2019 by an orchard mason bee as a linear nest for her eggs and, at the time of our specimen collecting, still contained two chambers with bee larvae and their food provisions.

Here, the paleobotany of the Morrison Formation offers us a window into understanding not only the Upper Jurassic vegetation, but also insight into the complex network of interrelationships in a 150-million-year-old ecosystem between plants, insects, and fungi. Beyond that, the web of interactions between the ancient tree, beetle, and white-rot fungi with a living bee show the intricacies of multitrophic interrelationships among organisms across geological time.

Declaration of Competing Interest

The authors declare that they have no known competing financial interests or personal relationships that could have appeared to influence the work reported in this paper.

Acknowledgments

Thanks go to Georg Oleschinski, University of Bonn, for photography of the fossil specimen shown in Plate I, A and Plate II, 1; to Mary Beth Bennis and Dale E. Gray for guiding us to the field site; to Steven D. Sroka, Mary Beth Bennis, and John Foster, Utah Field House of Natural History State Park Museum, for the use of facilities at the museum; to Conrad C. Labandeira, National Museum of Natural History, Smithsonian Institution, for helpful discussion; to Stephen T. Hasiotis, University of Kansas, for literature; to Yongdong Wang, Nanjing Institute of Geology and Paleontology, CAS, for assistance in the field; and to reviewer Victoria Egerton, University of Manchester, and an anonymous reviewer for their useful suggestions. Financial support for fieldwork in Utah from Open Funding grant no. 193101 from the State Key Lab of Palaeobiology and Stratigraphy State Grant to CTG is gratefully acknowledged. Financial support from the China Scholarship Council for the doctoral studies of AX (CSC no. 201804910527) is also appreciated. This is contribution no. 41 of the DFG Research Unit FOR 2685 “The Limits of the Fossil Record: Analytical and Experimental Approaches to Fossilization.”

References

Ash, S.R., Tidwell, W.D., 1998. Plant megafossils from the Brushy Basin Member of the Morrison Formation near Montezuma Creek Trading Post, southeastern Utah. Mod. Geol. 22, 321–339.

Beimforde, C., Seyfullah, L.J., Perrichot, V., Schmidt, K., Rikkinen, J., Schmidt, A.R., 2017. Resin exudation and resinicolous communities on *Araucaria humboldtensis* in New Caledonia. Arthropod–Plant Interact. 11, 495–505.

Bellamy, C.L., Williams, G.A., Hasenpusch, J., Sundholm, A., 2013. A summary of the published data on host plants and morphology of immature stages of Australian jewel beetles (Coleoptera: Buprestidae), with additional new records. Insecta Mundi 0293, 1–172.

Bosch, J., Kemp, W., 2001. How to Manage the Blue Orchard Bee as an Orchard Pollinator. Sustainable Agriculture Network, Handbook Series Book 5.

Brown, W., 2011. Wood-boring beetles of structures. Texas A&M AgriLife Extension E-394, pp. 1–5 Available online at https://cdn-ext.agnet.tamu.edu/wp-content/uploads/2019/01/E-394-structure-infesting-wood-boring-beetles.pdf Last accessed: 21 September 2021.

Cohen, K.M., Finney, S.C., Gibbard, P.L., Fan, J.-X., 2013. Updated 2021. The ICS international chronostratigraphic chart. Episodes 36, 199–204.

Collinge, D.B., 2009. Cell wall appositions: the first line of defence. J. Exp. Bot. 60, 351–352.

Dayvault, R.D., Hatch, H.S., 2003. Short shoots from the Late Jurassic Morrison Formation of southeastern Utah. Rocks Miner. 78, 232–247.

Gee, C.T., 2013. Applying microCT and 3D visualization to Jurassic silicified conifer seed cones: a virtual advantage over thin-sectioning. Appl. Plant Sci. 1, 1300039.

Gee, C.T., Tidwell, W.D., 2010. A mosaic of characters in a new whole-plant *Araucaria*, *A. delevoryasii* GEE sp. nov., from the Late Jurassic Morrison Formation of Wyoming, U.S.A. In: Gee, C.T. (Ed.), Plants in Mesozoic Time: Morphological Innovations, Phylogeny, Ecosystems. Indiana University Press, Bloomington, Indiana, pp. 67–94.

Gee, C.T., Dayvault, R.D., Stockey, R.A., Tidwell, W.D., 2014. Greater paleobiodiversity in conifer seed cones in the Upper Jurassic Morrison Formation of Utah, USA. Palaeobiodiv. Palaeoenviron. 94, 363–375.

Gee, C.T., Sprinkel, D., Bennis, M.B., Gray, D.E., 2019. Silicified logs of *Agathoxylon hoodii* (Tidwell et Medlyn) comb. nov. from Rainbow Draw, near Dinosaur National Monument, Uintah County, Utah, USA, and their implications for araucariaceous conifer forests in the Upper Jurassic Morrison Formation. Geol. Intermount. West 6, 77–92.

Gorman II, M.A., Miller, I.M., Pardo, J., Small, B.J., 2008. Plants, fish, turtles, and insects from the Morrison Formation: A Late Jurassic ecosystem near Cañon City, Colorado. In: Raynolds, R.G. (Ed.), Roaming the Rocky Mountains and Environs: Geological Field Trips. GSA Field Guide. Geological Society of America 10, p. 295.

Grimaldi, M., Engel, M.S., 2005. Evolution of the Insects. Cambridge University Press, Cambridge, UK.

Harper, C.J., Taylor, T.N., Krings, M., Taylor, E.L., 2016. Structurally preserved fungi from Antarctica: diversity and interactions in late Paleozoic and Mesozoic polar forest ecosystems. Antarct. Sci. 28 (3), 153–173.

Hasiotis, S.T., 2004. Reconnaissance of Upper Jurassic Morrison Formation ichnofossils, Rocky Mountain Region, USA: paleoenvironmental, stratigraphic, and paleoclimatic significance of terrestrial and freshwater ichnocoenoses. Sediment. Geol. 167, 177–268.

Hawkeswood, T.J., 2006. Review of the biology of *Prospheres aurantiopictus* (Laporte & Gory, 1837) (Coleoptera: Buprestidae). Calodema 5, 3–4.

Kervin, K., 2011. Pollinating fruit trees with blue orchard bees. Wild about Utah. https://wildaboututah.org/tag/blue-orchard-bees/ Last accessed on 29 July 2021.

Labandeira, C.C., 1998. The role of insects in Late Jurassic to Middle Cretaceous ecosystems. In: Lucas, S.G., Kirkland, J.I., Estep, J.W. (Eds.), Lower and Middle Cretaceous Terrestrial Ecosystems. New Mexico Museum of Natural History and Science Bulletin, vol. 14, pp. 105–124.

Labandeira, C.C., 2007. The origin of herbivory on land: the initial pattern of live tissue consumption by arthropods. Insect Sci. 14, 259–274.

Labandeira, C.C., 2013. Deep-time patterns of tissue consumption by terrestrial arthropod herbivores. Naturwissenschaften 100, 355–364.

Langenheim, J.H., 2003. Plant Resins: Chemistry, Evolution, Ecology, and Ethnobotany. Timber Press, Portland, Oregon.

Lara, M.B., Foster, J.R., Kirkland, J.I., Howells, T.F., 2020. First fossil true water bugs (Heteroptera, Nepomorpha) from Upper Jurassic strata of North America (Morrison Formation, southeastern Utah). Hist. Biol. 33, 1996–2004.

Manchester, S.R., Zhang, X., Hotton, C.L., Wing, S.L., Crane, P.R., 2021. Distinctive quadrangular seed-bearing structures of gnetalean affinity from the Late Jurassic Morrison Formation of Utah, USA. J. Syst. Palaeontol. 19, 743–760.

Mecke, R., Mille, C., Engels, W., 2005. *Araucaria* beetles worldwide: evolution and host adaptations of a multi-genus phytophagous guild of disjunct Gondwana-derived biogeographic occurrence. Pró-Araucária Online 1, 1–18.

Pereira, L.G., 2020. Mineralogy and Preservational Quality of Late Mesozoic Silicified Wood and Mineralized Dinosaur Bone. M.Sc. Thesis, University of Bonn, Germany.

Richmond, D., Lupia, R., Philippe, M., Klimek, J., 2019. First occurrence of the boreal fossil wood *Xenoxylon meisteri* from the Jurassic of North America: Morrison Formation of central Montana, USA. Rev. Palaeobot. Palynol. 267, 39–53.

Schwarze, F.W.M.R., Engels, J., Mattheck, C., 2000. Fungal Strategies of Wood Decay in Trees. Springer-Verlag, Berlin.

Smith, D.M., Gorman, M.A., Pardo, J.D., Small, B.J., 2011. First fossil orthoptera from the Jurassic of North America. J. Paleontol. 85, 102–105.

Smith, E.A., Loewen, M.A., Kirkland, J.I., 2020. New social insect nests from the Upper Jurassic Morrison Formation of Utah. Geology of the Intermountain West 7, 281–299.

Sprinkel, D.A., Bennis, M.B., Gray, D.E., Gee, C.T., 2019. Stratigraphic setting of fossil log sites in the Morrison Formation (Upper Jurassic) near Dinosaur National Monument, Uintah County, Utah, USA. Geology of the Intermountain West 6, 61–76.

Stubblefield, S.P., Taylor, T.N., 1985. Fossil fungi in Antarctic wood. Antarct. J. US 20 (5), 7–8.

Stubblefield, S.P., Taylor, T.N., 1986. Wood decay in silicified gymnosperms from Antarctica. Bot. Gaz. 147, 116–125.

Stubblefield, S.P., Taylor, T.N., Beck, C.B., 1985. Studies of Paleozoic fungi. IV. Wood-decaying fungi in *Callixylon newberryi* from the Upper Devonian. Am. J. Bot. 72, 1765–1774.

Taylor, T.N., Taylor, E.L., Krings, M., 2009. Paleobotany: The Biology and Evolution of Fossil Plants. Second edition. Academic Press, San Diego.

Taylor, T.N., Krings, M., Taylor, E.L., 2015. Fossil Fungi. Academic Press, San Diego.

Tian, N., Wang, Y., Zheng, S., Zhu, Z., 2020. White-rotting fungus with clamp-connections in a coniferous wood from the Lower Cretaceous of Heilongjiang Province, NE China. Cretac. Res. 105, 104014.

Tidwell, W.D., Ash, S.R., 1990. On the Upper Jurassic stem *Hermatophyton* and its species from Colorado and Utah, USA. Palaeontogr. Abt. B 218, 776–792.

Tidwell, W.D., Medlyn, D.A., 1993. Conifer wood from the Upper Jurassic of Utah, Part II: *Araucarioxylon hoodii* sp. nov. The Palaeobotanist 42, 70–77.

Tidwell, W.D., Skog, J.E., 1999. Two new species of *Solenostelopteris* from the Upper Jurassic Morrison Formation in Wyoming and Utah. Rev. Palaeobot. Palynol. 104, 285–298.

Trujillo, K.C., Kowallis, B.J., 2015. Recalibrated legacy $^{40}Ar/^{39}Ar$ ages for the Upper Jurassic Morrison Formation, Western Interior, U.S.a. Geology of the Intermountain West 2, 3–8.

Underwood, W., 2012. The plant cell wall: a dynamic barrier against pathogen invastion. Front. Plant Sci. 3 (85), 1–6.

USDA Forest Service, 2013. Field Guide to Insects and Diseases of Arizona and New Mexico Forests. United States Department of Agriculture, Forest Service, Southwestern Division. Available online at https://www.fs.fed.us/r3/resources/health/fieldguide/pdf/FieldGuide_AZ_NM.pdf Last accessed: 21 September 2021.

Wei, H.-B., Gou, X.-D., Yang, J.-Y., Feng, Z., 2019. Fungi–plant–arthropods interactions in a new conifer wood from the uppermost Permian of China reveal complex ecological relationships and trophic networks. Rev. Palaeobot. Palynol. 271, 104100.

Xia, G., Tian, N., Philippe, M., Yi, H., Wu, C., Li, G., Shi, Z., 2020. Oldest Jurassic wood with Gondwanan affinities from the Middle Jurassic of Tibetan Plateau and its paleoclimatological and paleoecological significance Review of Palaeobotany and Palynology 2020. Review of Palaeobotany and Palynology 281, 104283.

Xie, A., Gee, C.T., Bennis, M.B., Gray, D., Sprinkel, D.A., 2021. A more southerly occurrence of *Xenoxylon* in North America: *X. utahense* Xie et Gee sp. nov. from the Upper Jurassic Morrison Formation in Utah, USA, and its paleobiogeographic and paleoclimatic significance. Rev. Palaeobot. Palynol. 291, 104451.

Zabel, R.A., Morrell, J.J., 2020. Wood Microbiology: Decay and its Prevention. Second edition. Academic Press, San Diego.

Chapter 4

Ancient Basidiomycota in an extinct conifer-like tree, *Xenoxylon utahense*, and a brief survey of fungi in the Upper Jurassic Morrison Formation of USA

Publication

Xie, A.[1], Tian, N., and Gee, C.T., in revision, Ancient Basidiomycota in an extinct conifer-like tree, *Xenoxylon utahense*, and a brief survey of fungi in the Upper Jurassic Morrison Formation of USA: Journal of Paleontology, submitted in March 2022.

Author contributions

Xie and Tian designed the study. Xie and Gee collected the fossil wood. Xie made the thin-sections in the lab, studied the thin-sections, took micrographs, analyzed the fungal structures, wrote the preliminary manuscript, and created all the figures and plates. Tian and Gee revised the manuscript. Gee obtained funding for fieldwork.

Abstract from the submitted manuscript

Although the world-famous Upper Jurassic Morrison Formation has yielded abundant fossil plants since the first cycad fossil was reported in 1900, relatively little is known about the ecological interactions between the Morrison plants and fungi. Over two decades ago, the first evidence of fungal decay was noted in the fossil flora, and since then, a few more investigations on fungal interactions in Morrison plants have been published. However, up to now, detailed studies in paleomycology have not been carried out. Here we describe well-preserved fossil mycelia in detail in a silicified log of

[1] Corresponding author.

Xenoxylon utahense Xie et Gee from the Upper Jurassic Morrison Formation at Miners Draw, Blue Mountain, near Vernal in northeastern Utah, USA. The fungal hyphae are straight, slightly curved, highly coiled, or tubular in shape, measuring ca. 1.53 μm in diameter, and possess septa and clamp connections. The occurrence of typical clamp connections indicate a taxonomic affinity to the Basidiomycota, which are interpreted here as saprotrophs based on the patterns of wood decay in the *Xenoxylon* log. These fossil mycelia represent a new record of fossil Basidiomycota from the Upper Jurassic Morrison Formation in the state of Utah and provides further evidence for plant–fungal interactions in Jurassic terrestrial ecosystems.

Ancient Basidiomycota in an extinct conifer-like tree, *Xenoxylon utahense*, and a brief survey of fungi in the Upper Jurassic Morrison Formation of USA

Aowei Xie[1,*], Ning Tian[2], and Carole T. Gee[1,3,4]

[1]Institute of Geosciences, Division of Paleontology, University of Bonn, Nussallee 8, 53115 Bonn, Germany <awxie@uni-bonn.de; cgee@uni-bonn.de>

[2]College of Palaeontology, Shenyang Normal University, Shenyang 110034, China <tianning84@163.com>

[3]Huntington Botanical Gardens, 1151 Oxford Road, San Marino, California 91108, USA

[4]State Key Laboratory of Palaeobiology and Stratigraphy, Nanjing Institute of Geology and Palaeontology, CAS, Nanjing 210008, China

[*]Corresponding author.

4.1. Introduction

Although ecological associations between plants and fungi can be traced back to the Early Devonian times, ca. 400 million years ago (Stubblefield et al., 1985; Taylor et al., 2015), plant–fungal interactions are relatively poorly known throughout the geological history. In 1921, the Early Devonian plant–fungal interactions were described by Kidston and Lang on the basis of the ecological association between plant remains (e.g., *Aglaophyton major*) and fungi from the Lower Devonian Rhynie Chert in Scotland, which has yielded one of the most spectacular early terrestrial ecosystems throughout earth history. The scarcity of paleomycological reports is likely due to the inconspicuous fungal decay patterns in ancient plants, the microscopic size of many fungi, and the type of preservation in fossil plants.

Three major types of preservation are commonly recognized in fossil plants, namely, impressions, compressions, and permineralizations (Taylor et al., 2009). On impressions, it is extremely difficult to discover evidence of plant–fungal interactions, although some fossil leaves with

various spots had been interpreted as fungal remains in older reports (Unger, 1841; Meschinelli, 1898). On compressions, morphologically similar fungal structures, namely, small and black specks, are commonly found on the surface of leaf compressions or on cuticles, which have been studied as fungal remains using the scanning electron microscope (e.g., Alvin and Muir, 1970; Abu Hamad et al., 2008; Maslova et al., 2021). Compared to impressions and compressions, silicified plant remains provide the best fossil evidence of plant–fungal interactions (Taylor et al., 2015). For example, silicified woods, which are much more common than the foliar or reproductive organ remains of plants in sediments (Martín-Closas and Gomez, 2004; Philippe et al., 2004), have been widely found worldwide for hundreds of years (cf. Gothan, 1905). In recent years, there has been an increasing awareness of fossil fungal remains, especially of wood-decay fungi in permineralized woods (e.g., César et al., 2012; Harper et al., 2012, 2016; García et al., 2012; McLoughlin and Strullu-Derrien, 2016; Sagasti et al., 2019; Tian et al., 2020; Gee et al., 2022).

A silicified log with anatomically well-preserved wood was discovered in the Salt Wash Member of the Upper Jurassic Morrison Formation at the Miners Draw area in northeast Utah, USA, with structurally preserved fungal hyphae. The fossil log was recognized as a conifer-like tree *Xenoxylon utahense* Xie et Gee (Xie et al., 2021). The possible affinities of the fungi and the fungal decay pattern in the wood host are discussed. The present finding sheds new light on plant–fungal interactions in the Morrison ecosystems during the Late Jurassic times.

4.2. Geological setting

The fungal hyphae were found in a piece of wood collected from a fossil log from the Upper Jurassic Morrison Formation in Miners Draw, Blue Mountain, about 30 km southeast of Vernal in Utah, USA (Fig. 1). At this locality, the fossil wood-bearing strata occur as a series of light greenish-gray to brownish-gray, silty to very fine-grained sandstone with an exposed thickness of ca.10 m (Fig. 2; Gee et al., 2019; Sprinkel et al., 2019). Stratigraphically, the strata pertain to the Salt Wash Member of the Upper Jurassic Morrison Formation (Sprinkel et al., 2019). The Morrison Formation was originally established by Eldridge in the U.S. Geological Survey Monograph in 1896 (Eldridge, 1896) and consists of four members in northeastern Utah—the Windy Hill, Tidwell, Salt Wash, and Brushy Basin Members (Hasiotis, 2004; Sprinkel et al., 2019).

At Miners Draw, the Salt Wash Member of the Morrison Formation was divided into only three beds owing to part of the outcrop being covered (Sprinkel et al., 2019). The fossil wood specimen was collected from a log 3.0 m of a 4.3 m-thick silty sandstone, which crops out 21 m above the base of the Salt Wash Member (Fig. 2). The fossil log occurs 3.0 m above the base of the silty sandstone unit and 7.8 m below the top of the member. In Miners Draw, the Salt Wash Member represents a fluvial–lacustrine sedimentary environment (Sprinkel et al., 2019).

As described by Xie et al. (2021), the tree host is a fossil log with a preserved maximum diameter of 90 cm. Using new models to predict the height of a conifer tree from its diameter based on height–diameter relationships of living conifers, the Miner Draw tree has been estimated to have reached at a minimum height of about 40 m (Xie et al., 2021).

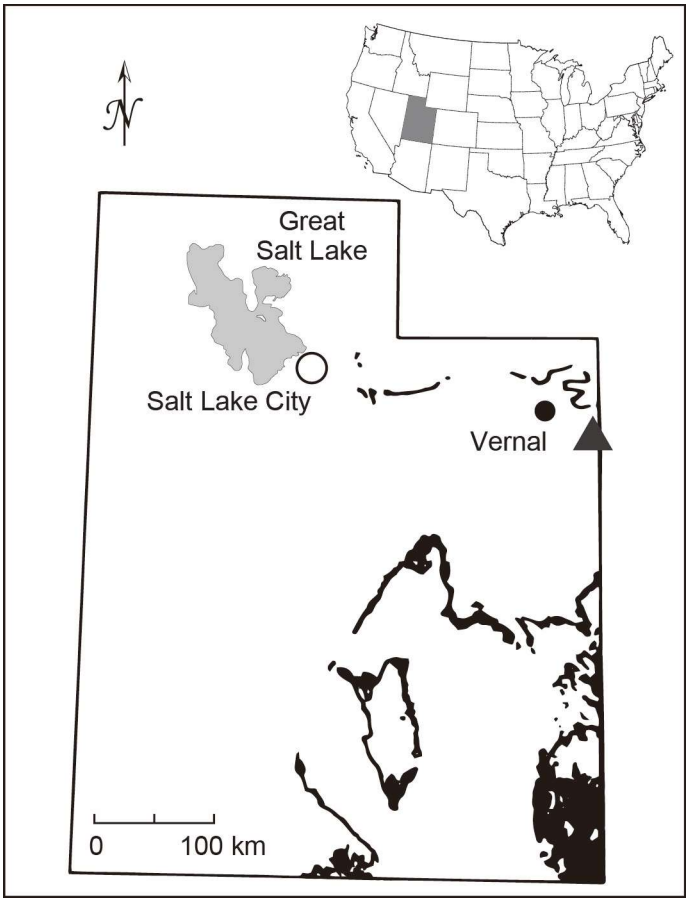

Figure 1. Map of fossil locality (triangle) bearing the fossil log of *Xenoxylon utahense* in Miners Draw near Vernal (solid circle), Utah (dark gray in inset), USA, superimposed on the outcrops of the Upper Jurassic Morrison Formation (black). Morrison outcrop map courtesy of Kenneth Carpenter.

4.3. Materials and methods

Three specimens of fossil wood were cut transversely, radially, and tangentially to make standard petrographic thin-sections in the three planes of section. In a reinvestigation of the thin sections

containing the type specimen of *X. utahense*, abundant and well-preserved fungal remains represented by fungal hyphae were found inside the wood tissue. They were studied and photographed using software ImageAccess easyLab 7 software adapted to a Leica DM2500 compound photomicroscope.

4.3.1. Repositories and institutional abbreviations

Wood samples are deposited at the Utah Field House of Natural History State Park Museum (FHNHM), Utah, USA, under FHPR Catalog Number FHPR11386. Thin-sections of the three samples are logged into the system at the University of Bonn, Bonn, Germany, as BMT-001a, BMT-001b, and BMT-001c.

4.4. Results

4.4.1. Tree host

The fossil log at Miners Draw area was previously recognized as *Xenoxylon utahense* Xie et Gee (Xie et al., 2021), an extinct gymnosperm which may pertain to the extinct family Miroviaceae (cf., Nosova and Kiritchkova, 2008; Philippe et al., 2013). *Xenoxylon utahense* is a conifer-like wood, dominated by tracheids and ray parenchyma, and lacking axial parenchyma and resin canals. Tracheid pitting on radial walls are mostly uniseriate, but also biseriate; when uniseriate, the bordered pits are strongly flattened. Cross-field pitting is fenestriform in type, with a single, large, simple pit which occupies nearly the entire crossfield, or occasionally two smaller oopores. Ray cells are mostly uniseriate, occasionally biseriate, homocellular, parenchymatous, with smooth and unpitted horizontal and end walls.

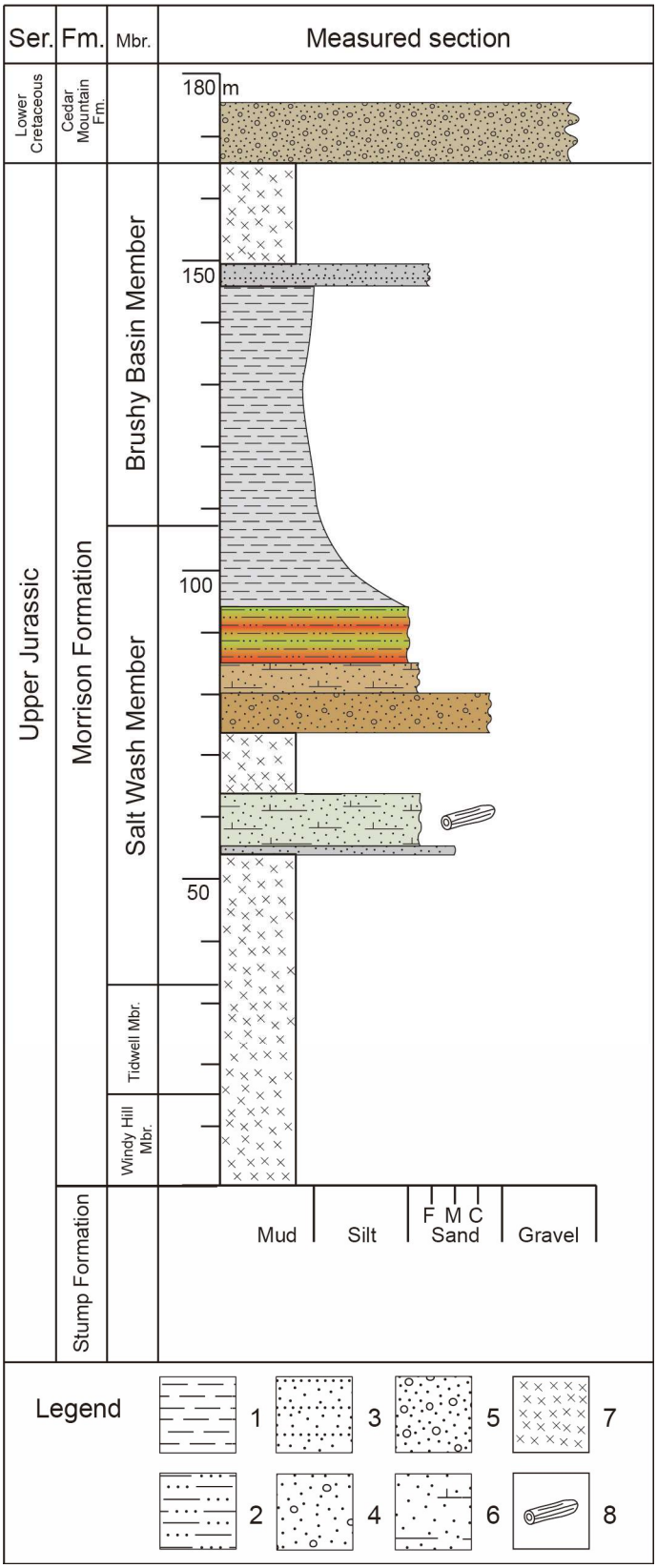

Figure 2. Lithostratigraphic column of the Upper Jurassic Morrison Formation in Miners Draw near Vernal, Utah, USA. Legend: (1) mudstone; (2) siltstone; (3) sandstone; (4) conglomeratic sandstone; (5) conglomerate; (6) silty sandstone; (7) covered and not measured outcrop; (8) fossil log. Section modified after Sprinkel et al. (2019).

4.4.2. Wood decay and fungal remains

The secondary xylem of the Miners Draw wood is strongly decayed by fungi. Abundant, well-preserved fungal remains are present, which are represented by the mycelia comprised of fungal hyphae distributed in the secondary xylem of the tree host. The transverse view of the tracheids shows wood decay at various stages, including during the decomposition of the middle lamellae (Fig. 3.1–4.4) and separation of the tracheid wall (Fig. 3.4). In the strongly decayed zone (decolored zone), only the faint outlines of tracheid walls are preserved (Fig. 3.5 and 3.6) and the tracheid pitting on radial walls can no longer be observed (Fig. 3.5 and 3.6).

The fungal hyphae run more or less vertically through the tracheids (Fig. 4.1–4.6), but are also able to penetrate through the ray cell walls (Fig. 4.7). Locally, some fungal hyphae are discontinuous, which morphologically seem to resemble so-called oidia (Fig. 4.2 and 4.3, white arrowhead). In the tracheid lumina, the fungal hyphae are straight, lightly curved (Fig. 4), highly coiled, or pseudosclerotia-like (Fig. 5.1, 5.2, and 5.8, white arrow), with a diameter from 1.21 to 2.09 μm, 1.53 μm on average. The hyphae are tubular in morphology and smooth-walled (Figs. 4 and 5). The cross walls of the hyphae, also called, septa, can be observed in some hyphae, which occurs near bifurcations (Fig. 5.3, black arrowhead). The hyphae can pass through the cross-fields, which also illustrate that the hyphae are capable of penetrating the walls of the ray parenchyma cells (Fig. 4.7). Globose swellings that may represent asexual fungal spore chlamydospores are also observed to be attached to hyphae. A large number of typical clamp connections are present in the hyphae (Fig. 5.4–5.9, black arrows). Tyloses are locally present in the tracheids, with the globose structures measuring 8 μm in diameter (Fig. 4.9, white arrowhead).

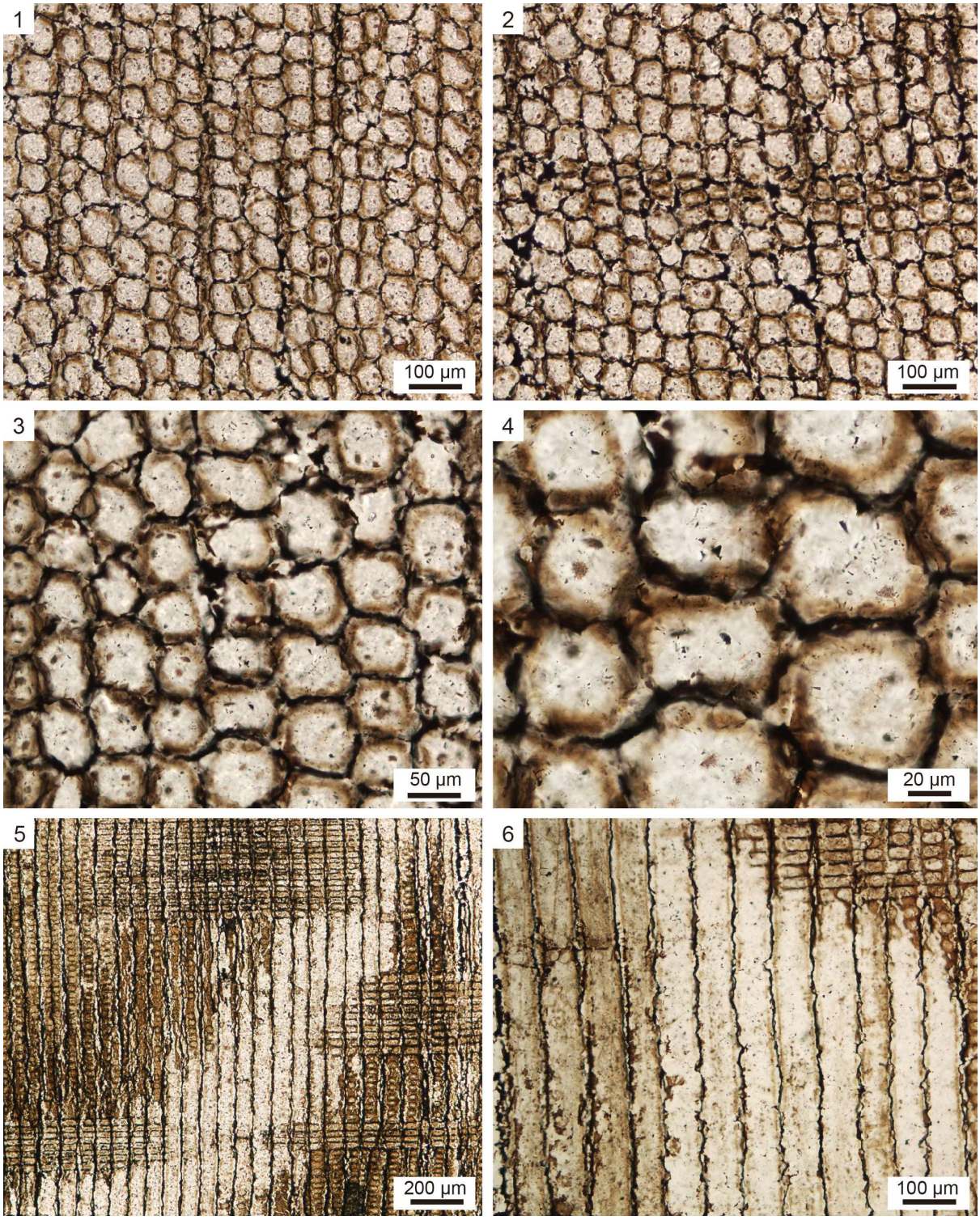

Figure 3. Tree host *Xenoxylon utahense* Xie et Gee from the Salt Wash Member of the Upper Jurassic Morrison Formation in Miners Draw, Blue Mountain, east of Vernal, Utah, USA: (1–2) cross section, showing the decomposition of middle lamellae between neighboring tracheids; (3–4) close-ups of (1) and (2), cross section, showing details of decomposition of middle lamellae; (5–6) radial section, showing the decomposition of middle lamellae between neighbor tracheids and faint outlines of tracheids in a strongly decayed and decolored zone.

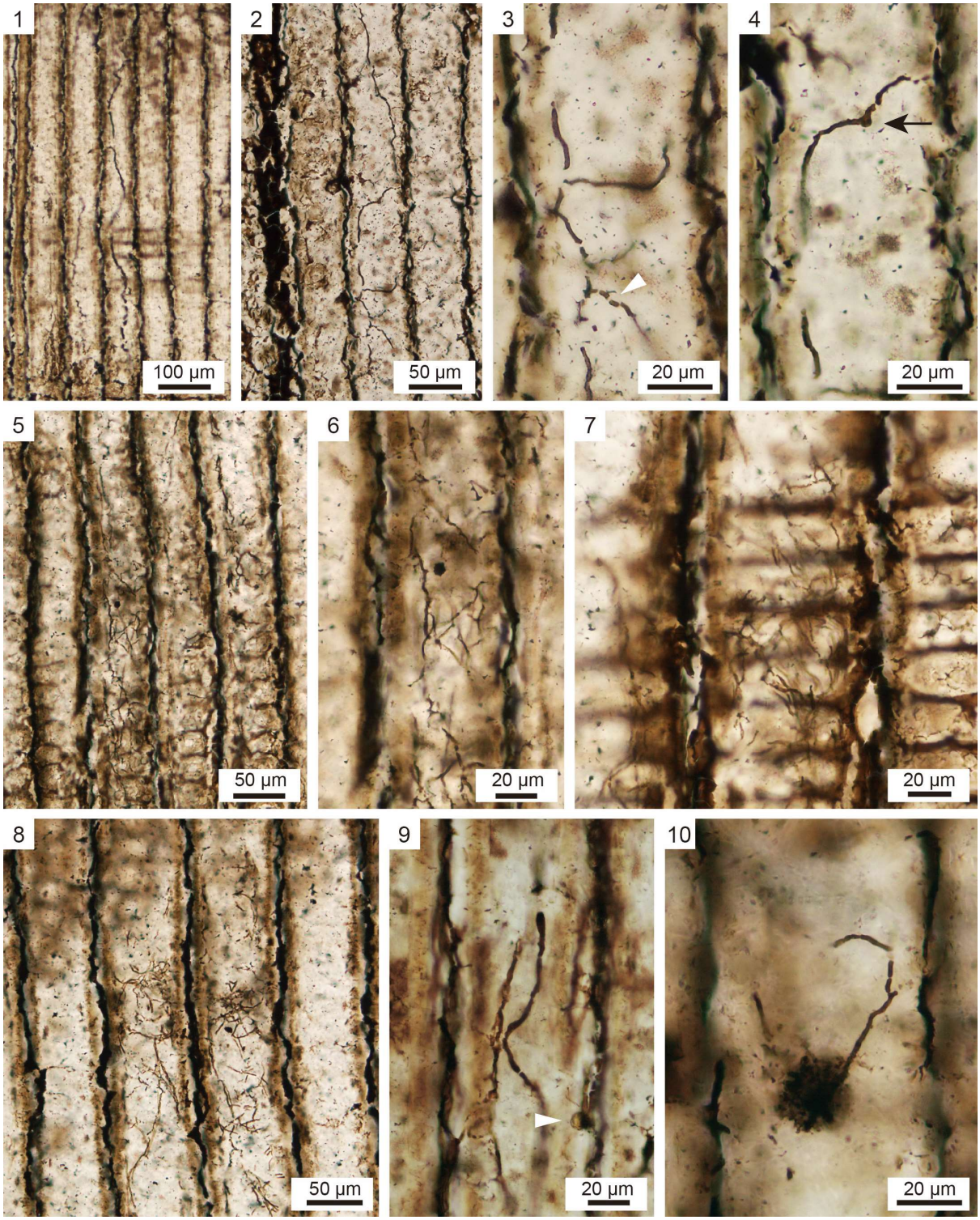

Figure 4. Radial section of thin sections of *Xenoxylon utahense* with fungal hyphae: (1) fungal hyphae passing through tracheid lumina; (2) fungal hyphae growing along the tracheid walls, with oidia and typical basidiomycetous clamp connections; (3) close-up of (2), with details of oidia (white arrowhead); (4) close-up of (2), with further details of clamp connection (black arrow); (5–6) abundant fungal hyphae in tracheids; (7) fungal hyphae penetrating the cross field zone; (8) abundant fungal hyphae growing in tracheids; (9) globose tylosis developing along the wall of one tracheid (white arrowhead); (10) detail of terminal chlamydospores.

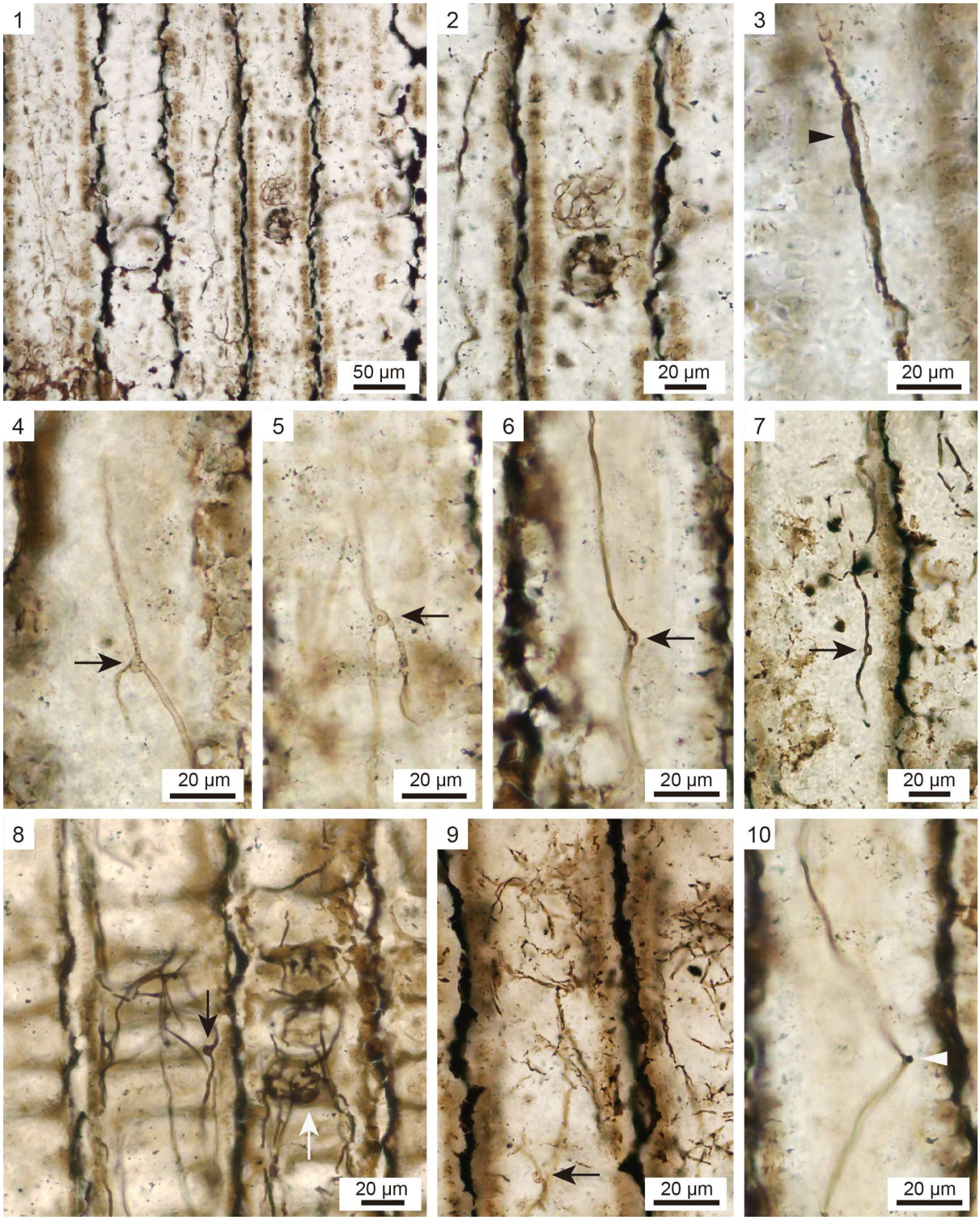

Figure 5. Radial section of thin sections of *Xenoxylon utahense* with fungal remains: (1) coiled fungal hyphae, likely pseudosclerotia; (2) close-up of (1), showing details of pseudosclerotia-like characters; (3) septum (black arrowhead) in a fungal hypha; (4–7) typical basidiomycetous clamp connections (black arrow); (8) pseudosclerotia-like feature (white arrow) and clamp connection (black arrow); (9) a typical clamp connection (black arrow); (10) probable intercalary chlamydospore (white arrowhead).

4.5. Discussion

4.5.1. Plant–fungal interactions and wood decay pattern in *Xenoxylon utahense*

In the Miners Draw wood, decolored pattern of wood tissue occurs in the secondary xylem, which is also found in modern white rot. In extant white rot, the fungal hyphae growing in the lumina of the tracheids produce decay enzymes that degrade the secondary wall of the tracheids during an early stage of simultaneous rot. Then, in a later stage, the secondary wall and the primary wall of the tracheids, and middle lamella are partially broken down, which results in the tracheid wall being thinner, and individual tracheid cells being somewhat separated from one another (Schwarze et al., 2000; Schwarze, 2007). These characters are well-developed in the decayed areas of the Miners Draw wood, which shows tracheids with the colonization by fungal hyphae and various cell wall alterations, including locally removal of the middle lamella, decomposition of the secondary wall of tracheids, and cell wall separation. Hence, these fungal damage characters indicate that wood decay in the Miners Draw tree had already reached the advanced stage of simultaneous white rot.

4.5.2. Fossil fungi and wood decay pattern

Although fungi have existed on the earth for perhaps more than one billion years (Parfrey et al., 2011; Berbee et al., 2017; Loron et al., 2019), evidence of fungi in the fossil record is relatively rare, not to mention evidence of plant–fungal interactions. The rarity of fungal records is very likely due to the small size of fungal structures and their cryptic lifestyles (Taylor and Taylor, 1997). In general, fungi are mainly associated with plants in three types of ecological interactions, which are parasitism, mutualism, and saprophytism (Newsham et al., 1995). Compared to parasitism and mutualism, saprophytism is the most common plant–fungal interaction (Schwarze et al., 2000; Schmidt, 2006) and plays a significant role in carbon recycling in ancient ecosystems (Stubblefield and Taylor, 1988; Taylor, 1993; Taylor and Krings, 2010; Taylor et al., 2015; Tian et al., 2021). For example, a fossil record of plant–fungal interactions from the Upper Devonian in Indiana, USA, was interpreted as saprophytism based on wood-decay structures (Stubblefield et al., 1985).

In regard to saprotroph, the wood-decay fungi are separated into three primary types in modern

woods according to their pattern of degradation process in wood: brown rot, white rot, and soft rot (Schwarze et al., 2000; Schwarze, 2007; Taylor et al., 2015). The brown rot and soft rot fungi usually destroy the thick middle layer (S_2) of secondary cell wall of tracheids first, whereas the white rot fungi generally bleach the wood tissue and degrade lignin, cellulose, and hemicellulose (Schwarze et al., 2000). Based on the degradation sequence of wood polymers, there are two major patterns that have been recognized in white rot, namely, selective delignification and simultaneous rot (Adaskaveg and Gilbertson, 1986; Rayner and Boddy, 1988). Simultaneous rot mainly occurs on broad-leaved trees but seldom on conifers, while selective delignification occurs on both broad-leaved trees and conifers, which is characterized by the initial degradation of lignin and hemicellulose of the cell walls of tracheids. This initial stage is then followed by degradation of cellulose in the cell walls (Schwarze et al., 2000).

4.5.3. Probable affinity of the fungus in *Xenoxylon utahense*

In general, the morphology of sexual reproductive organs is essential to the taxonomic identification of extant fungi. However, because the preservation of reproductive organs in fossil fungi is rare and the number of paleobotanical studies on fungi few, the systematic identification of fossil fungi is extremely difficult. Even so, the recognition of other diagnostic structural features has been recognized as a practical approach to identifying certain ancient fungi. For example, the structural character of clamp connections—a hyphal protrusion during cell division to maintain the binucleate (dikaryon) condition—is commonly used to identify fossil Basidiomycota in the absence of sexual reproductive structures (Krings et al., 2011; Taylor et al., 2015).

In the *Xenoxylon* wood from Miners Draw area, there are three lines of evidence that support the white rot fungus pertaining to the Basidiomycota, which are clamp connections, oidia, and pseudosclerotia-like features. The first and most conspicuous line of evidence in the *Xenoxylon* wood are the fungal hyphae with typical clamp connections, which are abundant in the fungal hyphae. The oldest fossil record of Basidiomycota with clamp connections was reported from the upper Visean of the Mississippian in France, which was found in the Carboniferous fern rachis *Botryopteris antiqua* (Krings et al., 2011), although molecular clock analysis suggests that the first Basidiomycota originated during the Cambrian times (Berbee and Taylor, 2001; Oberwinkler, 2012). Similar clamp

connections have also been described from the Pennsylvanian of North America (Denis, 1969, 1970), Lower Permian of North China (Wan et al., 2017), Triassic of Antarctic (Stubblefield and Taylor, 1986; Osborn et al., 1989), Jurassic of southwestern China (Feng et al., 2015), Lower Cretaceous of northeastern China (Tian et al., 2020), and Cretaceous of Mongolia and eastern China (Hsü, 1953; Krassilov and Makulbekov, 2003; Zhu et al., 2018).

Up to now, only three morphogenera have been established within fossil Basidiomycota on the basis of mycelia: *Palaeancistrus* Dennis, *Palaeofibulus* Osborn, Taylor et White, and *Palaeosclerotium* Rothwell (Dennis, 1970; Rothwell, 1972; Osborn et al., 1989). The first genus, *Palaeancistrus*, is defined by septate fungal hyphae with clamp connections, along with branching at mostly right angles (Dennis, 1970). The second genus, *Palaeofibulus*, is characterized by hyphal filaments with incomplete clamp connections (Osborn et al., 1989). The third genus, *Palaeosclerotium*, is recognized by fungal sclerotia, which are branched septate hyphae (Rothwell, 1972). However, when the type specimen of *Palaeosclerotium* was reexamined by Singer in 1977, he suggested that *Palaeosclerotium* shared affinities with the extant Ascomycota, an assessment that agrees with the conclusions of Dennis (1976). The fossil mycelia bearing septate fungal hyphae with typical clamp connections in the *Xenoxylon* tree from Miners Draw best correspond to the morphological features of *Palaeancistrus*.

Besides the clamp connections, there are two other diagnostic structural characters of fungal hyphae have been recognized in the Miners Draw wood. For example, the second line of evidence for the white rot fungus in the *Xenoxylon* wood that points to Basidiomycota is the oidia, which are produced by the breakup of the fungal hyphae (Schwarze et al., 2000).

The third line of evidence linking the possible affinity of white rot fungus in the *Xenoxylon* wood to Basidiomycota is the presence of pseudosclerotia-like features, which are inflated and bladder-like multicellular organs. For example, in *Polyporus squamosus* of Basidiomycota, pseudosclerotia form a defense function to keep pathogens out when affected by other fungi and unfavorable conditions (Schwarze et al., 2000).

4.5.4. Plant–fungal interactions in the Morrison Formation

Abundant fossil plants have been reported from the Upper Jurassic Morrison Formation for over

a century, however, little is known from the ecological interactions between the Morrison plants and fungi. It was only 22 years ago that the first mention of plant–fungal interactions in the Morrison Formation. Tidwell (1990) found fungal remains are preserved in some fossil woods and shoots, which represents the first report of plant–fungal interactions in the Morrison ecosystem during the Late Jurassic times. Tidwell (1990) noted numerous bore holes present in the tracheid walls, and suggested that these ancient trees had been decayed by a white rot fungus similar to *Polyporus* of the extant Basidiomycota (Tidwell, 1990). Although some other fungi can also produce bore holes in wood cell walls, such as blue stain fungi (Strullu-Derrien et al., 2022), howerer, the holes caused by these blue stain fungi were with a relatively smaller diameter, since they were made by the direct mechanical destruction of hyphae, rather than by chemical decomposition. The wood decay patterns in Tidwell's woods are the same as those found in the *Xenoxylon* wood from Miners Draw.

Another line of evidence supporting the plant–fungal interactions in the Morrison times are the abundant small and star-shaped decayed areas that were observed in the fossil conifer woods at the Mygatt-Moore Quarry (MMQ) in Colorado and recognized as modern brown rot (Tidwell et al., 1998). Moreover, Tidwell and colleagues proposed that the fungus in MMQ woods is similar to *Stereum sanguionolentum* of extant Stereaceae, although we argue for a white rot pattern on the basis of numerous disconnected, distorted, and collapsed tracheids in the MMQ woods.

Similar white rot decay has also been recently found in a giant *Agathoxylon* tree from the Upper Jurassic Morrison Formation in Rainbow Draw near Dinosaur National Monument in Utah. In the wood of this *Agathoxylon* log, the different fungal decay stages can be observed in neighbor cells. While the cell wall of a tracheid can appear seemingly intact, uniform, and dark in color, the cell wall of a neighboring tracheid can appear to have lost color in only one small part (Gee et al., 2022). In this *Agathoxylon* wood, the weakened and decomposed areas of wood tissue decayed by fungi facilitated the boring of large-diameter, vertical galleries by insects, most likely beetle larvae.

Beyond microscopical evidence of fungal decay, macroscopical characters have also been used to understand the relationship between plants and fungi in the Upper Jurassic Morrison Formation. For instance, small to large cavities measuring 1–5 cm in diameter, were found in the heartwood of a fossil conifer wood from the Morrison Formation, which was interpreted as the infestation of the tree by fungi (Hasiotis, 2004). However, the maker of these cavities may still be open to interpretation, because similar cavities can also be produced by beetles (e.g., Ponomarenko, 2003; Naugolnykh and

Ponomarenko, 2010; Feng et al., 2017; Gee et al., 2022).

Here, the newly reported plant–fungal interaction offers us more evidence into understanding the complex network of interrelationships in the Upper Jurassic, however, for a deeper and more comprehensive knowledge of trophic interactions in Morrison ecosystems further research is needed. Other ecological interactions between Morrison plants and fungi, such as parasitism and mutualism, have not been documented; up to now, only saprotrophic wood-decay fungi have been reported (Tidwell, 1990; Tidwell et al., 1998; Gee, 2015; Gee et al., 2022).

4.6. Conclusions

A new occurrence of plant–fungal interactions is described from the Upper Jurassic Morrison Formation at the Miners Draw area near Vernal in northeastern Utah. This wood-decay pattern is characterized by decolored wood tissue irregularly present in the secondary xylem, removal of the middle lamella, partial decomposition of the secondary wall in the tracheids, and tracheid wall separation, which are similar to the decay pattern in extant white rot. Abundant, well-preserved fungal hyphae with typical clamp connections, oidia, and pseudosclerotia-like features in the tracheids of Miners Draw wood shows that the white rot fungus in the Miners Draw wood is morphologically similar to the fossil genus *Palaeancistrus*. This new fossil discovery represents the first reliable record of Morrison Basidiomycota in Utah, which offers further evidence for paleomycological diversity in the Morrison Formation and sheds new light on plant–fungal interactions in the Morrison ecosystems during the Jurassic times.

4.7. Acknowledgments

We thank Mary Beth Bennis and Dale E. Gray, Utah Field House of Natural History State Park Museum, for guiding us to the fossil site; Yongdong Wang, Nanjing Institute of Geology and Palaeontology, CAS, for help in the field; and Steven Sroka, Utah Field House of Natural History State Park Museum for logistical support; Kenneth Carpenter for the outcrop map incorporated in figure 1; Douglas A. Sprinkel, Azteca Geosolutions, for the use of figure 2. Financial support from the China Scholarship Council for the doctoral studies of AX (CSC no. 201804910527) is gratefully

appreciated. Fieldwork funding from Open Funding grant no. 193101 from the State Key Laboratory of Palaeobiology and Stratigraphy (Nanjing Institute of Geology and Palaeontology, CAS) State Grant to CTG also supported this study. This is contribution no. 44 of the DFG Research Unit FOR 2685 "The Limits of the Fossil Record: Analytical and Experimental Approaches to Fossilization."

Chapter 5

Modeling the height–diameter relationship of living *Araucaria* trees to reconstruct ancient conifer height

Publication

Xie, A., Gee, C.T., and Griebeler, E.M., in prep. (nearing completion and subsequent submission), Modeling the height–diameter relationship of living *Araucaria* trees to reconstruct ancient conifer height.

Author contributions

Xie, Gee, and Griebeler designed the study. Xie collected the data, created all the text figures, and wrote the preliminary manuscript. Xie and Griebeler performed the statistical analysis. Griebeler wrote the R script. Griebeler and Gee revised the manuscript and guided the research with their excellent supervision.

Abstract from the manuscript

To reconstruct a fossil forest in three dimensions, an accurate estimation of tree height is crucial. However, modeling the height–diameter relationship of ancient trees is difficult, because the stems of woody fossil plants are usually fragmentary, which makes the direct measurements of their heights impossible. One practical approach for reconstructing the ancient tree height is to apply growth models based on the height–diameter relationships of the nearest living relatives of the fossil taxa. Here we applied 19 growth models to describe height–diameter relationships of living *Araucaria* trees to establish good growth models for ancient Araucariaceae trees. Data came from four living populations of the genus *Araucaria*: *Araucaria bidwillii* and *A*. *cunninghamii* in Queensland,

Australia, and *A*. *cunninghamii* and *A*. *hunsteinii* in New Guinea. According to AIC-based model selection, a power model with an exponent of 0.67 (hereafter the modified Mosbrugger model) was the best for each population and the entire dataset (157 trees), but normalization constants differed across populations. To find the best models for the genus *Araucaria*, 100 random samples (each population generating 25 random samples) from the entire dataset were used. Based on 100 curve fitting results on each model and multiple performance criteria, three median models were generated from the medians of their parameter estimates throughout the 100 random samples. The median Power model worked best for *Araucaria*, with the modified Mosbrugger model and Curtis model performing similarly well. We apply these three models to revise the existing height estimates of Late Jurassic araucariaceous logs in Utah, USA, to produce more accurate reconstructions of the ancient trees.

Modeling the height–diameter relationship of living *Araucaria* trees to reconstruct ancient conifer height

Aowei Xie[1,*], Carole T. Gee[1,2], and Eva M. Griebeler[3]

[1]Institute of Geosciences, Division of Paleontology, University of Bonn, Nussallee 8, 53115 Bonn, Germany; awxie@uni-bonn.de

[2]Huntington Botanical Gardens, 1151 Oxford Road, San Marino, California 91108, USA

[3]Institute of Organismic and Molecular Evolution, Evolutionary Ecology, Johannes Gutenberg-University, Mainz 55099, Germany

[*]Corresponding author.

5.1. Introduction

Although forests have played a dominant role in terrestrial ecosystems on earth for more than 300 million years (Berry and Marshall, 2015), the most informative evidence of ancient forests is usually preserved in the geological record as fossil stumps in original growth position or fossil logs. Fossil forests with in-situ stumps contain detailed information about the three-dimensional structure of the vegetation, such as taxonomy, tree density, tree age, height distribution and biomass (Mosbrugger et al., 1994), while fossil log assemblages offer information on tree age, height, and taxonomy. For instance, a silicified log flora described from the Upper Jurassic Morrison Formation at Rainbow Draw area in Utah, USA, contained variously sized tree trunks ranging from 71 to 127 cm in maximum preserved diameter, which were used as the basis for estimating the height of ancient trees. The largest log was reconstructed as a tree with a minimum height of 28 m, and the log assemblage was interpreted as forming a forest of large conifer trees that attained individual ages of over 100 years (Gee et al., 2019).

In present-day habitats, using the measurement of diameter at breast height (DBH) to estimate tree height has been implemented in practice management and silvicultural research, because DBH is more efficiently measured than tree height, yet is strongly correlated with tree height. Therefore,

height–diameter models commonly applied in forestry, are essential for the estimation of tree heights. Additionally, the estimation of biomass, stem basic density, growth and yield, and stand development over time in multilayered stands relies heavily on accurate height–diameter models (Huang et al., 1992; Temesgen et al. 2014; Nord-Larsen 2015; Sillett et al., 2019). It has also been shown that height–diameter models can even be used to estimate leaf, bark, cambium, sapwood, and heartwood quantities (Sillett et al., 2019).

For living trees, different models have been proposed to determine the height–diameter relationships in different species, regions, and ecological zones (Feldpausch et al., 2011; Temesgen et al., 2014; Chai et al., 2018), owing to multiple factors influencing tree growth. However, proposing specific height–diameter models is often not possible for ancient trees, because the stems of fossil plants are usually fragmented, which makes the direct measurements on the height–diameter of extinct plants rarely available (Thomas and Watson, 1976; Stewart et al., 1993; Taylor and Taylor, 1993). The practical approach of modeling height–diameter relationship for ancient trees is based on the nearest living relatives of the fossil taxa. Up to now, three height–diameter models have been commonly applied to the height reconstruction of fossil trees. In 1990, Mosbrugger and colleagues proposed a Power equation with an exponent off 0.67 for estimating the height of ancient trees based on the material strength of wood using Young's modulus and the specific weight of the wood of living conifers (Mosbrugger, 1990; Mosbrugger et al., 1994). In 1994, the second approach was proposed by Niklas based on the manner in which woody stems taper in girth along their length; this resulted in a curvilinear equation for estimating overall fossil plant height (Niklas, 1994). The third approach was taken five years later by Pole, who looked at the diameter and height data for three extant species of *Araucaria* growing in natural forests in Australia and New Guinea (Pole, 1999) and used a power model with an exponent fixed to 0.67 on height–diameter relationship. As the normalization constant of Pole's equation (1999) is about twice up to three times that in the Mosbrugger equation applied to conifers, Pole concluded that the heights of living trees are distinctly higher for any given diameter than the Mosbrugger curve would predict. All three approaches for the estimation of ancient tree heights were developed on the basis of tree architecture in living forests.

Here, we collected height–diameter data of living *Araucaria* from the scientific literature, which comprised four populations—*Araucaria bidwillii* and *A. cunninghamii* in Queensland, and *A. cunninghamii* and *A. hunsteinii* in New Guinea. We then established good height–diameter growth

models for each population and the whole dataset by ranking 19 different nonlinear height–diameter models and for the genus *Araucaria* by several model performance criteria. The final best growth models established for the genus *Araucaria* passed multiple performance criteria; each is based on 100 random samples from the whole dataset and can be applied to reconstruct ancient araucariaceous tree heights to have good estimates of tree height based on the maximum preserved diameter of fossil logs or stumps.

5.2. Materials and methods

5.2.1. Datasets on *Araucaria* trees

We compiled datasets on tree height–diameter information from three *Araucaria* species: *Araucaria bidwillii* (Pole, 1999), *A. cunninghamii* (Gray, 1975; Pole, 1999), and *A. hunsteinii* (Paijmans, 1970; Gray, 1975). These datasets had originally been collected to determine the size composition of natural stands, describe forest structure, or analyze height–diameter relationships. However, standard in each of these studies was taking the diameter at breast height (DBH) of each tree trunk and the height (H) of the respective tree. In our study, we used both measurements to establish the height–diameter growth models presented here.

Table 1. *Araucaria* species, localities, source of DBH-height records of this population, and population number designated here.

Species	Locality	Source Study
A. hunsteinii	New Guinea	Paijmans, 1970; Gray, 1975
A. cunninghamii	New Guinea	Gray, 1975
A. cunninghamii	Queensland, E. Australia	Pole, 1999
Araucaria bidwillii	Queensland, E. Australia	Pole, 1999

In total, we collected and analyzed the height–diameter data of 157 *Araucaria* trees. These trees had grown in different forests of New Guinea and eastern Australia (Queensland). Data were from trees inhabiting a diversity of forest habitats with variable floristic composition and site conditions and with varying heights. To have *Araucaria* trees growing in the same region and under roughly the

same climatic conditions, each tree from our whole dataset of 157 trees was assigned to one of four populations (Table 1), including *Araucaria bidwillii* and *A. cunninghamii* in Queensland, and *A. cunninghamii* and *A. hunsteinii* in New Guinea. In Queensland, 54 trees of *A. bidwillii* and 47 trees of *A. cunninghamii* were measured in the Bunya Mountains National Park (Pole, 1999). In New Guinea, *A. cunninghamii* (31 trees) and *A. hunsteinii* (25 trees) had all inhabited primeval forests in New Guinea (Paijmans, 1970; Gray, 1975). Thus, samples sizes substantially differed between populations.

To take into consideration that the height–diameter growth model(s) derived for the genus *Araucaria* could be biased towards the population with the largest sample, we modeled height against diameter not only for the whole dataset with 157 trees but also for 100 random samples taken from this dataset. Each random sample consisted of all 25 trees of *A. hunsteinii* from New Guinea, 25 randomly selected trees of *A. cunninghamii* from New Guinea, 25 randomly selected trees of *Araucaria bidwillii* from Queensland, and 25 randomly selected trees of *A. cunninghamii* from Queensland.

5.2.2. Height–diameter growth models considered

To find the best height–diameter growth model for each of the four populations, for each of the 100 random tree samples, and for all 157 trees, 19 height–diameter growth models were considered: Mosbrugger, Power, Niklas, von Bertalanffy, Näslund, Curtis, Schumacher, Meyer, Michaelis-Menten, Wykoff, Prodan, Logistic, Chapman-Richards, Weibull, Gompertz, Sibbesen, Korf, Ratkowsky, and Hossfeld IV (Table 2). All models are nonlinear and relate the height of an individual H (in meter) to its diameter D (in meter). They had been successfully applied to extant species, but their performance was rarely statistically tested against each other for *Araucaria*. Out of the 19 models, 16 models were already used in other studies on height–diameter relationships in extant species (Table 2) (Huang et al., 1992; Mehtätalo et al., 2015; Chai et al., 2018), whereas the other three, namely, Mosbrugger, Niklas, and von Bertalanffy models were so far never applied to rank height–diameter growth model for trees. These three growth models are thus briefly introduced hereafter.

Table 2. Nonlinear height–diameter growth models selected for establishing growth models for the genus *Araucaria*.

Model Name	**Function Type**	**Equation**	**References**
Mosbrugger	1-parameter	$H(D) = \mathrm{a}\ D^{0.67}$	Mosbrugger, 1990; Pole, 1999
Power	2-parameter	$H(D) = \mathrm{a}\ D^{\mathrm{b}}$	Stoffels and van Soest, 1953
Niklas	3-parameter	$\log_{10}H(D) = \mathrm{a} + \mathrm{b}(\log_{10}D) + \mathrm{c}(\log_{10}D)^2$	Niklas, 1994
von Bertalanffy	2-parameter	$H(D) = \mathrm{a} - (\mathrm{a} \times \exp(\mathrm{b}\ D))$	von Bertalanffy, 1938; 1957
Näslund	2-parameter	$H(D) = D^2 / (\mathrm{a}\ D + \mathrm{b})^2$	Näslund, 1937
Curtis	2-parameter	$H(D) = \mathrm{a}\ D / (1 + D)^{\mathrm{b}}$	Curtis, 1967
Schumacher	2-parameter	$H(D) = \mathrm{a} \times \exp(-\mathrm{b} / D)$	Schumacher, 1939
Meyer	2-parameter	$H(D) = \mathrm{a}\ (1 - \exp(-\mathrm{b}\ D))$	Meyer, 1940
Michaelis-Menten	2-parameter	$H(D) = \mathrm{a}\ D / (\mathrm{b} + D)$	Menten and Michaelis, 1913
Wykoff	2-parameter	$H(D) = \exp(\mathrm{a} - \mathrm{b} / (D + 1))$	Wykoff et al., 1982
Prodan	3-parameter	$H(D) = D^2 / (\mathrm{a}\ D^2 + \mathrm{b}\ D + \mathrm{c})$	Strand, 1959
Logistic	3-parameter	$H(D) = \mathrm{a} / (1 + \mathrm{b} \times \exp(-\mathrm{c}\ D))$	Pearl and Reed, 1920
Chapman-Richards	3-parameter	$H(D) = \mathrm{a}\ (1 - \exp(-\mathrm{b}\ D))^{\mathrm{c}}$	Richards, 1959
Weibull	3-parameter	$H(D) = \mathrm{a}\ (1 - \exp(-\mathrm{b}\ D^{\mathrm{c}}))$	Weibull, 1951
Gompertz	3-parameter	$H(D) = \mathrm{a} \times \exp(-\mathrm{b} \times \exp(-\mathrm{c}\ D))$	Gompertz, 1832
Sibbesen	3-parameter	$H(D) = \mathrm{a}\ D^{\mathrm{b}\ D^{-\mathrm{c}}}$	Sibbesen, 1981
Korf	3-parameter	$H(D) = \mathrm{a} \times \exp(-\mathrm{b} / D^{\mathrm{c}})$	Lundqvist, 1957
Ratkowsky	3-parameter	$H(D) = \mathrm{a} \times \exp(-\mathrm{b} / (D + \mathrm{c}))$	Ratkowsky, 1990
Hossfeld IV	3-parameter	$H(D) = \mathrm{a} / (1 + 1 / (\mathrm{b}\ D^{\mathrm{c}}))$	Peschel, 1938

Mosbrugger height–diameter growth model. The original Mosbrugger height–diameter model is based on a physical core principle, that is, any tree can be regarded as an upright and free-standing column that is stressed when it is loaded at the top by global buckling (Mosbrugger, 1990). Two parameters, Young's modulus and the specific weight of the column are used by its equation, see Eq. (1).

$$L_{\mathrm{g}} = \mathrm{C}\ (E/w)^{1/3}\ r^{2/3}, \tag{1}$$

where L_{g}, is the critical length (the free-standing column deforms by global buckling when length exceeds L_{g}, in meters), C equals 0.85 if a tree is regarded as an upright and free-standing ideal column, E is Young's modulus of the column, w is the specific weight of the column, and r is the radius of the column (in meters). For a typical conifer, Mosbrugger et al. (1994) suggested that C and E/w equal 0.32 and 1.7×10^6 m, respectively.

The Mosbrugger equation is in essence a 1-parameter power model that relates stem length to

stem radius, where the exponent is a constant equal to 0.67. Its normalization constant is given by C $(E/w)^{1/3}$ and is taxon-dependent. Thus, the formulation of the Mosbrugger model used in this study and fitted to height–diameter records of *Araucaria* is a power model that is parametrized by its normalization constant, whereas its exponent is fixed to 0.67 (Table 2). It not only simulates Mosbrugger'a formula (Eq. 1) but also that of Pole (1999) with the latter also being a power function with an exponent of 0.67 and a normalization constant that was inferred from the three *Araucaria* species studied herein (Table 1).

Niklas height–diameter growth model. The Niklas height–diameter model is a curvilinear function relating stem length measured from the tip of a stem to the stem diameter. This 3-parameter allometric model was used to describe growth in non-woody and woody species (Niklas, 1994). For log-transformed stem lengths and diameters, the formulation of the Niklas model reads as follows

$$log_{10}(L) = \beta + \alpha_1 log_{10}(d) + \alpha_2 (log_{10}(d))^2, \quad (2)$$

where L is the stem length, d is the stem diameter, β is the normalization constant, and both α_1 and a_2 are (allometric) exponents. For its polynomial formulation relating tree height H to DBH, see Eq. (2) and table 2.

Von Bertalanffy height–diameter growth model. The 2-parameter von Bertalanffy growth model has been commonly used to describe growth in body size in relation to an individual's age. This asymptotic model has been applied to many animal taxa, including birds, snakes, lizards, turtles, crocodiles, and extinct sauropod dinosaurs (Ricklefs, 1968; Frazer and Ehrhart, 1985; Halliday and Verrell, 1988; Shine and Charnov, 1992; Magnusson and Sanaiotti, 1995; Lehman and Woodward, 2008; Griebeler et al., 2013). The specific formulation of the von Bertalanffy model that fitted to height–diameter records of *Araucaria* is shown in table 2.

5.2.3. Establishment of growth models for the four populations and the whole dataset

All 19 height–diameter growth models (Table 2) were applied to each of the four *Araucaria*

populations and to the dataset with all 157 trees in order to identify the best model(s) to predict height H from DBH for each. Nonlinear curve fitting was done with the R function *nls*. For the Niklas model, its double log-transformed equation (2) with log-transformed DBH and H values was used (Niklas, 1994). For each *Araucaria* dataset the best fitting model was identified from the Akaike's information criterion (AIC, *nls* provides the log-likelihood-based AIC value of a model) and the AIC based model selection approach suggested by Burnham and Anderson (2002). Therefore all height–diameter growth models with significant parameter estimates found for the dataset were ranked based on their AIC values, and the model with the lowest AIC (min(AIC)) was identified. ΔAIC (AIC – min(AIC)) was then calculated for each model. ΔAIC scores less than 2 suggest similar well-supported models; ΔAIC scores ranging from 2 to 10 indicate a moderate support of the model with the lowest AIC over these models; ΔAIC scores greater than 10 indicate that the respective model is weakly supported compared to the model with the lowest AIC (with the lowest AIC). Differences in model performance were further assessed by AIC based Akaike weights (Burnham and Anderson, 2002).

5.2.4. Establishment of growth models for the genus *Araucaria*

To identify the best sample-size corrected growth model(s) for the genus *Araucaria*, each of the 19 different height–diameter models (Table 2) was fitted to each of the 100 randomly generated samples as already described for the four populations and the whole dataset. Based on the 100 curve fitting results obtained for each growth model and respective AIC values, we applied the following two criteria to the ten growth models obtaining significant parameter estimates for any of the four populations or the whole dataset. The first criterion was that the fitting algorithm had converged for all 100 random samples and the parameter estimates were all significant. The second criterion was that parameter estimates and AIC values had a small variation throughout the 100 random samples, which indicated that parameter estimates and goodness-of-fit are robust against the random sample used for curve fitting. Then, so-called "median models" were generated on the basis of the median values of their parameter estimates throughout the 100 random samples for each model meeting both criteria. These were used as reference to visually inspect the variation in parameter estimates and the resulting inaccuracies in model predictions.

Three “median models” satisfying both criteria at best, having the smallest AIC values and showing a small parameter variation were passed to our final detailed evaluation. For this, their predictive performance was checked for each the four populations and whole dataset with 157 trees. Specifically, we assessed how well each of the three median models predicted tree height H from DBH when compared to the model that was established for the respective dataset (e.g., a comparison between the Mosbrugger model obtained for *Araucaria bidwillii* in Queensland and the median Mosbrugger model; the power model attained for the whole dataset of 157 trees and the median power model). Five criteria were used—the residual sum of squares (RSS, i.e., the total sum of squared residuals), the residual standard deviation (RSD, i.e., the standard deviation of the residuals), the residual standard error (RSE, i.e., the standard error of the residuals), the root mean square error (RMSE, i.e., RSS divided by the difference of sample size and the number of parameters used by the growth model), and the AIC value (RMSE based). RSD and RSE tell the residual variation, while RSS, RMSE, and AIC evaluate overall model performance. For each growth model, RSS, RSD, RSE, RMSE and AIC values were calculated for both the median model and the respective model established for each height–diameter dataset. The best median model was the model that had the lowest RSS, RSD, RSE RMSE, and AIC value for a given height–diameter dataset. Consequently, the median model(s) passing this final detailed evaluation at best was (were) the height–diameter growth model(s) for the genus *Araucaria* presented in this study.

5.2.5. Software

All *Araucaria* height–diameter information was extracted with WebPlotDigitizer 4.2 (WebPlotDigitizer, Pacifica, California, USA; Rohatgi, 2020) from graphs in the respective papers (Paijmans, 1970; Gray, 1975; Pole, 1999). All statistical analysis were performed with the free software R statistics (version 4.1.1, https://www.r-project.org/).

5.3. Results

5.3.1. Height–diameter growth models for the four populations and the whole dataset

We were able to successfully apply 13 out of 19 growth models (Table 2, i.e., the fitting algorithm revealed parameter estimates) to the four populations and the 157 trees (Table S1–S5) growing in Queensland of Eastern Australia and New Guinea. Specifically, the Mosbrugger, Power, Niklas, von Bertalanffy, Näslund, Curtis, Schumacher, Wykoff, Prodan, Chapman–Richards, Weibull, Sibbesen, and Ratkowsky growth models worked for the four populations and their composite dataset, whereas the Meyer, Michaelis–Menten, Logistic, Gompertz, Korf, and Hossfeld IV growth models were never applicable (i.e., the fitting algorithm did not converge and revealed no parameter estimates). For all populations and the 157 trees, one model parameter estimate was always non-significant for the Ratkowsky, Chapman–Richards and Weibull growth model. Only for the *Araucaria cunninghamii* population in Queensland, one parameter estimate of the Niklas model was also not significant. Parameter estimates of the Prodan model were always significant and identical across the four populations. The Schumacher growth model had also identical and significant parameter estimates for the population *A. hunsteinii* in New Guinea and all 157 trees. They were also significant and identical for the other three populations, but parameter estimates were different. Parameters estimated for all remaining growth models, that is, Mosbrugger, Power, Niklas, von Bertalanffy, Näslund, Curtis, Wykoff, and Sibbesen growth models were significant and differed across the five datasets analyzed. Overall, ten growth models yielded significant estimates for all their parameters in any of the four populations or for the whole dataset. These so called "significant models" ($p \leq 0.05$) were the Mosbrugger, Power, Niklas, von Bertalanffy, Näslund, Curtis, Schumacher, Wykoff, Prodan and Sibbesen model.

Model of Araucaria hunsteinii *population in New Guinea*. Out of these ten significant models (Table S1, Figure 1), the Näslund and Prodan model had residual standard errors being about a magnitude larger than that of the other models (Table S1) and generated no monotonic increase in tree height H with increasing DBHs (Figure 1). Out of the other eight significant models, the Mosbrugger model obtained the lowest AIC value (8.684). ΔAIC values smaller than two suggested that the von

Bertalanffy (ΔAIC = 1.217), Curtis (ΔAIC = 1.288) and Power (ΔAIC = 1.883) models were similar well supported as the Mosbrugger model. The ΔAIC values of the Wykoff (ΔAIC = 2.467), Niklas (ΔAIC = 3.197) and Sibbesen (ΔAIC = 3.217) model were also small, whereas that of the Schumacher model was much larger (ΔAIC = 6.970).

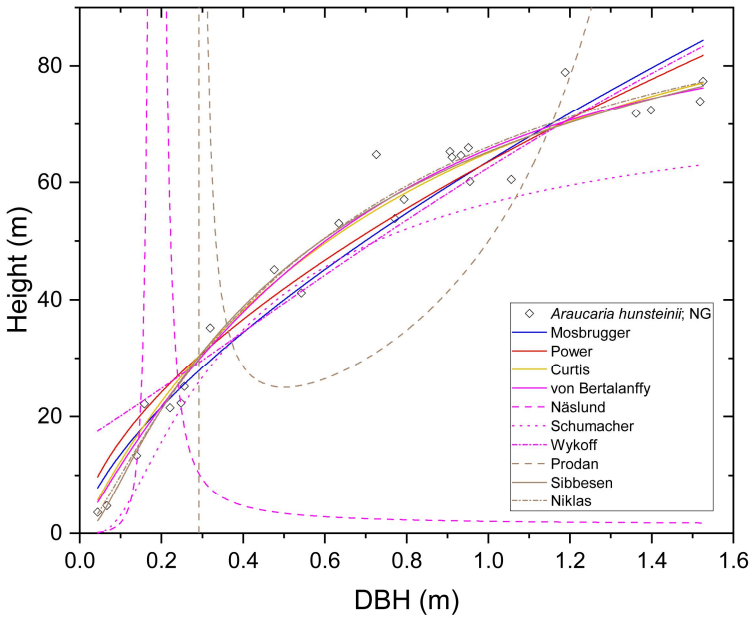

Figure 1. Fitted significant height–diameter growth curves of *Araucaria hunsteinii* population in New Guinea (NG).

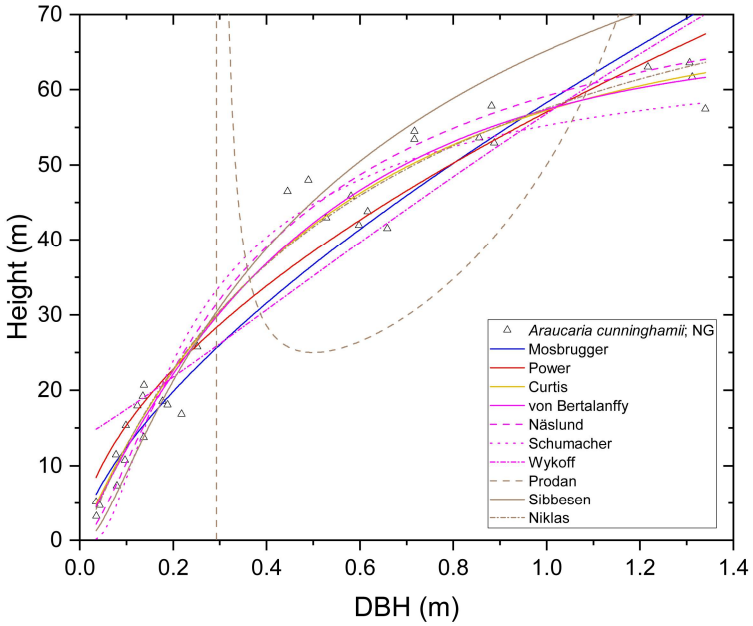

Figure 2. Fitted significant height–diameter growth curves of *Araucaria cunninghamii* population in New Guinea (NG).

Model of Araucaria cunninghamii *population in New Guinea*. Out of the ten growth models with significant parameters (Figure 2), only the Prodan model had a residual standard error substantially larger than that of the other nine significant models (Table S2) and it rendered no monotonic increase

in tree height H with increasing DBHs (Figure 2). The Mosbrugger growth model had again the lowest AIC value (8.800). ΔAIC values less than two suggested that the von Bertalanffy (ΔAIC = 1.115), Curtis (ΔAIC = 1.129), Näslund (ΔAIC = 1.233), Schumacher (ΔAIC = 1.669) and Power (ΔAIC = 1.782) model were similar well supported as the Mosbrugger model. A comparatively high support was also found for the Wykoff (ΔAIC = 2.523) and Niklas (ΔAIC = 3.172) model, whereas the ΔAIC value (7.414) of the Sibbesen model was much larger.

Model of Araucaria cunninghamii *population in Queensland*. Out of nine growth models with significant parameter estimates established for this population (the Niklas model was not a significant model, Table S3, Figure 3), only the Näslund and Prodan models had a residual standard error substantially larger than the other seven significant models (Table S3), and both models did not produce a monotonic increase in tree height H with increasing DBHs (Figure 3). The Mosbrugger growth model had again the lowest AIC value (8.323) out of the other seven models yielding a monotonic increase in tree height. ΔAIC values of the Power (1.928) and von Bertalanffy (1.895) model were smaller than two and suggest that both models were similar well supported as the Mosbrugger model. Only the Wykoff model had a ΔAIC value close to two (2.265), whereas that of the Curtis (4.667), Sibbesen (4.844), and Schuhmacher (5.782) model were clearly larger (Table S3).

Model of Araucaria bidwillii *population in Queensland*. Out of the ten growth models with significant parameters (Figure 4), only the Prodan model had a residual standard error substantially larger than the other nine significant models (Table S4) and its curve's shape indicated no monotonic increase in tree height H with increasing DBHs (Figure 4). The Mosbrugger growth model attained again the lowest AIC value (8.248). Four growth models had ΔAIC less than two, namely, the Näslund (1.601), von Bertalanffy (1.621), Curtis (1.633), and the Power (1.962) models, indicating that they were similar well supported as the Mosbrugger model. The ΔAIC of the Wykoff model (2.621) was close to two, whereas those of the Niklas (3.738), Sibbesen (4.756) and Schumacher (6.088) model were clearly larger.

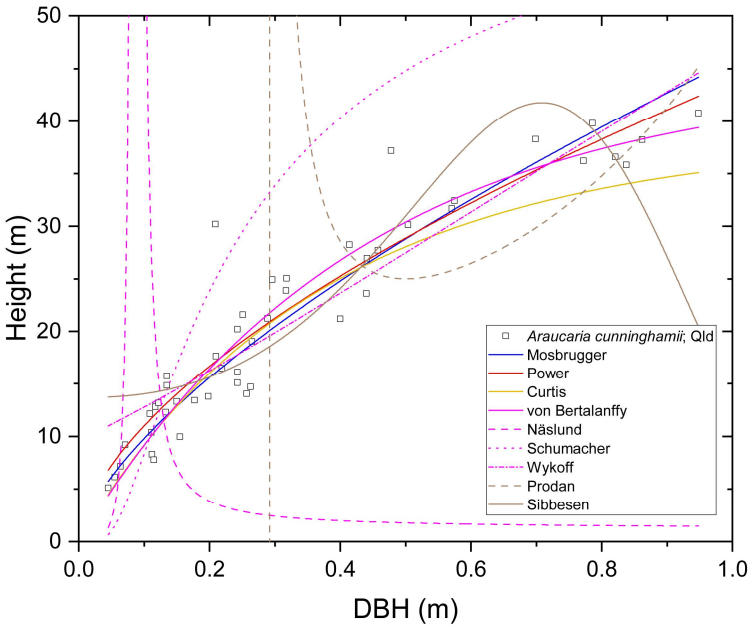

Figure 3. Fitted significant height–diameter growth curves of *Araucaria cunninghamii* population in Queensland (Qld).

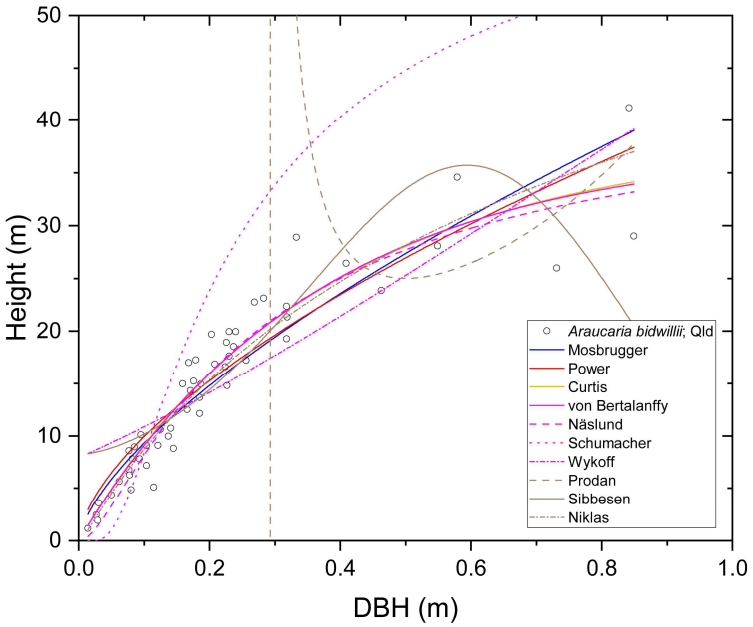

Figure 4. Fitted significant height–diameter growth curves of *Araucaria bidwillii* population in Queensland (Qld).

Composite model of all Araucaria *populations*. Out of the ten significant growth models (Figure 5) on the 157 trees, only the Prodan and Sibbesen model had a residual standard error substantially larger than the other eight models (Table S5), and the shape of their curves indicated a non-monotonic increase in tree height H with increasing DBHs (Figure 5). The Mosbrugger growth model had the lowest AIC value (10.753). Three growth models had ΔAIC less than two—Power (1.947), Curtis (1.948), and von Bertalanffy (1.965), suggesting that these models were similar well supported as the Mosbrugger model. The ΔAIC of the Näslund (2.120) and Wykoff models (2.172) were close to two,

whereas those of the Niklas (3.955) and Schumacher (4.935) models were clearly larger.

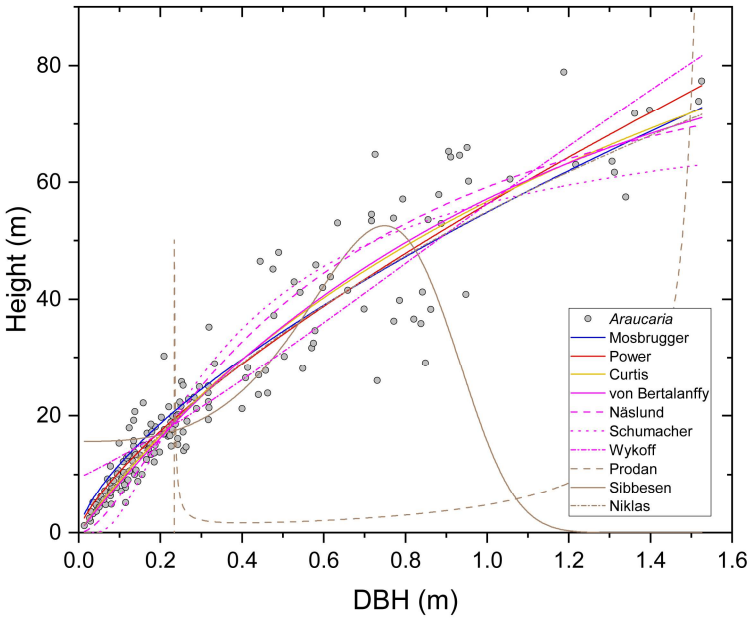

Figure 5. Fitted significant height–diameter growth curves of whole dataset of *Araucaria*.

When comparing modelling results obtained for the four populations to those from all 157 trees, the Mosbrugger model was the best one for all five datasets; the Power and von Bertalanffy models always had a ΔAIC less than two; the Curtis model always had a ΔAIC smaller than two, except for the *Araucaria cunninghamii* in Queensland (4.667); the Wykoff model always had ΔAIC values around two. The Schumacher model always had a ΔAIC clearly larger than two, except for the *Araucaria cunninghamii* in New Guinea (1.469), the Niklas model had ΔAICs clearly larger than two for the four datasets for which its parameter estimates were significant (*A. cunninghamii* in Queensland). The Näslund, Sibbesen, and Prodan model worked worse for all four populations and the whole dataset. The Näslund model had a residual standard error substantially larger than that of the other significant models and did not render a monotonic increase in height with increasing DBHs for two datasets (populations 2 and 4); the Sibbesen model had only for the whole dataset a residual standard error substantially larger than that of the other significant models, but its shape was also not a monotonic increase for the populations 1 and 2, and for the whole dataset; the Prodan model always had a residual standard error substantially larger than the other significant models and the curve's shape did not always render a monotonic increase in tree height H with increasing DBHs.

5.3.2. Height–diameter growth models for the genus *Araucaria*

Out of the ten growth models having significant parameter estimates in any of the four populations and the 157 trees, only seven (Mosbrugger, Power, von Bertalanffy, Curtis, Schumacher, Wykoff, and Sibbesen model) had significant parameters for all 100 random samples (Table S6). The variability in parameter estimates and AIC values of the 100 random samples differed between these models (Table S6, Figure S1). Curves derived from the 100 samples were the most variable for the Schumacher and Sibbesen model, and the Sibbesen model did not render a monotonic increase in tree height with increasing DBHs (Figure S1). Although parameter variability was small for the Wykoff model, all 100 models substantially overestimated tree heights for small DBHs (Figure S1). The 100 Mosbrugger models showed the lowest variability in predicted heights across the DBHs covered by the 157 trees, followed by the Power, von Bertalanffy, and Curtis model. Based on the median AIC values, these four growth models were similar well supported, with the Mosbrugger model attaining the lowest (median) AIC (Table S6). The curves of the 100 von Bertalanffy models were very similar (Figure S1) and the median AIC value across the 100 von Bertalanffy model was small, however, we only conducted our final detailed evaluation with the Mosbrugger, Power, and Curtis "median model". This was justified as the estimated asymptotic heights (parameter a) of the von Bertalanffy model for the four *Araucaria* populations differed considerably (Tables S1–S4), which lined with the large variation that we observed in the 100 random samples for the parameter estimating asymptotic height (Table S6).

Our final detailed evaluation of these three median models showed that the best fits in terms of RSS, RSD, RSE, RMSE, and (RMSE-based) AIC were performed by the respective established model for the four populations (Figure 6, Table S7). There were only two exceptions: for the *Araucaria cunninghammii* in New Guinea, RSD and RSE values of the Mosbrugger model were somewhat smaller than those of the median Mosbrugger model. For the whole dataset on *Araucaria*, differences in RSS, RSD, RSE, RMSE, and AIC observed between median models and the respective ones established for the whole dataset were much smaller than that observed in the four populations (Table S7). Contrary to our finding on the four populations and the whole dataset (the Mosbrugger model always performed best), RSS, RSD, RSE, RMSE and (RMSE-based) AIC values were smallest for the median Power model and the Power model in the whole dataset. Consistent with our results on the

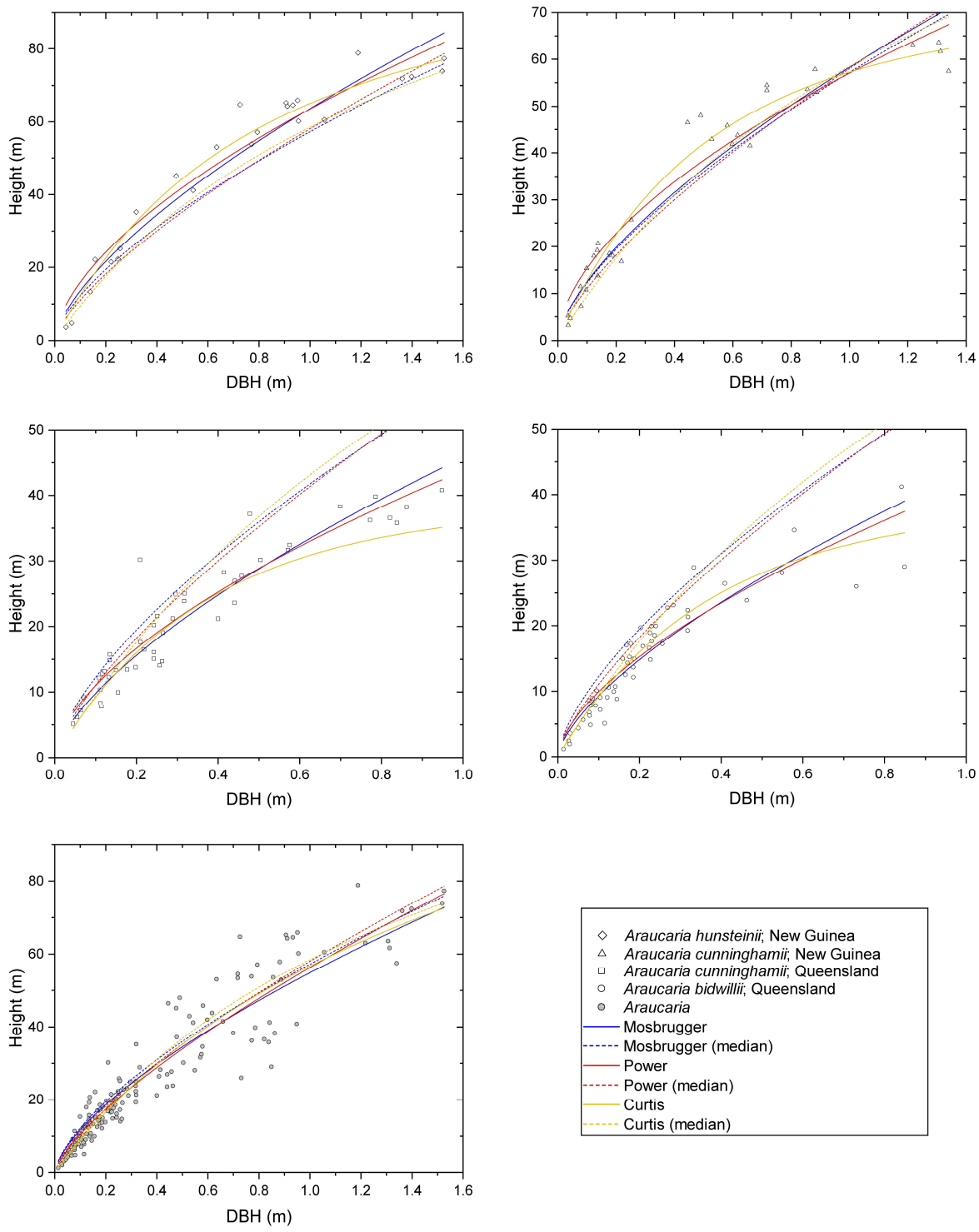

Figure 6. The curves of three median models on the genus *Araucaria* and curves derived from fitting the respective model to DBH-height records of the four populations and of the 157 trees.

four populations (except for the *Araucaria cunninghamii* in Queensland, ΔAIC = 4.667 of the Curtis model) and the whole dataset (log-likelihood-based AIC values), differences in (RMSE-based) AIC

values smaller than two indicate that the median Mosbrugger, Power and Curtis model were similar-well supported. The values of the exponent of the 100 Power models ranged between 0.69 and 0.74 with a median value of 0.72. This indicates that the Mosbrugger model (exponent = 0.67) and the Power model differ for the genus *Araucaria*.

5.4. Discussion

5.4.1. Growth model performance

Most of the selected height–diameter growth models were successfully fitted to the four populations, whole dataset (157 trees), and 100 random samples of *Araucaria*. For the four populations and whole dataset of *Araucaria*, the Mosbrugger model turned out to be the best model for describing the height–diameter relationship of *Araucaria* trees on the basis of AIC-based model selection; the Power and von Bertalanffy models were similar well supported as the Mosbrugger model according to the log-likelihood-based AIC values ($\Delta AIC < 2$). For the 100 random samples, the Mosbrugger, Power, and Curtis models were found to show the lowest variability in parameter estimates. They described the height–diameter relationships of *Araucaria* trees at best and generated three median models—the median Mosbrugger, median Power, and median Curtis models. Based on multiple model performance criteria, i.e., RSS, RSD, RSE, RMSE, and (RMSE-based) AIC, the median Power model was identified as the best median model in the final detailed evaluation of three median models; nevertheless, the median Mosbrugger and median Curtis models were rather similar well supported as the median Power model.

However, our results on selecting the best growth models for the four populations, whole dataset, and 100 random samples of *Araucaria* are inconsistent with previous studies on modeling height–diameter relationships of trees in ranking 19 different height–diameter growth models mentioned above (Table 2; Huang et al.,1992; Mehtätalo et al.,2015; Chai et al., 2018). For example, Huang and colleagues found that Chapman–Richards and Weibull models gave the most satisfactory results when modeling the height–diameter relationship of major Alberta species (angiosperms and conifers) in Canada (Huang et al., 1992). Mehtätalo et al. (2015) realized that the Näslund model provided a satisfactory fit in most height–diameter datasets of trees from Europe, Asia, North America and South

America. Another study proposed that the Chapman–Richards, Weibull, and Näslund models best performed in modeling height–diameter relationship of *Cryptomeria fortunei* trees (conifer family Cupressaceae) in Guizhou Province of southwestern China (Chai et al., 2018). None of all these models worked sufficiently for any of the populations studied herein (Table S1–S5). The reason for the inconsistency might be that the growing conditions and tree taxon would influence the height–diameter relationships. For example, mature trees of *Thuja plicata* (western redcedar, Cupressaceae), a common species in the northwestern USA, obtain an average height of 40 m (25–52 m) when DBH equals 1 m (VanderSchaaf, 2013); in northern California, USA, the native coastal redwood *Sequoia sempervirens* (Cupressaceae) generally obtains tree heights of about 33–70 m, averaging about 50 m, when DBH equals 1 m (Sillett et al., 2019; Earle, 2020; Vaden, 2020). The trees (Cupressaceae) obtaining same DBHs would reach different heights in the different growing conditions. Further support for growing conditions affecting the height–diameter relationship comes from this study. Parameter estimates of the median Power, Mosbrugger, and Curtis model differed between *Araucaria cunninghamii* from Queensland and New Guinea (Table S7). However, a strong taxon-effect on the best model (Table 2) in extant taxa asks for similar modeling studies on other extant tree genera to estimate most accurately ancient tree height from growth models in their living closest relatives.

We are aware that the uncertainties involved in establishing the good growth models for the genus *Araucaria* are greater than for each population of *Araucaria*. Nevertheless, we believe our approach for establishing good median models for the genus *Araucaria* is justified. Because the good median models obtained a small variation of significant parameter estimates and AIC values throughout the 100 random samples, and differences in (RMSE-based) AIC values between the good median models and the respective model of the 157 trees were small (2.76–3.29). Nevertheless, it should be noticed that the best model established for the respective dataset is always better than the median models, because each dataset of trees experiencing different growing conditions attains more or less different height–diameter relationships.

5.4.2. Pitfalls based on the preservation of fossil logs

Collecting precise diameter data of fossil logs is essential to the accurate estimation of ancient tree height, although there is commonly some deformation in the horizontal plane of trees during the

deep times. Nearly four decades ago, Rex and Chaloner showed experimentally that cylindrical objects (e.g., fossil logs) are likely to be preserved their original horizontal dimensions even when compressed vertically during geological burial (Rex and Chaloner, 1983). Another study based on the thin sections of fossil logs showed that compression is mostly accommodated by tracheids crushing or squashing in the parallel plane of compression (Falcon-Lang and Bashforth, 2005). Hence, the width of a fossil log is assumed to approximate the original diameter of the ancient tree even though the fossil log may have been compressed vertically during geological burial.

In general, measuring the diameter where there is apparent damage, swellings near exposed branches, and trunk near the root flare should be avoided (e.g., Williams et al., 2003). However, fossil logs found in the fluvial sediments commonly lack their root system, and any evidence of root flare or the tree trunk–substrate interface, making the measurements at exactly the DBH of fossil trunks impossible. Given that a trunk is not an ideal column but that diameter decreases along the height, using a diameter from a stump above breast height in a DBH-height model would underestimate and a diameter below breast height would overestimate tree height. The amount of underestimation and overestimation of tree height respectively finally depends on the shape of the tree's trunk, namely, how strong the trunk deviates from an ideal column.

Regarding bark layers, they are rarely completely preserved with fossil logs or trunks in the deep time, because the bark is easily detached from the central cylinder of secondary xylem after the tree has died or fallen (Staccioli et al., 1998). Bark thickness is strongly positively correlated with DBH (Pinard and Huffman, 1997; Paine et al., 2010; Zeibig-Kichas et al., 2016). Although the ratio of bark thickness to DBH varies widely among families, an average ratio of 5% may be generally applied when reconstructing ancient tree heights (Pinard and Huffman, 1997; Zeibig-Kichas et al., 2016). Neglecting bark layers generally leads to a light underestimation of tree height from DBH.

5.4.3. Revised height of Upper Jurassic araucariaceous trees in Utah, USA

The Upper Jurassic has yielded one of the most spectacular terrestrial faunas throughout the earth history, that is, the gigantic sauropods of the Morrison Formation in the Western Interior of North America (Foster, 2020; Gee et al., 2022), however, fossil plants have also been known in the Upper Jurassic Morrison Formation for over a century. For instance, fossil logs and woods are locally

abundant in this formation. Up to now, fossil wood remains have been reported from more than 20 localities in Utah, Colorado, Wyoming, South Dakota, and Montana (e.g., Tidwell, 1990; Ash and Tidwell, 1998; Tidwell et al., 1998; Gee and Tidwell, 2010; Gee et al., 2019; Richmond et al., 2019; Xie et al., 2021).

Recently, Gee and colleagues described a local flora of fossil log and wood in the Morrison Formation at the Rainbow Draw area near Dinosaur National Monument, northeastern Utah of USA, which represents a monospecific wood flora of the araucariaceous tree *Agathoxylon hoodii*. These large fossil trunks of a similarly large size were measured from 71 to 127 cm in preserved diameter (Gee et al., 2019). Based on the formula proposed by Mosbrugger et al. (1994) to estimate ancient tree height (Eq. 3), Gee et al. (2019) reconstructed the minimum heights of Rainbow Draw trees as 19–28 m with the maximum preserved diameter ranging from 0.712 to 1.270 m (Table 3). As the Mosbrugger and Pole curves are both power models with an exponent of 0.67 and the normalization constant of the Pole model (Eq. 4) is at least about twice that calculated from the formula proposed by Mosbrugger et al. (1994) for conifers (Eq. 3), the latter generally underestimates tree height H (in meter) by half (Eq. 4a) or a third (Eq. 4b) from tree diameter D (in meter) compared to that inferred by Pole (1999) for *Araucaria bidwillii* and *A*. *cunninghamii* in Queensland.

Table 3. Revised heights of Upper Jurassic araucariaceous trees in Utah, USA.

Field No.	FHNHM Inventory No.	Max. Preserved Diameter (cm)	Reconstructed Min. Tree Height (m)			
			Gee et al. (2019)	Mosbrugger median model	Power median model	Curtis median model
RD, Site 1, Log 1	FHPR 13360	127.0	28.4	67.2	68.9	67.1
RD, Site 2, Log 1	FHPR 11749	71.2	19.3	45.6	45.4	47.1
RD, Site 2, Log 2	FHPR 11361	91.4	22.8	53.9	54.4	55.3
RD, Site 4, Log 1	FHPR 11753	101.6	22.4	57.8	58.7	59.0
RD, Site 4, Log 2	FHPR 13362	105.4	25.0	59.3	60.3	60.3

Note: Utah Field House of Natural History State Park Museum (FHNHM). Specimens and diameters from Gee et al. (2019). Eq. 5-7 used for estimates of median models.

$$H = 24.00 \times D^{0.67} \quad (3)$$

$$H = 48.00 \times D^{0.67} \quad (4a)$$

$$H = 72.00 \times D^{0.67} \quad (4b)$$

Here, we applied our good models for the genus *Araucaria*, the Mosbrugger (Eq. 5), Power (Eq. 6), and Curtis (Eq. 7) median models to reconstruct heights of araucariaceous trees in Rainbow Draw on the basis of maximum preserved diameter of each fossil log.

$$H = 57.22 \times D^{0.67} \quad (5)$$

$$H = 58.03 \times D^{0.72} \quad (6)$$

$$H = 101.78 \times D / (1+D)^{0.80} \quad (7)$$

Although the uncertainties involved in applying these height–diameter growth models are much greater than in an extant dataset are awarded, we feel our approach is justified because the nearest living relatives of the fossil araucariaceous trees were used to modeling the height–diameter relationships and best models were established on the basis of multiple model performance criteria.

The Mosbrugger median model gave the new reconstructed heights of Rainbow Draw trees from 46 to 67 m; the Power median model reconstructed the tree heights ranging from 45 to 69 m; the Curtis median model estimated the tree heights as 47 to 67 m (Table 3). Our new results for reconstructed heights of Rainbow Draw trees are very consistent across the three models applied and work well for each of the four populations. They indicate that the formula proposed by Mosbrugger et al. (1994) would underestimate tree height for about two and a half times (Eq. 3, 19–28 m, Gee et al. 2019). Estimates from the Pole's curve yielding heights twice that of the Mosbrugger equation (Eq. 4a) are smaller than (36 to 54 m) that from the median models (Eq. 5-7), whereas those from the curve yielding three times larger heights (Eq. 4b) are even larger (57-84 m) than those from the median models (Eq. 5-7). Based on the thorough evaluation of our three median models and because of that they performed well for the four *Araucaria* populations and all 157 trees, we are convinced that the Mosbrugger, Power, and Curtis median models can be commonly utilized to reconstruct the heights of ancient araucariaceous trees.

5.5. Conclusions

In this study, 19 nonlinear height–diameter growth models were utilized to fit the four populations, whole dataset, and 100 random samples of *Araucaria* in New Guinea and Queensland.

The Mosbrugger model was the best model to describe the height–diameter relationship of the four populations and whole dataset of *Araucaria*, and the Power and von Bertalanffy models were similar well supported as the Mosbrugger model. Three significant growth models with small parameter-estimate variations and small AIC values were identified for the 100 random samples, which generated three median models. The median Power model was identified as the best median model to describe the height–diameter relationship of the genus *Araucaria*; the median Mosbrugger and median Curtis models were similar well supported as the median Power model. To obtain good estimates of heights of Rainbow Draw trees in the Upper Jurassic Morrison Formation of Utah, USA, we applied our three good median models based on the maximum preserved diameter of each fossil log (0.712 to 1.27 m), which results in the reconstructed tree heights, ca. 45–70 m, much greater than the heights given by Gee et al. (2019).

5.6. Acknowledgments

We thank Moritz Liesegang, Freie Universität Berlin, for helpful discussions. Financial support from the China Scholarship Council for the doctoral studies of AX (CSC no. 201804910527) is greatly appreciated.

5.7. Supporting information

Additional supporting information can be found online (https://drive.google.com/file/d/154KqSSu3M6nbi5x8pqLpgaJnTfWR5fiE/view?usp=sharing):

Table S1. Modelling results of 19 height–diameter growth models applied to the *Araucaria hunsteinii* population in New Guinea.

Table S2. Modelling results of 19 height–diameter growth models applied to the *Araucaria cunninghamii* population in New Guinea.

Table S3. Modelling results of 19 height–diameter growth models applied to the *Araucaria cunninghamii* population in Queensland.

Table S4. Modelling results of 19 height–diameter growth models applied to the *Araucaria bidwillii*

population in Queensland.

Table S5. Modelling results of 19 height–diameter growth models applied to the whole dataset on *Araucaria*.

Table S6. Modelling results on the 100 randomly generated samples and different height–diameter growth models.

Table S7. Parameter estimates and performance criteria of three median models and respective models either established for each of the four populations or for the whole dataset on *Araucaria*.

Figure S1. Accuracy of growth models with respect to the 100 random samples.

Chapter 6

Linking silicification cycles, trace element gradients, and biomolecule preservation in Upper Jurassic gymnosperm wood

Publication

Liesegang, M.[1], Schnell, A., Xie, A., Gee, C.T., Tahoun, M., Engeser, M., and Müller, C.E., in review, Linking silicification cycles, trace element gradients, and biomolecule preservation in Upper Jurassic gymnosperm wood: Geochimica et Cosmochimica Acta, submitted in April 2022.

Author contributions

Liesegang designed the study, collected, and analyzed the data from light microscopy, SEM, electron probe microanalysis, and Raman spectroscopy, and wrote the first draft of the manuscript. Schnell and Engeser collected and analyzed the MALDI-ToF data. Xie and Gee wrote the paleobotanical description and geological background. Tahoun and Müller collected and analyzed FT-IR data. All authors reviewed and edited the manuscript.

Abstract from the submitted manuscript

The exceptional potential of wood silicification for the preservation of plant structure and biomolecules is largely due to the chemical and physical stability of crystalline silica over hundreds of millions of years. However, a significant uncertainty exists regarding the link between the silicification process and organic compound structure and preservation. To identify the preservation potential of wood organic compounds and the linked primary and secondary trace element distribution, we investigated silicified, gymnosperm wood with macroscopically distinct color

[1] Corresponding author.

domains from the Upper Jurassic Morrison Formation. MALDI-ToF-MS, FT-IR, and Raman spectroscopy identify the preserved organic compounds as highly disordered carbon, lignin dimers, and hexose disaccharide or coniferin with a distinct distribution and abundance. This is the first documentation of hexose disaccharide or coniferin in original wood material as old as about 150 Ma. Electron probe microanalysis of trace elements reveals that the quality and quantity of the organic compounds correlates with the primary calcium and secondary sulfur distribution in cell walls overprinted chemically and structurally during fossilization and diagenesis. The episodical ingress of diagenetic fluid into the cell walls resulted in partial degradation of lignin, cellulose and hemicellulose followed by localized sealing of pore space with silica. This transient fluid-solid interaction encased parts of the wood organic compounds and the corresponding primary calcium signature in a silica matrix resistant to the destructive action of a later sulfur-rich fluid. Our results suggest that wood silicification conserves complex organic compounds that might be valuable paleoecological proxies and are usually vanished from the fossil record due to diagenetic fluids or acid hydrolysis extraction.

Linking silicification cycles, trace element gradients, and biomolecule preservation in Upper Jurassic gymnosperm wood

Moritz Liesegang [a,b,*], Anne Schnell [c], Aowei Xie [b], Carole T. Gee [b,d], Mariam Tahoun [e], Marianne Engeser [c], and Christa E. Müller [e]

[a] Institut für Geologische Wissenschaften, Arbeitsbereich Mineralogie-Petrologie, Freie Universität Berlin, Malteserstrasse 74-100, 12249 Berlin, Germany

[b] Institute of Geosciences, Division of Palaeontology, University of Bonn, Nussallee 8, 53115 Bonn, Germany

[c] Kekulé Institute of Organic Chemistry and Biochemistry, University of Bonn, Gerhard-Domagk-Str. 1, 53121 Bonn, Germany

[d] Huntington Botanical Gardens, 1151 Oxford Road, San Marino, California 91108, USA

[e] Pharmaceutical Institute, Department of Pharmaceutical & Medicinal Chemistry, University of Bonn, An der Immenburg 4, 53121 Bonn, Germany

[*]Corresponding author. E-mail address: m.liesegang@fu-berlin.de (M. Liesegang).

6.1. Introduction

Silicification is the major process for preserving delicate anatomical structures in plants in three dimensions and is also the most important fossilization process responsible for the exquisite cellular preservation of ancient woods (Buurman, 1972; Sigleo, 1978; Jefferson, 1987; Rößler et al., 2012; Kerp, 2017; Edwards et al., 2017; Liesegang and Gee, 2020; Gee et al., 2021; Jones and Renaut, 2021). The silicification of wood and other plants may take place within a very short time, for example, in hydrothermal springs or after volcanoclastic burial, and preserves plant material across length scales, from single cells to trees to entire ecosystems (Karowe and Jefferson, 1987; Ballhaus et al., 2012; Rößler et al., 2012; Edwards et al., 2017; Kerp, 2018; Hellawell et al., 2015). However, despite the exceptionally high preservation potential of plant matter entrapped in a silica mineral

matrix, only few studies have approached the issue of the coupling between the abiogenic silicification process, the quality and quantity of organic compounds, and the trace element distribution at the cellular level (Sigleo, 1978; Boyce et al., 2001; Witke et al., 2004).

It is commonly argued that the preferential silicification of buried wood begins with the direct binding of silanol groups to the organic matrix (Leo and Barghoorn, 1976; Hellawell et al., 2015; Liesegang and Gee 2020). Subsequent diagenetic silica dissolution–precipitation processes inside cell walls and lumina are expected. However, recent studies have pointed out that the properties of silica-precipitating fluids and their evolution over timescales have a direct impact on the preservation potential of cell wall architecture and trace element chemistry, as well as plant tissue degradation and quantity (Boyce et al. 2001; Mustoe, 2008; Trümper et al., 2018; Liesegang and Gee, 2020; Rößler et al., 2021; Mustoe and Ditthoff, 2022). Apparently, bulk silica diagenesis is incompatible with the variety of silica phases and silicification episodes preserved in fossil wood, for example, as a fluid-assisted, pervasive cell wall overprint (cf. Witke et al., 2004; Matysová et al., 2016; Trümper et al., 2018; Liesegang et al., 2021).

Previously identified organic matter in silicified wood comprises variably ordered organic carbon and lignin derivatives (Sigleo, 1978; Witke et al., 2004; Sweeney et al., 2009). In an analysis of 200 Ma old silicified wood from the Triassic Chinle Formation in Arizona (USA), Sigleo (1978) found that organic compounds are preserved in black carbonaceous samples. Pyrolysis–gas chromatography–mass spectrometry (Py-GC/MS) indicates that the remnant phenolic compounds in the demineralized fossil wood are most likely lignin derivatives. These organic compounds and potential cellulose/hemicellulose indicators are absent from wood that does not contain remnants of biological structures from the same site. Generally, an important limitation in identifying biomolecules in silicified wood is the potential loss of soluble species during sample preparation, for example, acid hydrolysis (Marynowski et al., 2018; Marynowski and Simoneit, 2022). Although recent studies show that unsilicified fossil wood of Middle Jurassic age contains primary monosaccharide (Marynowski et al., 2018), such information is absent from studies on silicified wood.

In this paper, we use electron probe microanalysis and MALDI-ToF-MS to understand the coupling between the trace element distribution and organic compounds, and the relationship between the quality of morphological and chemical preservation in silicified wood. In a novel approach, we

probe different color domains in mineralized wood without hydrolysis extraction to determine the diagenetically altered distribution of wood primary and secondary ions and the preservation of biomolecules. These new findings allow us to link the preservation of organic compounds to systematic changes of fluid-accessible pore space and the diagenetic fluid composition. Since wood and a significant number of terrestrial biota in the fossil record do not contain any biomineralized tissues (Briggs et al., 2000; Locatelli, 2014), the exceptional quality of preserved organic compounds in silicified wood may help to expand our access to the paleoecology of ancient environments and the evolution of plant organic compounds at least as old as the Jurassic.

6.2. Materials and Methods

6.2.1. Locality and sample description

The gymnosperm wood studied here was collected from Six Mile Draw, Uintah County, Utah, USA (Fig. 1A). Here, sediments of the upper part of the Upper Jurassic Morrison Formation crop out. In northeastern Utah, the Morrison Formation comprises four members: the Windy Hill, Tidwell, Salt Wash, and Brushy Basin Members in ascending chronostratigraphic order (Hasiotis, 2004; Sprinkel et al., 2019). According to lithological and paleontological analysis, the Windy Hill and Tidwell members indicate a marine to marginal marine to coastal plain depositional environment (Turner and Peterson, 2004), whereas the Salt Wash and Brushy Basin members represent a fluvial–lacustrine depositional environment (Turner and Peterson, 2004; Sprinkel et al., 2019). It is still unclear if the fine sandstone bearing the wood pertains to the Salt Wash or Brushy Basin Member, but in any case, the age of the deposit would range from 156–150 Ma (cf. Rainbow Draw; Trujillo and Kowallis, 2015).

The wood specimen was collected from a fossil log (Fig. 1B) and measured roughly 10 × 6 cm (Fig. 1C). Thin sections in the standard cross and radial planes of section were produced using conventional petrographic methods. The gymnosperm wood is tracheid-dominated, and does not show any resin canals nor other remarkable features in cross section. The quality of anatomical preservation, or specifically, the visibility of cell outlines, ranges from good to fair. The most noteworthy characteristic of this wood specimen are the three macroscopically distinct domains that

are pale beige, beige, or black in color. Hereafter, these domains will be referred to as light (pale beige), medium (beige), and dark (black), respectively.

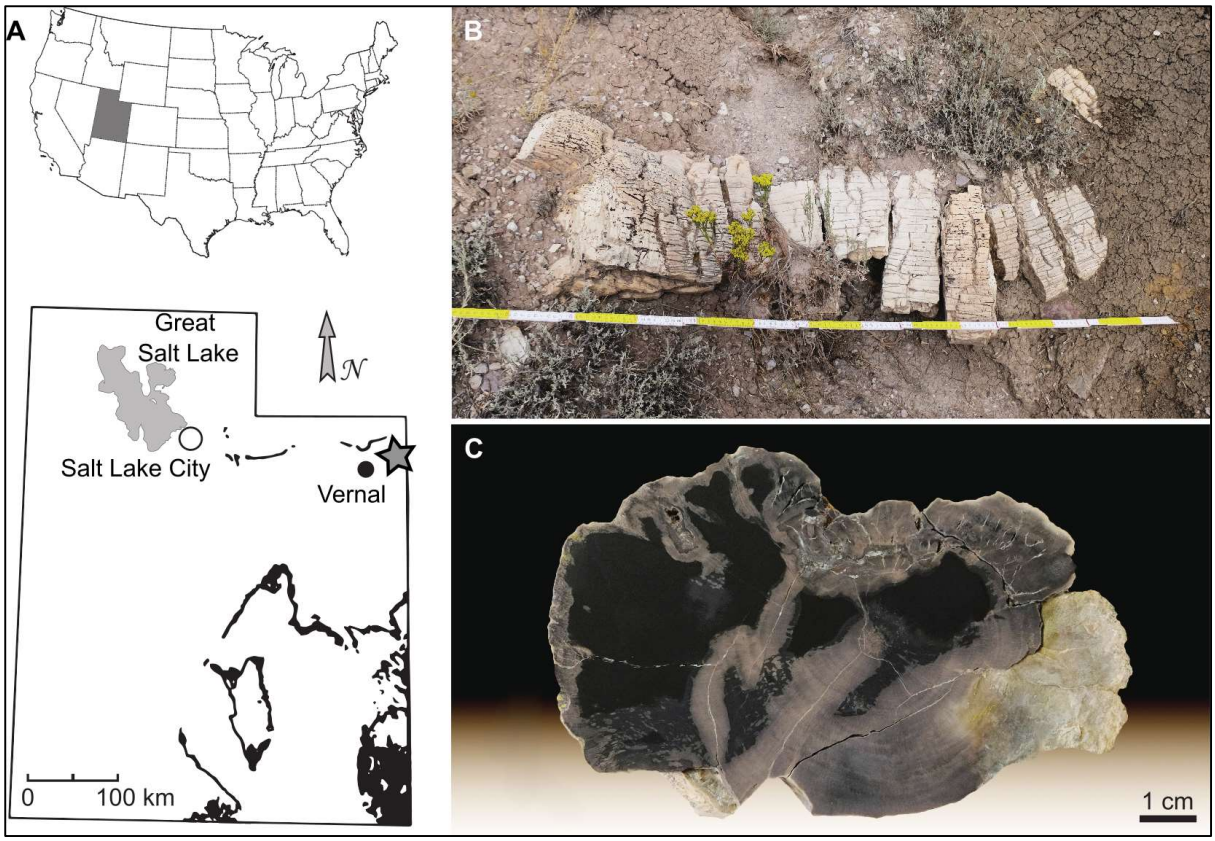

Figure 1. (A) Above, location of the state of Utah in the western USA; below, collecting site of fossil wood at the Six Mile Draw (star) site in NE Utah, near Vernal (black circle), USA. (B) Weathered log in outcrop at Six Mile Draw. (C) Cross section through the wood specimen.

6.2.2. Sample powder preparation

Sample material from each of the three color domains was drilled from the specimen with a diamond drill to obtain a fine powder for analysis with MALDI-ToF-MS, Raman spectroscopy, and FT-IR. Additional powders from sawn and crushed dark domains of the silicified wood samples were demineralized with hydrofluoric acid (HF) and subsequently washed with cold 6N hydrochloric acid (HCl) and distilled water followed by centrifugation. Previous studies suggested that this HF demineralization procedure would not significantly affect the organic compound distribution in silicified wood (cf. Sigleo, 1978). The domains richest in calcium were too small (<300 µm wide) to prepare the quantities of powder necessary for further analysis.

6.2.3. Electron beam microanalysis

Cross and radial thin sections of the specimen were epoxy-embedded, polished, and carbon-coated for scanning electron microscopy (SEM) and electron probe microanalysis (EPMA). High-resolution backscatter electron (BSE) images were obtained using a Zeiss Sigma 300 VP Field-Emission Scanning Electron Microscope operated at 15 kV. Compositional mapping for Al, Fe, Mg, Ca, Na, K, C, S, and P was obtained with a JEOL JXA 8200 Superprobe using the wavelength-dispersive WDX detectors. The operating conditions were 15 kV acceleration voltage and 70 nA beam current, with a beam diameter of 1 µm and 300 ms counting time per 2 µm pixel size.

6.2.4. Raman spectroscopy

Raman spectroscopy mapping analyses across the three different color domains in thin section were conducted on a confocal Horiba Jobin Yvon LabRAM HR 800 spectrometer coupled to an Olympus BX41 microscope. Powder of untreated and HF-extracted samples were analyzed at the same conditions for comparison and yielded identical Raman spectra. A 785 nm air-cooled diode laser was used to excite the sample with a 100 x objective (numerical aperture 0.9), a spectral integration time of 2 s and 2 accumulations, with a 2 µm pixel size. Scattered Raman light was collected in backscattering geometry and dispersed by a grating of 600 grooves/mm after passing through a 100 µm entrance slit. The confocal hole size was set to 1000 µm. Unpolarized spectra were collected with the LabSpec 6 software at a spectral resolution of ~3.5/cm^{-1}. An internal intensity correction (ICS, Horiba) was used to correct detector intensities. The instrument was calibrated using the Raman band of a silicon wafer at 520.7 cm^{-1}. A linear baseline between 1000-1800 cm^{-1} was used to subtract the background for carbon thermometry. The spectra were decomposed into four pseudo-Voigt functions representing the D1, D3, D4, and GL-band (Kouketsu et al., 2015; Visser et al., 2018). The position of the D3- and D4-band was fixed at 1510 cm^{-1} and 1245 cm^{-1}, respectively.

6.2.5. Fourier-transformed infrared spectroscopy (FT-IR)

A small amount of a powdered sample was triturated with 10–100 times its mass of pure anhydrous potassium bromide (KBr) using a small agate mortar and pestle. The sample was then pressed into a disc and analyzed with a Perkin Elmer Spectrum 100 FT-IR Spectrometer in the wavenumber range of 4000–450 cm^{-1}. The spectra were processed using the software Spectrum and PeakFit 4. Peak positions were determined after a linear background subtraction from 3695–2782 and 1800–780 cm^{-1}, according to Faix (1991).

6.2.6. Matrix-assisted laser desorption/ionization mass spectrometry (MALDI-ToF-MS)

To analyze the insoluble powdered fossil samples with MALDI-MS, several sample preparation methods and MALDI matrices (Hillenkamp and Peter-Katalinić, 2013; Kosyakov et al., 2014) were tested. Best results were obtained with the following suspension preparation method. For each powdered sample, about 0.6 mg were suspended in 0.5 µl of a solution of the matrix 2′,4′,6′-trihydroxyacetophenone (THAP) in dimethylformamide (DMF), transferred to a ground-steel MALDI target, spread out as thinly as possible, and dried. For the analysis of graphite powder, a sample preparation with rubbing was used. Graphite and THAP were added in a 1:10 ratio to a mortar and ground with the pestle. The powdery mixture was transferred to the ground-steel MALDI target and rubbed into its surface furrows with the flat side of a plastic spatula. Loose solids were scraped of the edge of the target. MALDI measurements were performed with a Bruker Daltonik ultrafleXtreme MALDI mass spectrometer. Relatively high laser intensities were needed to obtain reasonably high signal intensities from the silicified material. The powdered samples from each of the light, medium, and dark wood domains, as well as additional powder gained from desilicifying the dark domain through hydrofluoric acid (HF) extraction were measured several times.

6.3. Results

6.3.1. Optical Microscopy

The three color domains—previously designated here as light, medium, and dark—can be identified macroscopically based on the intensity of their brown coloration (Fig. 2). Some anatomical

structure is well-preserved in the wood and its optical visibility decreases toward the lighter domains. The cell walls are generally intact, even in the lightest domains. The sharp interfaces between differently colored domains unselectively traverse all anatomical features including individual cell walls, resulting in a mottled appearance of the thin section. Comparison of the sections in cross section with those in radial section shows that this decoloration pattern is a three-dimensional feature. Some dark-brown organic material is located at cell corners, which coincides with the position of the lignin-rich middle lamella in gymnosperm wood (Fig. 2e; Schwarze, 2007). Thin section observation with polarizers crossed indicates that the sample consists of chalcedony with a fibrous microstructure, enclosing organic matter of the cell walls and filling lumina. Wall-lining chalcedony fills late, randomly oriented cracks along cell wall boundaries. A difference between the mineralogy and degree of preservation of the earlywood and latewood was not observed.

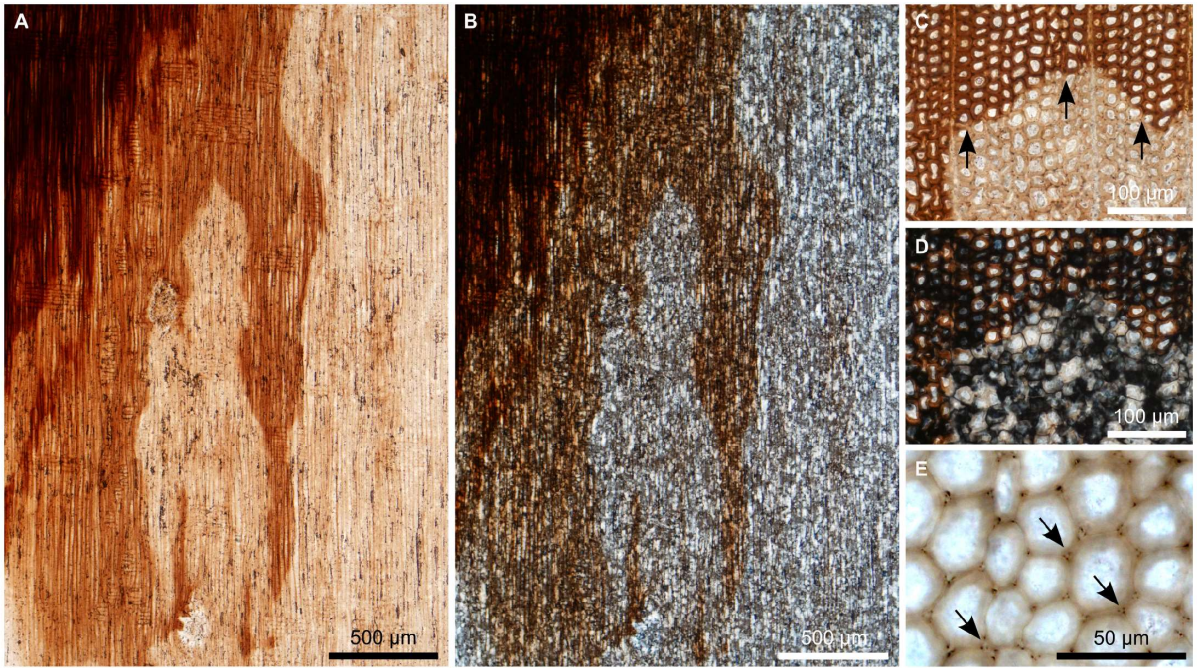

Figure 2. Photomicrographs of differently colored domains of Jurassic silicified wood taken under plane-polarized light (A, C, E) and crossed polarizers (B, D). (A–B) Radial section with three differently colored domains consisting of chalcedony. (C–D) Sharp boundaries separate domains across single cell walls (arrows). (E) Dark particles are located at the cell corners associated with lignin (arrows).

6.3.2. SEM imaging and microprobe analyses

EPMA element distribution mapping shows that calcium and sulfur highlight wood anatomy, that

is, they follow the outlines of the cell walls (Fig. 3). However, each of these trace elements defines anatomy to a different extent. The sulfur trace element distribution correlates positively with the optical darkness of the sample, and the sulfur concentration is highest in the cell walls in the darkest domain. The calcium concentration shows a more complex distribution pattern. While the bulk of the dark cell walls contains calcium at background level concentrations, a calcium-rich region up to ~250 µm thick occurs in the dark color domain, at the interface to the medium domains. The concentration gradient is steep at the dark–medium interface and smoother toward the dark domain. Apart from this calcium-rich zone, the medium domains contain the highest amount of calcium. The concentration of other elements such as Al and Na occurs only at background levels, with a distribution that is decoupled from cellular detail and allows for no differentiation between lumen-filling silica precipitates and those constituting the cell walls.

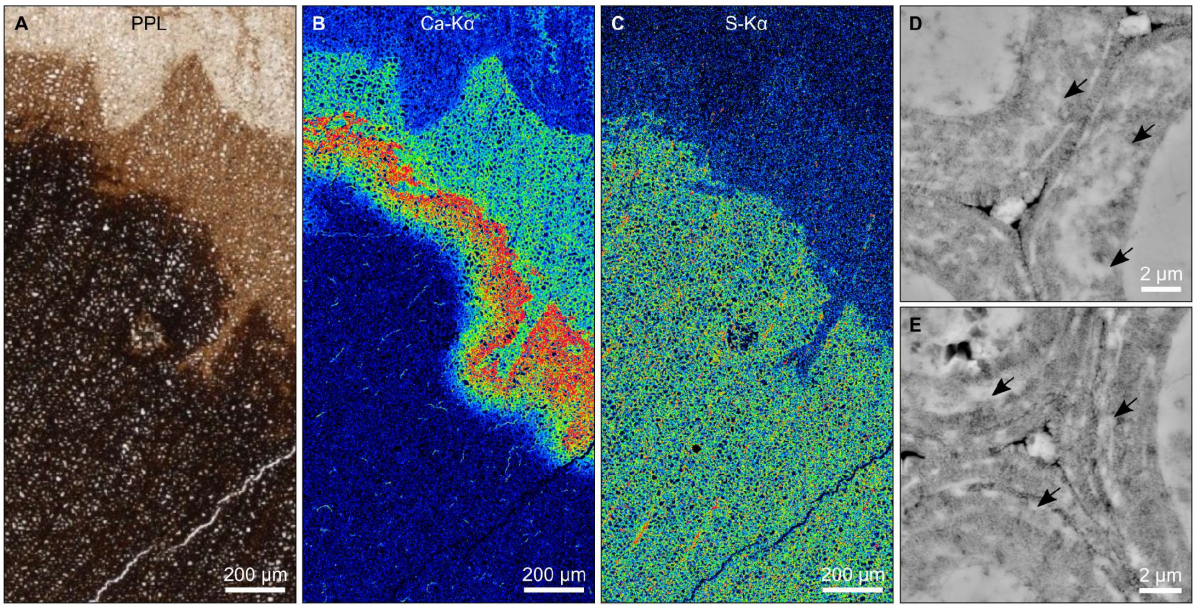

Figure 3. WDX element distribution maps (B–C) and BSE images of porous cell walls (D–E) on a polished thin section. (A–C) Photomicrograph taken under plane-polarized light (A) and element distribution maps of calcium (B) and sulfur (C). Only the cell walls contain significant amounts of calcium and sulfur. The darkest domains contain sulfur but lack calcium apart from a thin rim that outlines the dark domains. (D–E) Cell walls in medium (D) and dark (E) earlywood consist of granular submicrometer-sized quartz crystals. Cell corners contain round, silicified particles. Cell walls in medium wood (D) contain large patchy chalcedony domains (arrows) that significantly occlude porosity between granular quartz crystals. Compared to medium wood, cell walls in dark wood (E) contain abundant preserved porosity and only few compact chalcedony domains (arrows).

The chalcedony micromorphology differs between cell lumina and cell walls (Fig. 3D–E). While

chalcedony in cell walls consists of randomly oriented, granular quartz crystals <200 nm, dense chalcedony and minor ~1 μm-sized euhedral quartz crystals fill the lumina. Commonly, a layer of ~250 nm large quartz crystals is located on the outer surface of cell walls, with their longest axis normal to the surface, pointing toward the position of the compound middle lamella. Chalcedony traversing the cell walls was not observed.

6.3.3. Raman spectroscopy

Raman spectroscopy shows that among all domains in the sample, the spectra display prominent α-quartz bands (most intense band centered at 465 cm^{-1}) with a moganite band at 502 cm^{-1} (Fig. 4a). The area ratio (moganite/α-quartz, A_{502}/A_{465}) of these main symmetric stretching-bending modes of chalcedony varies unsystematically from ~0.13 to 0.24 in cell walls, lumina, and late veins. The cell walls contain variable amounts of amorphous carbon (Fig. 4B), with the highest concentrations found in the darkest domains. The spectra of the disordered carbon in thin section as well as untreated and HF-extracted powders are identical and the shape and peak positions of the carbon band from 1000–1800 cm^{-1} are qualitatively indistinguishable throughout the specimen. The intensity ratio of the carbon GL-band at ~1600 cm^{-1} and the most intense 465 cm^{-1} α-quartz band increases with the color intensity of the cell wall (i.e., higher carbon concentration in darker wood), which directly reflects the changes of the carbon/silica ratio (Fig. 4c). The peak temperature experienced by the organic matter has been calculated from the full width at half-maximum of the D1-band at 1361 cm^{-1} on average (Homma et al., 2015; Visser et al., 2018) and falls in the range of 100 ± 6 °C (n = 92). Raman bands associated with lignin or cellulose, or potential coloring agents such as iron oxides/hydroxides were not observed. The calcium-rich band at the interface of dark and medium domains is reproduced by a high relative concentration of highly disordered carbon. However, the spectra show no indication of carbonates or sulfates/sulfides that could account for the calcium or sulfur distribution in the cell walls visible in EPMA element distribution maps.

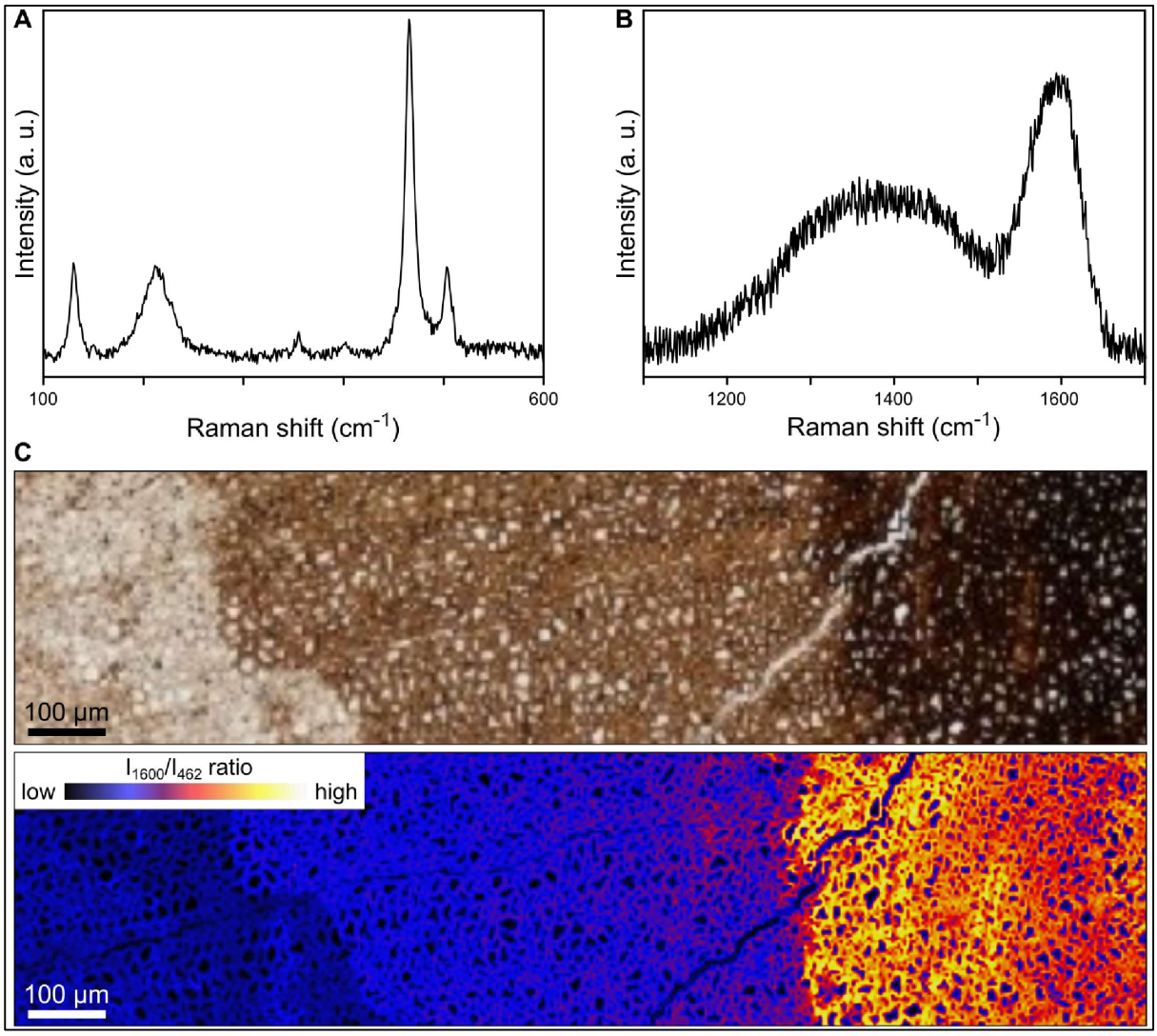

Figure 4. Raman spectra (A–B) and mapping (C) of different domains prepared as a petrographic thin section (A, C) and drilled from the hand specimen (B). (A) Chalcedony in cell walls with α-quartz bands (e.g., 462 cm^{-1}) and the characteristic moganite band at 502 cm^{-1}. (B) A representative Raman spectrum of highly disordered organic material drilled from the darkest domain. (C) Photomicrograph taken under plane-polarized light and corresponding Raman map of the intensity ratio of the carbon G_L-band at ~1600 cm^{-1} and the 462 cm^{-1} α-quartz band indicating higher concentrations of highly disordered organic carbon within dark cell walls compared to decolored domains.

6.3.4. FT-IR spectroscopy

Figure 5 shows the FT-IR spectrum of demineralized (HF-treated) dark fossil wood. The spectrum indicates the dominantly aromatic character of the fossil organic matter relative to modern gymnosperm wood. Compared to Raman spectroscopic and MALDI-TOF analysis of the dark domains, FT-IR allows identification of some organic compounds or at least functional groups with a

significantly lower suppression effect from amorphous carbon, revealing guaiacyl ring vibrations of lignin (Table S1) that would not occur in plain amorphous carbon spectra. Intense stretching absorptions of O-H and C-H are located at 3395 and 2953–2850 cm^{-1} (aromatic methoxyl groups and methyl and methylene groups of side chains), respectively. The main absorption bands in the region between 1800 and 600 cm^{-1} are guaiacyl ring vibrations at 1443, 1270, and 1218 cm 1 and the pronounced band of a skeletal vibration and of condensed aromatic rings at 1602 cm^{-1} (aromatic C=C, C=O stretch; Faix, 1991; Dirckx et al., 1992; Pandey, 1999). The aromatic C H in-plane deformation at 1031 cm^{-1} and the aliphatic C-H stretch at 1370 cm^{-1} are only present as shoulders. In the low frequency range, the two bands at 860 and 816 cm^{-1} indicate aromatic C H out-of-plane vibrations of guaiacyl units (Bock et al., 2020). The characteristic skeletal vibrations of lignin at 1515–1505 cm^{-1} are not present as a discrete band in the spectra of fossil wood extracts. However, a weakly developed band at ~1500 cm^{-1} could be related to these vibrations. The spectra generally lack evidence for bands that can solely be attributed to a cellulose or hemicellulose component.

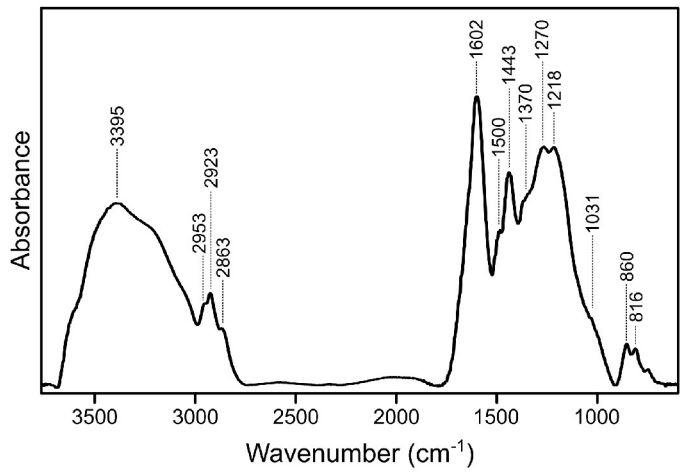

Figure 5. FT-IR spectrum of HF-extracted organic matter from dark domains showing typical lignin-related bands. The band assignment is collated in Table S1.

6.3.5. MALDI-ToF mass spectrometry

Figure 6 shows an overview of the MALDI-ToF mass spectra for samples drilled out of the light, medium, and dark domains, additional powder gained from desilicifying the dark domain by HF extraction, and a blank measurement of the matrix in DMF solution. Table S2 lists the signal assignments. Several differences between the domains are apparent.

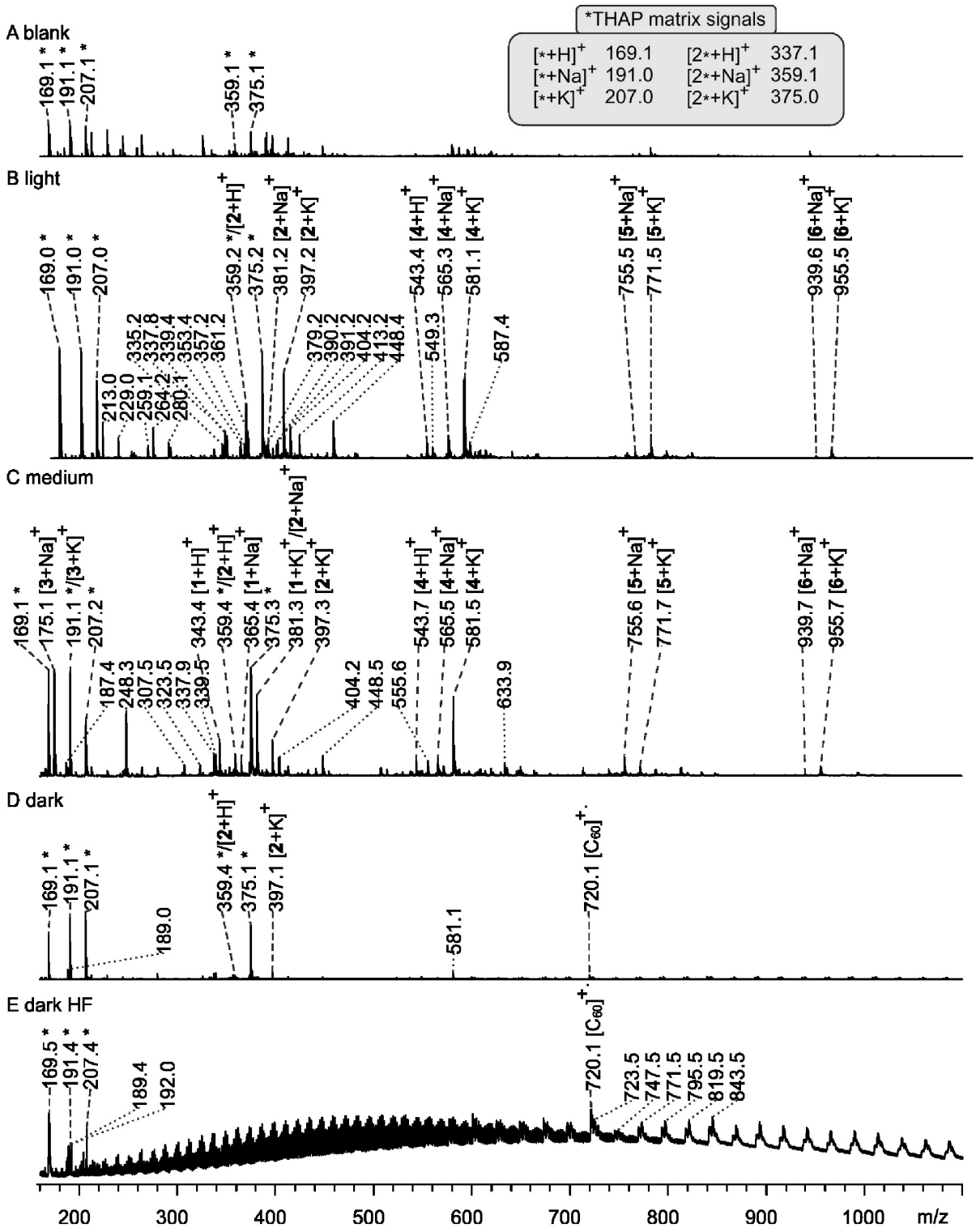

Figure 6. MALDI mass spectra (matrix THAP) of a blank measurement (A) and the three wood domains (B-E). Signals with a relative intensity >10% are annotated. The fully annotated spectrum of the blank is shown in Fig. S1. All signals were assigned after the spectra of the mass region up to *m/z* 400 were recalibrated (Table S2). Due to superposition, the following signals are assigned to multiple species: *m/z* 381 to $[1+K]^+$ and $[2+Na]^+$, *m/z* 191 to $[THAP+Na]^+$ and $[3+K]^+$ in medium spectra (C). $[2*THAP+Na]^+$ and minor amounts of $[2+H]^+$ are assigned to *m/z* 359.

The three signals *m*/*z* 343, 365, and 381 indicate the presence of a neutral molecule **1** with a mass of 342.12 Da (Fig. 6) which is detected as protonated molecule $[\mathbf{1}+H]^+$ and as adducts with sodium and potassium ions ($[\mathbf{1}+Na]^+$, $[\mathbf{1}+K]^+$). The signal at *m*/*z* 381 of molecule **1** is prominent in the medium, but very weak in the blank and all other domains indicating lower abundances in the latter. The three signals *m*/*z* 359, 381, and 397 can be assigned to a neutral molecule **2** with mass 358.06 Da. Severe superposition with other signals (Table 2) prevents a more distinct assignment in this case. Four other molecular compounds, **3** – **6**, could be detected as well.

The spectra of the dark domain before and after HF extraction show a regular pattern of signals from 700 *m*/*z* upwards that is absent in the other sampled domains or the blank (Fig. S2). This pattern consists of repeated signal groups with distances of 24 Da, indicative of plain carbon. Graphite shows the same regular pattern of signal groups every 24 Da at the same *m*/*z* values, the same form within the signal groups, and the same prominent signal at *m*/*z* 720 for fullerene C_{60}. Apparently, treating the sample powder with HF not only effectively removes silica, but also a majority of the organic substances (Fig. 6D and E). Only the dominant signals of carbon are detected in demineralized wood (Fig. 6E; Fig. S2), whereas organic compounds are detected in all untreated samples. Their presence is obvious in the light and medium domain, and possible but not constrained in the untreated dark domain, as suppression effects by easily ionizable substances are common in MALDI measurements of complex mixtures (Hillenkamp and Peter-Katalinic, 2013).

6.4. Discussion

Trace element mappings, electron microscopy, and MALDI-ToF-MS indicate an intimate coupling between primary and secondary ions, microstructure, and the organic geochemical properties of differently colored domains in silicified wood. Radial sections of the specimen show that decoloration and sharp interfaces between differently colored domains are three-dimensional features. The decoloration pattern and high degree of preservation is too pervasive for photooxidation and too intact for microbially-induced decoloration. Through EPMA and Raman mapping, we did not detect impurities such as iron oxide/hydroxide that could account for variations in cell wall coloration. Instead, differences in color correlate primarily with the abundance of highly disordered carbon (Fig. 4C). Calcium and sulfur are enriched only in the cell walls, showing that they preferentially bond to

the organic matrix. This is further evidenced by the absence of calcium- or sulfur-rich mineral precipitates in the cell walls. The observed chemical pattern suggests that silicification physically protected the specimen from rapid degradation while it was periodically immersed in solutions of variable composition.

6.4.1. Calcium and sulfur trace element distribution

Electron probe microanalysis indicates that none of the measured trace elements is universally present (Fig. 3). WDX mapping of the calcium distribution shows that the fronts between the differently colored domains are sharp and coincide on the microscale with optically and spectroscopically determined organic matter abundances. Calcium in trace quantities is usually considered to be a primary cell wall constituent and suggestive of remnant woody tissue in silicified wood (Sigleo, 1978; Boyce et al., 2001). If the organic material had a specific affinity for diagenetically derived calcium, it would be expected that the most pristine material, which is commonly assumed to be the darkest and most lignin-rich, would show the highest calcium concentration (Sigleo, 1978). This, however, is contrary to our observation of the lowest calcium concentration in the bulk dark domain and the tendency of secondary calcium to preferentially bond to lignin (cf. Torre et al., 1992). In the specimen studied here, the ~250 µm thick band that is the most calcium-rich and located at the interface of the dark and medium domains coincides with the highest concentration of highly disordered carbon (Fig. 4), however, not in the form of carbonate minerals, as indicated by Raman spectroscopy. Assuming that calcium is a primary cell wall constituent, this band represents the least altered remnant of lignin and potentially of holocellulose in the specimen. The bulk of dark domains in the specimen contain the least amount of calcium, which suggests a significant late-stage chemical overprint via unobstructed fluid pathways.

In contrast to calcium, sulfur is usually not considered as a primary trace element that follows wood anatomy in silicified or carbonate-mineralized wood (Boyce et al., 2001; Marynowski et al., 2011). In fact, previous studies have shown that secondary sulfur can readily be organically bound and accumulates preferentially in lignin-rich parts of the cell walls (Stankiewicz et al., 1997; Fors et al., 2012; Qi and Volmer, 2019), for example, by incorporation into alkenes during diagenesis (Boyce et al., 2001). Accordingly, we interpret the secondary sulfur concentration to reflect the amount of fluid-

accessible lignin and/or its degradation products to which sulfur can bond. High sulfur concentrations in the most calcium-rich and calcium-poor parts of the wood indicate sulfur bonding to organic substances which exist in both the least and most overprinted parts. FT-IR analysis of the demineralized dark domains shows that this organic residue contains abundant aromatic rings of guaiacyl units typical of gymnosperm lignin (Sarkanen and Ludwig, 1971). Diagenetically altered evaporite minerals from the ephemeral lakes and ponds of the Brushy Basin Member (cf. Currie, 1998), for example, would be a likely source for the preferentially incorporated sulfur.

6.4.2. Organic signatures

The degradation of buried wood is a complex interplay of processes such as oxidation, demethylation, de-methoxylation, loss of hydroxyl groups and condensation, which result in a continuous decrease in polysaccharides and increasing aromaticity with time since burial (Sigleo, 1978; Fengel, 1991; Briggs et al., 2000; van Bergen et al., 2000; Boyce et al., 2002; Marynowski et al., 2007; Bardet and Pournou, 2015). While holocellulose commonly resists degradation only for a few million years, lignin derivatives can frequently survive a diagenetic overprint of several million years long (Sigleo, 1978; Fengel, 1991; Marynowski et al., 2021). Here, the long-term preservation of lignin-related compounds is supported by FT-IR analysis of the dark domains that yields typical features of guaiacyl units (Fig. 5; Table S1).

MALDI-ToF-MS provides the opportunity for the direct assignment of molecules to the three differently colored domains. The different spatial distribution and abundance of these molecules is evidence for their primary origin. The neutral molecule **1** with a mass of 342.12 Da is detected in high intensity only in the medium domains. Two important molecules in wood cell walls fit to the measured mass value of 342.12 Da within the mass accuracy of the experiment: **1a** coniferin (Kaneda et al., 2008; Aoki et al., 2016; Yoshinaga et al., 2016) or **1b** a hexose disaccharide like cellobiose or sucrose (Ren et al., 2005; Aoki et al., 2016; Lee et al., 2021) (Fig. 7).

Due to the uneven sample preparation (suspension method) of the mineralized specimen, no higher mass accuracy could be achieved to distinguish between the non-isomeric structures **1a** and **1b**. Coniferin is a monolignol glucoside of coniferyl alcohol (Kaneda et al., 2008; Yoshinaga et al., 2016) and plays a fundamental role in the lignification process of wood (Freudenberg and Harkin, 1963;

Freudenberg and Torres-Serres, 1967; Yoshinaga et al., 2016). The hexose disaccharides **1b** can be built up by many different combinations of sugars, which are not easily distinguished by mass spectrometry (Pagel and Harvey, 2013; Hofmann and Pagel, 2017; Lee et al., 2021). However, the *m*/*z* of the protonated molecule and the adducts agree comparably well with those of disaccharide isomers including cellobiose (Ren et al., 2005; Aoki et al., 2016; Zhan et al., 2018). Interestingly, the relative signal intensity of **1** is much higher in the medium domains compared to the dark domains where the most unaltered plant substance would be usually expected. The negative calcium-sulfur correlation in the dark domain (Fig. 3) indicates a late natural fluid overprint that likely removed holocellulose degradation products, but retained the more resistant lignin and/or its degradation products. Although we cannot assign molecule **1** unequivocally to either a hexose disaccharide or coniferin, both of which are basic building blocks of wood, it is an important find that it could be either one of them, or both, in the Upper Jurassic wood studied here. Only recently have disaccharides been identified in significant concentrations in lignites (Marynowski et al., 2018). In the same study, it was shown with GC–MS analyses that fossil wood of Middle Jurassic age contains anhydro- and monosaccharide but lacks disaccharides. We infer that the preservation of a disaccharide from holocellulose degradation or coniferin is likely coupled to the silicification process that physically protects the organic substances from early diagenetic degradation and removal. The exceptional quality of preserved plant biomolecules is considered to indicate reductive conditions during fossilization (Marynowski et al., 2021).

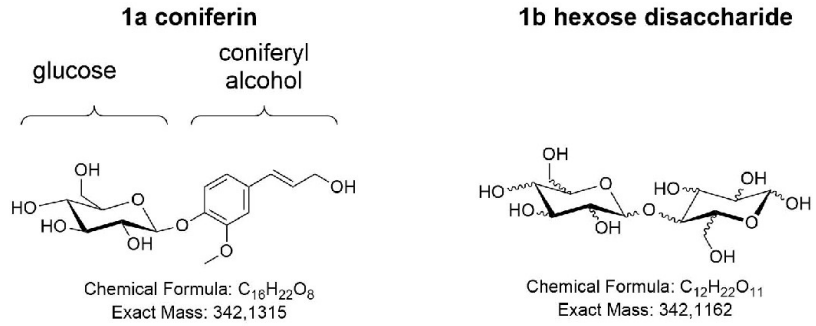

Figure 7. Structures of **1a** coniferin and **1b** hexose disaccharide.

Further signals in the MALDI mass spectra indicate relict organic substances. Mass spectra of lignin-containing samples typically show remaining soluble monomers and oligomers (Araújo et al., 2014; Kiyota et al., 2012; Saito et al., 2005a, b), *inter alia* lignin dimers of two monolignols. Some of these dimers have the elemental composition $C_{20}H_{22}O_6$ with a mass of 358.14 Da. In principle,

molecule **2** detected in all three domains of the silicified wood with a measured mass of 358.1 Da can be assigned to one or both of two lignin-related isomers: **2a** is a dimer formed from a cumaryl and a sinapyl alcohol whereas **2b** consists of two coniferyl alcohols (Fig. 8). Considering that coniferyl alcohol is the most abundant monolignol in conifers (Kaneda et al., 2008; Wagner et al., 2012) and guaiacyl ring vibrations of G lignin polymerized from coniferyl alcohol are abundant in FT-IR spectra, assigning **2** to isomer **2b** (two coniferyl alcohols) agrees well with the gymnosperm wood studied here. For the four low-intensity signals of species **3** – **6**, no molecular structure could be allocated.

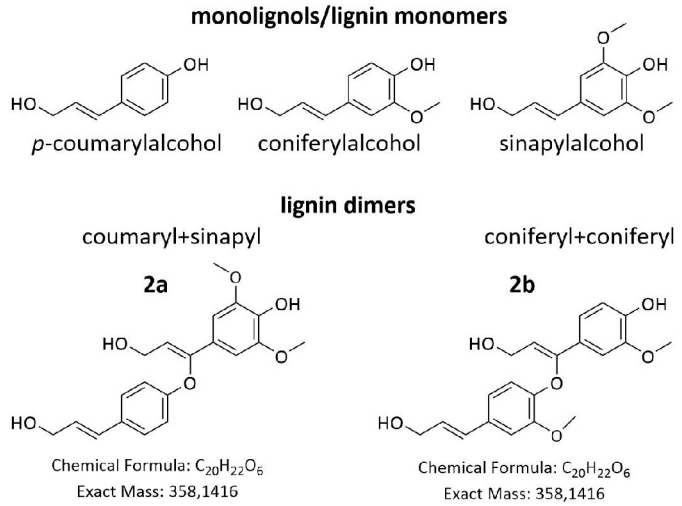

Figure 8. Structures of the monolignols/lignin monomers *p*-coumaryl-, coniferyl-, and sinapylalcohol, and lignin dimers **2a** and **2b**. The guaiacyl subunit in coniferyl is encircled.

6.4.3. Silicification cycles

When silica-rich fluid enters wood, silica monomers are expected to bond to the reactive surface groups of holocellulose on internal and external cell wall surfaces (Leo and Barghoorn, 1976; Liesegang and Gee, 2020). Cell lumina are usually unfilled at this early stage of fossilization (Mustoe and Dillhoff, 2022). Due to their hydrophobic character, the lignin-rich cell wall constituents (e.g., middle lamellae) initially remain largely unaffected (Liesegang and Gee, 2020). Lignin remnants preserved as dark dots at cell corners (Fig. 2E) likely document both the hydrophobic character of lignin and its stability over geological timescales.

Several studies showed that multiple silicification episodes can overprint the structure and chemistry of silicified wood while preserving cell wall morphology (Matysová et al., 2016; Trümper et al. 2018). If the commonly assumed diagenetic silica maturation involving dissolution-precipitation

processes in the cell walls proceeded in the studied specimen, it took place without a significant volumetric change that could otherwise severely damage plant tissue due to crystallization pressure (Liesegang and Gee, 2020). The direct precipitation of ordered silica phases, such as chalcedony, from diluted solutions has been invoked to explain a high degree of wood structural preservation and silica maturity (Liesegang et al., 2021; Mustoe and Dillhoff, 2022). To retain dimensional stability and organic matter distribution, episodes of diagenetic silica dissolution-precipitation in cell walls must proceed at the nano- to microscale, potentially via the formation of nanoscale dissolution channels in the cell wall. This process creates transient porosity that is subsequently filled with silica.

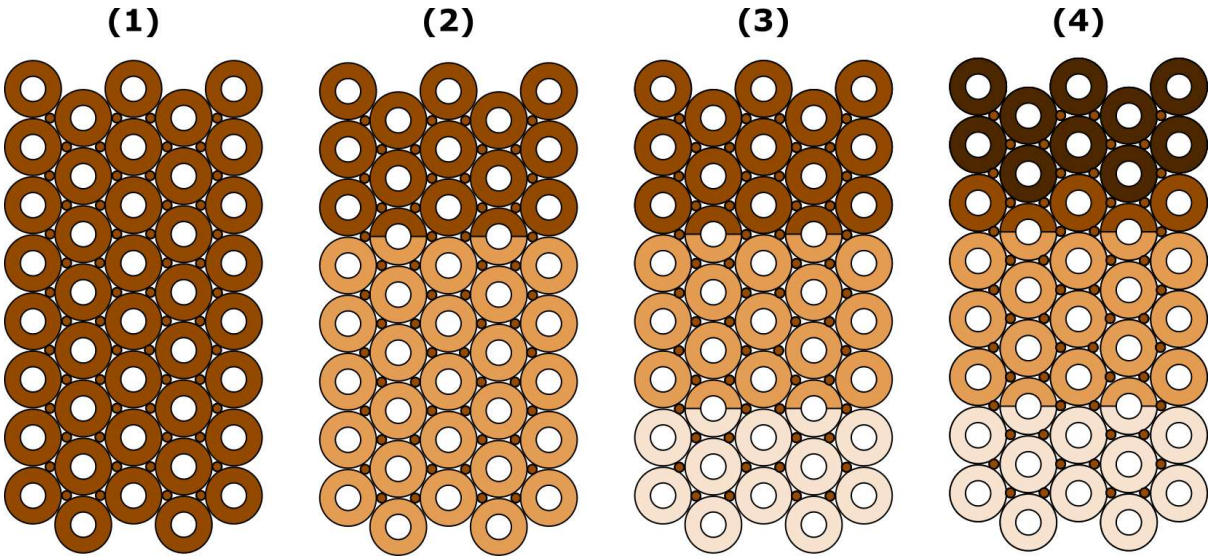

Figure 9. Schematic representation of the episodical silicification and decoloration of Upper Jurassic wood, beginning with a homogeneously silicified specimen (1). Progressive silicification (2–3) is associated with decoloration and loss of primary calcium (see Fig. 3), resulting in medium and light domains. The lightest domains have the lowest amount of fluid-accessible pore space. During the last wood silicification episode (4), the ingress of a sulfur-rich fluid results in the formation of the darkest, most sulfur-rich domain (top), and loss of primary calcium (see Fig. 3).

The distinct trace element distribution, particularly of primary calcium (Fig. 3B), indicates the amount of qualitatively well-preserved organic matter and provides evidence for at least four silicification episodes (Fig. 9). These episodes are: (1) incipient silicification of the entire specimen which preserves organic matter across all domains, (2) fluid access and silicification resulting in transport of soluble species, decoloration, and the formation of the medium domain, (3) further decoloration of the previous medium domain and formation of a light domain. The final overprint event (4) is preserved as a sulfur enrichment in the dark domain including the calcium-rich band. The

unsystematic scattering of the moganite/α-quartz ratio of chalcedony inside lumina and veins suggests that silica precipitation occurred within a short time span and/or at a similar degree of silica polymerization of the fluid (Heaney, 1993; Götze et al., 1998). Peak temperature calculations from Raman spectra of highly disordered carbon in the cell walls indicate that all silicification episodes took place at temperatures below ~100 °C.

Two major consequences result from ingress of silica-rich fluid into wood: degradation/transport of organic compounds and subsequent sealing of fluid-accessible pore space with newly-precipitated silica from fluids with variable dissolved silica concentration (e.g., Mustoe and Dillhoff, 2022). The higher the initial organic content, the more pore space is potentially available for fluid access and mass transport upon its degradation. The entrapment of organic matter in the silica matrix also reduces the potential impact of oxidation processes that cause gradual chemical changes (Marynowski et al., 2007). For the first three silicification events, the cell wall decoloration pattern highlights the fluid-accessible pathways during episodic immersion in water. The spatial extent of these pathways is limited by the overall penetration depth of the fluid into the bulk porous wood and the cell walls. As additional silica can precipitate in the cell wall only where organic matter has been previously removed, we observe a positive correlation between the abundance of dark organic matter and fluid-accessible pore space (Fig. 2D and E). However, MALDI-ToF-MS analysis shows that coniferin or a hexose disaccharide is preferentially preserved in lighter domains, which underlines that the quantitative and qualitative preservation of organic matter in silicified wood can be decoupled to some extent. The preservation of coniferin and/or hexose disaccharide and the molecules **3**-**6** in decolorized domains shows that cell wall clogging by silica is an effective mechanism to protect plant tissue from degradation.

The last silicification episode in the wood is characterized by an ingress of sulfur-rich fluid that effectively reduces the amount of primary calcium and, accordingly, the organic substance to which it was bound. The thin calcium-rich band at the interface of medium and dark domains indicates where the fluid ceased (Fig. 3B). Based on the significantly lower stability of holocellulose compared to lignin derivatives during diagenesis (Sigleo, 1978; Fengel, 1991), moderate primary calcium concentrations in the decolored domains indicate that lignin availability was of limited importance for the apparent difference in sulfur distribution. It is more likely that the bonding of sulfur to lignin-rich organic matter in dark domains is a function of sufficient fluid-accessible pathways. After silica clogs

relevant amounts of pore space in decolored domains, the most evident fluid pathway is the remaining pore space of the darkest domains. The aggressive degradation process of the organic matter was possibly similar to kraft pulping, which leads to the liberation of lignin fragments and their dissolution (Gierer, 1980). Here, the product of this process is characterized by abundant highly disordered carbon and guaiacyl ring vibrations indicating remnant lignin signatures. The silicification process ends with unselective fracturing across all wood domains and infilling of these veins with wall-lining chalcedony. Late fractures passing along the cell wall boundaries indicate cell separation after cell wall silicification and solidification.

6.5. Conclusions

We have presented organic compound and trace element characteristics of a varicolored Upper Jurassic gymnosperm wood analyzed with MALDI-ToF-MS, electron probe microanalysis, and vibrational spectroscopy and identified well-preserved wood biomolecules. Their distribution is consistent with the abundance of primary calcium and secondary sulfur in cell walls. These relationships demonstrate the effect of multiple silicification episodes on the decoupled quality and quantity of wood organic compounds. Our analytical results suggest that the key to the excellent preservation of biomolecules is the localized, transient opening and clogging of fluid pathways in silicified cell walls. To the best of our knowledge, using MALDI-ToF-MS analysis on mineralized material without acid hydrolysis, this study provides the first direct identification of lignin dimers and a hexose disaccharide or coniferin in silicified wood and thus highlights the significant potential of silicified plant analysis for future biomolecule identification in deep time.

6.6. Declaration of Competing Interest

The authors declare that they have no known competing financial interests or personal relationships that could have appeared to influence the work reported in this paper.

6.7. Acknowledgments

Funding for this research was provided by grants GE 751/5-1 (to CTG and Chris Ballhaus), EN 711/2-1 (to ME), and 396703500 (to CEM) from the German Research Foundation (DFG).

We thank Mary Beth Bennis and Dale E. Gray (Utah Field House of Natural History State Park Museum, Vernal, Utah, USA) for assistance in the field, Tanja Mohr-Westheide and Kirsten Born for access to the Raman spectroscopy facilities at the Museum für Naturkunde in Berlin, Germany, Karen Schmeling for desilicification of sample material at the University of Bonn, Germany, and Martina Menneken for assistance with the Raman spectrometer at the University of Bonn, Germany. This is contribution number #47 of the DFG Research Unit FOR 2685, “The Limits of the Fossil Record: Analytical and Experimental Approaches to Fossilization.”

6.8. Supplementary Material

Supplementary material, including FT-IR band assignments and details for the MALDI-ToF-MS calibration and additional spectra, can be found online at https://doi.org/--. In addition, Raman, FT-IR, and SEM data are available in the Zenodo Repository, at https://doi.org--.

Chapter 7

New occurrence of *Agathoxylon* from the Upper Jurassic Morrison Formation in Wyoming, USA and its implications for the paleohabitat

7.1. Introduction

Although plant fossils and vertebrate remains are rarely found together in the same fossiliferous sediments, abundant fossil plants along with the dinosaur remains have been found in the Howe Ranch in north-central Wyoming, USA (Tidwell et al., 1998; Ayer, 2000; Gee and Tidwell, 2010). As one of the most famous dinosaur localities in the Upper Jurassic Morrison Formation, Howe Ranch was first discovered by Barnum Brown of the American Natural History Museum in New York about one century ago (Bird, 1985). Soon after, a large-scale dinosaur excavation in Howe Ranch was carried out, which recovered approximately 3000 bones from Howe Quarry at Howe Ranch, representing a diversified dinosaur fauna of the megaherbivores *Diplodocus*, *Barosaurus*, and *Apatosaurus* (Tschopp et al., 2020). At Howe Ranch, another main fossil site about 450 m southwest of Howe Quarry, known as Howe-Stephens Quarry, has offered about 2500 bones of more than ten dinosaur individuals since the first excavation in 1992. These dinosaurs are comprised of three megaherbivorous dinosaurs (*Diplodocus*, *Camarasaurus*, *Stegosaurus*), and one carnivorous dinosaur *Allosaurus* (Ayer, 2000; Carballido et al., 2012).

Hundreds of coalified plant compressions were also found in the same geological horizon of the dinosaur remains, which is in the Brushy Basin Member of the Upper Jurassic Morrison Formation at Howe-Stephens Quarry. According to a study by Gee and Tidwell in 2010, this fossil flora is composed of woody shoots with leaves, ovulate cones, cone scales, seeds, and pollen cones, and these fossil plants were recognized as a single whole-plant, *Araucaria delevoryasii*, which may represent a monospecific araucariaceous forest at the Howe-Stephens Quarry area in the Morrison time.

Two fossil logs with anatomically well-preserved wood were discovered in the Brushy Basin Member of the Morrison Formation in Howe-Stephens Quarry of north-central Wyoming, USA. Here

we take a close look at the logs from Howe-Stephens Quarry to describe their wood anatomy in detail, reconstruct the ancient tree heights based on the preserved diameter of the logs, interpret the flora composition and ecological structure of the Morrison forests, and shed new light onto the dinosaur habitats of the Morrison. The fossil logs are recognized as a single species of *Agathoxylon*, *A. hoodii*, in the conifer family Araucariaceae and is now the only valid occurrence of *Agathoxylon* from the Upper Jurassic Morrison Formation in Wyoming.

7.2. Geological setting

The fossil wood specimens were collected from the Howe Ranch near Greybull in north-central Wyoming, USA, which is between the Bighorn Basin in the west and the Bighorn Mountains in the east (Fig. 1). These fossil wood specimens were preserved in the Upper Jurassic Morrison Formation,

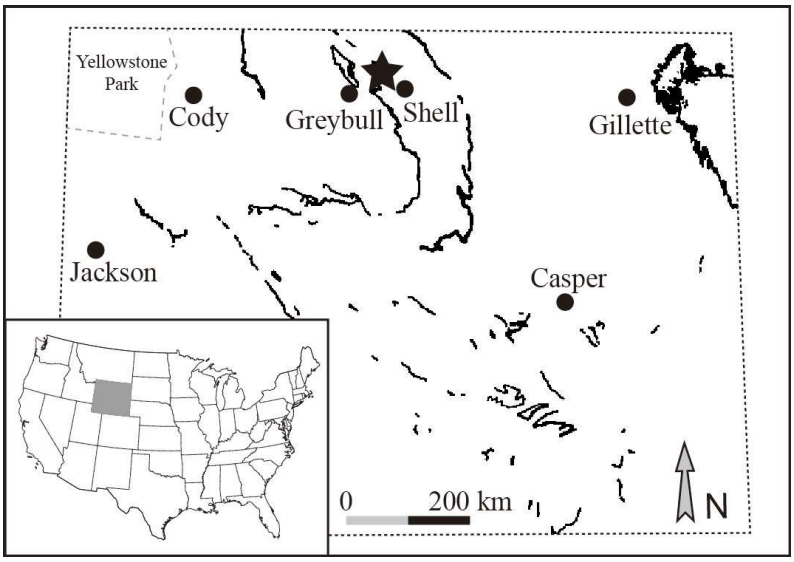

Figure 1. Sketch map of fossil locality (star) for fossil logs at Howe-Stephens Quarry in north-central Wyoming (dark gray state in USA map), USA, superimposed on the outcrops of the Upper Jurassic Morrison Formation. Map of Morrison outcrops courtesy of Kenneth Carpenter.

which is generally laterally distributed in the western United States, mostly in the Rocky Mountain region (Foster, 2020). In Howe Ranch, the Morrison Formation distributes in a southwest–northeast direction and consists primarily of sandstones and mudstones with rare layers of limestone with a thickness of ca. 55 m. Carbonaceous plant remains are usually concentrated in lenses in the cross-bedded sandstones, ranging from a few centimeters to several decimeters in thickness (Ayer, 2000). The fossil wood occurred in the dinosaur bed in the Howe-Stephens Quarry on the Howe Ranch. The matrix of the bone bed is composed of a light brown cross-bedded sandstone, which may represent part of a point bar sequence (Fig. 2) (Ayer, 2000).

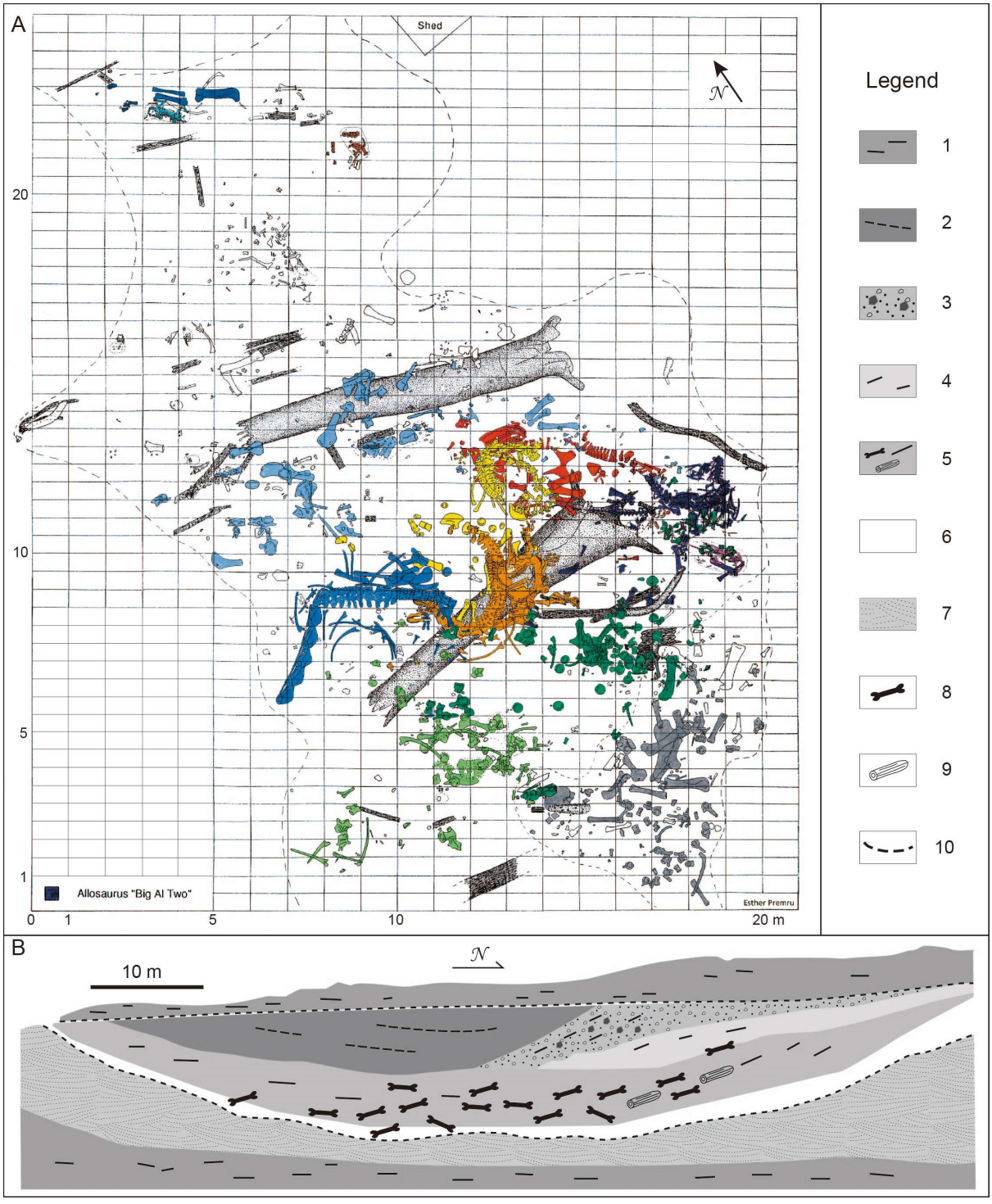

Figure 2. (A) Schematic map of the Howe-Stephens Quarry in north-central Wyoming, USA, with the 1992–2001 finds (courtesy of the Sauriermuseum Aathal, Aathal, Switzerland). (B) Sketch map of cross section through the Howe-Stephens Quarry in north-central Wyoming, USA (modified after Gee and Tidwell, 2010). Legend: (1) gray to greenish lithic mudstones; (2) gray mudstones; (3) gray sandstones with decimetric clay pebbles (breccias); (4) light gray sandstones; (5) highly fossiliferous brownish sandstones (the dinosaur bones and fossil plants are intimately associated in the same stratigraphic bed); (6) light weathering gray to yellowish sandstone; (7) light coarse-grained sandstones; (8) dinosaur bones and skeletons; (9) large fossil logs, fossil wood pieces, plant compressions and impressions; (10) erosional surface.

In general, the age of the Morrison Formation is considered to be the Late Jurassic, specifically the late Oxfordian to the Tithonian, but mostly Kimmeridgian (Litwin et al., 1998; Schudack et al., 1998; Turner and Peterson, 2004; Trujillo and Kowallis, 2015). The Morrison flora is comprised of conifers and ginkgophytes, with an understory of ferns, seed ferns, cycads, bennettitaleans, representing a warm and humid climate (Tidwell, 1990; Tidwell and Medlyn, 1992; Ash, 1994; Ash and Tidwell, 1998; Gee and Tidwell, 2010; Hotton and Baghai-Riding, 2010; Gee et al., 2019). The dominant vegetation type of the Morrison Formation is conifer forest (e.g., Gee and Tidwell, 2010; Hotton and Baghai-Riding, 2010; Gee et al., 2019).

7.3. Materials and Methods

Twenty-three specimens of silicified wood were selected for study from the paleobotanical collection of the Sauriermuseum Aathal near Zurich, Switzerland. They were inventoried at the University of Bonn with the prefix HSQ in consecutive sequence from HSQ-001 to HSQ-023. To make petrographic thin-sections for wood identification, all specimens were cut in the three planes of section, that is, transversely, radially, and tangentially. The thin-sections were investigated with a Leica DM2500 compound photomicroscope. Images and measurements were taken with software ImageAccess easyLab 7 integrated with the photomicroscope. The fossil wood specimens were returned to the Sauriermuseum Aathal, while the thin-sections are kept at the University of Bonn, Division of Paleontology. In the descriptions of the fossil wood, we follow the anatomical terms defined by the IAWA Committee (IAWA Committee, 2004).

7.4. Results

7.4.1. Systematic paleobotany

Order Coniferales

Family Araucariaceae

Genus *Agathoxylon* Hartig

Species *Agathoxylon hoodii* (Tidwell et Medlyn) Gee, Sprinkel, Bennis, et Gray (Fig. 3 and 4)

Synonymy:

1993 *Araucarioxylon hoodii*—Tidwell and Medlyn, pl. 1, figs, 1–6; pl. 2, figs. 1–6

2019 *Agathoxylon hoodii*—Gee, Sprinkel, Bennis, and Gray, figs. 5 and 6

Locality: Howe-Stephens Quarry, Howe Ranch, near Greybull, Wyoming, USA.

Specimens studied: HSQ-001 to 023.

Horizon and age: Brushy Basin Member, Morrison Formation, Late Jurassic (Kimmeridgian).

Repository: Fossil wood specimens in the Sauriermuseum Aathal near Zurich, Switzerland; thin sections in the Division of Paleontology, Institute of Geosciences, University of Bonn, Germany.

Description: Based on secondary xylem, because bark, pith, and primary xylem are absent. In transverse section, true growth rings absent (Fig. 3a–c); irregular, discontinuous concentric bands of tracheids with narrower lumina locally apparent (Fig. 3b, c), ranging from 1 to 4 cells thick and developing asynchronously during the growth of the tree. Tracheids subround to elliptical to polygonal in transverse section; lumina ranging from 25 to 66 μm in tangential diameter, those of normal-size cells about 46 μm (Fig. 3e). Axial parenchyma and resin canals absent.

In radial section, tracheids on average 61 μm wide (52–75 μm). Radial tracheid pits usually uniseriate, but also locally biseriate. When uniseriate, arrangement of tracheary pits contiguous and compressed (Fig. 3g, h), occasionally distant (Fig. 4c); when biseriate, alternate (Fig. 4a, b), occasionally opposite (Fig. 4c). Bordered pits generally oblate in outline. Crassulae not observed. Resinous remains coalesced along the periphery in ray cells and the cell corners (Fig. 4d). Crossfield pitting araucarioid type sensu IAWA Committee (2004). Each crossfield bearing numerous pits, 7–16 cupressoid pits with a circular or oval outline, contiguous, arranged in 3–5 alternate vertical rows (Fig. 4e, f). Rays consisting of parenchymatous cells with thin, smooth horizontal and end walls (Fig.

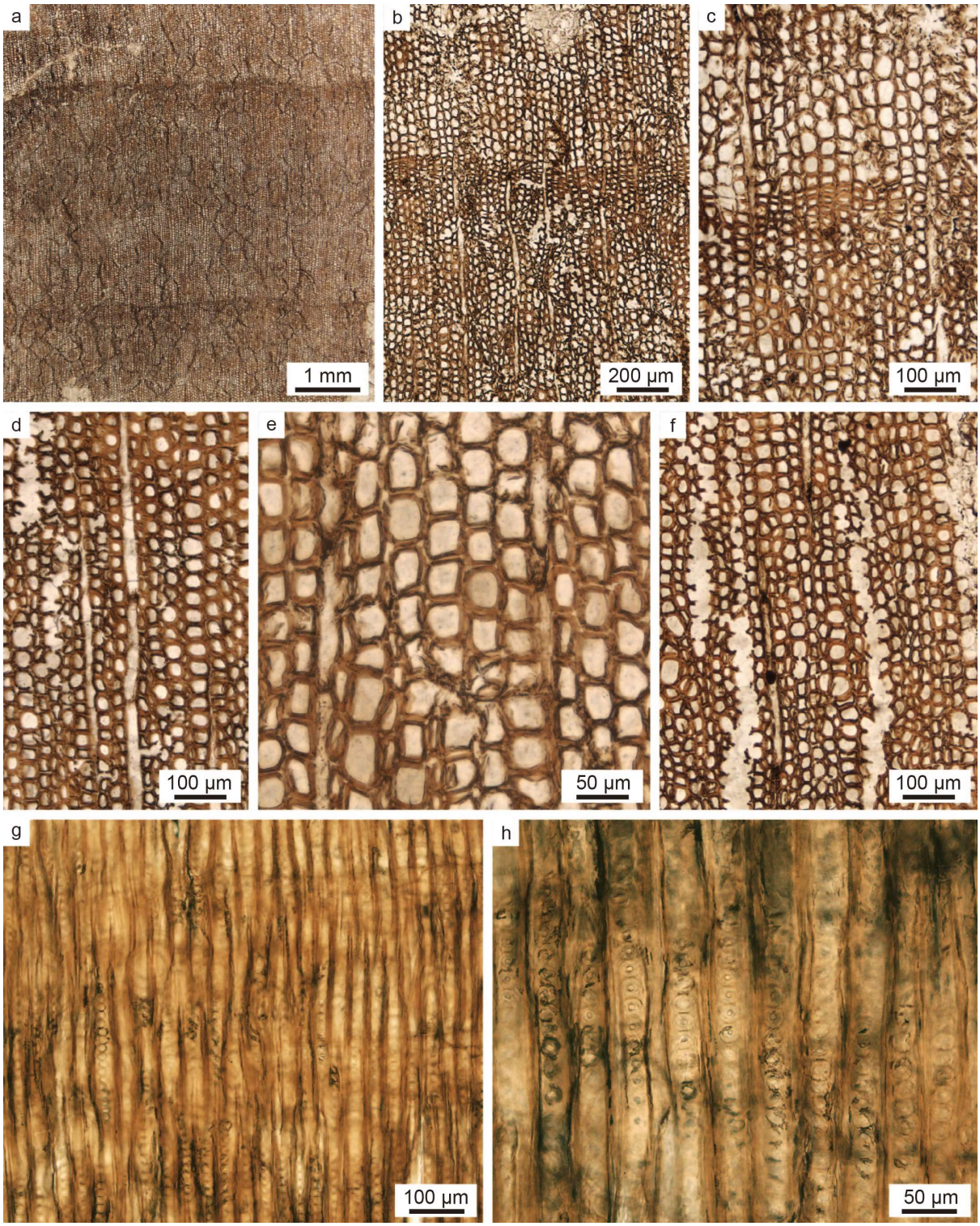

Figure 3. *Agathoxylon hoodii* (Tidwell et Medlyn) Gee, Sprinkel, Bennis, et Gray from the Upper Jurassic Morrison Formation at the Howe-Stephens Quarry in north-central Wyoming, USA; all photographs were taken of transverse and radial sections of thin section HSQ-021. (a) Transverse section, showing growth rings indistinct, true growth rings absent. (b) Transverse section, showing irregular, discontinuous concentric bands of tracheids with narrower lumina apparent. (c) Close-up of b, transverse section, showing details of tracheids with narrower lumina. (d) Transverse section, showing ray cells. (e) Transverse section, showing details of tracheids, subround to elliptical to polygonal. (f) Transverse section, showing details

of decayed tracheids. (g) Radial section, showing tracheids with uniseriate, contiguous, and compressed bordered pits. (h) Close-up of g, radial section, showing details of radial tracheid pits.

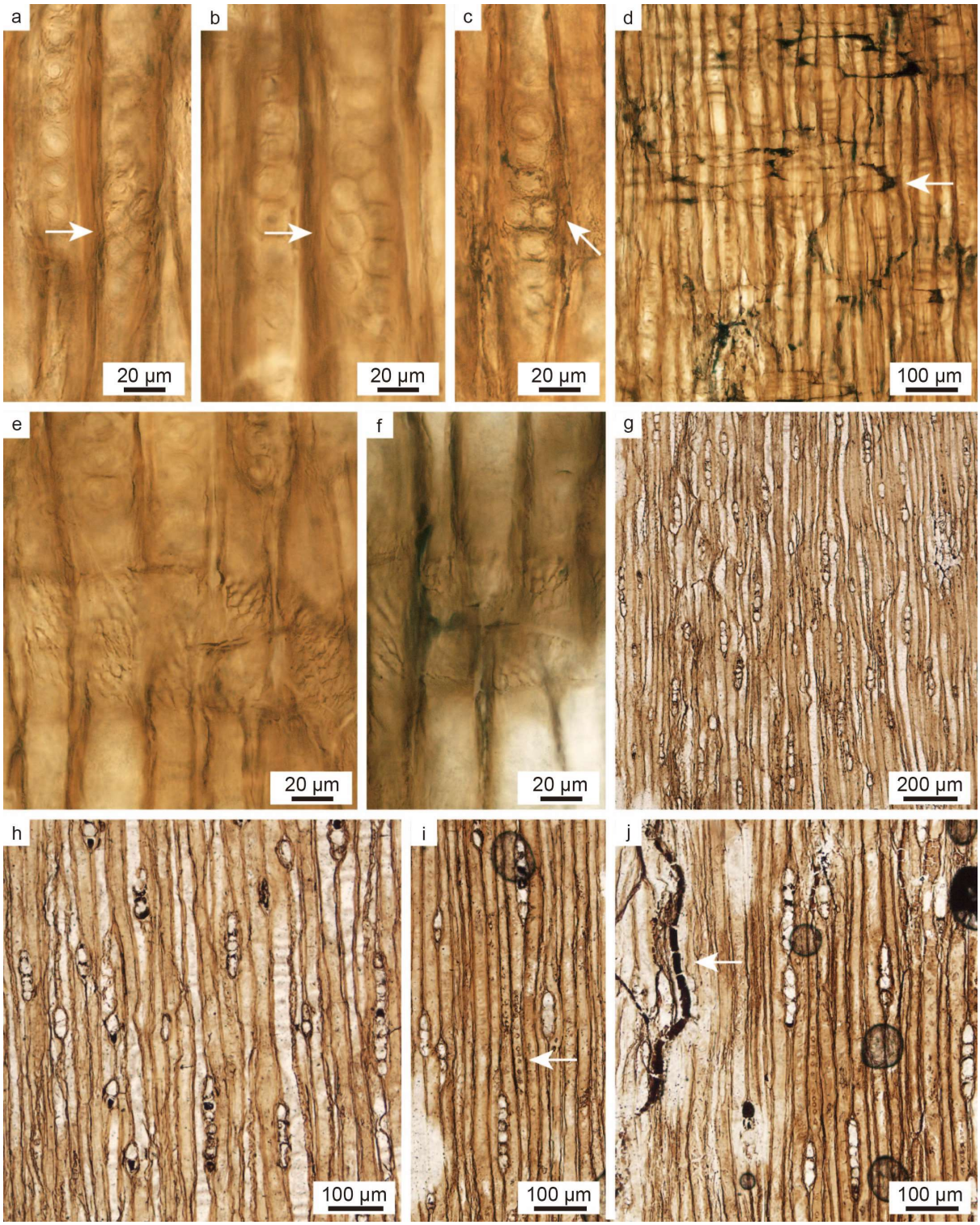

Figure 4. *Agathoxylon hoodii* (Tidwell et Medlyn) Gee, Sprinkel, Bennis, et Gray from the Upper Jurassic Morrison Formation at the Howe-Stephens Quarry in north-central Wyoming, USA; all photographs were taken of radial and tangential sections of thin section HSQ-021. (a–b) Radial section, showing tracheids with biseriate alternate bordered pits (arrow). (c) Radial section, showing tracheids with biseriate opposite bordered pits (arrow). (d) Radial section, showing

resinous remains coalesced along the periphery in ray cells and the cell corners (arrow). (e–f) Radial section, showing details of araucarioid cross-field pits in which each cross-field bears 7–16 cupressoid pits. (g) Tangential section, showing uniseriate rays. (h) Close-up of g, tangential section, showing details of uniseriate rays. (i) Tangential section, showing uniseriate tangential tracheid pitting (arrow). (j) Tangential section, showing resin plugs (arrow).

4d–f).

In the tangential section, rays are homogenous, parenchymatous, uniseriate (Fig. 4g–j). The rays are variable in height, ranging from very low to high, 2–25 cells high, mostly 3–8 cells tall. Bordered pits on the tangential tracheary walls circular, 15.8 μm in diameter, usually uniseriate distant, but also locally contiguous (Fig. 4i, j). Resin plugs evident in tracheids of axial system (Fig. 4j).

Remarks: Although numerous pieces of fossil wood were collected from the Howe-Stephens Quarry, 23 specimens were selected for thin-sectioning and study. Of these, only seven wood specimens yielded anatomical characters sufficient for unequivocal identification due to the generally poor preservation of the fossil wood flora from the Howe-Stephens Quarry. Two specimens, HSQ-021 and 022, are so well-preserved that they form the basis of the anatomical description here (Fig. 3 and 4). Tangential tracheid pits occur in these specimens, showing an arrangement that is usually uniseriate distant, occasionally contiguous. Because this character was not mentioned in the original description of *Araucarioxylon hoodii* from Mount Ellen in SE Utah, by Tidwell and Medlyn (1993), nor in the description of the new combination of *Agathoxylon hoodii* from Rainbow Draw in NE Utah, by Gee et al. (2019), we have added this detail here to the wood from Howe-Stephens Quarry, north-central Wyoming.

7.4.2. Reconstruction of Minimum Tree Height of *Agathoxylon hoodii*

Based on the height–diameter relationship of living *Araucaria* trees, three good height–diameter growth models (Eqs. 1, 2, and 3) were established for the estimation of minimum tree height from preserved diameter of fossil araucariaceous logs (Xie, Gee, Griebeler, unpubl. data). These three growth models for ancient Araucariaceae conifers can be given as:

$$H = 57.22 \times D^{0.67} \quad (1)$$

$$H = 58.03 \times D^{0.72} \quad (2)$$

$$H = 101.78 \times D / (1+D)^{0.80} \quad (3)$$

where H = estimated tree height, D = maximum preserved diameter of fossil log.

The preserved diameter at breast height (DBH) of the fossil logs at the Howe-Stephens Quarry is 1.15 m and 1.49 m (Fig. 2). Hence, this results in a reconstructed minimum height of the *Agathoxylon* tree at Howe-Stephens Quarry of about 63 m (62.84 m, 64.17 m, and 63.45 m) and 75 m (74.75 m, 77.33 m, and 73.10 m) respectively.

7.4.3. Tree taper of *Agathoxylon hoodii*

Based on analysis of living trees, an equation (Eq. 4) has been developed to extrapolate tree stem diameter at any height from tree taper. Generally, the portion of the tree stem from breast height to the base of the crown produces a linear or nearly linear stem profile (Larsen, 2017). Drawn from Eq. (4), the Eq. (5) for calculating tree taper can be given as:

$$d_h = dbh + p \times (h - bh) \quad (4)$$

$$p = (d_h - dbh) / (h - bh) \quad (5)$$

where d_h = the trunk diameter at height h of the tree in m, dbh = the trunk diameter at breast height of the tree in m, normally measured at approximately 1.3 m of tree above ground from the interface between the trunk and root system, p = the tree taper rate, h = any height of the tree in m, and b_h = the breast height of the tree in m.

Although tree taper can be used to describe trunk diameter decrease in girth along their length, the tree taper rate below breast height is generally different from the taper rate above breast height (Larsen, 2017). Hence, we carried out two taper rates for each fossil log. The results reveal that fossil log 1 obtains a stump taper rate (portion below breast height) equal to 0.06 and a stem taper rate (portion above breast height and below crown base) equal to 0.05, whereas the fossil log 2 acquires a

stump taper rate equivalent to 0.28 and a stem taper rate equaling 0.11.

7.5. Discussion

Although only two fossil logs are described from Howe-Stephens Quarry, they represent the only valid systematic report of the fossil wood *Agathoxylon* from the Upper Jurassic Morrison Formation in Wyoming. Previously, Knowlton (1900), and Andrews and Pannell (1942) described two species of fossil araucariaceous wood from the Morrison Formation of Wyoming, *Araucarioxylon*? *obscurum* and *A. wyomingense*, respectively; however, these taxa have been determined to be invalid (cf., Rößler et al., 2014). Hence, the recognition of a valid occurrence of fossil araucariaceous woods, which is described here as *Agathoxylon hoodii* from Howe-Stephens Quarry, contributes to a more profound understanding of Upper Jurassic conifer diversity in Wyoming and the composition of the forest vegetation in the Morrison.

7.5.1. Taxonomic assignment and comparison

All silicified wood from the Howe-Stephens Quarry described here can be assigned to the genus *Agathoxylon* based on a shared suite of characters: araucarian radial tracheid pitting and araucarioid crossfield pitting; many radial tracheid pits uniseriate, contiguous, and compressed, but also uniseriate contiguous to distant, or biseriate alternate to opposite; crossfields each bearing seven to sixteen densely arranged cupressoid pits.

Up to now, only two species of fossil araucariaceous woods have been reported from Wyoming, namely *Araucarioxylon*? *obscurum* Knowlton from the Morrison Formation in the Freezeout Hills of Wyoming (Knowlton, 1900) and *Araucarioxylon wyomingense* Andrews et Pannell from the Gros Ventre Canyon in western Wyoming (Andrews and Pannell, 1942). When the Freezeout Hills wood was described in 1900, Knowlton was uncertain of its generic position and tentatively assigned the wood to *Araucarioxylon* because it had obscure growth rings and relatively low ray height (Knowlton 1900; Medlyn and Tidwell, 2002). Although the Freezeout Hills wood was transferred to *Mesembrioxylon obscurum* on the basis of its podocarpaceaous anatomy (Medlyn and Tidwell, 2002), the genus *Mesembrioxylon* Seward 1919 is invalidly published owing to this generic name proposed

to replace Gothan's two valid genera *Podocarpoxylon* and *Phyllocladoxylon* (Bamford and Philippe, 2001; Philippe and Bamford, 2008). The Freezeout Hills wood differs from the Howe-Stephens Quarry wood by having mostly uniseriate, distant radial tracheid pits and 1–3 thin-bordered podocarpaceous pits per crossfield (Medlyn and Tidwell 2002), whereas our wood shows mostly uniseriate, contiguous, and compressed radial tracheid pits and araucarioid crossfield pitting. The second species, *Araucarioxylon wyomingense*, is marked by very low rays (1–3 cells high), locally strongly flattened radial tracheid pits, and a lack of tangential tracheid pits (Andrews and Pannell, 1942), while our wood has mostly uniseriate, distant tangential tracheid pits, higher rays (1–9 cells high), and a lack of strongly flattened radial tracheid pits.

Recently, Gee et al. (2019) reported a local wood flora of *Agathoxylon hoodii* (Tidwell et Medlyn) Gee, Sprinkel, Bennis et Gray from the Upper Jurassic Morrison Formation in Rainbow Draw, NE Utah, which was originally described as *Araucarioxylon hoodii* Tidwell et Medlyn (1993) from the same formation occurring on the eastern flank of Mt. Ellen in the Henry Mountains, southern Utah. Anatomical characters of *Agathoxylon hoodii* were described by Gee et al. (2019) as containing a dominance of axial tracheids and the lack of axial parenchyma and resin canals; the presence of abundant resin plugs and other resinous remains; an arrangement of the circular bordered pits on the tracheid walls as uniseriate, contiguous or occasionally distant, or alternate to opposite when biseriate; smooth, unpitted horizontal walls and end walls in ray cells; numerous, crowded, cupressoid pits in the crossfields; and an absence of true growth rings. Some wood samples show asynchronously occurring slowdowns in growth. These bands of smaller cells with thicker cell walls do not necessarily reach around the entire trunk (Gee et al. 2019). This suite of anatomical characters in *Agathoxylon hoodii* from Utah is extremely similar to the wood from the Howe-Stephens Quarry (Fig. 3 and 4).

There is only one minor difference between the fossil wood specimens from 13 logs in Rainbow Draw and the 23 specimens of wood from the Howe-Stephens Quarry, which is that the Rainbow Draw wood appears to contain a greater number of resin plugs or resinous remains, especially in the ray cells. Differences in resin abundance were also already noted by Gee et al. (2019) when comparing the Rainbow Draw wood flora with the species holotype from Mt. Ellen (cf. Tidwell and Medlyn 1993). Because a scantiness or absence of organic deposits such as resin plugs is not diagnostic for systematic identification (IAWA Committee, 2004), all fossil wood specimens from the

Howe-Stephens Quarry studied here are assigned to *Agathoxylon hoodii* (Tidwell et Medlyn) Gee, Sprinkel, Bennis et Gray (2019).

7.5.2. Height, age of Morrison trees and forest

The preserved lengths of 9.0 m and 8.7 m with DBH of 1.15 m and 1.49 m of the fossil logs at Howe-Stephens Quarry, as well as their reconstructed heights of at least 63 m and 75 m respectively, confirms the presence of old-growth forests in the Morrison Formation. A similarly large fossil trunk of 90 cm in preserved diameter has been reported from the Gros Ventre Canyon of western Wyoming (Andrews and Pannell, 1942), which is located about 240 km southwest of the Howe-Stephens Quarry, although the reconstructed tree height of the Gros Ventre Canyon log was not given by Andrews and Pannell. Based on the three good height–diameter growth models for the extrapolation of ancient araucariaceous tree height (Xie, Gee, Griebeler, unpubl. data), the preserved diameter of 90 cm of the Gros Ventre Canyon fossil log results in a tree height of about 54 m (53.32 m, 53.79 m, and 54.82 m).

A height of about 60–80 m corresponds to the size of many conifer trees native to tropical regions today. For example, mature trees of *Araucaria cunninghamii* and *A. hunsteinii*, which are very common species in the primary forests at the east coast of Papua New Guinea, reach an average height of about 60 m, ranging from 52 m to 66 m, when DBH equals to 1 m (Gray, 1975). In the temperate forests of western USA, the native coastal redwood *Sequoia sempervirens* normally reaches an average height of about 50 m (33–70 m), when DBH reaches 1 m (Sillett et al., 2019; Earle, 2020; Vaden, 2020).

In general, the age of trees is positively related to their diameter and height, namely, tree age may be estimated on the basis of tree size (Xing et al., 2012). For example, mature trees of *Araucaria araucana*, which is a very common species in the Andes Mountains of Northern Patagonia, attain an average height of 5 m with a DBH of 25 cm at 140 years of age, while older trees reach an average height of 25 m with a DBH of 85 cm at 450 years of age (Hadad et al., 2020). Nonetheless, the relationship between tree age and the diameter and height of the tree is not always positive correlation; for example, the largest trees may not always be the oldest because older trees in an adverse environment may have lost canopy biomass and height (Scipioni et al., 2019). For example, in

the tropical forests of southern Brazil, the native species of *Araucaria angustifolia* reaches a tallest tree height of about 45 m when the DBH equals to about 2 m, whereas the older *Araucaria* trees in the same region attain an average height of about 38 m with the DBH equal to about 3 m (Scipioni et al., 2019). Thus, extrapolating from the sizes and ages of tall forest conifer trees, specifically those of extant *Araucaria*, these Howe-Stephens Quarry trees of *Agathoxylon hoodii* with reconstructed tree heights of 63 m and 75 m most likely were over 500 years old before they died.

7.5.3. Paleohabitats of the Morrison dinosaur bones bed in Howe-Stephens Quarry

With the discovery of our new fossil logs from Howe-Stephens Quarry, Wyoming, the occurrence of *Agathoxylon* trees confirms the presence of tall forest trees in the Morrison Formation in the Howe-Stephens Quarry area. Another line of evidence supporting the presence of forests in this region during the deposition of the Late Jurassic Morrison Formation are the other coalified plant compressions from Howe-Stephens Quarry. These plant compressions consist of woody shoots with leaves, ovulate cones, cone seeds, seeds, and pollen cones, which were recognized as a single whole-plant species of *Araucaria* (Gee and Tidwell, 2010). The presence of an araucariaceous forest with gigantic trees suggests that humid environments prevailed in the Howe-Stephens Quarry area during the Morrison times.

If the Red Gulch Dinosaur Tracksite, about 15 km southeast of the Howe-Stephens Quarry in Wyoming, is included, there is also palynological evidence supporting humid environments in the Howe-Stephens Quarry area during the Late Jurassic. The palynological studies show a high overall species diversity and a high abundance and diversity of spores, including bryophytes, lycophytes, ferns, Araucariaceae, Podocarpaceae, Cupressaceae and Cheirolepidiaceae (Hotton and Baghai-Riding, 2010).

Such a flourishing forest of conifers with a dense understory of ferns and bryophytes during the Late Jurassic in the Howe-Stephens Quarry area (Gee and Tidwell, 2010; Hotton and Baghai-Riding, 2010) would have offered the bulk of the food supply consumed by the Morrison herbivores. For example, in Howe-Stephens Quarry, a very dense accumulation of dinosaur bones, yields a high diversity of dinosaur fauna, including the megaherbivorous dinosaurs *Diplodocus*, *Camarasaurus*, and *Stegosaurus*, as well as the carnivorous dinosaur *Allosaurus* (Ayer, 2000; Carballido et al., 2012),

which suggests that these dinosaurs might inhabit an araucariaceous forest.

Although abundant dinosaur bones have been found in Howe-Stephens Quarry, the preliminary sedimentological study shows that these dinosaur skeletons were transported by a devastating flood in the river for some distance before being deposited. For instance, the caudal vertebrae of the dinosaur "Big Al Two" were detached from the rest and lay on the front part of the dinosaur (Fig. 2), which indicates the carcass may have been transported after the dinosaur died and subsequently stopped by an obstacle (Ayer, 2000).

7.6. Conclusions

Newly discovered fossil logs and wood in the Howe-Stephens Quarry at Howe Ranch in north-central Wyoming were found to pertain to *Agathoxylon hoodii*, the first unequivocal occurrence of this genus in this state. The fossil logs measure 1.15 m and 1.49 m in diameter, respectively. Based on diameter–height calculations, the fossil logs of *Agathoxylon hoodii* attained at least 60 m and 71 m in height, respectively, which presumably represents two individuals within a larger forest community with many more trees of similar size that reached individual ages of over 500 years. The Howe-Stephens Quarry conifer forest suggests that humid environments prevailed in the Morrison times, which likely would have constituted the bulk of the food supply consumed by Morrison herbivores.

7.7. Acknowledgments

I thank Hans-Jakob (Köbi) Sieber and team for many years of collection at the Howe-Stephens Quarry, as well as for access to the collections at and loan of material from the Sauriermuseum Aathal. I would also like to thank Olaf Dülfer, Nicki Karyofylli, and Vincent Cheng for the thin sectioning of fossil wood specimens. Financial support from the China Scholarship Council for the doctoral studies of AX (CSC no. 201804910527) is greatly appreciated.

Chapter 8

Synthesis: What we can contribute to the reconstruction of Morrison landscape based on the fossil woods and logs in the Upper Jurassic Morrison Formation in western USA

Although six chapters in this dissertation have already presented recent scientific research on fossil woods from the Upper Jurassic Morrison Formation in the Western Interior of North America, there are still more scientific questions that need to be answered to understand the vegetation composition, paleoclimate, and paleoenvironment during Morrison times. This chapter aims to provide insights into the reconstruction of landscape based on the fossil woods and logs in the Upper Jurassic Morrison Formation in the western USA, including approaches of research on woody flora, height structure and age of the forests, biodiversity of the vegetation, implications of flora for Morrison dinosaurs, and paleoclimate reconstruction based on plants. In addition, future perspectives in the reconstruction of Morrison landscape using fossil woods and logs are also discussed, which include the new approaches that have not been used in this dissertation as well as the further approaches that need to be applied to newly discovered fossil woods and logs from other fossil localities in Utah.

8.1. Approaches of research on fossil woods

Beyond the numerous examples of wood anatomy for systematic paleobotany studies described since the middle of the nineteenth century (e.g., Endlicher, 1847; Gothan, 1905; Kräusel, 1949; Philippe and Bamford, 2008; Boura et al., 2021), an increasing number of different approaches have been carried out on the fossil wood studies. For example, tree growth ring analysis has commonly been implemented on fossil woods to reconstruct the growth conditions and the leaf longevity of ancient trees (e.g., Falcon-Lang 2000a; 2000b; Brison et al., 2001; Brea et al., 2008; Falcon-Lang et al., 2016; Krapiec et al., 2016; Gee et al., 2019; Jiang et al., 2020; Gou et al., 2021; Xie et al., 2021).

In this dissertation, the mean sensitivity analysis of growth rings was applied to the fossil conifer-like tree *Xenoxylon utahense* from the Upper Jurassic Morrison Formation in Utah. That the *Xenoxylon* tree had a mean sensitivity equal to 0.53 suggests that it grew in a warm and humid climate, because a mean sensitivity value varying from 0.35 to 0.6 corresponds to living conifers growing in a warm, humid climate in the southeastern United States or on the North Island of New Zealand, especially in flooding-disturbed, streamside habitats (Falcon-Lang, 2005). Although this interpretation is only based on a single occurrence of the *Xenoxylon* tree in the Morrison Formation, this understanding is justified, owing to a warm and humid climate which is consistent with the Late Jurassic paleoclimate inferred from the abundant fossil plant records in this formation (Tidwell, 1990; Tidwell and Medlyn, 1992; Ash, 1994; Ash and Tidwell, 1998; Gee and Tidwell, 2010; Hotton and Baghai-Riding, 2010; Gee et al., 2019; Xie et al., 2021), although other studies argue for a semiarid to arid climate with sparse vegetation (Demko and Parrish, 1998; Demko et al., 2004; Parrish et al. 2004; Rees et al. 2004; Turner and Peterson, 2004). Furthermore, this new occurrence of *Xenoxylon* in Utah with distinct growth ring characters indicating a warm and humid climate argues for *Xenoxylon* not always a reliable indicator of cool climate that has been extensively considered.

Recently, there is an increasing awareness behind the meaning of boreholes and fungal remains in fossil woods and the understanding of the ecological associations between plants, insects, and fungi (e.g., Césari et al., 2012; Harper et al., 2012, 2016; García et al., 2012; McLoughlin and Strullu-Derrien, 2016; Feng et al., 2017; Sagasti et al., 2019; Wei et al., 2019; Tian et al., 2020). In this dissertation, plant–insect–fungal interactions in the Upper Jurassic Morrison Formation in Utah are described in chapters 3 and 4. In chapter 3, an araucariaceous host tree in the Morison Formation in Utah bearing two insect boreholes, two cocoons of extant orchard mason bee in the larger borehole, and white rot fungal damage in the wood tissue was described, which represent the multitrophic interactions between an ancient tree–insect–white rot fungi and an extant insect across 150 million years. Similar white rot characters are also found in an ancient conifer-like tree *Xenoxylon utahense* in Utah. In chapter 4, the white rot fungi occurring in this *Xenoxylon* tree were described in detail based on the decay of the middle lamellae and abundant fossil mycelia with typical clamp connections that can be assigned to Basidiomycota. This occurrence of Basidiomycota represents the first reliable white rot fungi in the Jurassic of Utah.

Based on the preserved maximum diameter of fossil log or stump, estimating ancient tree height

has also been commonly applied to the reconstruction of fossil forests using specific height–diameter growth models (e.g., Mosbrugger, 1990; Mosbrugger et al., 1994; Niklas, 1994; Pole, 1999; Williams et al., 2003; Gee et al., 2019). In this dissertation, the height of a conifer-like tree in the Morrison Formation in Miners Draw in Utah was reconstructed as ca. 40 m based on our preliminary results of height–diameter growth model for conifers of unknown family affinity, which indicates that this Miners Draw tree was a mature tree, probably one individual in a larger forest community of many more trees of similar size. In the Jurassic times, Araucariaceae were dominant in the forest vegetation. To estimate ancient araucariaceous tree height based on the maximum preserved diameter of fossil logs, we established three good height–diameter growth models for ancient araucariaceous trees using the height–diameter relationship of living *Araucaria* trees in New Guinea and Queensland of Australia. To test our new growth models, these models were applied to the araucariaceous log flora in Utah reported by Gee et al. (2019) to end up with good estimates of araucariaceous tree heights.

In general, the preservation of fossil wood varies on the quality of internal structures. Anatomically well-preserved fossil woods normally contain more organic matter than the poorly preserved woods, as well as more silica or calcium carbonate than iron carbonate (e.g., Williams et al., 2010). In this dissertation, the results are consistent with the interpretation of preservation of fossil woods previously suggested based on a silicified wood from the Upper Jurassic Morrison Formation in Utah (chapter 6; Pereira, 2020).

8.2. Height structure and age of Morrison forests

In Miners Draw, near Vernal of northeastern Utah, a large fossil conifer-like log was measured with a maximum preserved diameter of 0.90 m. Based on our previous height–diameter growth model of a general conifer, the height of this ancient Miners Draw tree was reconstructed as ca. 40 m (Xie et al., 2021). In Rainbow Draw, located about 30 km northwest of the Miners Draw, the fossil wood flora of Morrison Formation contains five large araucariaceous logs measuring 0.36–0.64 m in maximum preserved diameter, as reported by Gee and colleagues in 2019. Gee et al. (2019) reconstructed the minimum heights of these Rainbow Draw trees as 19–28 m according to the height–diameter growth model of ancient conifers proposed by Mosbrugger et al. (1994). However, based on our new height–diameter growth models for the estimation of tree heights of ancient araucariaceous

trees, we revise the tree heights of the Rainbow Draw trees in chapter 5 to be ca. 45–69 m, that is, about two times greater than the tree height estimates in Gee et al. (2019). In the Howe-Stephens Quarry of north-central Wyoming, located ca. 450 km northeast of Vernal, Utah, the dinosaur bone bed of Morrison Formation yielded two gigantic fossil araucariaceous logs, measuring 1.15 m and 1.49 m in preserved maximum diameter, which was estimated as ca. 63 m and 75 m respectively by using the newly established height–diameter growth models for ancient conifers pertaining to the family Araucariaceae (chapter 7). The additional evidence of other large fossil logs confirms the presence of tall forest trees in the Upper Jurassic Morrison Formation.

In general, the age of the trees is generally positively related to the diameter and height of trees (Xing et al., 2012). Regarding the age of these araucariaceous trees in the Morrison Formation, the age–size (height and diameter) relationship of living *Araucaria* trees in northern Patagonia was consulted to get a perspective on the age of these Morrison Araucariaceae trees based on the preserved diameter and reconstructed height. In the Andes Mountains of northern Patagonia, for instance, mature trees of *Araucaria araucana* usually obtain an average height of 5 m with a DBH of 25 cm at 140 years of age, while older trees reach an average height of 25 m with a DBH of 85 cm at 450 years of age (Hadad et al., 2020). Hence, the araucariaceous trees during the Late Jurassic with greater tree heights and similar trunk diameters may have attained a tree age of at least 500 years, which suggests these trees may have inhabited old-growth Morrison forests with many more trees of similar size.

8.3. Biodiversity of the Morrison vegetation

Based on a newly discovered fossil log in Miners Draw, Utah, a new species of the conifer-like genus *Xenoxylon*, *X. utahense*, in the Upper Jurassic Morrison Formation in the Western Interior of USA was recognized (chapter 2, Xie et al, 2021). Previously, only a single occurrence of *Xenoxylon* is known from the Morrison Formation in central Montana, although two invalid species of Xenoxylon had been described in west-central Colorado and south-central Utah (Medlyn and Tidwell, 1975; Tidwell et al., 1998; Richmond et al., 2019). The establishment of the new species of *Xenoxylon utahense* increased the fossil conifer-like wood diversity to six genera and eight species in the Morrison Formation: *Cupressinoxylon jurassicum* Lutz (1930), *Mesembrioxylon carterii* Tidwell et al. (1998), *M. obscurum* (Knowlton) Medlyn et Tidwell (2002), *Protocupressinoxylon medlynii* Tidwell

et al. (1998), *Protopiceoxylon resiniferous* Medlyn et Tidwell (1979), *Agathoxylon hoodii* (Tidwell et Medlyn) Gee et al. (2019), *Xenoxylon meisteri* Palibin and Jarmolenko (1932), and *X. utahense* Xie et Gee (2021). When identified at the family level, the first three conifer taxa pertain to two families, Cupressaceae and Podocarpaceae. The following three conifer taxa represent two families, Cupressaceae and Araucariaceae. The last two taxa belong to an extinct family Miroviaceae (chapter 2, Xie et al., 2021), which shows that a diversity of conifers grew throughout the Morrison Formation during the Late Jurassic.

A variety of conifers growing throughout the Morrison Formation is also supported by other fossil evidence, such as conifer leaves, shoots, seed cones, and pollens. For conifer leaves and shoots, there are two conifer families that can be recognized, the Cupressaceae and Araucariaceae (Ash and Tidwell, 1998; Gee and Tidwell, 2010). Among conifer seed cones, three conifer families have been discovered, the Araucariaceae, Pinaceae, and extinct family Cheirolepidiaceae (Gee and Tidwell, 2010; Gee et al., 2014), which is also in agreement with the fossil conifer pollen. Moreover, conifer pollen grains also represent the family Podocarpaceae (Hotton and Baghai-Riding, 2010). Hence, all the fossil evidence linked to conifers shows a diversity of conifers growing throughout the Morrison Formation, including the Araucariaceae, Cupressaceae, Pinaceae, Podocarpaceae, and extinct families of Cheirolepidiaceae and Miroviaceae.

Besides conifers, there are other plants growing throughout the Morrison Formation based on the evidence from fossil leaves and palynology. Based on fossil evidence, the Morrison vegetation has been reconstructed as a conifer-dominated forest with other tall trees such as ginkgophytes and an understory of ferns, fern allies, cycads, and bennettitaleans (Tidwell, 1990; Ash and Tidwell, 1998; Tidwell et al., 1998; Hotton and Baghai-Riding, 2010; Gee et al., 2014; Foster, 2020; Xie et al., 2021).

8.4. Implications of vegetation for Morrison dinosaurs

As mentioned earlier, the Morrison vegetation flourished under warm and humid growth conditions during Late Jurassic times with the dominance of large conifer trees (Tidwell, 1990; Tidwell and Medlyn, 1992; Ash, 1994; Ash and Tidwell, 1998; Gee and Tidwell, 2010; Hotton and Baghai-Riding, 2010; Gee et al., 2019; Xie et al., 2021), which would have benefited the herbivorous dinosaurs, because conifers could provide a huge quantity of nutritious biomass for these herbivorous

dinosaurs (Gee, 2011; Gee, 2015).

One of the direct lines of evidence for these herbivorous dinosaurs living in a green Morrison landscape is the dinosaur bone bed of Howe-Stephens Quarry in north-central Wyoming (chapter 7). In this bone bed, abundant dinosaur remains along with the fossil plants have been discovered, which is not very common, because these two kinds of fossils are rarely found together in the same fossiliferous sediments owing to their differing preferred pH conditions in the depositional environment (Retallack et al., 1984; Britt, 1991; Tidwell et al., 1998).

In Howe-Stephens Quarry, the dinosaur bone bed yielded various dinosaurs, including megaherbivorous dinosaur *Diplodocus*, *Camarasaurus*, *Stegosaurus*, and carnivorous dinosaur *Allosaurus*, which may have inhabited an Araucariaceae-dominated forest (chapter 7). The first evidence supporting the dominance of araucariaceous trees is the fossil woods and logs found in this dinosaur bone bed, which pertain to the conifer family Araucariaceae. The second evidence of an Araucariaceae-dominated forest is the coalified plant compressions—woody shoots with leaves, ovulate cones, cone seeds, seeds, and pollen cones—found in the dinosaur bone bed, which was considered as a single species of *Araucaria* (Gee and Tidwell, 2010; chapter 7). These araucariaceous trees in the Howe-Stephens Quarry may have provided a high-energy food source for the herbivorous dinosaurs, because the studies of Hummel et al. (2008) and Gee (2011) suggested that the living *Araucaria* trees bear energy-rich foliage. Hence, the dinosaur bone bed in the Morrison Formation in Howe-Stephens Quarry suggests that the Morrison dinosaurs have lived in a green landscape with enough food supplies.

8.5. Paleoclimate reconstruction based on Morrison plants

In general, growth rings reflect the growth conditions of trees (Fritts, 1962, 1966; Creber and Chaloner, 1984; Tidwell et al., 1998; Brison et al., 2001). In the internal structures of the fossil log discovered in Miners Draw, northeastern Utah, true growth rings with narrow latewood were observed, which suggests that the growth conditions of the tree were only slightly variable in regard to mild seasonality during the entire year. Moreover, mean sensitivity analysis of growth rings was applied to the Miners Draw tree. The results showed a mean sensitivity equal to 0.53, which falls within the range of the mean sensitivity (0.35–0.60) of the living conifers growing in warm, humid

climatic conditions found in the southeastern United States and on the North Island of New Zealand, especially in flooding-disturbed, streamside habitats (Falcon-Lang, 2005). Therefore, the mean sensitivity of the Miners Draw tree suggests warm and humid growing conditions, although it only represents those of a single tree (chapter 2, Xie et al., 2021). In Rainbow Draw, the araucariaceous trees lack true growth rings, which indicates the tree growth conditions were equable during the entire year without seasonality (Gee et al., 2019). Similar characters of growth rings were also observed in the fossil woods of the Morrison Formation in Howe-Stephens Quarry (HSQ), north-central Wyoming, that is, true growth rings of the HSQ trees are absent, which conforms the tree growth conditions were more or less stable with no seasonality during the entire year (chapter 7).

Although warm and wet growth conditions are strongly expressed by the Miners Draw tree based on the growth ring features, there is other evidence of fossil leaves supporting a warm and wet climate throughout the Morrison Formation in the Upper Jurassic. For example, more than 20 species of ferns (e.g., *Hausmannia*, *Coniopteris*, and *Adiantites*), fern allies (e.g., *Equisetum* and *Selaginellites*), and tree fern (e.g., *Ashicaulis* and *Osmundacaulis*) widely distributed throughout the Morrison Formation, which indicates a warm and humid climate.

8.6. Future perspectives

8.6.1. Composition of Morrison vegetation

Except for the fossil localities of Miners Draw, Rainbow Draw, and Six Mile Draw in Utah, and Howe-Stephens Quarry in Wyoming that are mentioned in this dissertation, there are more fossil localities that yield fossil woods and logs in the Upper Jurassic Morrison Formation in Utah, such as Wagon Bench East and Manwell Log Site near Vernal, northeastern Utah and Escalante Petrified Forest State Park in Escalante, south-central Utah (Fig. 1).

Preliminary systematic paleobotany studies on these fossil woods from these new fossil localities have been carried out by Xie and Gee. The preliminary results showed that the fossil woods in Wagon Bench East and Manwell Log Site may pertained to the same fossil wood genus *Agathoxylon* (Araucariaceae) according to their anatomical structures, but the fossil woods in Escalante and Six Mile Draw showed the different familial anatomical characters—*Ginkgo*-like anatomical structures.

Therefore, further systematic studies on these fossil woods need to be carried out, which will contribute to a further and deeper understanding of the composition of the Morrison vegetation, at least to the woody flora of the Morrison forests during Late Jurassic times in what is today Utah.

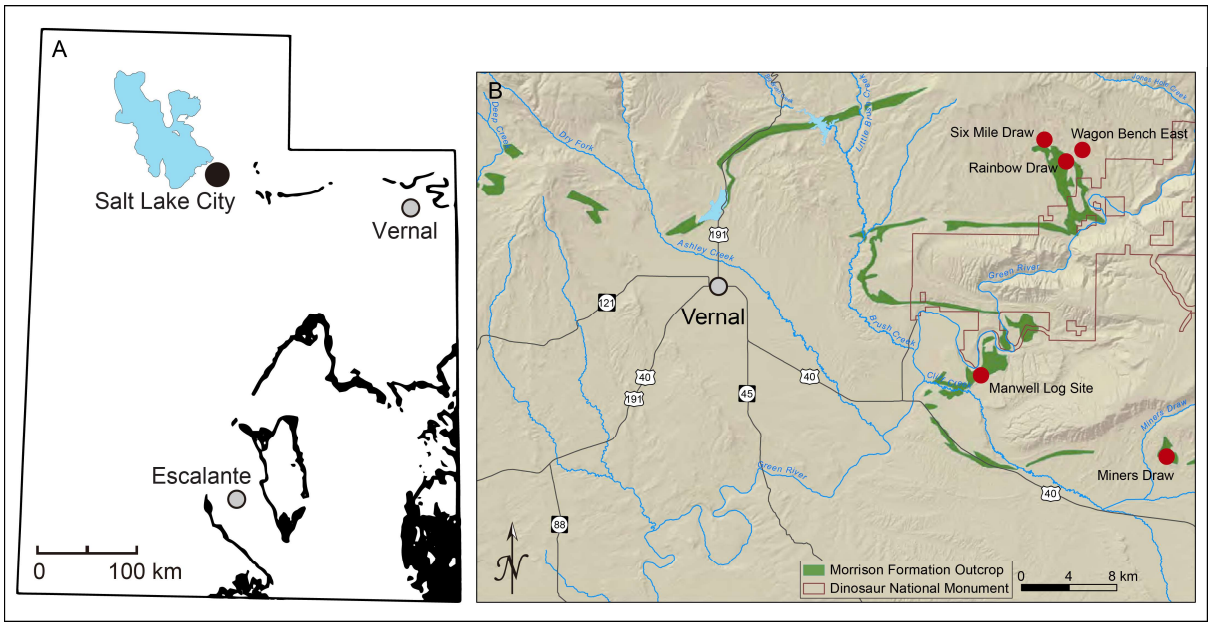

Figure 1. (A) Sketch map of fossil log locality, Vernal and Escalante, in Utah, USA, superimposed on the outcrops of the Upper Jurassic Morrison Formation. Map of Morrison outcrops courtesy of Kenneth Carpenter. (B) Map showing fossil localities (red dots) for fossil logs near Vernal in detail (modified after Sprinkel et al., 2019).

8.6.2. Reconstruction of ancient tree height

To reconstruct the ancient tree height, accurate height–diameter growth models are essential. In this dissertation, height–diameter growth models were established for ancient araucariaceous trees to reconstruct their tree heights, which could be utilized in the estimation of ancient tree heights of fossil logs in Wagon Bench East and Manwell Log Site in Utah. However, for the fossil logs in Escalante and Six Mile Draw, applying our growth models of ancient araucariaceous trees to the estimation of tree heights of these *Ginkgo*-like trees would not be accurate, because the height–diameter relationship of trees is strongly influenced by taxon, the araucariaceous and *Ginkgo*-like trees would have had different height–diameter growth models. We therefore intend to collect height–diameter data of living *Ginkgo* trees to establish height–diameter growth models for the reconstruction of ancient *Ginkgo*-like trees.

8.6.3. Leaf longevity analysis of the Morrison trees

Using tree growth rings, not only can the mean sensitivity analysis in understanding the tree growth conditions be carried out (chapter 2), but leaf longevity analysis can also be applied (e.g., Falcon-Lang, 2000b; Brea et al., 2008; Gulbranson et al., 2014; Shi et al., 2017; Jiang et al., 2021; Hoff, 2022). Leaf longevity analysis is based on the calculation of the cumulative algebraic sum of deviation of each radial diameter of tracheid from the mean radial diameter of tracheids of trees (CSDM) to plot the zero-trending CSDM curve for tree growth rings, which will indicate if a tree was evergreen (right skew of CSDM curve) or deciduous (left skew of CSDM curve) (Falcon-Lang, 2000b). For example, the living evergreen conifer *Araucaria araucana* shows a strong right-skewed CSDM curve, while the extant deciduous conifer *Larix gmelinii* normally attains a left-skewed CSDM curve (Fig. 2). We therefore plan to utilize leaf longevity analysis on the growth rings observed in the fossil logs from the Morrison Formation, to better describe the Morrison vegetation.

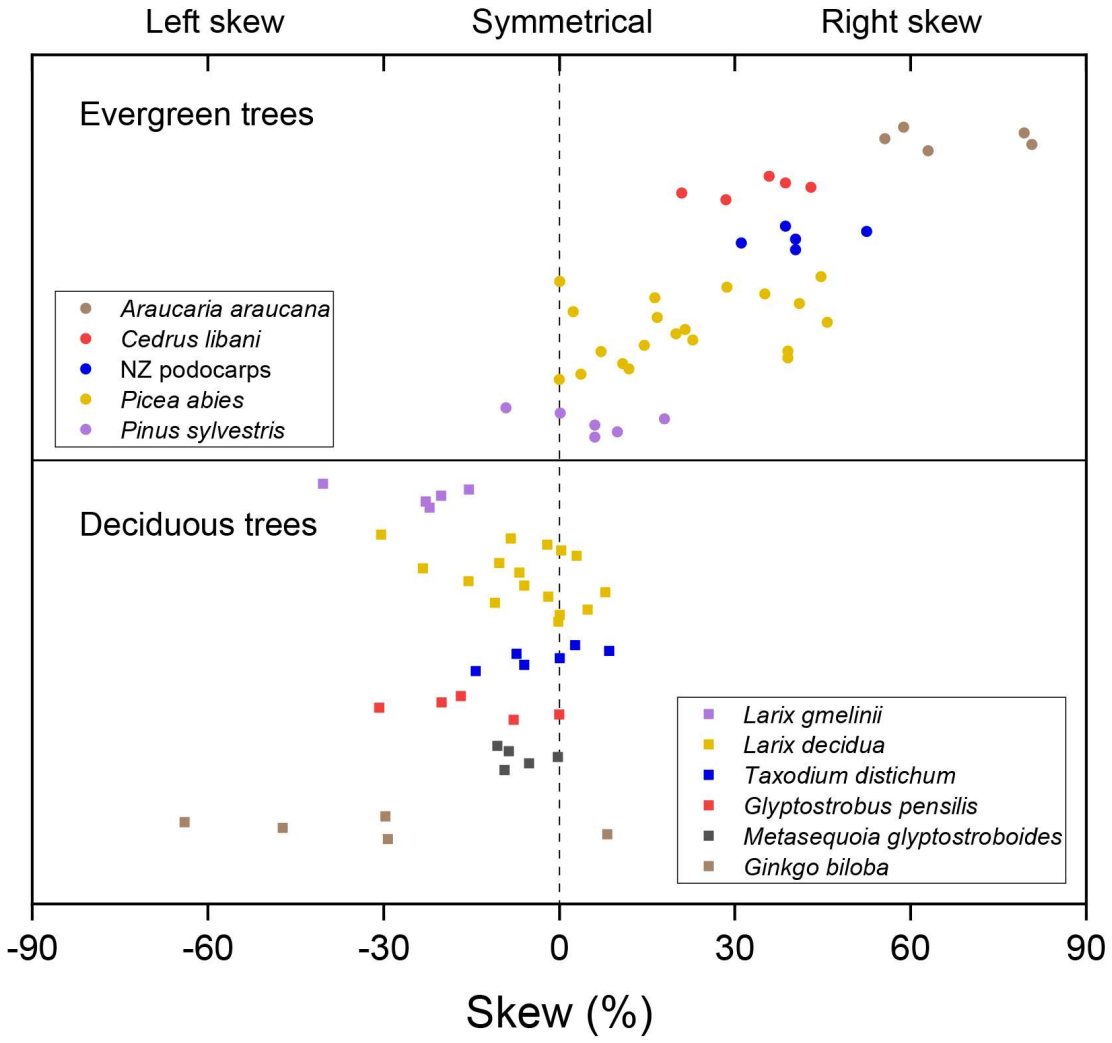

Figure 2. Example of CSDM curve skews of deciduous and evergreen conifers (modified after Falcon-Lang, 2000b). Generally, the evergreen conifers show a right-skewed CSDM curve, whereas the deciduous conifers attain a left-skewed CSDM curve.

References

Abu Hamad, A., Kerp, H., Vörding, B., and Bandel, K., 2008, A Late Permian flora with *Dicroidium* from the Dead Sea region, Jordan: Review of Palaeobotany and Palynology v. 149, p. 85–130.

Adaskaveg, J.E., and Gilbertson, R.L., 1986, In vitro decay studies of selective delignification and simultaneous decay by the white rot fungi *Ganoderma lucidum* and *Ganoderma tsugae*: Canadian Journal of Botany, v. 64, p. 1615–1629.

Alvin, K.L., and Muir, M.D., 1970, An epiphyllous fungus from the Lower Cretaceous: Biological Journal of the Linnean Society, v. 2, p. 55–59.

Andrews, H.N., and Pannell, E., 1942, A fossil araucarian wood from western Wyoming: Annals of the Missouri Botanical Garden, v. 29, p. 283–286.

Aoki, D., Hanaya, Y., Akita, T., Matsushita, Y., Yoshida, M., Kuroda, K., Yagami, S., Takama, R., and Fukushima, K., 2016, Distribution of coniferin in freeze-fixed stem of *Ginkgo biloba* L. by cryo-TOF-SIMS/SEM: Scientific Reports, v. 6, 31525.

Araújo, P., Ferreira, M.S., de Oliveira, D.N., Pereira, L., Sawaya, A.C.H.F., Catharino, R.R., and Mazzafera, P., 2014, Mass spectrometry imaging: An expeditious and powerful technique for fast *in situ* lignin assessment in *Eucalyptus*: Analytical Chemistry, v. 86, p. 3415–3419.

Ash, S., 1994, First occurrence of *Czekanowskia* (Gymnospermae, Czekanowskiales) in the United States: Review of Palaeobotany and Palynology, v. 81, p. 129–140.

Ash, S.R., and Tidwell, W.D., 1998, Plant megafossils from the Brushy Basin Member of the Morrison Formation near Montezuma Creek Trading Post, southeastern Utah: Modern Geology, v. 22, p. 321–339.

Ayer, J., 2000, The Howe Ranch Dinosaurs: Aathal, Switzerland: Sauriermuseum Aathal.

Bamford, M., and Philippe, M., 2001, Gondwanan Jurassic–Early Cretaceous homoxylous woods: A nomenclatural revision of the genera with taxonomical notes: Review of Palaeobotany and Palynology, v. 113, p. 287–297.

Bardet, M., Pournou, A., 2015, Fossil wood from the Miocene and Oligocene epoch: Chemistry and morphology: Magnetic Resonance in Chemistry, v. 53, p. 9–14.

Berbee, M.L., and Taylor, J.W., 2001, Fungal molecular evolution: gene trees and geologic time, *in* McLaughlin, D.J., McLaughlin, E.G., and Lemke, P.A., eds., The Mycota VIIB: Systematics and Evolution: Springer-Verlag, Berlin, p. 229–245.

Berbee, M.L., James, T.Y., and Strullu-Derrien, C., 2017, Early diverging fungi: diversity and impact at the dawn of terrestrial life: Annual Review of Microbiology, v. 71, p. 41–60.

Berry, C.M., and Marshall, J.E.A., 2015, Lycopsid forests in the early Late Devonian paleoequatorial zone of Svalbard: Geology, v. 43, p. 1043–1046.

Bice, K.L., and Norris, R.D., 2002, Possible atmospheric CO_2 extremes of the Middle Cretaceous (late Albian–Turonian): Paleoceanography, v. 17, p. 22-1–17.

Bird, R.T., 1985, Bones for Barnum Brown: Adventures of a dinosaur hunter: Fort Worth: Texas Christian University Press.

Bock, P., Nousiainen, P, Elder, T., Blaukopf, M., Amer, H., Zirbs, R., Potthast, A., and Gierlinger, N., 2020, Infrared and Raman spectra of lignin substructures: Dibenzodioxocin: Journal of Raman Spectroscopy, v. 51, p. 422–431.

Boeriu, C.G., Bravo, D., Gosselink, R.J., and van Dam, J.E., 2004, Characterisation of structure-dependent functional properties of lignin with infrared spectroscopy: Industrial Crops and Products, v. 20, p. 205–218.

Boura, A., Bamford, M., and Philippe, M., 2021, Promoting a standardized description of fossil tracheidoxyls: Review of Palaeobotany and Palynology, v. 295, 104525.

Boyce, C.K., Hazen, R.M., and Knoll, A.H., 2001, Nondestructive, in situ, cellular-scale mapping of elemental abundances including organic carbon in permineralized fossils: Proceedings of the National Academy of Sciences, v. 98, p. 5970–5974.

Brea, M., Artabe, A., and Spalletti, L.A., 2008, Ecological reconstruction of a mixed Middle Triassic forest from Argentina: Alcheringa, v. 32, p. 365–393.

Briggs, D.E.G., Evershed, R.P., and Lockheart, M.J., 2000, The biomolecular paleontology of continental fossils: Paleobiology, v. 26, p. 169–193.

Brison, A.L., Philippe, M., and Thévenard, F., 2001, Are Mesozoic wood growth rings climate induced: Paleobiology, v. 27, p. 531–538.

Burnham, K.P., and Anderson, D.R., 2002, Model selection and multimodal inference: a practical information-theoretic approach: New York: Springer, 488 p.

Buurman, P., 1972, Mineralization of wood: Scripta Geologica, v. 12, p. 1–43.

Carballido, J.L., Marpmann, J.S., Schwarz-Wings, D., and Pabst, B., 2012, New information on a juvenile sauropod specimen from the Morrison Formation and the reassessment of its systematic position: Palaeontology, v. 55, p. 567–582.

Césari, S.N., Busquets, P., Méndez-Bedia, I., Colombo, F., Limarino, C.O., Cardo, R., and Gallastegui, G., 2012, A late Paleozoic fossil forest from the southern Andes, Argentina: Palaeogeography, Palaeoclimatology, Palaeoecology, v. 333, p. 131–147.

Chai, Z., Tan, W., Li, Y., Yan, L., Yuan, H., and Li, Z., 2018, Generalized nonlinear height–diameter models for a *Cryptomeria fortunei* plantation in the Pingba region of Guizhou Province, China: Web Ecology, v. 18, p. 29–35.

Cohen, K.M., Finney, S.C., Gibbard, P.L., and Fan, J.X., 2013, The ICS International Chronostratigraphic Chart: Episodes, v. 36, p. 199–204.

Creber, G.T., and Chaloner, W.G., 1984, Influence of environmental factors on the wood structure of living and fossil trees: The Botanical Review, v. 50, p. 357–448.

Currie, B.S., 1998, Upper Jurassic–Lower Cretaceous Morrison and Cedar Mountain formations, NE Utah-NW Colorado; relationships between nonmarine deposition and early Cordilleran foreland-basin development: Journal of Sedimentary Research, v. 68, p. 632–652.

Demko, T.M., and Parrish, J.T., 1998, Paleoclimatic setting of the Upper Jurassic Morrison Formation: Modern Geology, v. 22, p. 283–296.

Demko, T.M., Currie, B.S., and Nicoll, K.A., 2004, Regional paleoclimatic and stratigraphic implications of paleosols and fluvial/overbank architecture in the Morrison Formation (Upper Jurassic), Western Interior, USA: Sedimentary Geology, v. 167, p. 115–135.

Dennis, R.L., 1969, Fossil mycelium with clamp connections from the Middle Pennsylvanian: Science, v. 163, p. 670–671.

Dennis, R.L., 1970, A Middle Pennsylvanian basidiomycete mycelium with clamp connections: Mycologia, v. 62, p. 578–584.

Dennis, R.L., 1976, *Palaeosclerotium*, a Pennsylvanian age fungus combining features of modern ascomycetes and basidiomycetes: Science, v. 192, p. 66–68.

Dirckx, O., Triboulot-Trouy, M.C., Merlin, A., and Deglise, X., 1992, Modifications de la couleur du bois d'*Abies grandis* exposé à la lumière solaire: Annals of Forest Science, v. 49, p. 425–447.

Earle, C.J., 2020, The Gymnosperm Database: Retrieved February 13, 2021, from https://www.conifers. org/cu/Sequoia.php.

Edwards, D., Kenrick, P., and Dolan, L., 2018, History and contemporary significance of the Rhynie cherts—Our earliest preserved terrestrial ecosystem: Philosophical Transactions of the Royal Society B, v. 373, 20160489.

Eldridge, G.H., 1896, Mesozoic geology, *in* Emmons, S.F., Cross, W., and Eldridge, G.H., eds., Geology of the Denver basin in Colorado: U.S. Geological Survey Monograph, v. 27, p. 51–151.

Endlicher, S.F.L., 1847, Synopsis coniferarum: Scheittin et Zollikofer, 368 p.

Faix, O., 1991, Classification of lignins from different botanical origins by FT-IRspectroscopy: Holzforschung, v. 45, p. 21–27.

Falcon-Lang, H.J., 2000a, The relationship between leaf longevity and growth ring markedness in modern conifer woods and its implications for palaeoclimatic studies: Palaeogeography, Palaeoclimatology, Palaeoecology, v. 160, p. 317–328.

Falcon-Lang, H.J., 2000b, A method to distinguish between woods produced by evergreen and deciduous coniferopsids on the basis of growth ring anatomy: a new palaeoecological tool: Palaeontology, v. 43, p. 785–793.

Falcon-Lang, H.J., and Bashforth, A.R., 2005, Morphology, anatomy, and upland ecology of large cordaitalean trees from the Middle Pennsylvanian of Newfoundland: Review of Palaeobotany and Palynology, v. 135, p. 223–243.

Falcon-Lang, H.J., Kurzawe, F., and Lucas, S.G., 2016, A Late Pennsylvanian coniferopsid forest in growth position, near Socorro, New Mexico, USA: Tree systematics and palaeoclimatic significance: Review of Palaeobotany and Palynology, v. 225, p. 67–83.

Feldpausch, T.R., Banin, L., Phillips, O.L., Baker, T.R., Lewis, S.L., Quesada, C.A., Affum-Baffoe, K., et al., 2011, Height-diameter allometry of tropical forest trees: Biogeosciences, v. 8, p. 1081–1106.

Feng, Z., Wang, J., Rößler, R., Ślipiński, A., and Labandeira, C., 2017, Late Permian wood-borings reveal an intricate network of ecological relationships: Nature Communications, v. 8, p. 8–13.

Feng, Z., Wei, H.B., Wang, C.L., Chen, Y.X., Shen, J.J., and Yang, J.Y., 2015, Wood decay of *Xenoxylon yunnanensis* Feng sp. nov. from the Middle Jurassic of Yunnan Province, China: Palaeogeography, Palaeoclimatology, Palaeoecology, v. 433, p. 60–70.

Fengel, D., 1991, Aging and fossilization of wood and its components: Wood Science and Technology, v. 25, p. 153–177.

Fors, Y., Jalilehvand, F., Risberg, E.D., Björdal, C., Phillips, E., and Sandström, M., 2012, Sulfur and iron analyses of marine archaeological wood in shipwrecks from the Baltic Sea and Scandinavian waters: Journal of Archaeological Science, v. 39, p. 2521–2532.

Foster, J., 2020, Jurassic West: the Dinosaurs of the Morrison Formation and Their World: Indiana University Press, Bloomington, 531 p.

Frazer, N.B., and Ehrhart, L.M., 1985, Preliminary growth models for Green, *Chelonia mydas*, and Loggerhead, *Caretta caretta*, turtles in the wild: Copeia, v. 1, p. 73–79.

Freudenberg, K., and Harkin, J.M., 1963, The glucosides of cambial sap of spruce: Phytochemistry, v. 2, p. 189–193.

Freudenberg, K., and Torres-Serres, J., 1967, Conversion of the phenylalanines in lignin-component glucosides: Justus Liebigs Annalen der Chemie, v. 703, p. 225–230.

Fritts, H.C., 1962, An approach to dendroclimatology: screening by means of multiple regression techniques: Journal of Geophysical Research, v. 67, p. 1413–1420.

Fritts, H.C., 1966, Growth-rings of trees: their correlation with climate: Science, v. 154, p. 973–979.

García Massini, J.L., Falaschi, P., and Zamuner, A., 2012, Fungal–arthropod–plant interactions from the Jurassic petrified forest Monumento Natural Bosques Petrificados, Patagonia, Argentina: Palaeogeography, Palaeoclimatology, Palaeoecology, v. 329, p. 37–46.

Gee, C.T., 2015, Conifer paleobiodiversity in the Late Jurassic Morrison Formation, USA, and implications for sauropod herbivory [Habilitationsschrift]: Bonn, Universität Bonn, 304 p.

Gee, C.T., and Tidwell, W.D., 2010, A mosaic of characters in a new whole-plant *Araucaria*, *A. delevoryasii* Gee sp. nov., from the Late Jurassic Morrison Formation, *in* Gee, C.T., ed., Plants in Mesozoic Time: Morphological Innovations, Phylogeny, Ecosystems: Indiana University Press, p. 67–94.

Gee, C.T., Anderson, H.M., Anderson, J.M., Ash, S.R., Cantrill, D.J., van Konijnenburg-van Cittert, J.H., and Vajda, V., 2020, Postcards from the Mesozoic: Forest landscapes with giant flowering trees, enigmatic seed ferns, and other naked-seed plants, *in* Martinetto, E., Tschopp, E., and Gastaldo, R.A., eds., Nature through Time: Springer, p. 159–185.

Gee, C.T., Dayvault, R.D., Stockey, R.A., and Tidwell, W.D., 2014, Greater palaeobiodiversity in conifer seed cones in the Upper Jurassic Morrison Formation of Utah, USA: Palaeobiodiversity and Palaeoenvironments, v. 94, p. 363–375.

Gee, C.T., McCoy, V.E., and Sander, P.M., 2021, Fossilization: Understanding the Material Nature of Ancient Plants and Animals: John Hopkins University Press, Baltimore.

Gee, C.T., Sprinkel, D., Bennis, M.B., and Gray, D.E., 2019, Silicified logs of *Agathoxylon hoodii* (Tidwell et Medlyn) comb. nov. from Rainbow Draw, near Dinosaur National Monument, Uintah County, Utah, USA, and their implications for araucariaceous conifer forests in the Upper Jurassic Morrison Formation: Geology of the Intermountain West, v. 6, p. 77–92.

Gee, C.T., Xie, A., and Zajonz, J., 2022, Multitrophic plant–insect–fungal interactions across 150 million years: A giant *Agathoxylon* tree, ancient wood-boring beetles and fungi from the Morrison Formation of NE Utah, and the brood of an extant orchard mason bee: Review of Palaeobotany and Palynology, v. 300, 104627.

Gothan, W., 1905, Zur Anatomie lebender und fossiler Gymnospermen-Hölzer: Abhandlungen der Preußischen Geologischen Landesanstalt, v. 44, p. 1–108.

Götze, J., Möckel, R., and Pan, Y., 2020, Mineralogy, geochemistry and genesis of agate–A review: Minerals, v. 10, 1037.

Götze, J., Nasdala, L., Kleeberg, R., and Wenzel, M., 1998, Occurrence and distribution of "moganite" in agate/chalcedony: a combined micro-Raman, Rietveld, and cathodoluminescence study: Contributions to Mineralogy and Petrology, v. 133, p. 96–105.

Gou, X.D., Wei, H.B., Guo, Y., Yang, S.L., and Feng, Z., 2021, Leaf phenology, paleoclimatic and paleoenvironmental insights derived from an *Agathoxylon* stem from the Middle Jurassic of Xinjiang, Northwest China: Review of Palaeobotany and Palynology, v. 289, 104416.

Gray, B., 1975, Size-composition and regeneration of *Araucaria* stands in New Guinea: The Journal of Ecology, p. 273–289.

Griebeler, E.M., Klein, N., and Sander, P.M., 2013, Aging, maturation and growth of sauropodomorph dinosaurs as deduced from growth curves using long bone histological data: an assessment of methodological constraints and solutions: PloS one, v. 8, e67012.

Gulbranson, E.L., Ryberg, P.E., Decombeix, A.L., Taylor, E.L., Taylor, T.N., and Isbell, J.L., 2014, Leaf habit of Late Permian Glossopteris trees from high-palaeolatitude forests: Journal of the Geological Society, v. 171, p. 493–507.

Hadad, M.A., Arco Molina, J.G., and Roig, F.A., 2020, Dendrochronological Study of the Xeric and Mesic *Araucaria araucana* Forests of Northern Patagonia: Implications for Ecology and Conservation, *in* Pompa-García, M., and Camarero, J.J., eds., Latin American Dendroecology: Springer, p. 283–315.

Halliday, T.R., and Verrell, P.A., 1988, Body size and age in amphibians and reptiles: Journal of Herpetology, v. 22, p. 253–265.

Harper, C.J., Bomfleur, B., Decombiex, A., Taylor, E.L., Taylor, T.N., and Kring, M., 2012, Tylosis formation and fungal interactions in an Early Jurassic conifer from northern Victoria Land, Antarctica: Review of Palaeobotany and Palynology, v. 175, p. 25–31.

Harper, C.J., Taylor, T.N., Kring, M., and Taylor, E.L., 2016, Structurally preserved fungi from Antarctica: diversity and interactions in late Palaeozoic and Mesozoic polar forest ecosystems: Antarctic Science, v. 28, p. 153–173.

Hasiotis, S.T., 2004, Reconnaissance of Upper Jurassic Morrison Formation ichnofossils, Rocky Mountain Region, USA: paleoenvironmental, stratigraphic, and paleoclimatic significance of terrestrial and freshwater ichnocoenoses: Sedimentary Geology, v. 167, p. 177–268.

Heaney, P.J., 1993, A proposed mechanism for the growth of chalcedony. Contributions to Mineralogy and Petrology, v. 115, p. 66–74.

Hillenkamp, F., and Peter-Katalinić, J., 2013, MALDI MS: A Practical Guide to Instrumentation, Methods and Applications: Wiley-Blackwell, Hoboken.

Hoff, F.V., 2022, A new occurrence of the fossil wood genus *Circoporoxylon* from the Upper Jurassic Morrison Formation of Montana, USA: Seasonality, growth ring markedness, evergreen habit, paleoclimate [Bachelor thesis]: Bonn, Universität Bonn, 48 p.

Hofmann, J., and Pagel, K., 2017, Glycan analysis by ion mobility–mass spectrometry: Angewandte Chemie International Edition, v. 56, p. 8342–8349.

Homma, Y., Kouketsu, Y., Kagi, H., Mikouchi, T., and Yabuta, H., 2015, Raman spectroscopic thermometry of carbonaceous material in chondrites: Four–band fitting analysis and expansion of lower temperature limit: Journal of Mineralogical and Petrological Sciences, v. 110, p. 276–282.

Hotton, C.L., and Baghai-Riding, N.L., 2010, Palynological evidence for conifer dominance within a heterogeneous landscape in the Late Jurassic Morrison Formation, USA, *in* Gee, C.T., ed., Plants in Mesozoic Time: Morphological Innovations, Phylogeny, Ecosystems: Indiana University Press, p. 295–328.

Hsü, J., 1953, On the occurrence of a fossil wood in association with fungous hyphae from Chimo of East Shantung: Acta Palaeontologica Sinica, v. 1, p. 80–86.

Huang, S., Titus, S.J., and Wiens, D.P., 1992, Comparison of nonlinear height–diameter functions for major Alberta tree species: Canadian Journal of Forest Research, v. 22, p. 1297–1304.

IAWA Committee, 2004, IAWA list of microscopic features for softwood identification: IAWA Journal, v. 25, p. 1–70.

Jefferson, T.H., 1987, The preservation of conifer wood: Examples from the Lower Cretaceous of Antarctica: Palaeontology, v. 30, p. 233–249.

Jiang, Z., Wu, H., Tian, N., Wang, Y., and Xie, A., 2021, A new species of conifer wood *Brachyoxylon* from the Cretaceous of Eastern China and its paleoclimate significance: Historical Biology, v. 33, p. 1989–1995.

Kaneda, M., Rensing, K.H., Wong, J.C.T., Banno, B., Mansfield, S.D., and Samuels, A.L., 2008, Tracking monolignols during wood development in lodgepole pine: Plant Physiology, v. 147, p. 1750–1760.

Karowe, A.L., and Jefferson, T.H., 1987, Burial of trees by eruptions of Mount St Helens, Washington: implications for the interpretation of fossil forests: Geological Magazine, v. 124, p. 191–204.

Kerp, H., 2018, Organs and tissues of Rhynie chert plants: Philosophical Transactions of the Royal Society B, v. 373, 20160495.

Kidston, R., and Lang, W.H., 1921, On Old Red Sandstone plants showing structure, from the Rhynie Chert Bed, Aberdeenshire. Part V. The Thallophyta occurring in the peat-bed; the succession of the plants throughout a vertical section of the bed, and the conditions of accumulation and preservation of the deposit: Transactions of the Royal Society of Edinburgh, v. 52, p. 855–902.

Kiyota, E., Mazzafera, P., and Sawaya, A.C., 2012, Analysis of soluble lignin in sugarcane by ultrahigh performance liquid chromatography–tandem mass spectrometry with a do-it-yourself oligomer database: Analytical Chemistry, v. 84, p. 7015–7020.

Knowlton, F.H., 1900, Description of a new species of *Araucarioxylon* from the cycad bed of the Freezeout Hills, Carbon County, Wyoming: US Geological Survey Twentieth Annual Report, v. 1898–1899, p. 418–419.

Kosyakov, D.S., Ul'yanovskii, N.V., Sorokina, E.A., and Gorbova, N.S., 2014, Optimization of sample preparation conditions in the study of lignin by MALDI mass spectrometry, Journal of Analytical Chemistry, v. 69, p. 1344–1350.

Krąpiec, M., Margielewski, W., Korzeń, K., Szychowska-Krąpiec, E., Nalepka, D., and Łajczak, A., 2016, Late Holocene palaeoclimate variability: The significance of bog pine dendrochronology related to peat stratigraphy. The Puścizna Wielka raised bog case study (Orawa–Nowy Targ Basin, Polish Inner Carpathians): Quaternary Science Reviews, v. 148, p. 192–208.

Krassilov, V.A., and Makulbekov, N.M., 2003, The first finding of Gasteromycetes in the Cretaceous of Mongolia: Paleontological Journal, v. 37, p. 439–442.

Kräusel, R., 1949, Die fossilen Koniferen-Hölzer (Unter Ausschluß von *Araucarioxylon* Kraus). II: Kritische Untersuchungen zur Diagnostik lebender und fossiler Koniferen-Hölzer: Palaeontographica Abteilung B, v. 89, p. 83–203.

Krings, M., Dotzler, N., Galtier, J., and Taylor, T.N., 2011, Oldest fossil basidiomycete clamp connections: Mycoscience, v. 52, p. 18–23.

Larsen, D.R., 2017, Simple taper: Taper equations for the field forester, *in* Kabrick, J.M., Dey, D.C., Knapp, B.O., Larsen, D.R., Shifley, S.R., and Stelzer, H.E., eds., Proceedings of the 20th Central Hardwood Forest Conference, p. 265–278.

Lee, D., Kim, Y., Jalaludin, I., Nguyen, H.Q., Kim, M., Seo, J., Jang, K.S., and Kim, J., 2021, MALDI-MS analysis of disaccharide isomers using graphene oxide as MALDI matrix: Food Chemistry, v. 342, 128356.

Lehman, T.M., and Woodward, H.N., 2008, Modelling growth rates for sauropod dinosaurs: Paleobiology, v. 34, p. 264–281.

Leo, R.F., and Barghoorn, E.S., 1976, Silicification of wood: Botanical Museum leaflets, Harvard University, v. 25, p. 1–47.

Liesegang, M., and Gee, C.T., 2020, Silica entry and accumulation in standing trees in a hot-spring environment: cellular pathways, rapid pace and fossilization potential: Palaeontology, v. 63, p. 651–660.

Liesegang, M., Tomaschek, F., and Götze, J., 2021, The structure and chemistry of silica in mineralized wood: Techniques and analysis, *in* Gee, C.T., McCoy, V.E., and Sander, P.M., Fossilization: Understanding the Material Nature of Ancient Plants and Animals in the Paleontological Record: John Hopkins University Press, Baltimore, p. 159–186.

Litwin, R.J., Turner, C.E., and Peterson, F., 1998, Palynological evidence on the age of the Morrison Formation: Modern Geology, v. 22, p. 297–319.

Locatelli, E., 2014, The exceptional preservation of plant fossils: A review of taphonomic pathways and biases in the fossil record: The Paleontological Society Papers, v. 20, p. 237–258.

Loron, C.C., François, C., Rainbird, R.H., Turner, E.C., Borensztajn, S., and Javaux, E.J., 2019, Early fungi from the Proterozoic era in Arctic Canada: Nature, v. 570, p. 232–235.

Lutz, H.T., 1930, A new species of *Cupressionoxylon* (Goeppert) Gothan from the Jurassic of South Dakota: Botanical Gazette, v. 90, p. 92–107.

Magnusson, W.E., and Sanaiotti, T.M., 1995, Growth of Caiman crocodilus in Central Amazonia, Brazil: Copeia, v. 2, p. 498–501.

Martin-Closas, C., and Gomez, B., 2004, Taphonomie des plantes et interprétations paléoécologiques. Une synthèse: Geobios, v. 37, p. 65–88.

Marynowski, L., and Simoneit, B.R., 2022, Saccharides in atmospheric particulate and sedimentary organic matter: Status overview and future perspectives: Chemosphere, v. 288, 132376.

Marynowski, L., Bucha, M., Lempart-Drozd, M., Stępień, M., Kondratowicz, M., Smolarek-Lach, J., Rybicki, M., Goryl, M., Brocks, J., and Simoneit, B.R.T., 2021, Preservation of hemicellulose remnants in sedimentary organic matter: Geochimica et Cosmochimica Acta, v. 310, p. 32–46.

Marynowski, L., Bucha, M., Smolarek, J., Wendorff, M., and Simoneit, B.R., 2018, Occurrence and significance of mono-, di-and anhydrosaccharide biomolecules in Mesozoic and Cenozoic lignites and fossil wood: Organic Geochemistry, v. 116, p. 13–22.

Marynowski, L., Otto, A., Zatoń, M., Philippe, M., and Simoneit, B.R., 2007, Biomolecules preserved in ca. 168 million year old fossil conifer wood: Naturwissenschaften, v. 94, p. 228–236.

Marynowski, L., Szełęg, E., Jędrysek, M.O., and Simoneit, B.R., 2011, Effects of weathering on organic matter: Part II: Fossil wood weathering and implications for organic geochemical and petrographic studies: Organic Geochemistry, v. 42, p. 1076–1088.

Maslova, N.P., Sokolova, A.B., Kodrul, T.M., Tobias, A.V., Bazhenova, N.V., Wu, X.K., and Jin, J.H.,

2021, Diverse epiphyllous fungi on *Cunninghamia* leaves from the Oligocene of South China and their paleoecological and paleoclimatic implications: Journal of Systematics and Evolution, v. 59, p. 964–984.

Matysová, P., Götze, J., Leichmann, J., Škoda, R., Strnad, L., Drahota, P., and Grygar, T.M., 2016, Cathodoluminescence and LA-ICP-MS chemistry of silicified wood enclosing wakefieldite–REEs and V migration during complex diagenetic evolution: European Journal of Mineralogy, v. 28, p. 869–887.

McLoughlin, S., and Strullu-Derrien, C., 2016, Biota and palaeoenvironment of a high middlelatitude Late Triassic peat-forming ecosystem from Hopen, Svalbard archipelago, *in* Kear, B.P., Lindgren, J., Hurum, J.H., Milàn, J., and Vajda, V., eds., Mesozoic Biotas of Scandinavia and its Arctic Territories: Geological Society, London, Special Publications, v. 434, p. 87–112.

Medlyn, D.A., and Tidwell, W.D., 1975, Conifer wood from the Upper Jurassic of Utah. Part I: *Xenoxylon morrisonense* sp. nov.: American Journal of Botany, v. 62, p. 203–208.

Medlyn, D.A., and Tidwell, W.D., 1979, A review of the genus *Protopiceoxylon* with emphasis on North American species: Canadian Journal of Botany, v. 57, p. 1451–1463.

Medlyn, D.A., and Tidwell, W.D., 2002, *Mesembrioxylon obscurum*, a new combination for *Araucarioxylon*? *obscurum* Knowlton, from the Upper Jurassic Morrison Formation, Wyoming: Western North American Naturalist, v. 62, p. 210–217.

Mehtätalo, L., De-Miguel, S., and Gregoire, T., 2015, Modeling height-diameter curves for prediction: Canadian Journal of Forest Research, v. 45, p. 826–837.

Meschinelli, A., 1898, Fungorum Fossilium Omnium Hucusque Cognitorum Iconographia: 31 Tabulis Exornata, Volumen Unicum, Typis Aloysii Fabris, 144 p.

Mosbrugger, V., 1990, The tree habit in land plants: Springer-Verlag, Berlin Heidelberg, 161 p.

Mosbrugger, V., Gee, C.T., Belz, G., and Ashraf, A.R., 1994, Three-dimensional reconstruction of an in-situ Miocene peat forest from the Lower Rhine Embayment, northwestern Germany—new methods in palaeovegetation analysis: Palaeogeography, Palaeoclimatology, Palaeoecology, v. 110, p. 295–317.

Mustoe, G.E., 2008, Mineralogy and geochemistry of late Eocene silicified wood from Florissant Fossil Beds National Monument, Colorado, *in* Meyer, H.W., and Smith, D.M., eds., Paleontology of the Upper Eocene Florissant Formation, Colorado: Geological Society of America, Boulder, p.

127–140.

Mustoe, G.E., 2015, Late Tertiary petrified wood from Nevada, USA: Evidence of multiple silicification pathways: Geosciences, v. 5, p. 286–309.

Mustoe, G.E., and Dillhoff, T.A., 2022, Mineralogy of Miocene Petrified Wood from Central Washington State, USA: Minerals, v. 12, p. 131.

Naugolnykh, S.V., and Ponomarenko, A.G.,2010, Possible traces of feeding by beetles in coniferophyte wood from the Kazanian of the Kama River Basin: Paleontological Journal, v. 44, p. 468–474.

Newsham, K.K., Fitter, A.H., and Watkinson, A.R., 1995, Multifunctionality and biodiversity in arbuscular mycorrhizas: Trends in Ecology & Evolution, v. 10, p. 407–411.

Niklas, K.J., 1994, Predicting the height of fossil plant remains: an allometric approach to an old problem: American Journal of Botany, v. 81, p. 1235–1242.

Nord-Larsen, T., and Nielsen, A.T., 2015, Biomass, stem basic density and expansion factor functions for five exotic conifers grown in Denmark: Scandinavian Journal of Forest Research, v. 30, p. 135–153.

Nosova, N.V., and Kiritchkova, A.I., 2008, First records of the genus *Mirovia reymanówna* (Miroviaceae, Coniferales) from the Lower Jurassic of western Kazakhstan (Mangyshlak): Paleontological Journal, v. 42, p. 1383–1392.

Oberwinkler, F., 2012, Evolutionary trends in Basidiomycota: Stapfia, v. 96, p. 45–104.

Osborn, J.M., Taylor, T.N., and White Jr., J.F., 1989, *Palaeofibulus* gen. nov., a clamp-bearing fungus from the Triassic of Antarctica: Mycologia, v. 81, p. 622–626.

Pagel, K., and Harvey, D.J., 2013, Ion mobility–mass spectrometry of complex carbohydrates: collision cross sections of sodiated N-linked glycans: Analytical Chemistry, v. 85, p. 5138–5145.

Paijmans, K., 1970, An analysis of four tropical rain forest sites in New Guinea: The Journal of Ecology, p. 77–101.

Paine, C.E.T., Stahl, C., Courtois, E.A., Patino, S., Sarmiento, C., and Baraloto, C., 2010, Functional explanations for variation in bark thickness in tropical rain forest trees: Functional Ecology, v. 24, p. 1202–1210.

Pandey, K.K., 1999, A study of chemical structure of soft and hardwood and wood polymers by FTIR spectroscopy: Journal of Applied Polymer Science, v. 71, p. 1969–1975.

Parfrey, L.W., Lahr, D.J.G., Knoll, A.H., and Katz, L.A., 2011, Estimating the timing of early eukaryotic diversification with multigene molecular clocks: Proceedings of the National Academy of Sciences, USA, v. 108, p. 13624–13629.

Parrish, J.T., Peterson, F., and Turner, C.E., 2004, Jurassic "savannah": plant taphonomy and cli- mate of the Morrison Formation (Upper Jurassic, western USA): Sedimentary Geology, v. 167, p. 137–162.

Pereira, L.G., 2020, Mineralogy and preservational quality of Late Mesozoic silicified wood and mineralized dinosaur bone [Master thesis]: Bonn, Universität Bonn, 110 p.

Philippe, M., and Bamford, M.K., 2008, A key to morphogenera used for Mesozoic conifer-like woods: Review of Palaeobotany and Palynology, v. 148, p. 184–207.

Philippe, M., Bamford, M., McLoughlin, S., Da Rosa Alves, L.S., Falcon-Lang, H., Gnaedinger, S., Ottone, E., Pole, M., Rajanikanth, A., Shoemaker, R.E., Torres, T., and Zamuner, A., 2004, Biogeography of Gondwanan terrestrial biota during the Jurassic–Early Cretaceous as seen from fossil wood evidence: Review of Palaeobotany and Palynology, v.129, p. 141–173.

Philippe, M., Thévenard, F., Nosova, N., Kim, K., and Naugolnykh, S., 2013, Systematics of a palaeoecologically significant boreal Mesozoic fossil wood genus, *Xenoxylon* Gothan: Review of Palaeobotany and Palynology, v. 193, p. 128–140.

Pinard, M.A., and Huffman, J., 1997, Fire resistance and bark properties of trees in a seasonally dry forest in eastern Bolivia: Journal of Tropical Ecology, v. 13, p. 727–740.

Pole, M., 1999, Structure of a near-polar latitude forest from the New Zealand Jurassic: Palaeogeography, Palaeoclimatology, Palaeoecology, v. 147, p. 121–139.

Ponomarenko, A.G., 2003, Ecological evolution of beetles (Insecta: Coleoptera): Acta Zoologica Cracoviensia, v. 46, p. 319–328.

Qi, Y., and Volmer, D.A., 2019, Chemical diversity of lignin degradation products revealed by matrix-optimized MALDI mass spectrometry: Analytical and Bioanalytical Chemistry, v. 411, p. 6031–6037.

Rayner, A.D.M., and Boddy, L., 1988, Fungal Decomposition of Wood: Its Biology and Ecology: John Wiley, Chichester, UK.

Ren, S.F., Zhang, L., Cheng, Z.H., and Guo, Y. L., 2005, Immobilized carbon nanotubes as matrix for MALDI-TOF-MS analysis: applications to neutral small carbohydrates: Journal of the American Society for Mass Spectrometry, v. 16, p. 333–339.

Rex, G.M., and Chaloner, W.G., 1983, The experimental formation of plant compression fossils: Palaeontology, v. 26, p. 231–252.

Richmond, D., Lupia, R., Philippe, M., and Klimek, J., 2019, First occurrence of the boreal fossil wood *Xenoxylon meisteri* from the Jurassic of North America: Morrison Formation of central Montana, USA: Review of Palaeobotany and Palynology, v. 267, p. 39–53.

Ricklefs, R.E., 1968, Patterns of growth in birds: Ibis, v. 110, p. 419–451.

Rohatgi, A., 2020, WebPlotDigitizer, version 4.4: Website: https://automeris.io/WebPlotDigitizer [accessed 13 Feb 2020].

Rößler, R., Philippe, M., van Konijnenburg-van Cittert, J.H.A., McLoughlin, S., et al., 2014, Which name(s) should be used for Araucaria-like fossil wood?—Results of a poll: Taxon, v. 63, p. 177–184.

Rößler, R., Trümper, S., Noll, R., Hellwig, A., and Niemirowska, S., 2021, Wood shrinkage during fossilisation and its significance for studying deep-time lignophytes: Review of Palaeobotany and Palynology, v. 292, 104455.

Rößler, R., Zierold, T., Feng, Z., Kretzschmar, R., Merbitz, M., Annacker, V., and Schneider, J.W., 2012, A snapshot of an early Permian ecosystem preserved by explosive volcanism: New results from the Chemnitz Petrified Forest, Germany: Palaios, v. 27, p. 814–834.

Rothwell, G.W., 1972, *Palaeosclerotium pusillum* gen. et. sp. nov.: A fossil eumycete from the Pennsylvanian of Illinois: Canadian Journal of Botany, v. 50, p. 2353–2356.

Sagasti, A.J., Massini, J.L.G., Escapa, I.H., and Guido, D.M., 2019, Multitrophic interactions in a geothermal setting: Arthropod borings, actinomycetes, fungi and fungal-like microorganisms in a decomposing conifer wood from the Jurassic of Patagonia: Palaeogeography, Palaeoclimatology, Palaeoecology, v. 514, p. 31–44.

Saito, K., Kato, T., Takamori, H., Kishimoto, T., and Fukushima, K., 2005b, A new analysis of the depolymerized fragments of lignin polymer using ToF–SIMS: Biomacromolecules, v. 6, p. 2688–2696.

Saito, K., Kato, T., Tsuji, Y., and Fukushima, K., 2005a, Identifying the characteristic secondary ions of lignin polymer using ToF−SIMS: Biomacromolecules, v. 6, p. 678–683.

Sarkanen, K.V., and Ludwig, C.H., 1971, Lignins. Occurrence, formation, structure, and reactions: Wiley, New York.

Schmidt, O., 2006, Wood and Tree Fungi. Biology, Damage, Protection, and Use: Springer, Heidelberg, 334 p.

Schopf, J.M., 1971, Notes on plant tissue preservation and mineralization in a Permian deposit of peat from Antarctica: American Journal of Science, v. 271, p. 522–543.

Schudack, M.E., Turner, C.E., and Peterson, F., 1998, Biostratigraphy, paleoecology, and biogeography of charophytes and ostracodes from the Upper Jurassic Morrison Formation: Modern Geology, v. 22, p. 379–414.

Schwarze, F.W.M.R., 2007, Wood decay under the microscope: Fungal Biology Reviews, v. 21, p. 133–170.

Schwarze, F.W.M.R., Engels, J., and Mattheck, C., 2000, Fungal Strategies of Wood Decay in Trees: Springer, 185 p.

Scipioni, M.C., Dobner, M., Longhi, S.J., Vibrans, A.C., and Schneider, P.R., 2019, The last giant *Araucaria* trees in southern Brazil: Scientia Agrícola, v. 76, p. 220–226.

Scurfield, G., and Segnit, E.R., 1984, Petrifaction of wood by silica minerals: Sedimentary Geology, v. 39, p. 149–167.

Seward, A.C., 1919, Fossil plants. Volume IV: Cambridge University Press, London.

Shi, X., Yu, J., Broutin, J., Pons, D., Rossignol, C., Bourquin, S., Crasquin, S., Li, Q., and Shu, W., 2017, *Turpanopitys taoshuyuanense* gen. et sp. nov., a novel woody branch discovered in Early Triassic deposits of the Turpan Basin, Northwest China, and its palaeoecological and palaeoclimate implications: Palaeogeography, Palaeoclimatology, Palaeoecology, v. 468, p. 314–326.

Shine, R., and Charnov, E.L., 1992, Patterns of survival, growth and maturation in snakes and lizards: The American Naturalist, v. 139, p. 1257–1269.

Sigleo, A.C., 1978, Organic geochemistry of silicified wood, Petrified Forest National Park, Arizona: Geochimica et Cosmochimica Acta, v. 42, p. 1397–1405.

Sillett, S.C., Van Pelt, R., Carroll, A.L., Campbell-Spickler, J., Coonen, E.J., Iberle, B., 2019,

Allometric equations for *Sequoia sempervirens* in forests of different ages: Forest Ecology and Management, v. 433, p. 349–363.

Sprinkel, D.A., Bennis, M.B., Gray, D.E., and Gee, C.T., 2019, Stratigraphic setting of fossil log sites in the Morrison Formation (Upper Jurassic) near Dinosaur National Monument, Uintah County, Utah, USA: Geology of the Intermountain West, v. 6, p. 61–76.

Staccioli, G., Uçar, G., Bartolini, G., Coppi, C., and Mochi, M., 1998, Investigation on a fossil *Sequoia* bark from Turkey: Holz als Roh-und Werkstoff, v. 56, p. 426–429.

Stankiewicz, B.A., Mastalerz, M., Kruge, M.A., Van Bergen, P.F., and Sadowska, A., 1997, A comparative study of modern and fossil cone scales and seeds of conifers: A geochemical approach: New Phytologist, v. 135, p. 375–393.

Stewart, W.N., Stewart, W.M., and Rothwell, G.W., 1993, Paleobotany and the evolution of plants: Cambridge University Press, 521 p.

Stubblefield, S.P., and Taylor, T.N., 1986, Wood decay in silicified gymnosperms from Antarctica: Botanical Gazette, v. 147, p. 116–125.

Stubblefield, S.P., and Taylor, T.N., 1988, Recent advances in palaeomycology: New Phytologist, v. 108, p. 3–25.

Stubblefield, S.P., Taylor, T.N., and Beck, C.B., 1985, Studies of Paleozoic fungi. IV. Wood decaying fungi in *Callixylon newberryi* from the Upper Devonian: American Journal of Botany, v. 72, p. 1765–1774.

Sweeney, I.J., Chin, K., Hower, J.C., Budd, D.A., and Wolfe, D.G., 2009, Fossil wood from the middle Cretaceous Moreno Hill Formation: Unique expressions of wood mineralization and implications for the processes of wood preservation: International Journal of Coal Geology, v. 79, p. 1–17.

Taylor, E.L., Taylor, T.N., and Krings, M, 2009, Paleobotany: The Biology and Evolution of Fossil Plants: Elsevier, Academic Press, 1230 p.

Taylor, T.N., 1993, The role of late Paleozoic fungi in understanding the terrestrial paleoecosystem, *in* Archangelsky, S., ed., XII Congrès International de Géologie du Carbonifère-Permian (Buenos Aires): Comptes Rendus, p. 147–154.

Taylor, T.N., and Krings, M., 2010, Paleomycology: the rediscovery of the obvious: Palaios, v. 25, p. 283–286.

Taylor, T.N., and Taylor, E.L., 1997, The distribution and interactions of some Paleozoic fungi: Review of Palaeobotany and Palynology, v. 95, p. 83–94.

Taylor, T.N., Krings, M., and Taylor, E.L., 2015, Fossil Fungi, 1st edition: Elsevier/Academic Press Inc, London, San Diego CA, Waltham MA, Oxford, 398 p.

Temesgen, H., Zhang, C.H., and Zhao, X.H., 2014, Modelling tree height–diameter relationships in multi-species and multi-layered forests: A large observational study from Northeast China: Forest Ecology and Management, v. 316, p. 78–89.

Thomas, B.A., and Watson, J., 1976, A rediscovered 114-foot *Lepidodendron* from Bolton, Lancashire: Geological Journal, v. 11, p. 15–20.

Tian, N, Wang, Y.D., Zheng, S., and Zhu, Z.P., 2020, White-rotting fungus with clamp-connections in a coniferous wood from the Lower Cretaceous of Heilongjiang Province, NE China: Cretaceous Research, v. 105, 104014.

Tian, N., Wang, Y.D., and Jiang, Z.K., 2021, A new permineralized osmundaceous rhizome with fungal remains from the Jurassic of western Liaoning, NE China: Review of Palaeobotany and Palynology, v. 290, 104414.

Tidwell, W.D., 1990, Preliminary report on the megafossil flora of the Upper Jurassic Morrison Formation: Hunteria, v. 2, p. 1–11.

Tidwell, W.D., and Medlyn, D.A., 1992, Short shoots from the Upper Jurassic Morrison Formation, Utah, Wyoming, and Colorado, USA: Review of Palaeobotany and Palynology, v. 71, p. 219–238.

Tidwell, W.D., and Medlyn, D.A., 1993, Conifer wood from the Upper Jurassic of Utah, Part II—*Araucarioxylon hoodii* sp. nov.: Palaeobotanist, v. 42, p. 1–7.

Tidwell, W.D., Britt, B.B., and Ash, S.R., 1998, Preliminary floral analysis of the Mygatt-Moore Quarry in the Jurassic Morrison Formation, west-central Colorado: Modern Geology, v. 22, p. 341–378.

Trujillo, K.C., and Kowallis, B.J., 2015, Recalibrated legacy ^{40}Ar/^{39}Ar ages for the Upper Jurassic Morrison Formation: Geology of the Intermountain West, v. 2, p. 1–8.

Tschopp, E., Mehling, C., and Norell, M.A., 2020, Reconstructing the specimens and history of Howe Quarry (Upper Jurassic Morrison Formation; Wyoming): American Museum Novitates, v. 3956, p. 1–56.

Turner, C.E., and Peterson, F., 2004, Reconstruction of the Upper Jurassic Morrison Formation extinct ecosystem—a synthesis: Sedimentary Geology, v. 167, p. 309–355.

Unger, F., 1841, Chloris Protogaea: Beiträge zur Flora der Vorwelt: Engelmann, Leipzig, Germany, 150 p.

Vaden, M.D., 2020, Data from: Tallest & Largest redwoods: Avaliable online at https://mdvaden.com/redwood_dimensions.shtml, accessed on 13 Feb 2020.

van Bergen, P.F., Blokker, P., Collinson, M.E., Damsté, J.S.S., and de Leeuw, J.W., 2004, Structural biomacromolecules in plants: what can be learnt from the fossil record? *in* Hemsley, A.R., Poole, I., eds., The Evolution of Plant Physiology, Academic Press, London, p. 133–154.

van Bergen, P.F., Poole, I., Ogilvie, T.M., Caple, C., and Evershed, R.P., 2000, Evidence for demethylation of syringyl moieties in archaeological wood using pyrolysis-gas chromatography/mass spectrometry: Rapid Communications in Mass Spectrometry, v. 14, p. 71–79.

Vanderschaaf, C.L., 2013, Mixed-effects height–diameter models for ten conifers in the inland Northwest, USA: Southern Forests: a Journal of Forest Science, v. 76, p. 1–9.

Visser, R., John, T., Menneken, M., Patzek, M., and Bischoff, A., 2018, Temperature constraints by Raman spectroscopy of organic matter in volatile-rich clasts and carbonaceous chondrites: Geochimica et Cosmochimica Acta, v. 241, p. 38–55.

Wagner, A., Donaldson, L., and Ralph, J., 2012, Lignification and lignin manipulations in conifers, *in* Jouanin, L., and Lapierre, C., eds., Lignins - Biosynthesis, Biodegradation and Bioengineering: Academic Press, Cambridge, p. 37–76.

Wan, M.L., Yang, W., He, X.Z., Liu, L.J., and Wang, J., 2017, First record of fossil basidiomycete clamp connections in cordaitalean stems from the Asseliane–Sakmarian (Lower Permian) of Shanxi Province, North China: Palaeogeography, Palaeoclimatology, Palaeoecology, v. 466, p. 353–260.

Ward, L.F., 1990, Description of a new genus and twenty new species of fossil cycadean trunks from the Jurassic of Wyoming: Proceedings of the Washington Academy of Sciences, v. 1, p. 253–300.

Wei, H.B., Gou, X.D., Yang, J.Y., and Feng, Z., 2019, Fungi–plant–arthropods interactions in a new conifer wood from the uppermost Permian of China reveal complex ecological relationships and trophic networks: Review of Palaeobotany and Palynology, v. 271, 104100.

Williams, C.J., Johnson, A.H., Lepage, B.A., Vann, D.R., and Sweda, T., 2003, Reconstruction of Tertiary *Metasequoia* forests. II. Structure, biomass, and productivity of Eocene floodplain forests in the Canadian Arctic: Paleobiology, v. 29, p. 271–292.

Williams, C.J., Trostle, K.D., and Sunderlin, D., 2010, Fossil wood in coal-forming environments of the late Paleocene–early Eocene Chickaloon Formation: Palaeogeography, Palaeoclimatology, Palaeoecology, v. 295, p. 363–375.

Willis, K., and McElwain, J., 2014, The evolution of plants: Oxford University Press, 398 p.

Witke, K., Götze, J., Rößler, R., Dietrich, D., and Marx, G., 2004, Raman and cathodoluminescence spectroscopic investigations on Permian fossil wood from Chemnitz—A contribution to the study of the permineralisation process: Spectrochimica Acta Part A, v. 60, p. 2903–2912.

Xie, A., Gee, C.T., Bennis, M.B., Gray, D., and Sprinkel, D.A., 2021, A more southerly occurrence of *Xenoxylon* in North America: *X. utahense* Xie et Gee sp. nov. from the Upper Jurassic Morrison Formation in Utah, USA, and its paleobiogeographic and paleoclimatic significance: Review of Palaeobotany and Palynology, v. 291, 104451.

Xing, P., Zhang, Q.B., and Baker, P.J., 2012, Age and radial growth pattern of four tree species in a subtropical forest of China: Trees, v. 26, p. 283–290.

Yoshinaga, A., Kamitakahara, H., and Takabe, K., 2016, Distribution of coniferin in differentiating normal and compression woods using MALDI mass spectrometric imaging coupled with osmium tetroxide vapor treatment: Tree Physiology, v. 36, p. 643–652.

Zeibig-Kichas, N.E., Ardis, C.W., Berrill, J.P., and King, J.P., 2016, Bark thickness equations for mixed-conifer forest type in Klamath and Sierra Nevada Mountains of California: International Journal of Forestry Research, p. 1–10.

Zhu, Z.P., Li, F.S., Xie, A.W., Tian, N., and Wang, Y.D., 2018, A new record of Early Cretaceous petrified wood with fungal infection in Xinchang of Zhejiang Province: Acta Geologica Sinica, v. 92, p. 1149–1162. (in Chinese with English abstract)

Appendix

Peer-reviewed publications

Xie, A.*[1], Gee, C.T., Bennis, M.B., Gray, D., and Sprinkel, D.A., 2021, A more southerly occurrence of *Xenoxylon* in North America: *X. utahense* Xie et Gee sp. nov. from the Upper Jurassic Morrison Formation in Utah, USA, and its paleobiogeographic and paleoclimatic significance: Review of Palaeobotany and Palynology, v. 291, 104451, DOI: 10.1016/j.revpalbo.2021.104451.

Gee, C.T.*, Xie, A.*, and Zajonz, J., 2022, Multitrophic plant–insect–fungal interactions across 150 million years: A giant *Agathoxylon* tree, ancient wood-boring beetles and fungi from the Morrison Formation of NE Utah, and the brood of an extant orchard mason bee: Review of Palaeobotany and Palynology, v. 300, 104627, DOI: 10.1016/j.revpalbo.2022.104627.

Xie, A.*, Tian, N., and Gee, C.T., in revision, Ancient Basidiomycota in an extinct conifer-like tree, *Xenoxylon utahense*, and a brief survey of fungi in the Upper Jurassic Morrison Formation of USA: Journal of Paleontology, submitted in March 2022.

Xie, A.*, Gee, C.T., and Griebeler, E.M., in prep. (nearing completion and subsequent submission), Modeling the height–diameter relationship of living *Araucaria* trees to reconstruct ancient conifer height.

Liesegang, M.*, Schnell, A., Xie, A., Gee, C.T., Tahoun, M., Engeser, M., and Müller, C.E., in review, Linking silicification cycles, trace element gradients, and biomolecule preservation in Upper Jurassic gymnosperm wood: Geochimica et Cosmochimica Acta, submitted in April 2022.

[1] *Corresponding author.